STRUCTURE AND PROPERTIES OF CONDUCTING POLYMERS MODIFIED WITH FUNCTIONAL MOLECULES

THESIS SUBMITTED TO THE
UNIVERSITY OF PUNE

FOR THE DEGREE OF
DOCTOR OF PHILOSOPHY

IN
CHEMISTRY

BY
S FRANCIS AMALRAJ

POLYMER SCIENCE AND ENGINEERING DIVISION
NATIONAL CHEMICAL LABORATORY (NCL)
PUNE – 411008, INDIA.
FEBRUARY-2008

Dedicated to My Parents
and
Uncle Rev. Fr. S. Savarimuthu

CERTIFICATE

This is to certify that the work incorporated in the thesis entitled **"Structure and Properties of Conducting polymers Modified with Functional molecules"** submitted by Mr. S. Francis Amalraj was carried out by him under my supervision at the Polymer Science and Engineering Division, National Chemical Laboratory, Pune. Such material as has been obtained from other sources has been duly acknowledged in the thesis.

Date: 01.02.2008

National Chemical Laboratory — Dr. S. Radhakrishnan

Pune 411 008 — Research Guide

DECLARATION

I hereby declare that the work incorporated in the thesis entitled **"Structure and Properties of Conducting polymers Modified with Functional molecules"** submitted for the degree of Doctor of Philosophy to the university of Pune, has been carried out by me at the National Chemical Laboratory, Pune under the supervision of Dr. S. Radhakrishnan. The work is original and has not been submitted in part or full by me for any other degree or diploma to this or any other university.

01-02-2008

National Chemical Laboratory, S.Francis Amalraj
Pune-8. Research student.

ACKNOWLEDGEMENT

First, I Thank God the Almighty for guiding me through inner voice in all phases of my life. I thank him for his divine providence and love showered during the course of my research.

I express my deep sense of gratitude to my research supervisor Dr. S. Radhakrishnan for his constant guidance and valuable advises that has enabled me to complete my research work. I am grateful to him for giving me liberty in the work undertaken and for continuous encouragement during the course of the present study. I appreciate his broad-base understanding in chemistry, physics and other related fields.

I am very grateful to Dr. B. D. Kulkarni and Dr. Vincent Paul for their invaluable help, and encouragement throughout my stay at NCL.

I am thankful to my senior colleagues Dr. Deshpande, Dr. Kanhegaokar, Dr. Arindam, Dr. Sreejith, Dr. Swarnendu, Dr. Subbu, Dr. Patil. for their extensive help and cooperation during my research tenure.

It gives me great pleasure to thank my present lab mates Dr. Santhosh Paul, Dr. Ramanujam, Dr. Pradip sonawane, Dr. Narendra sonawane, Siju, Biplab, Rajashree and Zope for their helping attitude at all times of need.

I sincerely thank my friends Malli, Ramesh, Victor, Prathap, Pradeep, Balakrishnan, Immanuel, Harikrishna for their cheerful company and kind help.

I would also like to thank Dr. Pavaskar , Mrs. Anuya for their timely help and support.

I am very grateful to my parents Susai-Helen, uncle Rev. Fr. S.Savarimuthu and brother Louis for their encouragement, unconditional love and moral support. Mere words cannot express my thanks to my brother Dr. Lawrence, who inspired me and co-operated with me throughout my research work. I thank my sister-in-laws for their wish and support.

A special thanks to my wife Amudha and daughter Reni for their support, love and care during the course of my research work. I appreciate their sacrifice and patience, for being away from home to accomplish this task. I also thank my father-in-law and mother-in-law for their concern and keeping me in their prayers.

Finally, I'm grateful to Dr P. Ratnaswamy and Dr. S. Sivaram, former and present directors of NCL, Pune for giving me the opportunity to work in this premier institute and making all the facilities available for my research work. My thanks are also duly acknowledged to CSIR, New Delhi for their valuable support in the form of a Research Fellowship.

National Chemical Laboratory
PUNE-2

S.Francis Amalraj

CONTENTS

Chapter 2: Experimental

Chapter 3: Synthesis and properties of iron and cobalt Phthalocyanine doped PANI

Chapter 4: Synthesis and properties of tetra sulfonated nickel phthalocyanine doped PANI

Chapter 5: Synthesis and properties of tetra sulfonated Copper phthalocyanine doped PANI

Chapter 6: Summary and Conclusion

LIST OF ABBREVIATIONS

APS	- Ammonium per sulphate
CP	- Conducting Polymer
CV	- Cyclic Voltammetry
DBSA	- Dodecylbenzene sulfonic acid
DMF	- Dimethyl Formamide
DMSO	- Dimethyl sulphoxide
d-value	- Inter-planar Distance
Ea	- Activation Energy
EDAX	- Electron Dispersion X-ray Microanalysis
EMI	- Electro Magnetic Interference
ES	- Emeraldine salt
eV	- Electron Volt
FET	- Field Effect Transistor
FT-IR	- Fourier Transform Infrared
GFAAS	- Graphite Furnace Atomic Absorption Spectroscopy
HCSA	- Camphor Sulfonic acid
HOMO	- Highest Occupied Molecular Orbital
ICP	- Inherently Conducting Polymer.
LEB	- Leucomeraldine base
LB	- Langmuir-Blodgett
LUMO	- Lowest Unoccupied Molecular Orbital
NMP	- N-Methyl Pyrolidone
$(NO)_2$	- Nitric Oxide
OD	- Optical Density
PA	- Polyacetylene
PANI	- Polyaniline
Pc	- Phthalocyanine

PEGME	- Poly(ethyleneglycol)monoethyl ether
PEO	- Polyethylene Oxide
PET	- Polyethylene Terephthalate
Pfu	- Polyfuran
PMAS	- Poly(2-methoxyaniline-5-sulfonic acid)
PNG	- Pernigraniline
ppm	- Parts per Million
PPP	- Poly(p-phenylene)
PPS	- Poly(p-phenylene) sulfide
PPy	- Polypyrrole
Pt	- Platinum
PTh	- Polythiophene
Py	- Pyrrole
RT	- Room Temperature
SCE	- Standard Calomal Electrode
SEM	- Scanning Electron Microscopy
SPAN	- Sulfonated Polyaniline
TBAP	- Tetra Butyl Ammonium Perchlorate
TGA	- Thermo Gravimmetric Analysis
THF	- Tetrahydrofuran
TSCuPc	- Tetra sulfonated copper phthalocyanine
TSFePc	- Tetra sulfonated iron phthalocyanine
TSNiPc	- Tetra sulfonated nickel phthalocyanine
UV-Vis.	- Ultra Violet–Visible
VOC	- Volatile Organic Compound
WAXD	- Wide Angle X-ray Diffraction.

LIST OF SYMBOLS

R	- Resistance.
R_0	- Initial Resistance
ΔR	- Change in Resistance
σ	- Conductivity
Ω	- Ohm
$M\Omega$	- Mega Ohm
mA	- milli Ampere
S/cm	- Siemens per Centimeter
V	- Voltage
mV	- milli Volt
μV	- micro Volt
% T	- Percentage Transmission
T	- Temperature
^0C	- Degree Centigrade
S	- Sensitivity Factor
%	- Percentage
μm	- micro meter
mg	- milli gram
g	- gram
π	- Pi
t	- Time
Sec	- Second
ml	- milli Liter
λ_{max}	- Wavelength at Maximum Absorption
υ	- Wavenumber
nm	- Nano meter
t_{50}	- Response Time of Sensor
$(r_{a/v})$	- Surface area to volume

Structure and Properties of Conducting polymers Modified with Functional molecules

Abstract

Conducting polymers functionalized with groups, which enhance specific physical and/or chemical properties are promising candidates for sensor, electrochromic, redox catalytic and energy conversion applications. In this respect, polyaniline substituted with redox or molecular recognizing groups represent very attractive combination for developing new materials. The sensors made from polyaniline have many improved characteristics like room temperature operation, shorter response time, ease of synthesis etc. when compared to metal oxide based sensors that operate at high temperature. Hence in the present investigation, the emeraldine salt form of polyaniline was incorporated with tetra sulfonated metal phthalocyanines in the form of dopant ion. The functional molecules namely iron, nickel and copper tetra sulfonated phthalocyanines were used to incorporate into polyaniline matrix by chemical and electrochemical methods. Initialy, polyaniline was modified with un-substituted iron and cobalt phthalocyanines which ended up with polyaniline-phthalocyanine composite with decrease in electrical conductivity. Hence, it was decided to use water soluble tetra sulfonated metal phthalocyanines as dopant during the synthesis of polyaniline.

The catalytic effect of phthalocyanine was observed as an increase in polyaniline conversion during synthesis with various metal phthalocyanines. The efficacy of incorporation and the structure of functionalized polyaniline was elucidated by various physico-chemical techniques. The effect of phthalocyanine incorporation in PANI was seen as a shift in the frequency of benzeniod structure towards lower wave number region. In WAXD studies, notable changes in the crystallinity of PANI has been observed due to

the addition of macrocyclic phthalocyanine moiety into polymer matrix. In the electronic spectra, the π - π^* and polaron to bipolaron transitions in PANI showed red shift due to the extension of conjugation with the highly conjugated phthalocyanine moiety. GFASS analysis revealed the proportionate increase in metal ion concentration as consistent with the concentration of sulfonated phthalocyanine used.

The electrical conductivity of Polyaniline modified with un-substituted phthalocyanine doesn't show any increase in conductivity instead a steady fall in conductivity was noted due to the formation of two phases namely, insulating phthalocyanine and conducting PANI. In the case of tetra sulfonated phthalocyanine incorporated PANI an increase in conductivity was observed with increase in phthalocyanine concentration and this is could be due to the strong interaction between the Pc and PANI providing better pathway for the transport of charges along and in between the polyaniline matrix. This is further confirmed from the IR and WAXD studies. The thermal stability of synthesized samples were analyzed by TGA. The added phthalocyanine has significant effect on the thermal stability of PANI by linking sulfonated phthalocyanine and PANI chains together to give better thermal stability. TSPc-PANI samples synthesized under electrochemical route showed clearly defined nano-fibrils where as PANI synthesized using HCl dopant doesn't show the fibrillar morphology. Similarly TSPc-PANI samples prepared through chemical route were particulate in nature. The redox behaviour of electrochemically synthesized Pc containing PANI films were studied by cyclic voltammetric technique.

The potentiality of the Pc functionalized PANI samples were tested to explore its final utility towards sensing of 100 ppm NO_2 gas. When the samples were exposed to NO_2 gas a decrease in resistance was observed with FePc and CoPc loaded PANI, which appear to

be a common process. On the other hand, an increase in resistance was observed with sulfonated Pc incorporated PANI samples. Hence, a different mechanism of NO_2 gas sensing has been suggested for the substituted phthalocyanine incorporated as dopants in PANI. The sulfonated Pc-PANI samples showed higher sensitivity factor and speed of response than FePc and CoPc incorporated PANI samples. Among the sensors made from chemically synthesized sulfonated phthalocyanine-PANI samples, 1 mol % TSCuPc incorporated PANI showed maximum sensitivity factor (R/R_o) of 30.9 with a response speed of 62 sec. In the case of sensors fabricated by electrochemical method, the response is very rapid and at the same time recovery is also fast when compared to the sensor made from chemical method. In all electrochemically functionalized PANI samples, the maximum sensitivity was reached at an optimum concentration of 0.5 mol % of TSPc in PANI. A high sensitivity factor of 335 was achieved by 0.5 mol % TSCuPc-PANI with rapid response time of 29 sec.

Therefore, among the sulfonated metal phthalocyanine incorporated PANI, the TSCuPc-PANI appear to be superior as a chemical sensor materials operating at room temperature. Additionally, the morphology also plays an important role since nano fibrous morphology is seen in the electrochemically deposited films, which give better response than the chemically synthesized polymers. These studies have clearly brought out the importance of functionalization of conducting polymers for specific application such as a chemical sensor. Thus, these sensors can lead to the development of artificial electronic nose, which can sniff out toxic gases and send alarms.

CHAPTER-1

Introduction

1.1. Origin of conducting polymer

Polymers are normally used in electrical and electronic applications as insulators, where advantage is taken of their resistivities and good dielectric performances. Polymers are also widely exploited because of their other advantageous properties, including mechanical strength, flexibility, stability, low cost and ease of processing. However, polymers with spatially extended π- boding system, for e.g., acetylene black, though known for many years, didn't draw significant research attention till mid 1970s. This was caused by the fact that they were intractable and in many respects showed inferior properties as compared to already developed polymers.

In 1977 Heeger, MacDiarmid and Shirakawa showed that polyacetylene (PA), which is the simplest polyconjugated system, can be rendered conductive by the reaction with bromine or iodine vapors [1]. Spectroscopic studies that followed demonstrated without ambiguity that this reaction is redox in nature and consists of the transformation of neutral polymer chains into polycarbocation with simultaneous insertion of the corresponding number of Br_3^- or I_3^- anions between the polymer chains in order to neutralize the positive charge imposed on the polymer chain in course of the doping reaction [2]. This important discovery initiated an extensive and systematic research devoted to various aspects of the chemistry and physics of conjugated polymers. This previously un-attended and underestimated family of macromolecular compounds turned out to be extremely interesting both from basic research and application point of view. As a result, in the year 2000, Heeger, MacDiarmid and Shirakawa – the founders of the 'conjugated polymer science' – were laureated with the Noble Prize in chemistry [3-5]. Another exciting event demonstrated by Batlogg et al [6] shortly after the attribution of

the Nobel Prize for the conducting polymers is that the regioregular conducting polymer poly(3-hexylthiophene) if used in a field effect transistor (FET) configuration becomes superconducting at 2.35 K. This is the first case of superconductivity in organic polymers, albeit not the first example of a superconducting polymer since superconductivity in an inorganic polymer-poly(sulfur nitride): $(SN)_x$ – was discovered more than two decades ago [7].

The discovery of highly conducting PA, therefore, led to a sudden spurt in research activity directed towards the study and discovery of new conducting polymeric systems. At present many new conducting polymers with properties similar to those of PA have been synthesized and studied. Such systems include [8-12] poly(p-phenylene) (PPP), poly(p-phenylene) sulfide (PPS), heterocyclic polymers such as polythiophene (PTh), polypyrrole (PPy), polyfuran (PFu) and their derivatives, i.e. polyquinolines, polyquinoxalines and pyrrones, etc. These polymers, though they share many structural similarities, show wide range of conductivity, depending upon the doping percent, the alignment of polymer chains, and the purity of the sample.

1.2. Classification of conducting polymers

There are essentially three major ways in which polymers can be made electrically conducting and these are

1. Conductively filled polymers
2. Ionically conducting polymers
3. Inherently conducting polymers

1.2.1. Conductively Filled Polymers

An insulating polymers like PVC, PMMA, PS and PP can be made electrically conducting by incorporating conductive additives or fillers [13]. Typical examples of conductive components used to prepare this type of conducting polymer include conducting solids such as carbon black, carbon fibers, aluminium flakes and metal particles, etc. Conductivity is introduced into the various insulating polymers by the addition of conducting components through various processing techniques like hot compression and extrusion. The conductively filled polymers were first made in 1930 for the prevention of corona discharge. Since then, conductively filled polymers have been used for a number of applications ranging from electrostatic discharge protection to electromagnetic interference / radio-frequency interference (EMI/RFI) shielding [14].

1.2.2. Ionically Conducting Polymers

Ionically conducting polymers are normally prepared by dissolving a salt species in a solid polymer host. Conductivity in polymer electrolytes [15] is believed to arise from the ion migration between coordination sites repeatedly generated by the local motion of polymer chain segments. Therefore, a desirable polymer host must possess: a) electron –donating atoms or groups for the coordinate bond formation with cations, b) low bond rotation barriers for an easy segmental motion of the polymer chain, and c) an appropriate distance between coordinating centers for multiple intra polymer bonding with cations. Although a large number of macromolecules can meet the above requirements, lithium or sodium salts dissolved poly(ethylene oxide) [16] , remains the most studied ionically conducting polymer.

1.2.3. Inherently Conducting Polymers

Inherently conducting polymers also referred to as highly conjugated polymers are a novel class of electrically conductive materials whose electrical properties are derived principally through their possession of extended π conjugation [17]. Owing to the delocalization of electrons in a continuously overlapped π-orbital along the polymer backbone reduces the energy difference between the HOMO/valence and LUMO/conduction bands, essentially making them small band gap semiconductors. Conduction of electric charges requires unoccupied energy states for extra electrons or electron deficiencies (holes) to be available and the relatively unhindered movement of charge throughout the conducting material [18]. The structure of some of representive conducting polymers are shown in Fig. 1.1. As can be seen from the figure 1.1, the conjugated structure with alternating single and double bonds or conjugated segments coupled with atoms providing p-orbitals for a continuous orbital overlap (e.g., N, S) seems to be necessary for the polymers to become intrinsically conducting. These materials differ from polymers filled with carbon black or metals because the latter are only conductive if the individual conductive particles are mutually in contact and form a coherent phase. Since our studies are mainly focused on conjugated polymers, the following topics will be discussed with respect to inherently conducting polymers.

1.3. Doping Processes

Conjugated conducting polymers have low ionization potential, high electron affinity and low energy optical transitions [19]. Most polymers containing these

structures behave, in their pristine forms, like insulators with conductivities of about 10^{-12} S/cm or lower.

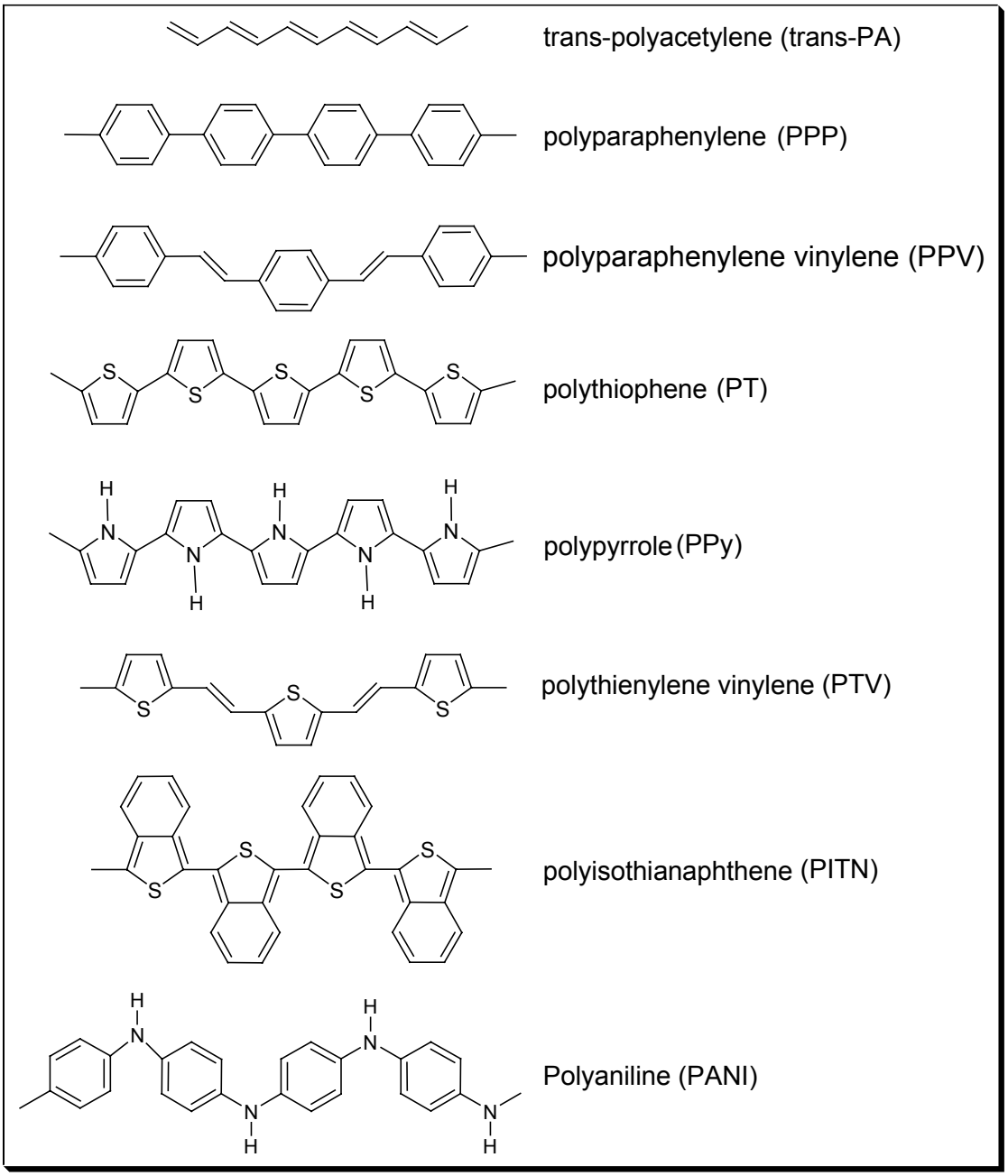

Fig. 1.1. Structure of few inherently conducting polymers.

Therefore, the insulating character displayed by conjugated polymers must be attributed to the low concentrations of charge carriers in these materials. An increase in charge carriers can be achieved by doping. Doping process involves [20] partial oxidation (*p*-doping) of the polymer chain with electron acceptors (e.g. I_2, AsF_5) or by partial reduction (*n*-doping) with electron donors (e.g., Na, K). Through such a doping process, charged defects (e.g., polaron, bipolaron and soliton) are introduced, which could then be available as charge carriers [21]. In practice, doping occurs by exposing the polymer, most often in the form of thin film or powder, to the doping agent in gas phase or in liquid phase. The doping can also be done electrochemically by using the polymer as an electrode. The principal methods of doping are as follows.

1.3.1. Chemical doping

The doping is accomplished by exposing the polymer to the vapor of a dopant such as I_2, AsF_3, or H_2SO_4, or by immersing the polymer film in a dopant solution, such as sodium naphthalide in THF, I_2 in hexane, and so on [22]. For example, the treatment of *trans*-polyacetylene with an oxidizing agent such as iodine leads to the doping reaction as shown in equation-1 and a concomitant increase in conductivity of about 10^{-5} to 10^{2} S/cm.

$$\textit{trans}\text{-}(CH)_x + 3/2xyI_2 \longrightarrow [CH^{+y}(I_3)_y^-]_x \quad \text{----------(1)}$$

Similarly, *trans*-polyacetylene can be doped with reducing agents (n-doping) to gain high conductivities (equation-2).

$$\textit{trans}\text{-}(CH)_x + [Na^+(C_{10}H_8)^-] \longrightarrow [(Na^+)_y (CH)^{-y}]_x + C_{10}H_8 \quad \text{---------(2)}$$

The amount of dopant incorporated in the material (doping level) depends on the vapour pressure of the dopant or its concentration, the doping time, and the temperature.

1.3.2. Electrochemical doping

Conjugated polymers can also be easily oxidized (*p*-doping) or reduced (*n*-doping) electrochemically with the conducting polymer acting as either electron source or an electron sink [23, 24]. In particular, the doping reaction (equation-3) can be accomplished by applying a DC power source between a *trans*-polyacetylene-coated positive electrode and a negative electrode. Both of them immersed in a solution containing $LiClO_4$ in propylene carbonate.

$$\textit{trans}\text{-}(CH)_x + (xy)(ClO_4)^- \longrightarrow [CH^{+y}\,(ClO_4)y^-]_x + (xy)e^- \quad (y \leq 0.1) \quad \text{---- (3)}$$

Compared with chemical doping, electrochemical doping has several distinct advantages. Firstly, a precise control of the doping level can be achieved simply by monitoring the amount of current passed. Secondly, doping-undoping is highly reversible.

1.3.3. Photo doping

The irradiation of a conjugated polymer with a light beam of energy greater than its band gap could promote electrons from the valence band into the conduction band (equation-4). Although the photo-generated charge carriers may disappear once the irradiation ceases, the application of an appropriate potential during irradiation could separate electrons from holes, leading to photoconductivity [25].

trans-$(CH)_x$ ⟶ 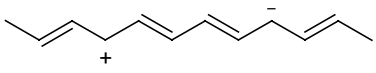 ----- (4)

1.3.4. Charge-injection doping

Using a field effect transistor (FET) geometry, charge carrier can be injected into the band gap of conjugated polymers [e.g. polyacetylene, poly(3-hexylthiophene)] by applying an appropriate potential on the metal/insulator/polymer multilayer structure [26, 27].

1.3.5. Secondary doping

When HCSA-doped PANI film cast from chloroform was treated with *m*-cresol [28, 29], an increase in conductivity was observed from 0.1 S/cm up to 400 S/cm. This concomitant increase in conductivity by up to several orders of magnitude can be due to the molecular interactions between HCSA-doped PANI and *m*-cresol which causes a conformational transition of the polymer chain from a "compact coil" to an "expanded coil". This process has been ascribed as "secondary doping". This effect has been observed as a free carrier tail in the near-infrared region which could arise from delocalization of electrons in the polaron band, leading to an increase in conductivity.

1.4. Charge transport process in conducting polymers

Conducting polymers actually behave more like highly doped semiconductors rather than metals. In their pristine state, conducting polymers are highly conjugated and neutral. Addition of dopants generates charged species (soliton, polaron and bipolaron) within the polymer which are mobile enough to conduct electric charges. The positive charges initially supplied to the polymer chain by electron acceptors fill the highest occupied molecular orbital (HOMO level) of the valence band. However, the negative charges provided to the chains by electron donors fill the lowest unoccupied molecular

orbital (LUMO level) of the conduction band. Distortions of the bond lengths in the vicinity of the doped charges occur as a consequence of the strong coupling between electrons and phonons [30, 31].

trans-polyacetylene presents an unusual ground state geometry that gives rise to two degenerate states for infinite chain length. The charge added to the polymer backbone can be stored as a radical, cation or anion defect, the motion of which in the chain, owing to the degenerate ground states of the polymer, can be described by the motion of the solitary wave, called a soliton [32] in field theory notation and it is shown in Fig. 1.2.

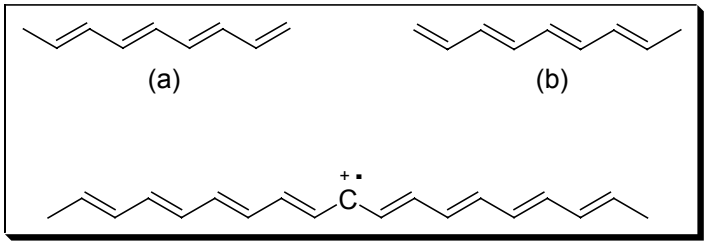

Fig. 1.2. Degenerate states of polydienes. A radical cation or anion defect on the polyacetylene backbone divide the polymer into sections (a) and (b)

The radical defect is called a neutral soliton, and both the cation and anion defects are referred to as charged solitons. These latter carriers are postulated to explain the spinless transport observed in polymers with degenerate ground states, because they carry charge but not spin. High doping in t*rans*-polyacetylene causes the soliton energy levels essentially to overlap the filled valence and empty conduction bands, leading to a conducting polymer.

Spinless transport also occurs in polymers with nondegenerate ground states, such as poly(*p*-phenylene) [33], although this polymer does not have two energetically equivalent structures, a requirement theoretically necessary for mobile solitons.

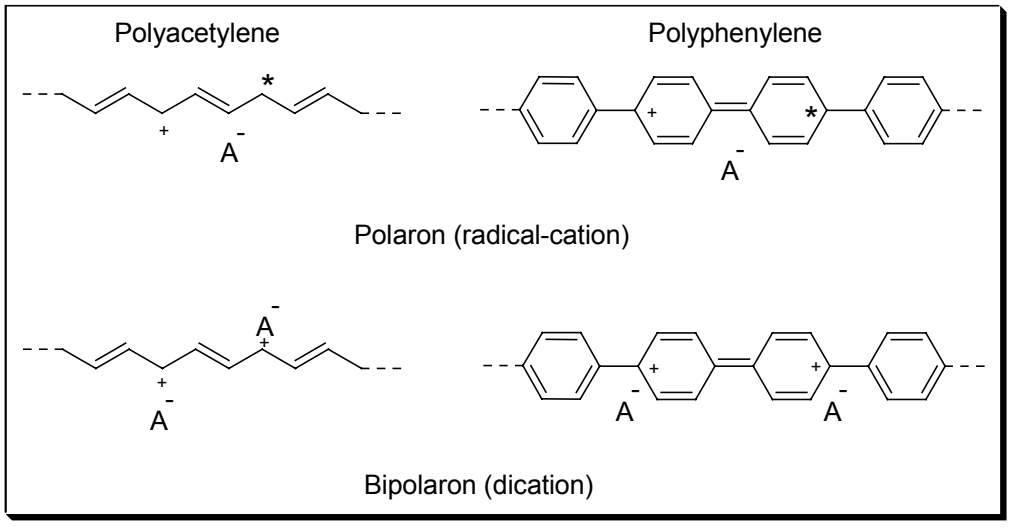

Fig. 1.3. Charge defects in polyacetylene and poly(p-phenylene)

Motions of the cation defect that create stable benzonoid structure give rise to an energy gain due to stabilizing effects of the aromatic rings. An energy loss occur if the motion takes place in the direction in which quinoidal structures are formed. The charged defects generated in polyacetylene and polyphenylene are shown in Fig. 1.3.

For nondegenerate systems (ie., polypyrrole, polythiophene, polyaniline, etc.) the charge introduced at low doping levels are stored as charged polarons and bipolarons. A polaron is a radical cation or a radical anion plus a lattice distortion around the charge [34,35]. Therefore, these species have spin and charge. An inspection of the positive polaron in poly(*p*-phenylene) shows that the radical and the cation are bound together, since an increase in the charge separation of these two defects would require the creation of additional high-energy quinoid units. The motion of the polaron in polyacetylene

involves motions of the neutral soliton and the charged soliton forming the radical cation. For nondegenerate polymers, high doping results in the polarons interacting to form a polaron lattice or electrically conducting, partially filled band. The exothermic reaction of two polarons on the same chain gives rise to a di-cation or di-anion, called a bipolaron [36]. Bipolarons have been detected spectroscopically in several doped polymers, though it's not clear whether these species arise from the combination of two radical ions or a second ionization of one polaron. Charged solitons can travel in chains of infinite length having degenerate ground states. Hopping of the charged soliton to an adjacent defect free chain should overcome high-barrier energies associated with the necessary geometrical reorganization [37]. However, this barrier will be rather low if hopping of two charged solitons to an adjacent chain occurs. This mechanism would explain the spinless transport observed in polymers with nondegenerate ground states. This transport mechanism is illustrated for polyacetylene in Fig. 1.4.

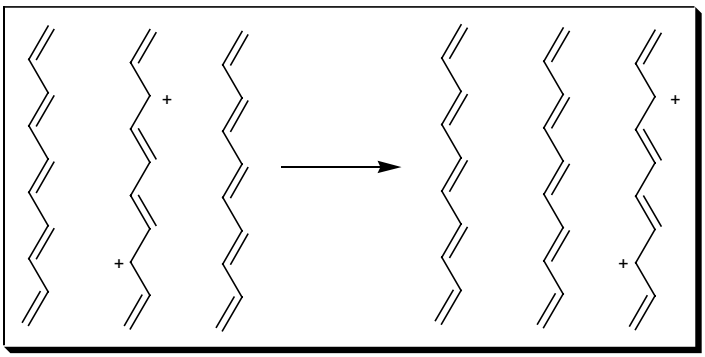

Fig. 1.4. Interchain transport of bipolarons in polyacetylene

Summing up, charge doped into the polymer is stored in novel states such as solitons, polarons, bipolarons, which involves distortion of the lattice surrounding it.

1.5. Applications of conducting polymers

In the most general way, the applications of conjugated polymer may be classified into two broad categories based on doping process.

1.5.1. Applications of doped conjugated polymers

Under this section, all applications which exploit specific physical properties of the polymer as a consequence of doping process are discussed. Doped conjugated polymers can be used as organic conductors in the preparation of conductive layers, antistatic coatings, fibers, and transparent electrode. The combination of high electrical conductivity with the excellent mechanical properties of plastics increases the application of conjugated doped polymers.

Synthetic fibers and textiles coated with conducting layers deposited by electrode less deposition frequently suffer from poor metal-polymer adhesion. Metallic fibers can be prepared by deposition of doped conjugated polymers on the surface of insulating fibers, in such a way that surface conductivity of 0.2 S/cm is easily reached [38-40]. This conductivity, though low, is much more than that necessary for charge dissipation. It's worth noting that doped conjugated polymers display an appropriate level of conductivity and relatively flat attenuation over a wide range of frequencies, which makes them appropriate as components of radio-absorbing materials [41]. Conducting polymers can also be used in electromagnetic interference (EMI) shielding, principally in the radio and microwave frequency ranges in computer and telecommunication technologies [42]. Although the conducting properties and therefore the shielding efficiency of doped polymers depend on the preparation and the resulting structural order, the shielding of

EMI increases as the thickness of the film increases. The shielding capabilities are in the range of utility for many commercial (~40 dB) and military (~80-100 dB) applications.

Conducting polymers are being used as anticorrosion coatings. Thus, polyaniline exhibits corrosion-protecting properties both in its neutral form [43] and doped form [44]. The protection of this conducting polymer in steel depends on the thickness of the iron oxide layer at the polymer–metal interface. Accordingly, polyaniline withdraws electron from the surface of the steel so that protection is of the anodic type. Owing to the fact that the redox potential of polyaniline is close to that of silver, this material behaves like a noble metal. Conducting polymers are also being used as electrodes in rechargeable batteries as a consequence of the redox reactions that takes place in these polymers. Some battery applications of electro-active polymers are discussed elsewhere [45].

Organic-inorganic hybrids are obtained by doping conjugated polymers with large anions of the Keggin type such as $[XM_{12}O_{40}]^{n-}$. These substances are excellent polymer supported catalyst in several important reactions of industrial importance, and their advantage over the classical catalysts is the molecular dispersion of the catalytic active species via the doping reaction. Several surface-doped conjugated polymers have been tested as heterogeneous catalysts, among them polyacetylene, polypyrrole, polyaniline, etc [46].

Doping –associated optical changes may be promoted electrochemically, leading to the so-called electrochromic effect. Electrochromic windows can be prepared by sandwiching a thin layer of a conducting polymer electrode, a suitable electrolyte and a transparent counter electrode. Electrochromic effects are displayed in polyaniline by changing the pH [47].

1.5.2. Applications of undoped conjugated polymers.

Undoped conjugated polymers are intrinsic semiconductors whose energy gap is strongly affected by both chemical structure and functionalisation of substituents. These materials may emit light under electric perturbations, a phenomenon known as electroluminescence. Electroluminescent diode can be prepared from a conducting polymers which in its simplest form consists of a single layer of electroluminescent polymer and two electrodes. One of them, usually the anode, transparent to the light generated during the electroluminescence effect and the cathode must be a metal of low work function such as calcium, magnesium, or aluminium. Upon application of an external electric field, holes and electrons are injected, respectively, in the valence band (HOMO level) and the conduction band (LUMO level). Injected charge carriers of different sign drift in opposite directions in the conjugated polymer matrix to form excited species, namely, singlet or triplet polaron-excitons. The radiative decay of singlet excitons gives out light whose wavelength depends on the band gap of the polymer and the relaxation process taking place in the excited state. Detailed information on the luminescent properties of conjugated polymer can be found elsewhere [48, 49].

Undoped conjugated polymers can also be used to construct polymer photovoltaic cells. As a consequence of the electron-donors nature of conjugated polymers, photoinduced charge separation may occur owing to photo-induced electron transfer if an electron-accepting molecule is in the vicinity of a conjugated chain. In this way, a positive polaron, which is highly delocalized and mobile, appears in the conjugated backbone. The power conversion efficiency of the conjugated polymer-based

photovoltaic cell increases considerably if a composite layer consisting of electron donor fullerenes (C_{60}) dispersed in the conjugated polymer matrix [50, 51].

Conjugated polymers based field effect transistors are being used in electronic applications. Polymers with highly ordered structures are the best candidates for FETs because charge mobility is much larger in these regions than in the amorphous regions [52, 53]. Therefore, polymers having high carrier mobility like poly(*p*-phenylene vinylene) family and polypyrrole are used for this purpose.

Finally, the conducting polymers are being used as a sensitive layer for the detection of various gases, toxic chemical and explosives [54, 55]. Conducting polymer sensors can be applied in a number of different modes, such as pH based (change in pH), conductometric mode (change in conductivity), amperometric mode (change in current), potentiometric mode (change in open circuit potential) and so on. Among various CP, polypyrrole and polyaniline are most commonly used for making gas sensors. Since conducting polymer based chemical sensors are the main focus of our investigation, it will be discussed in detail in a separate section (Section. 1.7).

1.6. Functionalization of conducting polymers

Functionalization of conducting polymers with groups providing specific physical and chemical properties, in addition to the particular electronic properties of the conjugated backbone, has become more and more prominent in recent years. These so-called ‘‘intelligent’’ materials are promising candidates for sensor, electrochromic, redox catalytic or energy conversion applications. In this respect, polyaniline, polypyrrole or polythiophenes substituted with redox or molecular recognizing groups represent very

attractive combinations. Consequently there is a keen interest in the methodology of chemical synthesis for the precursor monomer and oligomer units. Well developed methods for synthesis of substituted aniline, pyrrole, and especially thiophene monomers have been reported and substituents are numerous, including crown ethers [56], metallocenes [57], amino acids [58] and enzymes [59].

Various strategies for the functionalisation of conducting polymer is displayed schematically in Fig. 1.5.

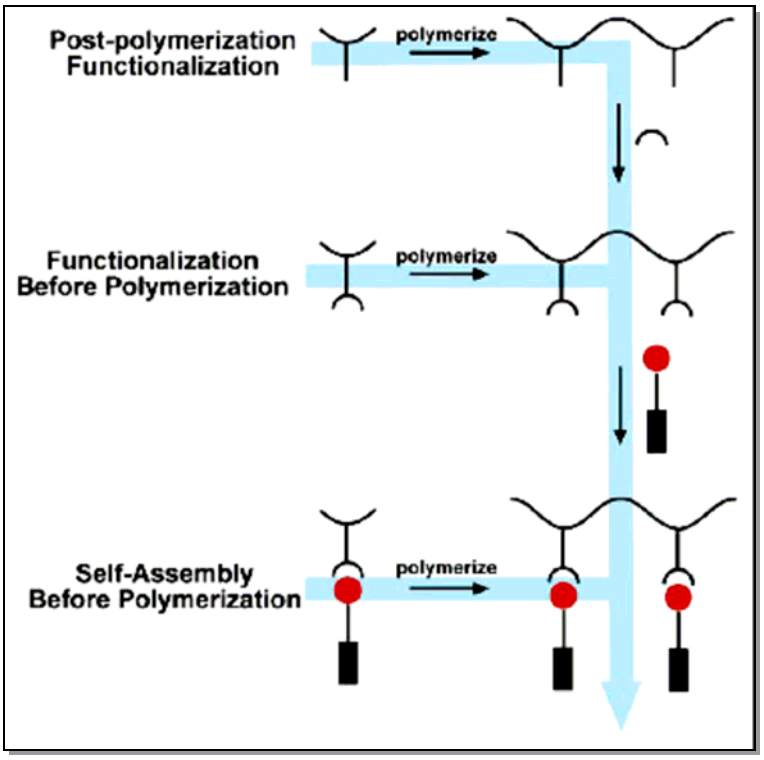

Fig. 1.5. Schematic display of various functionalization strategies.

Since a detailed discussion on functionalisation of polyaniline is given in section. 1.8.3., here we shall look upon the functionalisation of conducting polymers like PPy, and PTh.

The modification of the monomer by chemical bonding (i.e. covalent grafting) has been shown to be very efficient for obtaining functionalized conducting polymer. To induce specific properties in conducting polymer, one has to graft the functional moiety onto a monomer and then perform the polymerization, leading to a functionalized conducting polymer. A typical example is the functionalisation of pyrrole, mainly through the N-substitution. This consists of the substitution of the hydrogen atom by a specific functional molecule. This technique appears to be attractive, due to the large variety of possible modifications. One major problem is the polymerization step which is often more difficult to perform than with the pyrrole monomer alone. Bidan et al. [60] were the first authors to propose a systematic synthesis procedure to carry out the N-functionalization of pyrrole. With shortest chains, steric effects appear to be very important, and with longer chains, the polymer obtained is less conductive. It has been observed in general that the N-substitution of polypyrrole leads to a dramatic decrease in conductivity. This is attributed to the effect of neighboring group steric interactions that reduce the conjugation length of the polymer strands. In addition to this effect, a high density functional groups inhibits electron transfer and it lowers the conductivity [61].

The synthesis and the properties of conducting polymer films obtained from functionalized pyrrole have been extensively reviewed recently [62, 63]. Curran et al [64] has mentioned, the most straightforward way of functionalizing pyrrole at N centers involve electrophilic attack at nitrogen. A typical synthesis of pyrrole monomers bearing bipyridal ligands covalently attached to the pyrrole N centers is shown in Fig. 1.6.

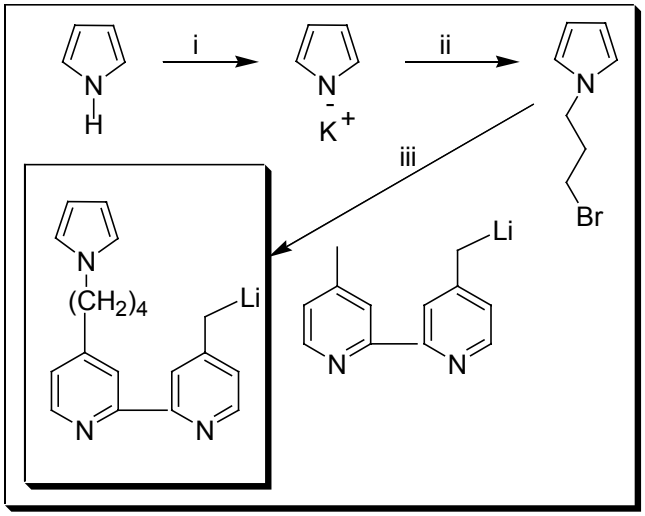

Fig. 1.6. Synthesis of N-functionalized pyrrole monomer. (i) potassium metal, THF; (ii) excess $Br(CH_2)Br$: (iii) THF

Similarly chiral polypyrroles have been synthesized by Elsenbaumer et al [65] by the electropolymerisation of pyrrole monomers bearing chiral substituents covalently attached to the pyrrole N centers.

The most interesting development in the functionalisation of 3-oligo oxyethlene substituted polythiophene has been demonstrated by marsella et al [66], that these polymer are responsive to alkali metal ions. Oligooxyethylene moieties twist the polymer chain as shown in Fig. 1.7. and hence alter the colour of the polymer, as well as its redox properties. The 'twisting' effect could be transmitted significantly to neighbouring rings, thus amplifying the response at low concentration of cation. One would predict a blue shift in the π - π^* transition on cation binding, as the degree of conjugation is lowered with twisting, and this was indeed observed for these polymers.

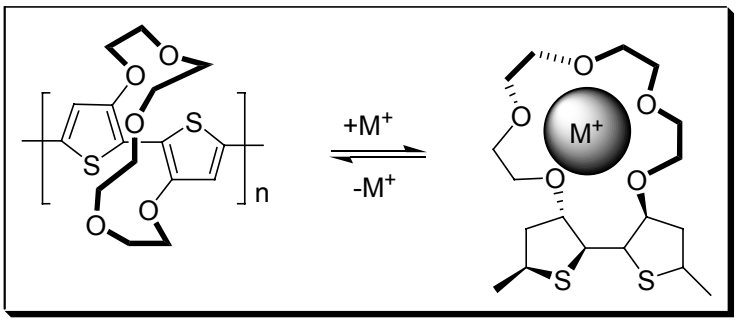

Fig. 1.7. Binding of an alkali metal cation causes twisting of the ionoresponsive polythiophene chain away from optimum conjugation.

Schaferling et al [67] have successfully synthesized the bi and terthiophenes covalently linked to tetraphenylporphyrins via oxaalkyl spacer (see Fig. 1.8.). The porphyrin functionalized polymer has been characterized by electrochemical, optical and in-situ conductivity measurements and they have been demonstrated as amperometric sensors.

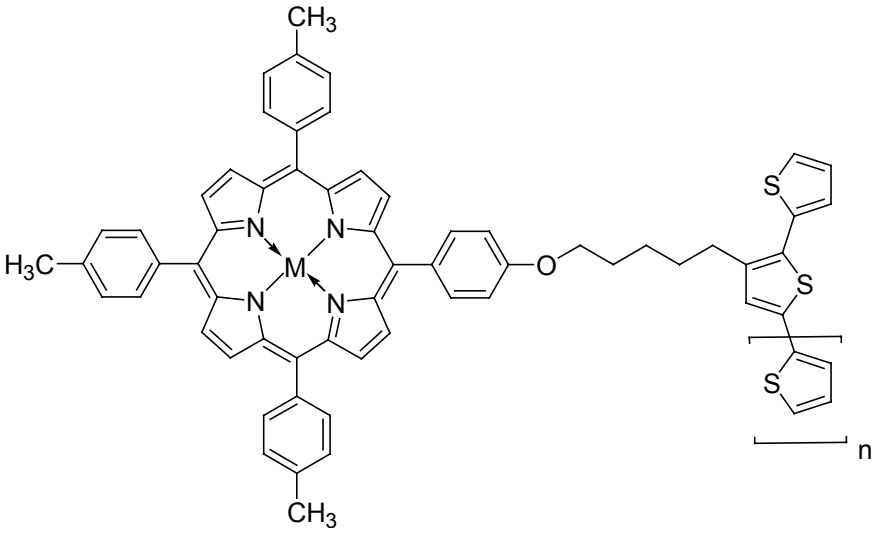

Fig. 1.8. Functionalisation of bi and terthiophene by tetra phenyl porphyrin containing various transition metal ions via oxaalkyl spacer.

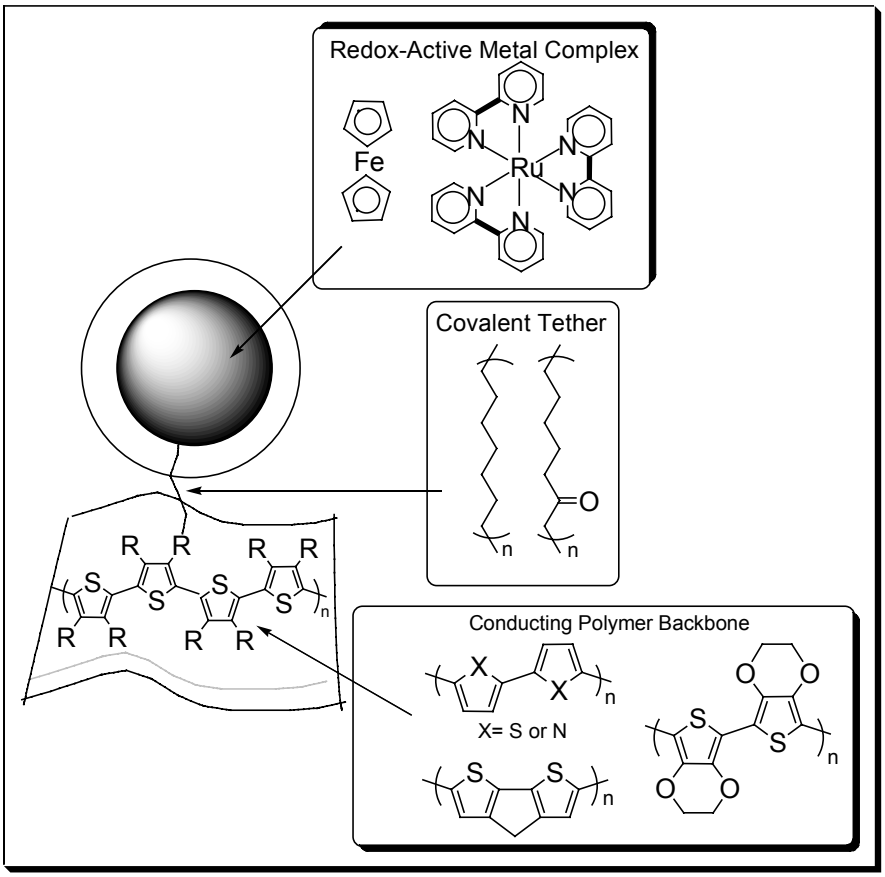

Fig. 1.9. Molecular components of transition metal incorporated conducting polymer structures.

A diverse collection of systems shown in Fig. 1.9. that incorporate transition metals into conducting polymer structures have been reported by Holliday et al [68]. In these type of functionalized polymers, the nature of the conducting polymer backbone as well as the length and nature of the tether has been varied to study the electron transport and electrochemical behavior of this functionalized polymers.

Consequently many research efforts have concentrated on copolymer material synthesized from a solution mixture of functionalized and non-functionalized monomers. This approach leads to materials with a lower proportion of functional groups and higher

conductivities are observed [69]. Despite the convenience of this approach there are key problems, for example, the resultant materials are usually intractable and so hard to characterize, control of copolymer composition is difficult because of the disparate nature of the monomer reactivities, and, it is difficult to prove that the resultant materials are indeed copolymers rather than blends of homogeneous strands. In response to these difficulties many research groups are focusing on functionalized oligomeric species such as sexithiophene [70] and dithienyl pyrrole [71] derivatives. On polymerization, these small oligomer units yield copolymer materials that have a well defined, prescribed structure in which the functional group substituents are spaced out to minimise steric interactions and spatial conflict. Consequently, this reduces the steric interactions between adjacent functional groups of a polymer chain resulting in improved conjugation length and high conductivity [72]. An additional motivation for studies involving functionalised oligomers also arises from reports that soluble polymers can be produced from these precursors thereby offering enhanced processibility for practical applications. The drawback to this approach, however, lies with the arduous nature of the chemical synthesis of the oligomeric precursors. Hence, by considering all the above facts, we thought of functionalising the conducting polymer by immobilizing the negatively charged sulfonated phthalocyanines as dopants in to the positively charged conducting polymer matrix in two different ways namely (a) Chemical polymerization and (b) Electrochemical polymerization.

1.7. Gas sensor based on conducting polymer

Conducting polymers such as polyaniline (PANI), polypyrrole (PPy), polythiophene (PTh) and their derivatives have been used as the active layers of gas sensors since early 1980s [73]. In comparison with most of the commercially available sensors based on metal oxides that operated at high temperatures, the sensors made of conducting polymers have many improved characteristics. They have high sensitivities and short response time especially; these feathers are ensured at room temperature. Furthermore, conducting polymers have good mechanical properties, which allow a facile fabrication of sensors. As a result, more and more attentions have been paid to the sensors fabricated from conducting polymers.

Active layer of sensor made of conducting polymer can be prepared by any one of the following methods namely: electrochemical deposition, spin coating, dip coating, Langmuir-Blodgett technique, drop coating, layer by layer self assembly technique, and vapor deposition polymerization. Among this, electrochemical deposition is the most convenient method to deposit conducting polymer films. The thickness of the film can be controlled by the total charge passed through the electrochemical cell during film growing process. Moreover, the film can be deposited on patterned microelectrodes [74]. However, if the insulating gap between the neighboring electrodes is close enough (~several tens of micrometer), the growing film can cover the insulated gap and connect electrodes [75]. This is important in fabricating chemiresistors. Some researchers also packed conducting polymer powders into pellets to fabricate the active layers [76].

1.7.1. Sensing principle

Chemical sensors transform the concentrations of analytes to other detectable physical signals, such as currents, absorbance, mass or acoustic variables. After exposing to the vapor of an analyte, the active sensing material of the sensor interacted with the analyte, which causes the physical property changes of the sensing material. According to different analytes and different active materials The interactions between the analytes and sensing materials are multiform, and they are discussed in the following sections.

1.7.1.1. Interactions between gas molecules and conducting polymer

(a) Chemical reactions between analytes and conducting polymers

The physical properties of conducting polymers strongly depend on their doping levels. Fortunately, the doping levels of conducting polymers can be easily changed by chemical reactions with many analytes at room temperature, and this provides a simple technique to detect the analytes. Most of the conducting polymers are doped/undoped by redox reactions; therefore, their doping level can be altered by transferring electrons from or to the analytes. Electron transferring can cause the changes in resistance and work function of the sensing material. This process occurs when PANI, PPy and PTh films exposed in NH_3, NO_2, I_2, H_2S and other redox-active gases [77-85]. Electron acceptors, such as NO_2 and I_2, can remove electrons from the aromatic rings of conducting polymers. When this occurs at a p-type conducting polymer, the doping level as well as the electric conductance of the conducting polymer is enhanced. An opposite process will occur when detecting an electron-donating gas. Ammonia is an electron-donor; when PPy reacts with ammonia, its electric resistance dwindles down sharply. However, after washing with dry nitrogen or air, the resistance of the sensing layer can be totally or

partly recovered. Following reactions are possibly involved in the ammonia sensing process [86].

$$PPy^{+} + \ddot{N}H_3 \longrightarrow PPy^{0} + NH_3^{+} \quad \text{Adsorption} \quad \text{------} \quad (5)$$

$$PPy^{0} + NH_3^{+} \longrightarrow PPy^{+} + \ddot{N}H_3 \quad \text{Desorption} \quad \text{------} \quad (6)$$

Based on this mechanism, all p-type conducting polymers are expected to dedope under ammonia atmosphere. In fact, some different phenomenon was observed in thin polycarbazole film sensor [87]. It was found that a decrease in resistance occurred when reacted with ammonia. Further studies are still needed to make the mechanism clear. Proton transfer is also present in PPy. Krivan et al. observed a decrease in resistance of PPy film when it was exposed to the vapor of weak acid such as H_2S and CH_3COOH, indicating a proton transfer from acidic gas to PPy and a increase of doping level of the polymer [88]. Geng et al. gave the same interpretation [89]. Furthermore, NH_3 was reported to be able to remove protons from PPy [90, 91]. Mohammad and Jung et al. considered the response of PTh film to ammonia as the result of formation of irreversible ionic pairs between the positively charged electric barrier of NH_4^+ ions and the doped anions [92]. In another case, HCl protonates the carboxylate groups on poly (thiophene-3-alkanoic acid), and allows the polymer chains to relax from twisted conformation to a π-stacked conformation [93].

(b) Weak interactions between analytes and conducting polymers

Many important organic analytes, such as benzene, toluene and some other volatile organic compounds (VOCs) are not reactive at room temperature and under mild conditions. Therefore, it is difficult to detect them by their chemical reactions with

conducting polymers. However, they may have weak physical interactions with the sensing polymers, involving absorbing or swelling the polymer matrixes, etc. These interactions do not change the oxidation levels of conducting polymers, but can also influence the properties of the sensing materials and make these gases detectable.

Absorbing of the analyte molecules on the surface of sensing film is widely used in gas sensing. In fact, absorption is the first step in all the sensing techniques, especially in quartz crystal microbalance sensors. The absorption of organic gases on conducting polymers has been experimentally studied. To detect the adsorption of analyte and further the concentration of them, the effects of adsorption and desorption on the properties of the sensing film were studied. A simple method to monitor the adsorption-desorption is measuring the mass uptake. By recording the response frequency change of a conducting polymer film coated quartz microbalance, water vapor, hydrocarbon, acetone, organic acids, benzene, toluene, ethylbenzene and xylene (BTEX compounds) can be detected [94-98]. Analyte adsorption also may enhance the potential barrier at the boundaries between the grains, eventually changing the electric properties of the sensing materials [99].

In addition to adsorption, another widely observed phenomenon in the process of swelling in conducting polymer when contact with vapors. Like other polymers, conducting polymers can swell in many organic solvents. This is controlled by the vapor molecular volume, the affinity of the vapor to the sensing polymer and the physical state of the polymer [100, 101]. However, swelling of the polymer film is an important mechanism to interpret sensing behavior of conducting polymer to organic vapors [102-105]. For a pure conducting polymer, inserting analyte molecule into polymer matrix

generically increases interchain distance, which affects the electron hopping between different polymer chains.

Hydrogen bonding and dipole-dipole interactions are also reported to play important roles in sensing process. The infrared spectra of a PPy film after exposing to acetone indicated the formation of hydrogen bonds (H-bonds) between C=O groups of acetone molecules and N−H groups of pyrrole units [106]. Furthermore, the weak intermolecular force is also used to distinguish enantiomer of chiral gas by PPy with chiral side group [107].

Experimental results demonstrated that some analyte, especially alcohols [108] and ketones [106], can change the crystallinity of conducting polymers. This fact has been confirmed by X-ray diffractions. Small alcohols such as methanol and ethanol interact and diffuse more efficiently in the polymeric matrixes than the alcohols with higher molecular weight do. Moreover, the high dielectric constants of small alcohols make them strongly interact with the nitrogen atoms of polyanilines, leading to an expansion of the compact PANI chains into more stretching conformations. This in turn, is expected to increase the crystallinity of the polymer and decrease its electric resistance. In contrast, alcohol molecules with high molecular weights can not diffuse into polymer matrix efficiently like small ones due to their long chain lengths and non-polar nature, they are likely to act as barriers among PANI chains, which results in an increase in resistance [76].

1.7.2. The parameters influence the performance of the gas sensors based on conducting polymers

Many factors are expected to influence the performances of conducting polymer based sensors. Here, we will just list few important factors.

1.7.2.1. Sensing materials

Much attempt has been devoted to improve the sensitivity, response time and stability of gas sensors by modifying the sensing materials. Nearly all the widely studied conducting polymers such as PPy, PTh and PANI have been used as the active materials in sensors. The methods of adjusting the sensing materials include modifying the polymer molecular structures, changing dopants and incorporating second component into conducting polymers. An advantage of using conducting polymer as the active material is that the structure of conducting polymer can be easily modified.

The introduction of grafts to the backbones of conducting polymers has two effects. Firstly, most of the side chains are able to increase the solubility of conducting polymers. This makes them to be processed into the sensing film by LB technology, spin-coating and other solution-assistant methods. Secondly, some functional chains can adjust the properties of conducting polymers, such as space between molecules [109] or dipole moments [110], or bring additional interactions with analytes, which may enhance the response, shorten the response time, or produce new sensitivity to other gases.

Dopants can influence the physical and chemical properties of conducting polymers. Conducting polymers doped with different ions may give distinct responses to a specific analyte. A representative example of conducting polymer is that PANI doped with small inorganic ions showed an increase in resistance to ammonia, while acrylic acid

doped PANI exhibited an inverse response [111]. Differences in sensing performances between Cl^-, $(SO_4)^{2-}$ and $(NO_3)^-$ doped PPy composites are also studied by Ratcliffe group [112]. Further, De Souza et al. tried to find the relationship between the response and the molecular sizes of dopants [113].

Incorporating second component into conducting polymer film is one of the most important methods to develop new sensors. In comparison with modification of molecular structure of conducting polymers, the advantage of this technique is that it can avoid complicated chemical synthesis. The functions of incorporating another component into the conducting polymers are manifold. We can classify these sensors according to sensing mechanisms. In some cases, the second components play an important role in sensing process. They may improve the properties of sensing film help in electron or proton transfer [114], or directly interact with analytes by swelling [115] or electron/proton exchange.

1.7.2.2. Device fabrication

The change in morphology of sensing layer can strongly influence the performances of chemi-resistors and diodes. These effects are usually attributed to be the results of changing the ratio of surface area to volume ($r_{a/v}$) [116]. A film with higher ($r_{a/v}$) makes analyte molecules diffuse and interact with the sensing layer more easily, which lead to a higher sensitivity and shorter response time. To increase the ($r_{a/v}$) of a flat film, we can either thin the film or make it porous. Many results demonstrated that sensors with thinner or more porous active films have higher sensitivities [117, 118]. On the other hand, as a thin film fabricated by LB technique was used as the sensing layers, the sensitivity of the sensor increased with the number of LB layer [119]. Nanofibers

(wires, tubes) have high ($r_{a/v}$) values, so they are perfect candidates preparing sensors with high sensitivities and fast response.

1.7.2.3. Working environment

The sensitivity of sensor depends on the temperature. As discussed above, sensing process involves two steps: adsorbing of analyte molecules in sensing film and then the reaction between them. Temperature is able to influence both of the two steps. Adsorption always prefers low temperature; increasing temperature will shift the equilibrium to desorption [120-122]. The performance of the sensors based on redox reactions usually increase with the increase of temperature [123, 124], mainly due to the acceleration of reaction.

The sensitivity of a sensor also strongly depends on the ambient humidity. In fact, water vapor itself is an important analyte, and many sensors are sensitive to humidity. Thus, the signal of other gas in humid atmosphere is a corporate response of the analyte and water. To reduce the influence of humidity, introducing hydrophobic substituted groups on polymer backbone was reported [125].

In conclusion**,** conducting polymers have been widely used as the sensing layers of gas sensors. The advantages of using conducing polymers as the sensing layers are room-temperature operations, facile property adjustment, high sensitivity and short response time, easy device fabrication. However, they have several disadvantages which needs to be improved: Long-time instability is a main drawback of the sensors based on conducting polymers. Not only the sensors based on conducting polymers, but also the other sensors have the problem of low selectivity. Thus, extending the lifetime of sensors

is the crisis in application of conducting polymers, and also the main challenge before the researchers in the field.

Conducting polymer nanocomposites, especially nanofibers and nanotubes, are good sensing materials due to their high surface/volume ratio. Although the fabrications of these nanomaterials are more complicate than film, they can enhance the performance of gas sensors efficiently. Thus, synthesizing new nanocomposites is still a focus of future works in gas sensing field.

1.8. Polyaniline (PANI)

Polyaniline is the oxidative product of an aniline under acidic conditions and has been known since 1862 as an aniline black [126]. Polyaniline is a typical phenylene based polymer having a chemically flexible -NH- group in a polymer chain flanked either side by a phenylene ring. Among all conducting polymers, polyaniline has been one of the most studied electroactive polymers due to easy synthesis, environmental stability, and simple non redox doping by protonic acid. The ability of aniline polymers to exist in a large number of intrinsic redox states [127] makes them a unquie and interesting class of polymeric material. Polyaniline also differs from polypyrrole and polythiophene in that the N hetero atom participates directly in the polymerization process and also participates in the conjugation of the conducting form of the polymer to a greater extent than the N and S heteroatoms in PPy and polythiophene.

Polyaniline represents a class of macromolecules whose electrical conductivity can be varied from an insulator to a conductor by the redox process. This polymer can achieve its highly conductive state either through the protonation of the imine nitrogens

or through the oxidation of amine nitrogens [128]. For example, the conducting state of PANI can be obtained in its 50% oxidized emeraldine state in aqueous acids like HCl and the resulting material is a p-type semiconductor [129]. With the extent of doping polyaniline can have four different oxidation states [130] like Leucomeraldine base (LEB), Emeraldine base (EB), Emeraldine salt (ES) and Pernigraniline (PNG) shown in Fig. 1.10.

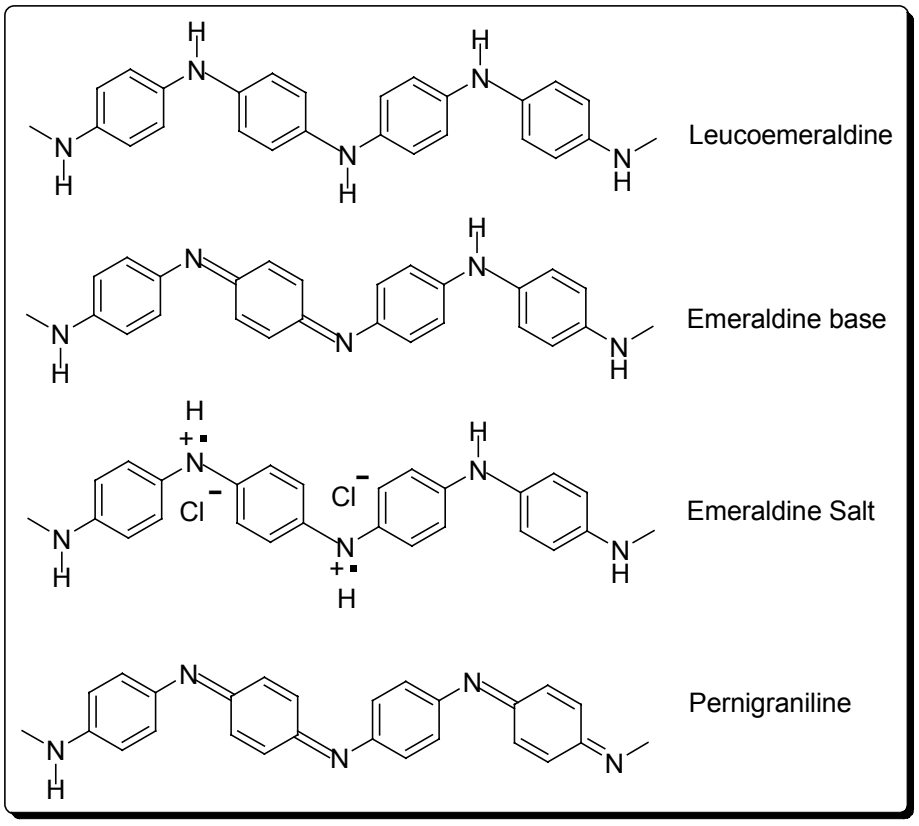

Fig. 1.10. Different oxidation states of PANI

Oxidative doping of the leucoemeraldine base or protonic acid doping of the emeraldine base material produces the conducting emeraldine salt whose conductivity varies between 0.5 S/cm and 400 S/cm depending on the means of preparation. Extensive studies of the

emeraldine salt (ES) material have shown that the metallic state is governed by in-homogeneous disorder. That is, in the conducting state, there are regions that are three-dimensionally ordered in which the conducting electrons are three-dimensionally delocalized and regions where the polymer is strongly disordered, in which conduction electrons diffuse through one-dimensional polymer chains. One dimensional localization in these nearly isolated chains lead to decrease in conductivity with decrease in temperature.

Polyanilines are most commonly prepared through the chemical or electrochemical oxidative polymerization of the respective aniline monomers in acidic solution. However, the method of synthesis depends on the intended application of the polymer. For bulk production chemical method, where as for thin films and better patterns electrochemical method is preferred.

1.8.1. Chemical synthesis

The general procedure for the chemical synthesis of polyaniline involves, oxidation of aniline monomer in the presence of acidic medium for 4 -8 hr at 0-5°C resulted in a dark green coloured product polyaniline. Various oxidizing agents have been used by different authors; ammonium persulfate [131], potassium dichromate [132], hydrogen peroxide [133], ceric nitrate and sulfate [134]. MacDiarmid et al. [135] used a stoichiometric equivalent of the oxidant whereas Hand and Nelson [136] used oxidant excess of the stoichiometric quantity. Similarly, various authors have carried the reaction in different acidic media. MacDiarmid et al [131] used hydrochloric acid at pH 1, Genies et al [137] used a eutectic mixture of hydrofluoric acid and ammonia, the general formula of which is $NH_4F;2.3HF$. Cao, et al [138] studied the influence of synthesis parameters

on the inherent viscosity and conductivity of pressed pellets. Among different oxidants, ammonium presulfate was found to result in the highest conductivity and highest viscosity and finally a concentration of 1.2 M HCl in the reaction mixture yielded the best conductivity and inherent viscosity. It has been reported that [139], a higher molecular weight can be produced by synthesizing polyaniline at temperature below 5°C.

A number of researchers have studied the reaction mechanism of polyaniline. Wei et al. [140] proposed the reaction path shown in Fig. 1.11. It was reported that, the rate

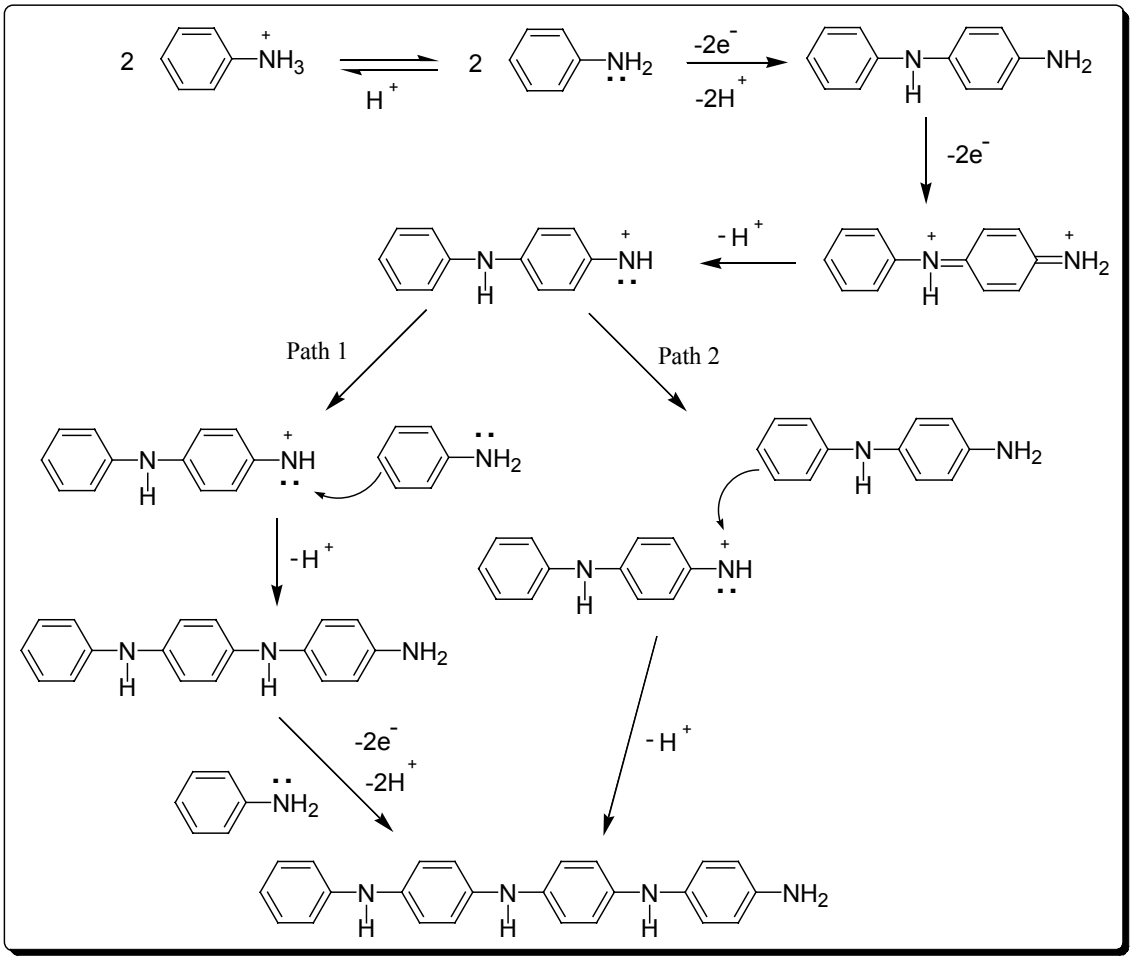

Fig. 1.11. Polyaniline reaction path proposed by Wei [140]

determining step in the oxidative polymerization of aniline is the formation of protonated dimer. The protonated dimer then reacts with either a (neutral) dimer or a neutral aniline molecule.

1.8.2. Electrochemical polymerisation

Polyaniline is often [141-143] prepared electrochemically by cycling the potential of aniline in aqueous acid between 0 and 700 mV versus a standard calomel electrode (SCE). When this is done, one obtains a film of polyaniline deposited on the working electrode. The resulting product is 'clean' and does not necessarily need to be extracted from the initial monomer/oxidant/solvent mixture. This method offers the possibility of coupling with physical spectroscopic techniques such as visible, IR, Raman, ellipsometry and conductometry, for in situ characterization. The anodic oxidation of aniline is generally effected on an inert electrode material which is usually platinum [144, 145]. However, several studies have been carried out with other electrode Materials like iron [146], copper [147], zinc [148], gold [149], and different types of carbon [150, 151]. The two electrochemical modes mainly employed are galvanostatic or potentiostatic. In the latter case, the potential is fixed or cycled, with the value of the applied potential being in the order of 0.7 to 1.2 V (versus SCE) and that of the cycled potential being --0.2 V to 0.7 - 1.2 V (versus SCE). It is generally accepted that potential cycling leads to a more homogenous product, as verified by scanning electron micrograph investigations [152]. The sweep rates most commonly used are between 10 and 100 mV/s. The mechanism generally accepted for the electropolymerization of aniline in an acid medium was presented by Genies and Tsintavis [153], as shown in Fig. 1.12.

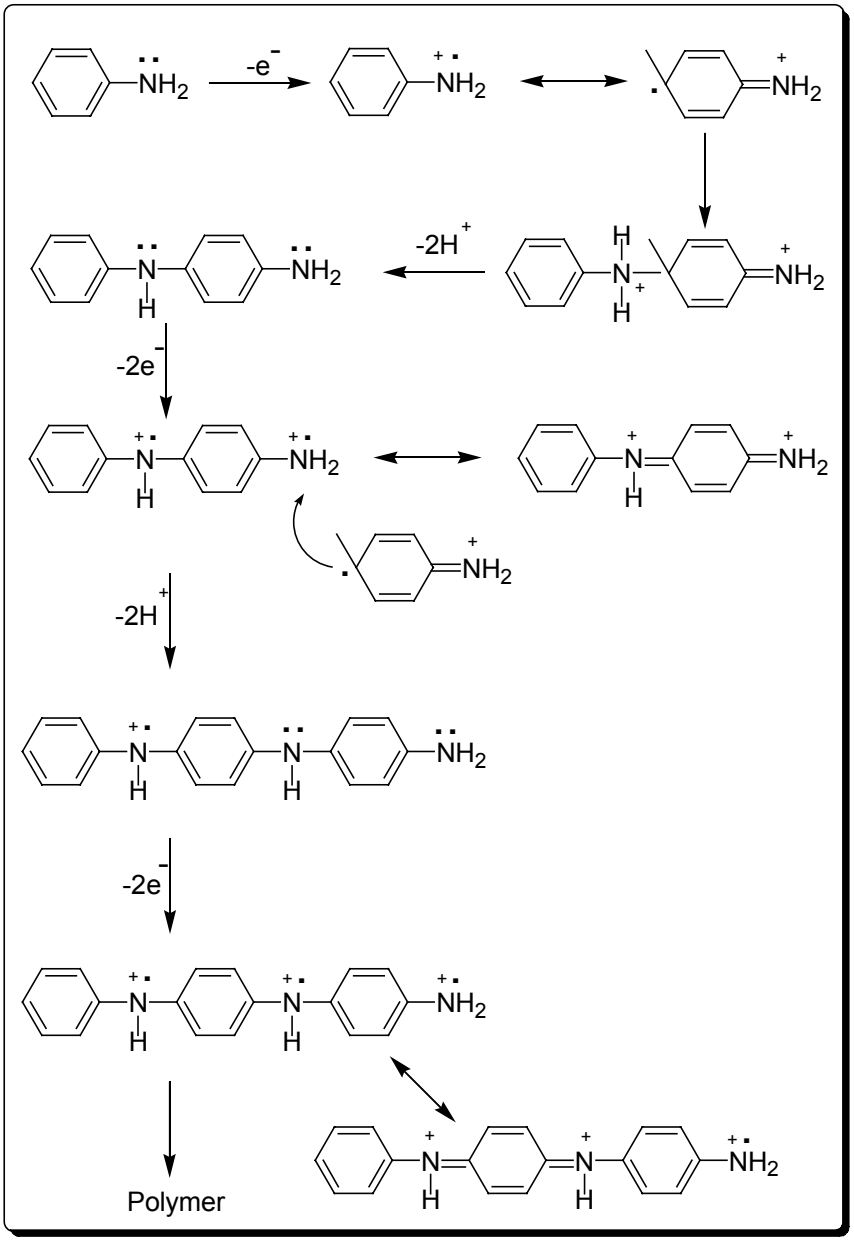

Fig. 1.12. Electropolymerization mechanism of polyaniline proposed by Genies [153]

1.8.3. Functionalization of Polyaniline

Polyaniline has been categorized as an intractable material, which is neither soluble nor fusible under normal conditions. Aside from finding better doping methods to achieve higher conductivity, various strategies have been worked out to induce solubility, processability and specific functionality in polyaniline. One such method is to substitute one or more hydrogens in the aniline nucleus with halogens, alkyl, alkoxy, aryl, hydroxyl and amino groups. Polyaniline with functional moiety appended as side group or dopant may have specific functions towards electrocatalysis, gas sensor and other applications. Although higher solubility can be achieved in many cases, these polyaniline derivatives show much lower conductivity and the molecular weights obtained are generally low. It seems that solubility and processability always come at the expense of conductivity. Functionalization of polyaniline can be classified into two categories.

(a) Substitution of aniline monomer at *o* or *m* positions and then polymerizing or introducing functional moiety as dopant during polymerization.

(b) post polymerization modification on polyaniline.

1.8.3.1. Polymerization of substituted aniline monomers

Polyanilines of the general types **1** and **2** substituted with alkyl and alkoxy group at *o*-position and at the N- center have been synthesized by the chemical or electrochemical oxidation of appropriately substituted aniline monomers [154-156]. The emeraldine salt product of such substituted product imparts solubility in organic solvents that is markedly improved over the parent (un-substituted) PANI-HA salts. The poly(2-methoxyaniline) (POMA) species, in particular, has been the subject of extensive studies

[155, 156] This species has the additional attractive feature of being soluble in water after being wet with acetone.

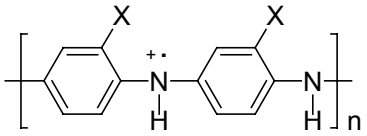

X= R, OR

(1)

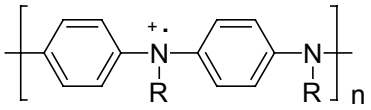

(2)

The substituted polyaniline products often have much lower molecular weights than the parent, unsubstituted PAn, although Mw values as high as 400,000 g mol^{-1} have been obtained for POMA by controlled chemical polymerization at –40°C. This improvement in processibility for substituted polyanilines is also generally gained at the expense of a large decrease in electrical conductivity due to twisting of the polymer chains from planarity by the bulky substituents. Oxidative polymerization of substituted aniline monomers is frequently more difficult than that of aniline itself.

Considerable interest in the polymerization of sulfonated aniline monomers in the hope of producing water-soluble sulfonated polyanilines has also been shown. Attempts to polymerize *o*- or *m*- aminobenzenesulfonic acid by both chemical and electrochemical means have generally been unsuccessful, which has been attributed to steric and electronic deactivation by the electron-withdrawing sulfonic acid substituent [157]. However, Young et al. [158] have reported that *o*- and *m*-aminobenzenesulfonic acid can be successfully synthesized by a novel high-pressure (19 kbar) procedure using $(NH_4)_2S_2O_8$ as oxidant in the presence of 5.0 M LiCl and 5% $FeSO_4$, yielding the fully sulfonated self-doped polyaniline **3** (SPAN). The related fully sulfonated polymer, poly(2-methoxyaniline-5-sulfonic acid) **4** (PMAS) can be prepared under normal

atmospheric pressure by the oxidation of 2-methoxyaniline-5-sulfonic acid with aqueous $(NH_4)_2S_2O_8$ in the presence of ammonia or pyridine [159].

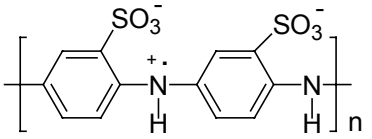

(3) SPAN

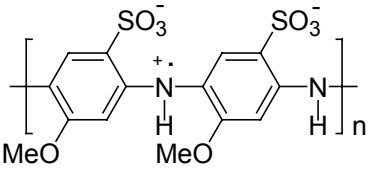

(4) PMAS

The self-doped polymer, poly[*N*-(4-sulfophenyl)aniline] **5**, bearing a sulfonated substituent on each of its N centers, has been similarly prepared by oxidizing the relevant monomer with $(NH_4)_2S_2O_8$ in aqueous HCl, [160, 161] Phosphonic acid substituents can also be utilized to generate self-doping polyanilines, as illustrated by the oxidation of the monomer *o*-aminobenzylphosphonic acid to give the novel polymer **6** [162]. Its low conductivity (10^{-3} S/cm) may arise from H-bonding between the $PO_2(OH)^-$ substituents and NH_4^+ radical cation sites on the polymer chain, causing significant charge-pinning.

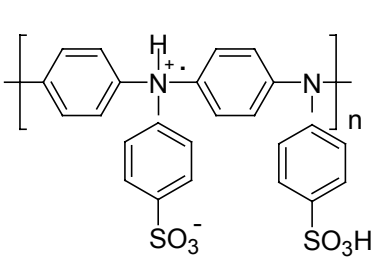

(5)

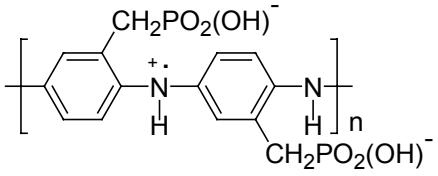

(6)

1.8.3.2. Post polymerization modification

A variety of postpolymerization methods have been utilized to increase the solubility and hence the processibility of PANI. Such modifications have also been pursued to introduce added functionality to PANI, allowing their use in a range of applications such as chemical and biochemical sensors. The postpolymerization

modifications typically involve either (a) chemical reactions on preformed emeraldine base (EB), leucoemeraldine base (LB) or pernigraniline base (PB) leading to covalent bonding of groups to the aniline rings or N centers, or (b) doping of preformed emeraldine base (EB) with agents such as Brönsted acids (HA), Lewis acids and metal complexes or organic electron acceptors. These various approaches are summarized below.

(a) chemical reactions on preformed conducting polymer

In addition to their direct synthesis from sulfonated aniline monomers (described earlier), a number of water-soluble self-doped sulfonated polyanilines can also be prepared by postpolymerization methods. Most widely investigated has been the synthesis of the ring-substituted SPAN (Structure **3**). Treatment of emeraldine base with fuming sulfuric acid gave a SPAN product with ca. 50% of the aniline rings sulfonated [157]. Subsequently, it was found that up to 70% of the aniline rings could be sulfonated by similar treatment of leucoemeraldine base, giving a polymer with enhanced electrical conductivity (ca. 1 S cm^{-1}) [162]. The substitution of amino and alkylthio groups onto the aniline rings of PANI has similarly been achieved through the treatment of emeraldine base (or pernigraniline base) with alkyl amines and alkylthiols [163].

Deprotonation of the amine centers in emeraldine base by treatment with NaH in DMSO, followed by reaction with 1,3-propanesulfone, provides a route to the water-soluble self-doped polymer **7**, in which a $–(CH_2)_3SO_3H$ group is covalently attached to approximately 50% of the N centers along the polymer chain [164]. A related approach to covalently attach chiral camphorsulfonate groups to N centers of PANI by the reaction of EB with (1S)-(+)-10-camphorsulfonyl chloride in NMP/pyridine has been demonstrated

by Reece et al [165]. The optically active product **8**, isolated as the HCl salt, is believed to preferentially adopt a one-handed helical conformation for its polymer chains. This provides the first example of chiral induction in a PANI species through a covalently attached group. A significant advantage for **8** over the chiral PANI.HCSA salts described earlier is that it consequently retains its optical activity upon alkaline dedoping in solution to its EB form.

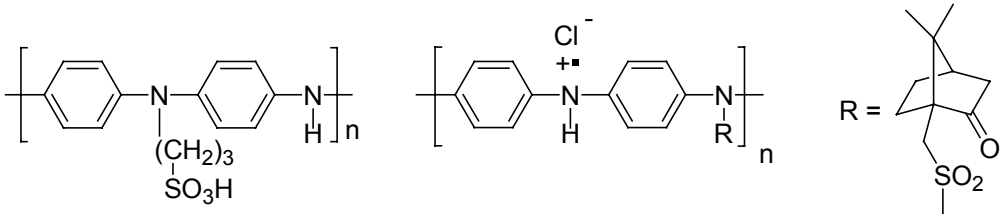

(7) **(8)**

A factor hindering the expansion of polyaniline chemistry to date has been the lack of a generic route to variously substituted derivatives. An exciting development in this respect is the recent synthesis of the novel poly(aniline boronic acid) [166]. Aromatic boronic acids are versatile chemical precursors undergoing a wide range of transformations, which provides a facile route to a range of substituted PANI that are difficult to synthesize directly from their respective monomers. This approach has been successfully demonstrated for the synthesis of poly(hydroxyaniline) and for poly(halogenoaniline).

(b) Doping of EB with Brönsted acids, HA

Polyaniline is unique among inherently conducting polymers in that it can be converted into a conducting form by a nonredox acid-doping process exemplified by the doping of emeraldine base with Brönsted acids (HA) to yield electronically conducting

PANI-HA emeraldine salts (Equation-7). A wide variety of acids can be employed, ranging from inorganic acids such as HCl, HNO_3, H_2SO_4, H_3PO_4 and HBF_4 to organic

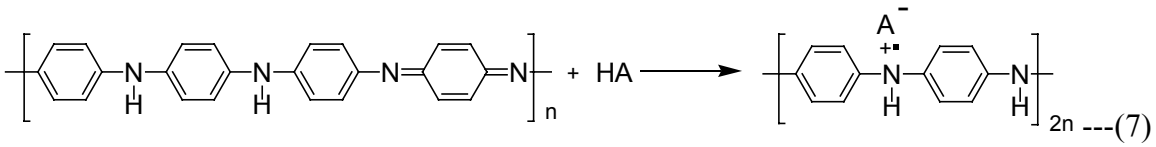

---(7)

sulfonic and carboxylic acids. In an important discovery in the early 1990s, Cao et al [167] found that organic solvent solubility can be imparted to conducting PANI salts by the incorporation of surfactant like dopant acids (HA). For example, by doping emeraldine base (EB) with large bifunctional protonic acids such as camphor-10-sulfonic acid (HCSA) or dodecylbenzenesulfonic acid (DBSA), it is possible to solubilize fractions of these polymers in their fully doped state into solvents such a *m*-cresol, chloroform, toluene and xylene. This solubilization is caused by the hydrocarbon "tail" in the dopants, while the sulfonate (SO_3^-) "head" forms an ionic bond with radical cation $NH^{+\cdot}$ sites on the PANI chains.

Water-soluble emeraldine salts can also be prepared by this acid-doping technique. For example, doping of emeraldine base with phosphonic acid containing poly(ethylene glycol)monoethyl ether (PEGME) as a hydrophilic tail gives a mildly conducting PANI that is soluble (or dispersible) in water [168]. With the water-soluble poly(*o*-methoxyaniline) (POMA), Mattoso et al. [169] have reported the self-assembly of multilayer conducting polymer films by depositing alternating layers of the POMA cation and polyanionic dopants such as poly(styrenesulfonate) and poly(vinylsulfonate) onto a glass substrate. This concept has been further developed with POMA by employing the anion of poly(3-thiopheneacetic acid) as the polyanionic dopant, giving novel self-

assembled films in which both the cationic and anionic components are electroactive polymers [170]

(c) Doping of EB with Lewis acids

Solutions of EB can be also readily doped with a range of metal salts and Lewis acids in a process reminiscent of the Brönsted acid doping of EB described above. In a fashion similar to protonic doping, binding of the metal ions to imine N sites on the EB chains is believed to occur, leading to conducting PANI products of the general type shown in equation–8. Considerable attention has been paid to the doping of EB with

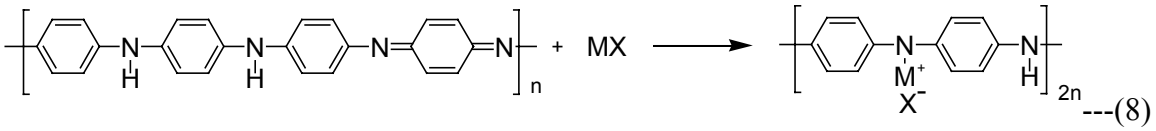

---(8)

LiCl and other lithium salts because of the significance to lithium ion rechargeable batteries [171]. The coordination of transition metal ions such as Zn(II) and Pd(II) to polyaniline N centers has also been described by several research groups [172].

Complexation (doping) of EB with classic Lewis bases such as $AlCl_3$, $GaCl_3$, $SnCl_4$ and $FeCl_3$ solubilizes PANI in acetonitrile and nitromethane, solvents that will not dissolve EB or its protonated PANI-HA emeraldine salts [173]. This improved solubility is attributed to metal doping at all the Pan basic sites, eliminating H-bonding between adjacent polymer chains that is one of the major contributors to poor PANI solubility.

(d) Doping of EB with organic electron acceptors

The doping of EB by a range of organic acceptors has also been reported by Kang et al. [174], producing charge transfer complexes with conductivities as high as 0.1 S/cm. On the basis of the maximum conductivity achieved, the complexing/doping ability of

the organic acceptors with EB decrease in the order: TCNE ~ *o*-chloranil > DDQ > *o*-bromanil > *p*-fluoranil > *p*-chloranil. With *o*-chloranil, X-ray photoelectron spectroscopic (XPS) studies show the formation of Cl^- ions and positively charged N centers on the PANI chains.

1.8.4. PANI as Chemical sensor

A great deal of polyaniline sensor research has been focused on changing the polymer structure to facilitate interaction between vapor molecules and polymer either by modifying the polymer backbone or the inter-chain connections. Since the conductivity of polyaniline depends on both its ability to transport charge carriers along the polymer backbone and for the carriers to hop between polymer chains [175], any interaction with polyaniline that alters either of these processes will affect its conductivity. This is the underlying chemical principle enabling polyaniline to be used as the selective layer in a chemical-vapor sensor, such as resistance type detectors known as chemiresistors. Due to their room temperature sensitivity, the ease of deposition onto a wide variety of substrates and the rich chemistry of structural modifications, polyaniline [176] as well as other conducting polymers [177] are becoming attractive materials for sensor applications.

PANI in its doped state can be controlled by acid/base reactions. This is widely used to detect acidic and basic gases. When exposed to ammonia gas, PANI undergo dedoping by deprotonation [178] leading to increase in resistance. The interaction PANI-ES with ammonia is shown in equation - 9.

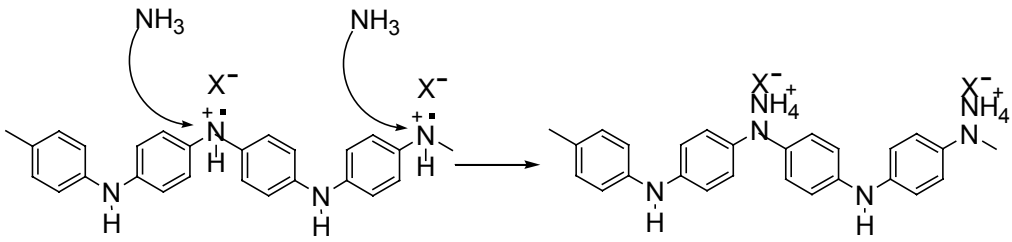

--------- (9)

The protons on –NH– groups were transferred to NH_3 molecules to form ammonium ions while PANI itself turned into its base form. This process is reversible, when ammonia atmosphere is removed, the ammonium ion can be decomposed to ammonia gas and proton.

PANI, when exposed to acidic gases such as HCl, H_2S and CO_2, PANI will be doped [179-181] giving rise to decrease in resistance. Weiller et al. reported that H_2 can be adsorbed on the positive charged nitrogen atoms of PANI, and then dissociate into hydrogen atoms. The formation of new N-H bonds between the hydrogen and nitrogen atom can reduce the resistance of PANI [182]. According to the results reported by Josowicz et al., partial charge transferring from conducting polymer leads to an alteration in the conductivity. The direction of partial electron transfer was determined by the electronegativity of the vapor and the work function of the polymer [183]. Some toxic gas, such as CO, doesn't undergo redox at room temperature. However, when PANI interacts with CO gas [184] a decrease in resistance of PANI film was observed. Furthermore, Densakulprasert et al. compared the UV-vis spectrums and XRD patterns of the film before and after exposing to CO, no discernable difference were found [185]. Thus, they speculated sensing mechanism as following: (equation –10)

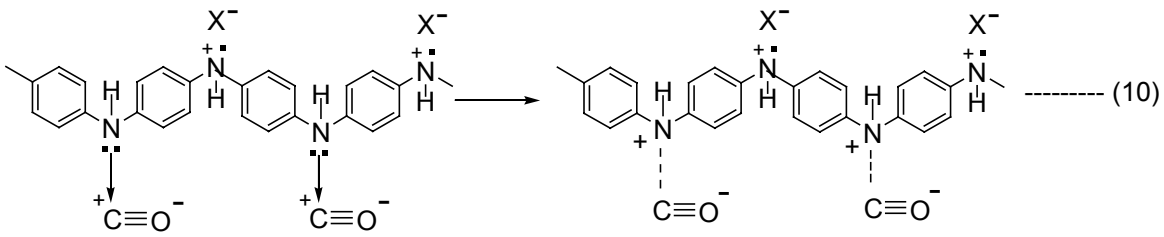

--------- (10)

The stable resonance structure of $^{+}C{\equiv}O^{-}$ with the positive charge at the carbon atom will withdraw a lone pair electron at the amine nitrogen. The positive charge at the carbon atom is transferred to amine nitrogen, which results in a net increase of positive charge carriers on the polymer backbones and therefore an increase in conductivity. The interaction between chlorinated hydrocarbon and PANI was also studied, and similar phenomena were observed [186].

In some cases, a catalyst incorporated in the conducting polymer film can help in detecting some inert analytes. Katre et al. prepared nanocomposite of Pd/PANI, and found its electrical resistance responses rapidly and reversibly in the presence of methanol [187]. They assumed that the effective positive charges on the imine nitrogen atoms were reduced by the methanol molecules in the presence of Pd nanoparticles: (equation-11)

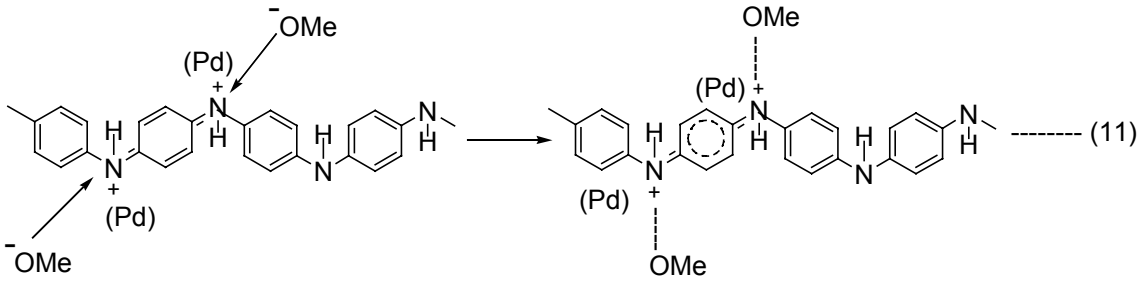

-------- (11)

Not only polymer chains but also the counter ions or the side chains may involve in the acid-base reaction. A decrease in resistance was found when acrylic acid doped PANI reacted with NH_3 [188]. The authors explained it as that the removal of protons from the free acrylic acid dopants by ammonia render free conduction sites in the polymer matrix. (equation – 12)

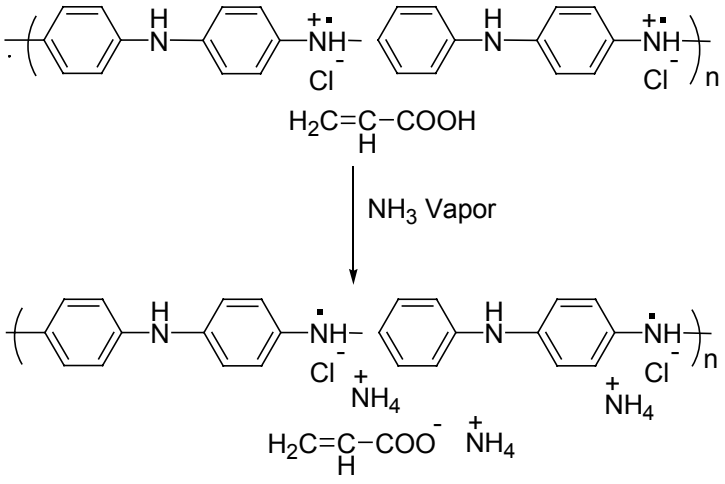

---------- (12)

The sensors fabricated from PANI with boronate groups showed poor reversibility for detecting ammonia, mainly due to ammonia reacted with boronate to form ion pairs [189]. Tan et al. investigated the interaction between methanol and PANI salt and base [190]. They found that the H-bonds in the two types PANI were different. In PANI base, one methanol molecule forms two H-bonds as a bridge between PANI chains. Twisting caused by these H-bonds localized the polarons and decrease the conductance of PANI.

Kulkarni et al [191] have studied the influence of the presence and the nature of substituents on aniline ring. The responses, under various alcohol vapors, of several

PANI substituted derivatives such as poly(*o*-toluidine), poly(*o*-anisidine), poly(*N*-methylaniline),poly(*N*-ethylaniline), poly(2,3-dimethylaniline), poly(2,5-dimethylaniline) and poly(diphenylamine) have been compared. It has been found that the layer resistance decreases in the presence of small chain alcohols (methanol, ethanol, propanol) and increases in the presence of butanol and heptanol vapors. The maximal sensitivity has been obtained for methanol irrespective of the layers. However, these sensors present high response times. Resistance alterations are explained on the basis of vapor-induced change of the polymer crystallinity. The extent of change is governed by the chain length of detected alcohol and by the value of its dielectric constant.

Agbor et al. [192] have studied the sensitivity of non-doped PANI layers. The tested gases are NO*x*, H_2S, SO_2, CO, and CH_4 diluted in N_2. Compared to N_2, the conductivity of all these sensors increases. The increase of PANI conductivity under H_2S is surprising since H_2S is a reducing gas and PANI, a p-type semiconductor. Similarly, few authors [193, 194] have observed a decrease in conductivity of PANI films when exposed to NO_2 gas and they have explained it based on the different protonated states of PANI used. It is well known that emeraldine salt has the greatest conductivity in the PANI family and its conductivity will decrease if its oxidation states becomes higher [195].

Collins and Buckley [196] have deposited PANI onto poly(ethylene terephtalate) or nylon threads which are then woven into a fabric mesh. The aim is to increase the sensitive surface in contact with the analyzed gas. But these layers have shown a detection limit in the ppm range for various pollutants including NH_3 and NO_2. Recently, a lot of research works deal with the use of a composite film with PANI as sensitive layer.

Hosseini and Entezami [197] have studied the response under various gases and organic vapors of layers made from PANI blends with polyvinyl acetate, polystyrene and polyvinyl chloride. Ogura et al. [198] have used a composite film of emeraldine base and polyvinyl alcohol to detect CO_2. The CO_2 adsorption leads to an increase of the film conductivity due to the incorporation of carbonate ions formed from CO_2 hydrolysis in the emeraldine base film. Matsuguchi et al. [199] have realized ammonia sensors based on PANI / polystyrene and PANI / polymethylmethacrylate (PMMA) blends.

El-Sherif and co-workers [200] have used a multi-mode optical fiber in which a small section of the original cladding material has been replaced by polyaniline or polypyrrole. The adsorption of gases or organic vapors results in refractive index and optical absorption fluctuations of the polymer, leading to an optical intensity modulation within the fiber. Results obtained in the case of HCl or NH_3 detection seem to be promising. Nicho and co-workers [201] have realized NH_3 sensors based on optical-transmittance changes of a PANI layer dip-coated onto PMMA and of a PANI/PMMA composite film spin-coated onto glass. The sensors work at room temperature and with a test wavelength of 632 nm. The PANI/PMMA composite sensor shows a better sensitivity with a detection limit lower than 10 ppm and a complete reversibility compared to the PANI layer dip-coated onto PMMA sensor. Compared to resistive sensors, these sensors have a lower response time.

The use of nanostructured polyaniline, such as nanowires, nanotubes, nanofibers, or nanorods, could greatly improve diffusion, since nanostructured polyanilines have much greater exposed surface area, as well as much greater penetration depth for gas molecules relative to their bulk counterparts. Since they have higher surface-to-volume

ratios due to their cylindrical morphology [202], the fibers should still outperform a thin film. The small diameter of the nanofibers (<100 nm) coupled with the possibility of gas approaching from all sides should give sensors with improved performance. However, few reports exist on nanostructured conducting polymer sensors [203] probably due to the lack of facile and reliable methods for making high quality conducting polymer nanostructures.

1.9. Phthalocyanine " a potential macrocycle"

Phthalocyanines (Pcs) have been one of the most widely studied class of organic functional material. The diverse functionality of the phthalocyanine macrocycle originates from its 18-π electron aromatic system which is closely related to that of the naturally occurring porphyrin ring [204]. The structure of phthalocyanine is shown in Fig. 1.13. In the last 20 years phthalocyanine chemistry is undergoing a renaissance, because

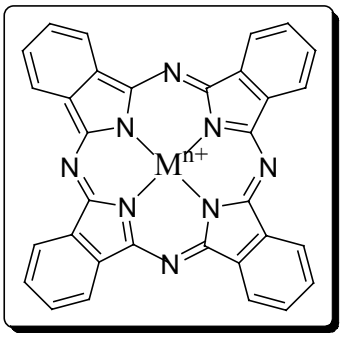

Fig.1.13. Structure of phthalocyanine macrocycle.

phthalocyanines and many of their derivatives exhibit unconventional physical properties interesting for application in material science. Thus, the interest of phthalocyanines, in

addition to the basic research, has been recently expanding into applied fields such as photovoltaics, electrochromism, liquid crystals, electrocatalyst, chemical sensors and photosensitizers for photodyanamic therapy and so on [205].

1.9.1. Synthesis of metal phthalocyanine

Most metal phthalocyanines can be prepared from phthalonitrile or phthalic anhydride and metal salts in high boiling solvents, such as 1-chloronaphthalene and quinoline. The synthesis of metal phthalocyanine is shown in Scheme-1. The use of phthalonitrile leads to clean reaction, where as phthalic anhydride is favoured in industry due to the cheap precursor. In both the reactions, metal ion acts as a template in forming the macrocycle. They are also obtained by metal insertion into the phthalocyanine. The

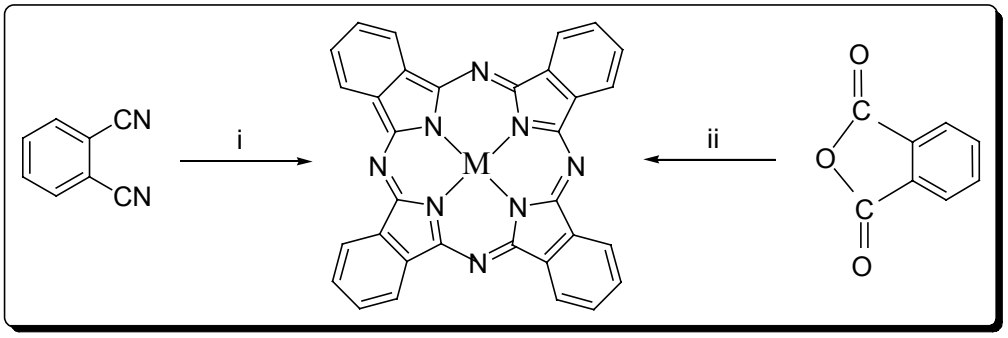

Scheme-1. The synthesis of phthalocyanine (Pc). Reagents and conditions: (i) metal or metal salt, heat; (ii) metal salt and nitrogen donor (e.g. urea), heat

phthalocyanine macrocycle (formally a Pc^{2-} anion) can hold almost 70 different metal ion in its central cavity and some transition metal ions (e.g. Cu^{2+} and Ni^{2+}) cannot be removed without the destruction of the macrocycle. However, metal-free Pc can be prepared by removal of labile metal ions such as Li^{2+} and Mg^{2+} after cyclotetramerization.

In order to exploit the interesting properties of Pc, precise control over the molecular packing and ordering in the solid phase is required. The Pc ring provides up to sixteen sites on the benzo group for a covalent attachment to a polymer and further two axial sites on the suitable metal ion held in the central cavity.

The combination of phthalocyanines with macromolecules is a powerful tool for designing new materials with outstanding properties. Phthalocyanines have been incorporated into polymers as side group, in the main chain and in a polymeric network [206]. The latter two approaches involve either polycyclotetramerization reactions of "bifunctional monomers" or the reaction of face-to-face tetra or disubstituted mononuclear phthalocyanine derivatives with another bifunctional compound [207]. In general, this type of polymer shows high electrical conductivities but they are insoluble in organic solvents, which makes difficult their processing. Pc derivatives which are substituted with flexible side chains form liquid crystals in which molecules self assemble into ordered columnar structures.

On the other hand, phthalocyanines can present several kinds of condensed phases such as single crystal, polycrystalline film, discotic liquid crystals and Langmuir Blodgett films. Thin film formulations have been playing an important role in incorporating Pcs into devices [208]. The LB technique has proved to be particularly useful for the fabrication of organized thin films of Pcs [209]. Other different techniques employed to form thin films with phthalocyanine derivatives are sublimation, chemical vapor deposition (CVD), molecular beam epitaxy (MBE), electrochemical deposition, spin coating, thin film casting, self assemble monolayers (SAMs) methodology, etc.

1.9.2. Electrical properties of phthalocyanine

The conducting properties of phthalocyanines have been a subject of a great interest for the few decades [210]. Cofacial stacking of phthalocyanine is necessary to achieve some supramolecular properties, for example, conductivity along main axis of the stacked system by electro-delocalization through coplanar macrocycles. Conductivity in metallophthalocyanine systems usually depends on the intrinsic properties of a particular kind of phthalocyanine, like bis(phthalocyaninato)lutetium (Pc_2Lu) and lithium phthalocyanine (PcLi), which are respectively typical narrow and broad band intrinsic molecular semiconductors and have been used for the preparation of devices such as field-efect transistors [211]. Phthalocyanines can also be readily doped by electron acceptors to give p-type columnar semiconductors.

Metallic conductivities close to 10^4 S/cm have been measured in ultra high pure iodinated nickel phthalocyanines [212]. Conductivities are also achieved in Pc-based polymers. Among the large variety of semiconducting polymers based on metallophthalocyanines, the most important families are the polyphthalocyanato-metalloxanes $[PcMO]_n$ (M = Si, Ge, Sn), studied in detail by Kenny and Marks [213, 214] and the self-assembled Pc coordination polymers $[PcM(L)]_n$, where L is the ligand, developed by Hanack using the so called "shish-kebab" approach [215]. The powder conductivies of some doped bridged phthalocyaninato transition metal complexes $[PcM(L)]_n$ are in the range of 10^{-5} – 10^{-1} S/cm. The polysiloxane backbone passes through the center of the rings, imposing a tight stacking of the Pc molecules that allow electrical conductivity due to orbital overlapping.

1.9.3. Phthalocyanine based gas sensors

Optical and electronic properties of phthalocyanines are known to be sensitive to the presence of foreign gases. The electrical conductivity is chosen as one of the most commonly used parameters to detect a gas, since this provides a ready method of interfacing the front end sensing element into a processor- based electronic instrumentation system for data analysis. The application of phthalocyanines as gas sensors arises due to their planar aromatic ring system with high chemical and thermal stability. The gas sensing is thought to occur though the charge transfer interaction in which the gas molecule to be detected acts as a planar π-electron acceptor forming a redox couple, and the positive charge produced is delocalized over the phthalocyanine ring causing the increase of the conductivity. It has been observed that acceptor gases such as oxygen, nitric oxide, and nitrogen dioxide cause an increase in phthalocyanine conductivities, a decrease in the activation energies, and the appearance of charge transfer bands in the visible spectra [216]. On the other hand, a donor gas such as ammonia causes a decrease in conductivity and reverses the effect of the acceptor gases. On the basis of the general response to donor and acceptor gases, phthalocyanines have been classified as *p*-type semiconductors.

In its simplest form, a phthalocyanine sensor consists of a planar interdigitated electrode coated with a thin phthalocyanine film which is termed as a chemiresistor, since phthalocyanines are generally weak conducting materials (e.g., 10^{-10} S/cm) the interdigitated electrode geometry is used because it can make possible the measurement of very small currents [217].

A critical operation in the construction of a sensor is the physical deposition of the phthalocyanine film onto the electronic substrate. The most commonly used techniques are vacuum sublimation and Langmuir- Blodgett (LB) methods. It is required that the deposition process provide films with reproducible electronic and vapor response characteristics. The resulting sensor device performance is evaluated in terms of (1) sensitivity range, (2) specificity, (3) reversibility, response times, and recovery rates, and (4) stability.

In vacuum sublimation, obtaining reproducible films is sometimes difficult and may require careful attention to sublimation conditions, phthalocyanine purity, and substrate cleanliness. The morphology of the phthalocyanine films is variable and strongly dependent on the sublimation conditions. It ranges from amorphous to highly crystalline. Compared with the vacuum sublimation, the LB technique offers excellent control over film thickness, uniformity and reproducibility, and is very compatible with microelectronics technology, The LB film phthalocyanine gas sensors show better performance than sensors made from vacuum sublimation, giving fast response and recovery, and good reversibility, because of the thinness and uniformity of the film.

1.9.3.1. Gas sensing mechanism

Much effort has been directed to the study of the phthalocyanine gas sensing mechanism. It is commonly observed that the sensor responses to the incoming gas show two stages of conductivity changes, an initial fast change followed by a slow drift to a steady-state value. It was suggested that the fast process is due to the surface adsorption of gas molecules and the slow process is due to the bulk diffusion of gas molecules into the film [218]. Since the sensor measurement electrodes are only in contact with the

bottom face of the sensing film, the permeation of the gas into the bulk of the film appears to be necessary for maximum response. Thus there still lacks a complete picture to describe the gas sensing mechanism.

1.9.3.2. The effect of phthalocyanine morphology on gas sensor performance

The phthalocyanine film crystal structure and morphology play an important role in the film's electrical response to gas exposure. The morphology must accommodate both +ve charge transfer process and charge carrier transport. The carrier transport is facilitated by a long-range stacking of cofacially oriented phthalocyanine rings. The film crystal structure are important determinants of how gas molecules can enter the lattice and interact with the phthalocyanine units. For most of the metal phthalocyanine films prepared by vacuum sublimation, several crytalline polymorphs exist, including the α, β, γ and δ structures. The α and β structures are the most common ones and have been studied in detail. Energetically, the β phase is more stable than a phase. Therefore the stable β -form phthalocyanine film is preferred for gas sensors application. For a particular crystalline form, the crystallite size and orientation in a thin film can affect a sensor's response to gases. It has been reported [219] that for a Pc single crystal, the conductivity change induced by NO_2 exposure is a surface and not a bulk. It is suggested that any bulk diffusion of NO_2 into the single crystal must occur so slowly that this effect can be negligible. The effect of heat treatment on gas sensing properties of phthalocyanine films has been studied extensively [220]. It was observed that the crystallite size increased with annealing temperature up to about 330°C, giving the sensor performance with smaller conductivity change, but fast response and recover time. The

second stage of conductivity change was reduced and the steady state was reached more rapidly.

Finally, substituted phthalocyanines, metal tetra-tertiarybutylphthalocyanines were vacuum sublimated and tested as a sensing film to NO_2 gas [221]. Higher resistivity and faster response and recovery were obtained, compared to the un-substituted Pc film, which could originate from the wider space for each stack and faster gas diffusion in the substituted Pc film.

1.10. Aim and Scope of the present investigation

Conducting polymer based chemiresistor are of increasing importance in the field of gas sensing, due to their ease of fabrication and ability to operate at room temperature. There are materials which are responsive to a wide variety of chemicals but are generally low on sensitivity and selectivity. Although conducting polymers have potential applications in gas sensors, further functionalization of such polymers will lead to new / better applications as well as enhancement of existing properties. Hence, detailed studies have been carried out towards the goal of developing new conjugated polyaniline with functional molecules that can have better sensitivity and selectivity. On the other hand, phthalocyanines also are sensitive to gases and chemical vapours but to fabricate sensors from these materials requires tedious physical vapour deposition technique involving expensive equipment. Further, undoped phthalocyanines have very high electrical resistivity ($>10^6$ ohm-cm). Hence, it was thought to incorporate these in conducting polymers so as to obtain lower resistivity material.

There are many functional molecules exhibiting special properties such as electrochromism, photochromism, chemiluminescence, catalysis, molecular recognition, etc. Among them, matallophthalocyanines have been one of the most studied class of organic functional materials. The diverse functionality of the phthalocyanine (Pc) macrocycle originates from its 18-π electron system which is closely related to that of the naturally occurring porphyrin ring. The incorporation of transition metal complexes like phthalocyanine into the conducting polymer framework especially has the potential to greatly expand the function and applications of polyaniline systems; more particularly, for molecular recognition and detection of very low concentration of analyte.

Hence, it was decided to have polyaniline whose matrix can be incorporated with functional molecule that can give better sensitivity and selectivity to specific gas. Compared to un-substituted parent metal phthalocyanines, peripherally substituted phthalocyanines are finding applications in the above said fields due to their ease of solubility in aqueous medium, better and uniform incorporation into the matrix. With the possibility of immobilizing the water soluble sulfonated metal phthalocyanines onto the polyaniline matrix, it can become an interesting material for gas sensing application, as phthalocyanines are known for their change in physico chemical properties upon coming in contact with foreign species. Many properties of the phthalocyanine can be varied by changing the central metal atom or by substituting groups at the periphery of the phthalocyanine macrocycle. For example, its redox properties can be varied and the sensing effect can be changed, by replacing central metal atom or the solubility can be increased, by attaching side groups. Hence, in the present investigation, the emeraldine salt form of conducting polyaniline was modified both chemically and electrochemically

by tetra sulfonated metal phthalocyanine as co-dopant. The phthalocyanine functionalized polyaniline was characterized by various physico chemical techniques like IR, UV, XRD. In order to investigate the effect of central metal atom towards NO_2 gas sensing, the polyaniline was functionalized with sulfonated phthalocyanine that carries different metal ion under identical macrocyclic frame work. The various physico chemical properties emerged from these functionalized conducting polymer prepared under chemical and electrochemical routes were compared and compiled at the end of this thesis.

1.11. References

[1] H. Shirakawa, E. J. Louis, A. G. MacDiarmid, C. K. Chiang and A. J. Heeger, J. Chem. Soc. Chem. Com., 16 (1977) 578.

[2] S. Lefrant, L. S. Lichtman, M. Temkin, D. C. Fichten, D. C. Miller and G. E. Whitwell, Solid. State. Com., 29 (1979) 191.

[3] H. Shirakawa, Angew. Chem. Int. Ed., 40 (2001) 2574.

[4] A. G. MacDiarmid, Angew. Chem. Int. Ed., 40 (2001) 2581.

[5] A. J. Heeger, Angew. Chem. Int. Ed., 40 (2001) 2591.

[6] J. H. Schon, A. Dodabalapur, Z. Bao, Ch. Kloc, G. Schenker and B. Batlogg, Nature., 410, (2001) 189.

[7] R. L. Greene, B. R. Street and L. J. Suter, Phys. Rev. Lett., 34 (1975) 577.

[8] A. F. Diaz and K.K. Kanazawa, in Extended Linear Chain Compounds, Vol.3, Ed. J. S. Miller, Plenum Publishing Corporation, 1983.

[9] G. Tourillon and F. Garnier, J. Electroanal. Chem., 135 (1982), 173.

[10] D. M. Ivory, G. G. Miller, J. M. Sowa, L. W. Shacklette, R. R. Chance and R. H. Baughman, J. Chem. Phys., 71 (1979) 1506.

[11] J. F. Rabolt, T. C. Clarke, K. K. Kanazawa, J. R. Reynolds and G. B. Street, J. Chem. Soc., Chem. Commun., (1980) 347.

[12] A. F. Diaz and J. A. Logan, J. Electroanal. Chem., 111 (1980) 111.

[13] S. K. Bhattacharya, Ed.; Metal-Filled Polymers: Properties and Applications; Marcel Dekker: New York, 1986.

[14] O. Olabisi, in Handbook of Thermoplastics, Marcel Dekker, New York, (1977).

[15] B. Scrosati, Ed. Application of Electroactive Polymers; Chapman and Hall: London,

(1993).

[16] F. Croce, G. B. Appetecchi, L. Persi, B. Scrosati, Nature., 394 (1998) 456.

[17] J. D. Stenger-smith, Prog. Polym. Sci., 23 (1998) 57.

[18] N. Gospodinova and L. Terlemezyan, Prog. Polym. Sci., 23 (1998) 1443.

[19] F. Gutmann and L. E. Lyons, Organic semiconductors, John wiley, New York, 1967.

[20] S. Pekker and A. Janossy, in Handbook of Conducting Polymers, T. A. Skotheim, ed.), Vol-1, Marcel Dekker, New York, (1986).

[21] J. L. Bredas and G. B. Street, Acc. Chem. Res., 18 (1985) 309.

[22] C. K. Chiang, M. A. Druy, S. C. Gau, A. J. Heeger, E. Louis, A. G. MacDiarmid and Y. W. Park, J. Am. Chem. Soc., 100 (1978) 1013.

[23] J. Tanguy, Synth. Met., 43, (1991) 2991.

[24] E. M. Genies and M. Lapkowski, J. Electroanal. Chem., 220, (1987) 67.

[25] A. J. Heeger, S. Kivelson, J. R. Schrieffer and W. P. Su, Rev. Mod. Phys., 60 (1988) 781.

[26] F. Garnier, R. Hajlaoui, A. Yasser and P. Srivastava, Science., 265 (1994) 1684.

[27] J. H. Schon, A. Dodabalapur, Z. Bao, Ch. Kloc, G. Schenker and B. Batlogg, Nature., 410, (2001) 189.

[28]. A. G. MacDiarmid and A. J. Epstein, Synth. Met., 65 (1994) 103.

[29] L. M. Huang, C. H. Chen, T. C. Wen and A. Gopalan, Electrochimica. Acta., 51 (2006) 2756.

[30] J. M. Ginder, A. J. Epstein, Phys. Rev., B 41 (1990) 10674.

[31] F. Devreux, F. Genoud, M. Nechtschein and B. Villeret, Springer. Ser. Solid-state. Sci., 76 (1987) 270.

[32] W. P. Su, J. R. Schrieffer and A. J. Heeger, Phys. Rev. Lett., 42 (1979) 1698.

[33] M. Peo, S. Roth, K. Dransfeld, B. Tieke, J. Hocker, H. Gross, A. Grupp and H. Sixl, Solid State Commun., 35 (1980) 119.

[34] J. L. Bre´das, J. C. Scott, K. Yakushi and G. B. Street, Phys. Rev., B 30 (1984) 1023.

[35] J. L. Bredas, R. R. Chance and R. Silbey, Mol. Cryst. Liq. Cryst., 77 (1982) 319.

[36] F. Genoud, M. Guglielmi, M. Nechtschein, E. Genies and M. Samon, Phys. Rev. Lett., 55 (1985) 18.

[37] N. F. Mott and E. A. Davis, "Electronic Process in Non-crystalline Materials", Clarendon Press, Oxford (1979).

[38] J. C. Thieblemont, M. F. Planche, C. Petrescu, J. M. Bouvier and G. Bidan, Synth. Met., 59 (1993) 81.

[39] R. V.Gregory, W. Kimbrell and H. H. Kuhn, Synth. Met., 8 (1989) C823.

[40] H. H. Jun and A. D.Child, In Handbook of Conducting Polymers, T. A. Skothein, R. L. Elsenbaumer, J. R. Reynolds, Eds., 2nd Ed, pp.993, Marcel Dekker, New York, (1998).

[41] P. R. Newman and P. H. Cunninham, US patent, 4,942,078.

[42] L.Olmedo, P. Hourquebie and F. Jousse, in Handbook of organic conductive molecules and polymers, H. S. Nalwa (Ed), vol.3. pp. 367, Wiley, (1997).

[43] S. Jasty and A. J. Epstein, Polym. Mat. Sci. Eng., 72 (1995) 565.

[44] A. J. Epstein, J. Joo, C.-Y. Wu, A. Benatar, C. F. Jr. Faisst, J. Zegarski, and A. G. MacDiarmid, in Intrinsically Conducting Polymers: An Emerging

Technology; Aldissi, M., Ed.; pp. 165, Kluwer Academic Publishers, Netherlands, (1993).

[45] B. Sorosati, Ed., Application of Electroactive Polymers, Chapman and Hall: London, 1993.

[46] P. Go´mez-Romero, Adv. Mat., 13 (2001) 163.

[47] A. Hugo-Le-Goff, in Handbook of organic conductive molecules and polymers, H. S. Nalwa (Ed), vol.3. pp. 745, Wiley, (1997).

[48] R. H. Friend and N. C. Greenham, in Handbook of Conducting Polymers, T. A. Skothein, R. L. Elsenbaumer, J. R. Reynolds, Eds., 2nd Ed, pp.823, Marcel Dekker, New York, (1998).

[49] A. Kraft, A. C. Grimsdale and A. B. Holmes, Angew. Chem. Int. Engl. Ed., 7 (1998) 403.

[50] N. S. Sariciftci, D. Braun, C. Zhang, V. Srdanov, A. J. Heeger, G. Stucky and F. Wudl, Appl. Phys. Lett., 62 (1993) 585.

[51] G. Yu, J. Gao, J. C. Hummelen and A. J. Heeger, Science., 270 (1995) 1789.

[52] H. Fuchigami, A. Tsumura and H. Koezuka, Appl. Phys. Lett., 63 (1993) 1372.

[53] H. Sirringhaus, N. Tessler and R. H. Friend,. Science., 280 (1998) 1741.

[54] J. J. Miasik, A. Hooper and B. C.Tofield, J. Chem. Soc., Faraday Trans., 1, 82 (1986) 1117.

[55] T. Hanawa, S. Kuwabata and H. Yoneyama, J. Chem. Soc., Faraday Trans., 1, 84 (1988) 1587.

[56] H. Kori-Youssou, M. Hmyene, F. Garnier and D. Delabouglise, J. Chem. Soc., Chem. Commun., (1993) 1550.

[57] G. Zotti, G. Schiavon, S. Zecchin, A. Berlin, A. Canavesi and G. Pagani, Synth. Met., 84 (1997) 239.

[58] C. J. Pickett and K. S. Ryder, J. Chem. Soc., Dalton Trans., (1994) 2128.

[59] S. Cosnier, M. Fontecave, D. Limosin and V. Niviere, Anal. Chem., 69 (1997) 3095.

[60] G. Bidan and M. Guglielmi, Synth. Met., 15 (1986) 49.

[61] G. Zotti, S. Martina, G. Wegner and A. D. Schluter, Adv. Mater., 4 (1992) 798.

[62] A. Deronzier and J-C. Moutet, Acc. Chem. Res., 22 (1989) 249.

[63] A. Deronzier and J-C. Moutet, Coord. Chem. Rev., 147 (1996) 339.

[64] D Curran, J Grimshaw and S D Perera, Chem Soc Rev., 20 (1992) 391.

[65] R. L. Elsenbaumer, H. Eckhardt, Z. Iqbal, J. Toth and R. H. Baughman, Mol. Cryst. Liq. Cryst., 118 (1985) 111.

[66] M J. Marsella, R. J. Newland, P. J. Carroll and T. M. Swager, J. Am. Chem. Soc., 117 (1995) 9842.

[67] M. Schaferling and P. Bauerle, J. Mater. Chem. , 14(2004) 1132.

[68] B. J. Holliday and T. M. Swager , Chem. Commun., (2005) 23.

[69] Y. Chen, C. T. Imrie, J. M. Cooper, A. Glidle, D. G. Morris and K. S. Ryder, Polym. Int., 47 (1998) 43.

[70] W. ten Hoeve, H. Wynberg, E. E. Havinga and E. W. Meijer, J. Am. Chem. Soc., 113 (1991) 5887.

[71] L. Groenendaal, M. J. Bruining, E. H. J. Hendrickx, A. Persoons, J. A. J. M. Vekemans, E. E. Havinga and E. W. Meijer, Chem. Mater., 10 (1998) 226.

[72] J. P. Ferraris and M. D. Newton, Polymer., 32 (1992) 391.

[73] C. Nylabder, M. Armgrath and I. Lundstrom, Proceedings of the International

Meeting on Chemical Sensors, Fukuoka, Japan, (1983) 203.

[74] G. W. Lu, L. T. Qu, G. Q. Shi, Electrochim. Acta., 51 (2005) 340.

[75] J. Reemts, J. Parisi, and D. Schlettwein, Thin Solid Films., 466 (2004) 320.

[76] A. A. Athawale and M. V. Kulkarni, Sens. Actuators B., 67 (2000) 173.

[77] V. C. Nguyen, K. Potje-Kamloth, Thin Solid Films., 338 (1999) 142.

[78] C. N. Van, K. Potje-Kamloth, Thin Solid Films., 392 (2001) 113.

[79] D. Xie, Y. D. Jiang, W. Pan, D. Li, Z. M. Wu and Y.R. Li, Sens. Actuators B., 81 (2002) 158.

[80] S. V. Mello, P. Dynarowicz-Latka, A. Dhanabalan, R. F. Bianchi, R. Onmori, R. A. J. Janssen and O. N. Oliveira, Colloid Surf. A-Physicochem. Eng. Asp., 198 (2002) 45.

[81] N. V. Bhat, A. P.Gadre, V. A. Bambole, J. Appl. Polym. Sci., 88 (2003) 22.

[82] K. H. An, S. Y. Jeong, H. R. Hwang and Y. H. Lee, Adv. Mater., 16 (2004) 1005.

[83] G. F. Li, M. Josowicz, J. Janata and S. Semancik, Appl. Phys. Lett., 85 (2004) 1187.

[84] J. Elizalde-Torres, H. L. Hu and Garcia-Valenzuela, Sens. Actuators B., 98 (2004) 218.

[85] M. K. Ram, O. Yavuz and M.Aldissi, Synth. Met., 151 (2005) 77.

[86] N. V. Bhat, A. P. Gadre and V. A. Bambole, J. Appl. Polym. Sci., 80 (2001) 2511.

[87] V. Saxena, S. Choudhury, S. C. Gadkari, S. K. Gupta and J.V.Yakhmi, Sens. Actuators B., 107 (2005) 277.

[88] E. Krivan, C. Visy, R. Dobay, G. Harsanyi and O.Berkesi, Electroanalysis., 12 (2000) 1195.

[89] L. Geng, S. R. Wang, Y. Q. Zhao, P. Li, S. M. Zhang, W. P. Huang and S. H. Wu,

Mater. Chem. Phys., 99 (2006) 15.

[90] G. Gustafsson, I. Lundrom, B. Liedberg, C. R. Wu, O. Inganas and O. Wennerstom, Synth. Met., 31 (1989) 163.

[91] N. Guernion, R. J. Ewen, K. Pihlainen, N. M. Ratcliffe and G. C. Teare, Synth. Met., 126 (2002) 301.

[92] F. Mohammad, J. Phys. D: Appl. Phys., 31 (1998) 951.

[93] P. C. Ewbank, R. S. Loewe, L. Zhai and J. Reddinger, G. Sauve and R. D. McCullough, Tetrahedron., 60 (2004) 11269.

[94] Z. P. Deng, D. C. Stone and M. Thompson, Analyst., 122 (1997) 1129.

[95] Z. K. Chen, S. C. Ng, S. F. Y. Li, L. Zhong, L. G. Xu and H. S. O. Chan, Synth. Met., 87 (1997) 201.

[96] G. Appel, R. Mikalo, K. Henkel, A. Oprea, A. Yfantis, I. Paloumpa and D. Schmeisser, Solid-State Electron., 44 (2000) 855.

[97] S. Rizzo, F. Sannicolo, T. Benincori, G. Schiavon, S. Zecchin and G. Zotti, J. Mater. Chem. 14 (2004) 1804.

[98] A. Mirmohseni and K. Rostamizadeh, Sensors., 6 (2006) 324.

[99] L. Torsi, M. C. Tanese, N. Cioffi, M. C. Gallazzi, L. Sabbatini and P. G. Zambonin, Sens. Actuators B., 98 (2004) 204.

[100] E. Segal, R. Tchoudakov, M. Narkis and A. Siegmann, Polym. Eng. Sci., 42 (2002) 2430.

[101] E. Segal, R. Tchoudakov, M. Narkis, A. Siegmann and Y.Wei, Sens. Actuators B., 104 (2005) 140.

[102] L. Ruangchuay, A. Sirivat and J.Schwank, Talanta., 60 (2003) 25.

[103] I. Matsubara, K. Hosono, N. Murayama, W. Shin and N. Izu, Bull. Chem. Soc. Jpn., 77 (2004) 1231.

[104] K. Hosono, I. Matsubara, N. Murayama, W. Shin and N. Izu, Thin Solid Films 484 (2005) 396.

[105] L. Torsi, A. Tafuri, N. Cioffi, M. C. Gallazzi, A. Sassella, L. Sabbatini and P.G. Zambonin, Sens. Actuators B., 93 (2003) 257.

[106] L. Ruangchuay, A. Sirivat, J. Schwank, Synth. Met., 140 (2004) 15.

[107] B. P. J. D. Costello, N. M. Ratcliffe, P. S. Sivanand, Synth. Met., 139 (2003) 43.

[108] V. Svetlicic, A. J. Schmidt and L. L. Miller, Chem. Mater., 10 (1998) 3305.

[109] B. Li, G. Sauve, M. C. Iovu, M. Jeffries-El, R. Zhang, J. Cooper, S. Santhanam, L. Schultz, J. C. Revelli, A. G. Kusne, T. Kowalewski, J. L. Snyder, L. E. Weiss, G. K. Fedder, R. D. McCullough and D. N. Lambeth, Nano Lett., 6 (2006) 1598.

[110] L.Torsi, M. C. Tanese, N. Cioffi, M. C. Gallazzi, L. Sabbatini, P. G. Zambonin, G. Raos, S. V. Meille and M. M. Giangregorio, J. Phys. Chem. B., 107 (2003) 7589.

[111] V. V. Chabukswar, S. Pethkar and A. A. Athawale, Sens. Actuators B., 77 (2001) 657.

[112] N. Guernion, B. P. J. D. Costello and N. M. Ratcliffe, Synth. Met., 128 (2002) 139.

[113] J. E. G. de Souza, F. L. dos Santos, B. Barros-Neto, C. G. dos Santos and C. P. de Melo, Synth. Met., 119 (2001) 383.

[114] K. Ogura, T. Saino, M. Nakayama and H. J. Shiigi, Mater. Chem., 7 (1997) 2363.

[115] E. Segal, R. Tchoudakov, M. Narkis, A. Siegmann and Y. Wei, Sens. Actuators B., 104 (2005) 140.

[116] E. Milella, F. Musio and M. B Alba, Thin Solid Films., 285 (1996) 908.

[117] E. Stussi, R. Stella and D. De Rossi, Sens. Actuators B., 43 (1997) 180.

[118] J. Huang, S. Virji, B. H. Weiller and R. B. Kaner, Chem. Eur. J., 10 (2004) 1315.

[119] D. Xie, Y. D. Jiang, W. Pan, D. Li, Z. M. Wu and Y. R. Li, Sens. Actuators B., 81 (2002) 158.

[120] J. H. Cho, J. B.Yu, J. S. Kim, S. O. Sohn, D. D. Lee and J. S. Huh, Sens. Actuators B 108 (2005) 389.

[121] N. T. Kemp, A. B. Kaiser, H. J. Trodahl, B. Chapman, R. G. Buckley, A. C. Partridge and P. J. S. Foot, J. Polym. Sci. B., 44 (2006) 1331.

[122] M. Matsuguchi, J. Io, G. Sugiyama and Y. Sakai, Synth. Met., 128 (2002) 15.

[123] L. Torsi, M. Pezzuto, P. Siciliano, R. Rella, L. Sabbatini, L. Valli and P.G. Zambonin, Sens. Actuators B., 48 (1998) 362.

[124] C. Conn, S. Sestak, A. T. Baker and J. Unsworth, Electroanalysis., 10 (1998) 1137

[125] R. A. Bissell, K. C. Persaud, and P. Travers, Phys. Chem. Chem. Phys., 4 (2002) 3482.

[126] H. Letheby, J. Am. Chem. Soc., 15 (1862) 161.

[127] E. T. Kang, K. G. Neoh and K. L. Tan, Prog. Polym. Sci., 23 (1998) 211.

[128] Wu-Song Huang, Alan G. MacDiarmid, and Arthur J. Epsteinb J. Chem. Soc., Chem. Commun., (1987) 1784

[129] J. C. Chiang and A. G. MacDiarmid, Synth. Met., 13 (1986) 193.

[130] A. G. MacDiarmid, J. C. Chiang and A. F.Richter, Synth. Met., 18 (1987) 317.

[131] A. G. MacDiarmid, J. C. Chiang, M. Halpern, W. S. Huang, S. L. Mu, N. L. D. Somasiri, W. Wu and S. I. Yaniger, Mol. Cryst., Liq. Cryst., 121 (1985) 173.

[132] E. M. Genies, C. Tsintavis and A. A. Syed, Mol. Cryst., Liq. Cryst., 121 (1985) 181.

[133] R. L. Hand and R. F. Nelson, J. Electrochem. Soc., 125 (1978) 1059.

[134] H. A. Pohl and E. H. Engelhardt, J. Phys. Chem., 66 (1962) 2085.

[135] A. G. MacDiarmid, N. L. D. Somasiri, W. R. Salaneck, I. LundstrSrn, B. Liedberg, M. A. Hasan, R. Erlandsson and P. Konrasson, Springer Series in Solid State Sciences, Vol.63, pp. 218, Springer, Berlin, 1985.

[136] R. L. Hand and R. F. Nelson, J. Am. Chem. Soc., 96 (1974) 850.

[137] E. M. Genies, C. Tsintavis and A. A. Syed, Ft. Patent No. EN 8 307958 (1983); U.S. Patent No. 698 183 (1985).

[138] Y. Cao, A. Andreatta, A. J. Heeger and P. Smith, Polymer., 30 (1989) 2305.

[139] J. Stejskal, R. G. Gilbert , Pure Appl. Chem., 74 (2002) 857.

[140] Y. Wei, X. Tang, Y. Sun and W. W. Focke, J. Polym. Sci.: Part A.: Polym. Chem., 27, (1985) 2385.

[141] A. G. MacDiarmid, J. C. Chiang, W. Huang, B. D. Humphrey, and N. L. D. Somasiri, Mol. Clyst. Liq. Cryst., 125 (1985) 309.

[142] E. M. Genies and C. Tsintavis, J. Eleciroanal. Chem., 195 (1985) 109.

[143] E. M. Genies and C. Tsintavis, J. Electroanal. Chem., 200 (1986) 127.

[144] D. M. Mohilner, R. N. Adams and W. J. Argersinger, J. Am. Chem. Soc., 84 (1962) 3618.

[145] J. Bacon and R. N. Adams, J. Am. Chem. Soc., 90 (1968) 6596.

[146] G. Mengoli, M. T. Munari, P. Bianco and M. M. Musiani, J. Appl. Polym. Sci., 26 (1981) 4247.

[147] G. Mengoli, M. T. Munari and C. Folonari, J. Electroanal. Chem., 124 (1981) 237.

[148] E. M. Genies and M. Lapkowski, Synth. Met., 24 (1988) 61.

[149] E. W. Paul, A. J. Ricco and M. S. Wrighton, J. Phys. Chem., 89 (1981) 1441.

[150] C. M. Carlin, L. J. Kepley and A. J. Bard, J. Electrochem. Soc., 132 (1985) 353.

[151] R. L. Hand and R. F. Nelson, J. Electrochem. Soc., 125 (1978) 1059.

[152] A. Thyssen, A. Hochfeld, R. Kessel, A. Meyer and J. W. Schulzte, Synth. Met., 29 (1989) E357.

[153] E. M. Genies and C. Tsintavis, J. Eleciroanal. Chem., 195 (1985) 109.

[154] G. D'Aprano, M. Leclerc, G. Zotti and G. Schiavon, Chem. Mater., 7 (1995) 33.

[155] L. H. Dao, J. Y. Bergeron, J. W. Chevalier, M. T. Nguyen and R. Paynter, Synth. Met., 41 (1991) 655.

[156] E. T. Kang, K. G. Neoh, K. L. Tan and H. K. Wong, Synth. Met., 48 (1992) 231.

[157] J. Yue, Z. H. Wang, K. R. Cromack, A. J. Epstein and A. G. MacDiarmid, J. Am. Chem. Soc., 113 (1991) 2665.

[158] H. S. O. Chan, A. J. Neuendorf, S. C. Ng, P. M. L Wong and D. J. Young, J.Chem. Soc., Chem. Commun., (1998)1327.

[159] S. Shimizu, T. Saitoh, M. Yuasa, K. Yano, T. Maruyama and K. Watanabe, Synth. Met., 85 (1997) 1337.

[160] C. DeArmitt, C. P. Armes, J. Winter, F. A. Uribe, J. Gottesfeld and C.Mombourquette, Polymer., 34 (1993) 158.

[161] M. T. Nguyen, P. Kasai, J. L. Miller and A. F. Diaz, Macromolecules., 27 (1994) 3625.

[162] X.-L. Wei, Y.Z. Wang, S.M. Long, C. Bobeczko and A.J. Epstein, J. Am. Chem. Soc., 118 (1996) 2545.

[163] C. C. Han, W. D. Hseih, J.-Y. Yeh and S.-P. Hong, Chem. Mater., 11 (1999) 480.

[164] S.-A. Chen and G.-W. Hwang, J. Am. Chem. Soc., 117 (1995) 10055.

[165] D. A. Reece, L. A. P. Kane-Maguire and G. G. Wallace, Synth. Met., 119 (2001) 101.

[166] E. Shoji and M. S. Freund, Langmuir., 17 (2001) 7183.

[167] Y., Cao, P. Smith and A.J. Heeger, Synth. Met., 48 (1992) 91.

[168] Y.H. Geng, Z. C. Sun, J. Li, X. B. Jing, X. H. Wang and F. S. Wang, Polymer., 40 (1999) 5723.

[169] L. H. C. Mattoso, V. Zucolotto, L. G. Patterno, R. V. Griethuijsen, M. Ferreira, S. P. Campana and O. N. Oliveira, Synth. Met., 71 (1995) 2.

[170] S. V. Mello, E. C. Pereira and O. N. Oliveira, Synth. Met., 102 (1999) 1204.

[171] A. V. Saprigin, K. R. Brenneman, W. P. Lee, S. M. Long, R. S. Kohlman and A. J. Epstein, Synth. Met., 100 (1999) 55.

[172] J. Ruokolainen, H. Eerikainen, M. Torkkeli, R. Serimaa, M. Jussila and O. Ikkala, Macromolecules., 33 (2000) 9272.

[173] F. Genoud, I. Kulszewicz-Bajer, A. Bedel, J. L. Oddou, C. Jeandey and A. Pron, Chem. Mater., 12 (2000) 744.

[174] E. T. Kang, K G.,Neoh, T. C., Tan, S. H. Khor and K. L. Tan, Macromolecules., 23 (1990) 2918.

[175] A. G. MacDiarmid, Synth. Met., 125 (2001) 11.

[176] G. G. Wallace, M. Smyth and H. Zhao, Trends. Anal. Chem., 18 (1999) 245.

[177] D. T. McQuade, A. E. Pullen and T. M. Swager, Chem. Rev., 100 (2000) 2537.

[178] K. H. Hong, K. W. Oh and T. J. J. Kang, Appl. Polym. Sci., 92 (2004) 37.

[179] S. Virji, J. X. Huang, R. B. Kaner and B. H. Weiller, Nano Lett., 4 (2004) 491.

[180] Q. L. Hao, X. Wang, L. D. Lu, X. J. Yang and V. M. Mirsky, Macromol. Rapid Commun., 26 (2005) 1099.

[181] K. Ogura and H. Shiigi, Electrochem. Solid State Lett., 2 (1999) 478.

[182] S. Virji, R. B. Kaner and B. H. Weiller, J. Phys. Chem. B., 110 (2006) 22266.

[183] D. Blackwood and M. Josowicz, J. Phys. Chem., 95 (1991) 493.

[184] V. Dixit, S. C. K. Misra and B. S. Sharma, Sens. Actuators B., 104 (2005) 90.

[185] N. Densakulprasert, L. Wannatong, D. Chotpattananont, P. Hiamtup, A. Sirivat and J. Schwank, Mater. Sci. Eng. B-Solid State Mater. Adv. Tech., 117 (2005) 276.

[186] G. Anitha and E. Subramanian, Sens. Actuators B., 107 (2005) 605.

[187] A. A. Athawale, S. V. Bhagwat and P.P. Katre, Sens. Actuators B., 114 (2006) 263.

[188] V. V. Chabukswar, S. Pethkar and A.A. Athawale, Sens. Actuators B., 77 (2001) 657.

[189] J. T. English, B. A. Deore and M. S. Freund, Sens. Actuators B., 115 (2006) 666.

[190] C. K. Tan and D. J. Blackwood, Sens. Actuators B., 71 (2000) 184.

[191] A. A. Athawale and M. V. Kulkarni, Sens. Actuators B., 67 (2000) 173.

[192] N. E. Agbor, M. C. Petty, A. P. Monkman, Sens. Actuators B., 28 (1995) 173.

[193] X. B. Yan, Z. J. Han, Y. Yang and B. K. Tay, Sens. Actuators B., 123 (2007) 107.

[194] D. Li, Y. Jiang, Z. Wu, X. Chen, Y. Li, Sens. Actuators B., 66 (2000) 125.

[195] E. T. Kang, K. G. Neoh and K. L. Tan, Prog. Polym. Sci., 23 (1998) 211.

[196] G. E. Collins and L. J. Buckley, Synth. Met., 78 (1996) 93.

[197] S. H. Hosseini and A. A. Entezami, Polym. Adv. Technol., 12 (2001) 482.

[198] K. Ogura, H. Shiigi, T. Oho and T. Tonosaki, J. Electrochem. Soc., 147 (2000)

4351.

[199] M. Matsuguchi, J. Io, G. Sugiyama and Y. Sakai, Synth. Met., 128 (2002) 15.

[200] M. A. El-Sherif, Y. Jianming and A. G. MacDiarmid, J. Intell. Mater. Syst. Struct., 11 (2000) 407.

[201] M. E. Nicho, M. Trejo, A. Garcia-Valenzuela, J. M. Saniger, J. Palacios and H. Hu, Sens. Actuators B., 3724 (2001) 1.

[202] U. Kang and K. D. Wise, IEEE Trans. Electron Devices., 47 (2000) 702.

[203] J. Liu, Y. H. Lin, L. Liang, J. A. Voigt, D. L. Huber, Z. R. Tian, E. Coker, B. Mckenzie and M. J. Mcdermott, Chem. Eur. J., 9 (2003) 605.

[204] N. B. McKeown, J. Mater. Chem., 10 (2000) 1979.

[205] H. Schultz, H. Lehmann, M. Rein and M. Hanack, Struct. Bonding., 74 (1991) 41.

[206] D. Wohrle, Macromol. Rapid. Commun., 22 (2001) 68.

[207] N. Trombach, O. Hild, and D. Whorle, J. Mater. Chem., 12 (2002) 879.

[208] M. J. Cook and I. Chambrier, in The Porphyrin Handbook, ed. K. M. Kadish, K. M. Smith and R. Guilard, vol. 17, pp. 37. Academic Press, San Diego, CA, (2003).

[209] J.-P. Bourgoin, F. Doublet, S. Palacin and M. Vandevyver, Langmuir, 12 (1996) 6473.

[210] N. B. McKeown, Phthalocyanine Materials: Synthesis, Structure and Function, Cambridge University Press, Cambridge, (1998).

[211] G. Guillaud, J. Simon and J. P. Germain, Coord. Chem. Rev., 178 (1998) 1433.

[212] J. A. Thompson, K. Murata, D. C. Miller, J. L. Stanton, W. E. Broderick, B. M. Hoffman and J. A. Ibers, Inorg. Chem., 32 (1993) 3546.

[213] R. S. Nohr, P. M. Kuznesof, K. J. Wynne, M. E. Kenney and P. G. Siebermann,

J. Am. Chem. Soc., 103 (1981) 4371.

[214] P. J. Toscano and T. J. Marks, J. Am. Chem. Soc., 108 (1986) 437.

[215] H. Schultz, H. Lehmann, M. Rein and M. Hanack, Struct. Bonding., 74 (1991) 41.

[216] J. Kaufhold, K. Hauffe and B. Bunsenges. Phys. Chem., 69 (1965) 168.

[217] C. C. leznoff and A. B. P. Lever, eds. Phthalocyanines: Properties and Applications, chapter-5, VCH Publisher, Inc., New Pork, (1989).

[218] S. Dogo, J.-P. Germain, C. Maleyaaon and A. Pauly, Thin solid flm., 219 (1992) 251.

[219] R. L. Van, A V. Chadwick, J. D. Wright, J. Chem. Soc. Faraday., 476 (1980) 2194.

[220] Y. Sadaoka, T. A. Jones, W. Gopel, Sens and Actuators B., l (1990) 148.

[221] K. Moriya, H. Enornoto and Y. Nhura, Sens and Actuators B., 13 (1990) 412.

CHAPTER-2

EXPERIMENTAL

2.1. Introduction

The detailed experimental procedures and various characterization techniques employed in the present studies are explained in this chapter. The polyaniline was functionalized with sulfonated metal phthalocyanines by two methods (a) chemical (b) electrochemical method. Three sulfonated metal phthalocyanines from transitional metal series namely iron, nickel and copper were chosen and used as functional molecule. The structure of the functionalized polymer was analysed by various physico chemical techniques. The properties like electrical conductivity, thermal stability, surface morphology and electrochemical studies were investigated on the functionalised polymer samples. Finally, the procedure for fabrication of sensor and testing the functionalized polymer towards NO_2 gas sensing is explained.

2.2. Materials

The various chemicals used in the present study along with their acronym and make are given in the following Table 2.1.

Table 2.1 Specifications of material used for the experiments.

Chemical	Acronym/Formula	Make
Aniline	$C_6H_5NH_2$	Merck, India
Ammonium persulphate	$(NH_4)_2S_2O_8$	Merck, India
Iron phthalocyanine	FePc	Aldrich, USA
Cobalt phthalocyanine	CoPc	Aldrich, USA
Tetra sulfonated iron phthalocyaine	TSFePc	Aldrich, USA

Tetra sulfonated nickel phthalocyanine	TSNiPc	Aldrich, USA
Tetra sulfonated copper phthalocyanine	TSCuPc	Aldrich, USA
Poly ethylene oxide	PEO	BDH, India
Copper chloride	$CuCl_2$	Merck, India
Tetrabutyl ammonium perchlorate	TBAP	Fluka,
Amberlite-120	---	Rohm and Hass, USA
Potassium chloride	KCl	Merck, India
Potassium bromide, IR grade	KBr	Merck, India
Styrene butadiene	SBS	Dupont, USA
Agar agar	---	Spectrochem Ltd., India
Silica gel	---	Spectrochem Ltd., India
1-methyl-2-pyrrolidinone AR	NMP	Merck, India
N,N-Dimethyl formamide	DMF	Merck, India
Methanol, AR	CH_3OH	Merck, India
Acetic acid, AR	CH_3COOH	Merck, India
Hydrochloric acid, AR	HCl	Merck, India
Nitric acid, AR	HNO_3	Merck, India

Aniline was distilled before use [1]. All other chemicals were used as received.

2.3. Synthesis of functionalized polyaniline

A general procedure on the synthesis of phthalocyanine functionalized PANI by chemical and electrochemical method is explained in this section. More details on the synthesis will be discussed in their respective chapters.

2.3.1. Chemical synthesis

The chemical synthesis of polyaniline was carried out by the usual method as reported in the literature [2]. The monomer aniline was distilled before use. The sulfonated transition metal phthalocyanine doped PANI was synthesized by in situ oxidative polymerization of aniline monomer. The polymerization was carried out in aqueous acid solution containing 1 M HCl. The oxidizing agent was added drop wise to the acidified solution of monomer under constant stirring at low temperature between 0–5 °C. The monomer to oxidizing agent ratio was kept as 1:1. The addition of sulfonated phthalocyanine to the reaction mixture containing aniline and HCl was done prior to the addition of oxidizing agent. After complete addition of oxidizing agent, the reaction mixture was kept under stirring for 4 hour. The precipitated polymer (emeraldine salt) was recovered from the reaction vessel by filtration, washing and followed by vacuum drying at room temperature for 24 hours.

2.3.2. Electrochemical synthesis

The electrochemical deposition was carried out in a single compartment cell with three electrode system as shown in Fig. 2.1. Polyaniline film doped with tetra sulfonated metal phthalocyanine was electrochemically grown by potential sweeps between -0.3 and +1V at a sweep rate of 0.05 V/sec, onto a platinum or ITO electrodes in a aniline and 1M HCl solution. A platinum wire was used as a counter electrode and all potentials were

referred to the saturated calomel electrode (SCE). Voltammograms recorded during continuous scans showed very similarly shaped CV curves with increasing current in each successive cycle which reflects the regular growth of the polymer film.

The electrochemical deposition was also carried out by chronoamperometric technique at a constant applied potential of +0.8 V against SCE for 300 Sec. The electrolytic solution containing aniline and aqueous hydrochloric acid along with metal phthalocyanine sulfonic acid was used. The conjugate base of sulfonated metal phthalocyanine was incorporated as dopant during electrochemical deposition. The grown film was rinsed with water prior to characterisation.

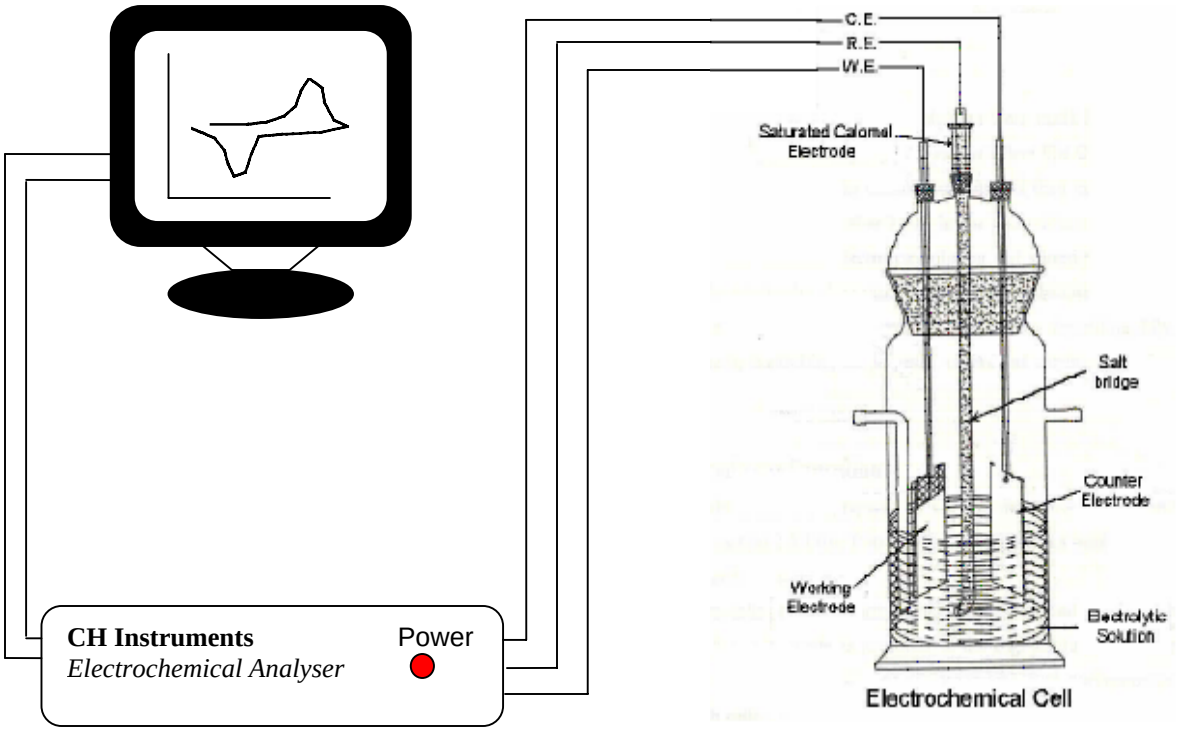

Fig. 2.1. Computer controlled electrochemical setup

2.4. Characterisation of the polymer

2.4.1. Structural identification techniques

2.4.1.1. Infrared spectroscopic studies

Infrared (IR) studies were carried out to confirm the incorporation of various metal phthalocyanine into the conducting polymer [3]. The frequencies of various modes of vibrations in the pristine PANI was compared with functionalized PANI. The sample was prepared by mixing 1 wt % polymer with KBr to form a thin wafer. These wafers were mounted in the IR cell in the conventional way to record the spectra. Infrared Spectra were collected in the range 400–4000 cm^{-1} with a Fourier transform Shimadzu FT-IR 8300 spectrometer and recorded by averaging 64 scans at a solution of 4 cm^{-1}

2.4.1.2. UV-Vis spectroscopic studies

The doping induced electronic transitions in PANI was studied through UV-Vis spectroscopy [4]. The UV-Vis. spectra of the functionalized samples were recorded by dissolving 10 mg of sample in 10 ml of solvent such as glacial acetic acid using spectro-photometer unit (model USB 2000, Ocean Optics, USA) with fiber optic cable connected to a computer. The spectra were scanned from 300 nm to 900 nm. The spectrophotometer utilizes a DH-2000 deuterium light source and a HR 2000 CG-UV-NIR detector.

2.4.1.3. Wide Angle X-ray Diffraction studies

Wide-Angle X-ray Diffraction (WAXD) studies [5] were done in order to analyze the structure of synthesized polyaniline as well as functionalized PANI. The incorporation of these functional moieties into polyaniline is expected to show some structural changes. The structural variation in the functionalized polyaniline were investigated by WAXD, using a powder X-ray diffractometer (Rigaku Geigerflex

refractometer) using CuKα source and β Ni filter. All the scans were recorded in the 2θ region of 5-50° at a scan rate of 4° per minute.

For the crystalline phase, the d- values can be calculated using Bragg's equation:

$$n\lambda = 2d \sin\theta$$

$$d = (n\lambda / 2 \sin\theta) \text{ ; where } n = 1 \text{ and } \lambda = 1.54 \text{ Å}$$

2.4.1.4. Graphite Furnace Atomic Absorption Spectrometry (GFAAS)

Graphite furnace (also known as an electrothermal atomizer or ETA) atomic absorption (AA) is generally considered an ultratrace and microtrace analytical technique with limits of detection (LODs) in the low pictogram range, precision of a few percent. An understanding of the free atoms formation process has facilitated the application of the technique to the analysis of a variety of complex samples.

In brief, the technique is based on the fact that free atoms will absorb light at frequencies or wavelengths characteristic of the element of interest (hence the name atomic absorption spectrometry) [6]. Here, we are interested in looking the presence of transition metals like iron, nickel and copper to confirm the presence of sulfonated metal phthalocyanine in the functionalized PANI. GFAAS has been done with GBC, AvantaΣ instrument. Within certain limits, the amount of light absorbed can be linearly correlated to the concentration of analyte present. Free atoms of most elements can be produced from samples by the application of high temperatures. In GFAAS, samples are deposited in small graphite or pyrolytic carbon coated graphite tube, which can then be heated to vaporize and atomize the analyte. The atoms absorb ultraviolet or visible light and make transitions to higher electronic energy levels. The transient nature of the ETA signal was collected and processed to give quantitative information about the metal present.

2.4.1.5. Energy Dispersive X-ray Analysis (EDAX)

Energy Dispersive X-ray Analysis (EDAX) was carried out to find out the doping levels in functionalized polyaniline [7]. From these studies the percentage of various elements like C, N, O, S, Cl and metals etc. were found out. The measurements were carried out on EDAX microanalysis, Phoenix (U.S.A.).

2.4.2. Property measurements

2.4.2.1. Electrical conductivity

The conductivity at room temperature was measured by a Keithley electrometer 6514 series with a standard two-probe method. The powder samples were made into a pellet of size 1cm x 1cm with approximately 1-2 mm thickness. The resistance measured is converted into conductivity using the formula

$$\rho = RA / l \qquad \text{----------} \qquad (2.1)$$

$$\sigma = 1 / \rho \qquad \text{----------} \qquad (2.2)$$

Where ρ is its resistivity, A is the cross sectional area, l is the thickness, R is the sample resistance and σ is conductivity.

2.4.2.2. Thermogravimetric Analysis (TGA)

The degradation pattern and thermal stability of the functionalized as well as pure PANI were followed by TGA [8] wherein the % weight loss of the sample was analyzed as a function of temperature using a Perkin Elmer Thermogravimetric analyzer. The sample masses were between 0.005-0.010 g and they were heated from 50ºC to 700ºC at the rate of 10ºC/min under nitrogen atmosphere. Onset of degradation, maximum

degradation temperature and the weight loss at the maximum degradation temperature were the parameters determined from the TGA curves.

2.4.2.3. Scanning Electron Microscopy

SEM [9]studies were performed to investigate the surface morphology of the chemically and electrochemically synthesized metal phthalocyanine doped PANI as well as pure PANI. All the samples were coated with a thin layer of gold in plasma coating unit ES000 to prevent charging of the specimen. The micrographs of the samples with 10 KV EHT and 25 PA beam current were recorded by a CCD camera attached on to the high resolution recording unit.

2.4.2.4. Electrochemical studies

Cyclic voltammetry experiments were used to obtain information on the mechanism of polymer growth as well as redox behaviour and understand the mode of electronic conduction [10]. In the present study, the redox behaviour of the metal phthalocyanine and polyaniline was investigated by carrying out the cyclic voltammetric studies separately in various electrolyte/solvent systems using CH electrochemical analyzer (USA) unit of model CH1604B. The electrochemical behaviour of metal phthalocyanine was recorded between the region 0 and -2 V against SCE in DMF solvent using tetra butyl ammonium perchlorate as supporting electrolyte where as aqueous 1 M HCl was used as electrolytic solution to record the cyclic voltammogram of PANI in the region -0.2 and +1 V. These studies were carried out at room temperature by using a three-electrode cell consisted of platinum as working electrode, a saturated calomel as reference and platinum wire as the auxiliary electrode.

2.5. Sensitivity of functionalized PANI towards NO_2 gas

2.5.1. Sensor fabrication

The sensor comprising an active layer of functionalized PANI film was made by first depositing gold films on 100 μm PET film to form interdigitated electrodes with interelectrode diamension of 0.1 mm x 10 mm. Polyethylene oxide along with 10% $CuCl_2$ was dissolved in methanol to form homogenous solution. The functionalized PANI samples (33 mg each) were then sonicated for 2 h to form a uniform slurry. This type of dispersion is more amenable to coat on the interdigitated electrode configuration and has been used for the purpose of sensing as reported in the literature [11, 12]. Two drops of this slurry were placed on the gold coated substrates and the solvent evaporated so as to form the test sensor in surface cell configuration as shown in Fig. 2.2.

In the case of electrochemically deposited films, the interdigited electrode deposited substrates were pretreated in 1M $FeCl_3$ for few hours so as to create active sites for binding the polyaniline between the two electrodes. These sensors were directly used for testing the sensitivity.

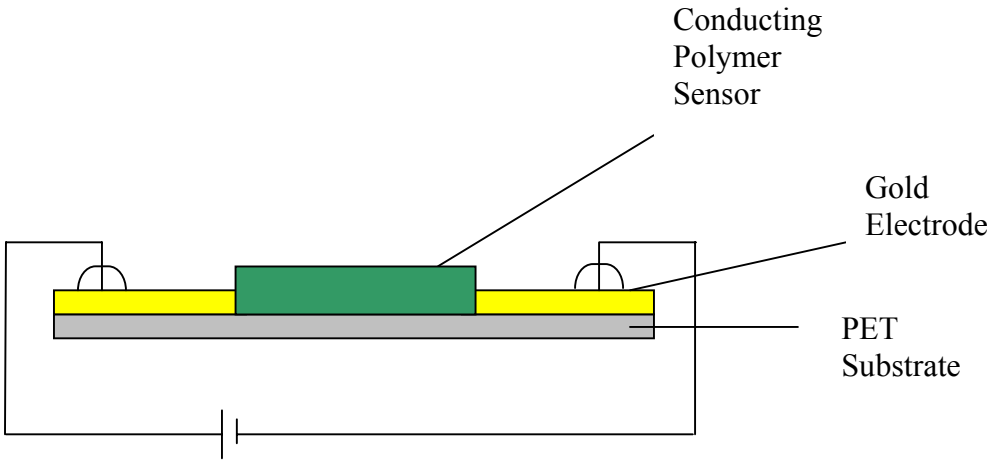

(a)

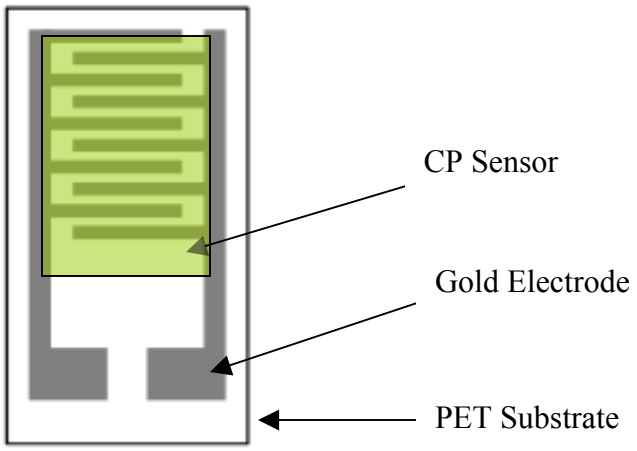

(b)

Fig. 2.2. Configuration of fabricated sensor (a) side view (b) top view

2.5.2. Sensitivity measurements

For the sensitivity measurement study, the fabricated sensor was taken in a specially designed gas testing chamber as shown in Fig. 2.3. Two leads taken from the sensor was connected to digital Keithley electrometer interfaced to a computer with test Point software so as to monitor the sample resistance continuously with fast sampling speed of ten points per second. The change in resistance was measured online from the time of exposing the material to NO_2 gas. The measurements were continued up to 600 Sec. The sensitivity factor (% sensitivity) was calculated using the formula,

$$S = R/R_0$$

Where, R is the resistance after exposing to NO_2 gas and R_0 is the resistance of the material before exposing to gas. Once the resistance reaches a maximum, recovery of the

material is carried out by applying vacuum. The change in resistance during recovery was also monitored with respect to time.

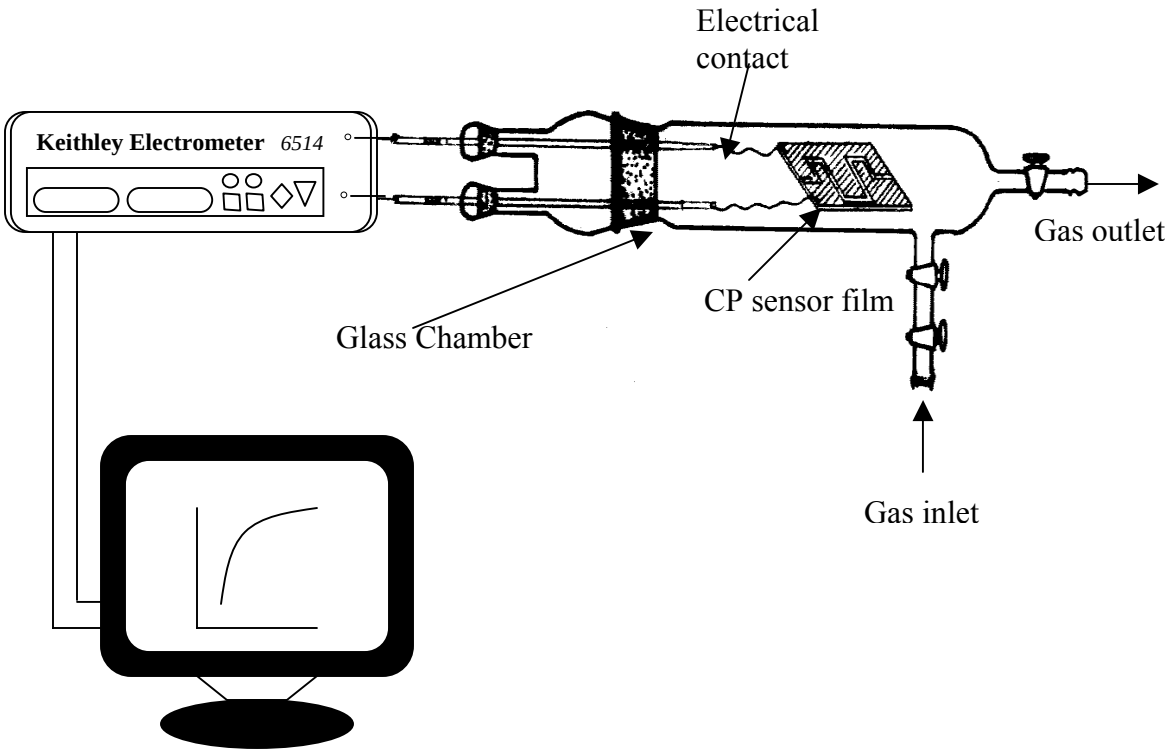

Fig. 2.3. Computer interfaced sensitivity measurement setup

2.6. References

[1] W. L. F. Armarego, D. D. Perrin, Purification of laboratory chemicals, 4th ed.,Butterworth-Heinemann, Oxford, London.

[2] S. Radhakrishnan and S. D. Deshpande, Sensors., 2 (2002) 185.

[3] J. F. Rabek, "Experimental Methods in Polymer Chemistry" John Wiley and Sons, New York (1980).

[4] H. Stubb, E. Punkka and J. Paloheimo, Mat. Sci. And Eng., 10, (1993) 85.

[5] L. E. Alexander, "X-ray diffraction methods in Polymer Science" Wiley-Intersci., John Wiley and Sons, Inc. (1969).

[6] R. Woodriff and G. Ramelow, Spectrochim.Acta, Part B., 23 (1968) 665.

[7] H. Miinstedt, Polymer 27 (1986) 899.

[8] V. G. Kulkarni, L. D. Campbell and W. R. Mathew, Synth. Met., 30 (1989) 321.

[9] W. –S. Huang, D. Brian, Humphrey and A. G. MacDiarmid, J. Chem. SOC., Faraday Trans. 1, 82 (1986) 2385.

[10] G. G, Wallace, G. M. Spinks, L. A. P. Kane-Maguire, P. T. Teasdale, Conductive electroactive polymers intelligent material systems, CRC press, Florida, (2003).

[11] S. D. Deshpande and S. Radhakrishnan, Mat. Lett., 48(3) (2001) 144.

[12] S. Radhakrishnan and S. D. Deshpande, Sensors., 2 (2002) 185.

CHAPTER-3

Synthesis and properties of iron and cobalt Phthalocyanine doped PANI

3.1. Introduction

Conducting polymer based chemical sensors have attracted much interest in recent years because they provide an easy method of fabricating cost effective, disposable device which can operate at room temperature [1]. However, many of the studies report that [2-4], though conducting polymers have good sensitivity, their selectivity needs to be improved especially for industrial gases such as ammonia and nitrous oxide etc. especially under normal conditions of operation.

In the present chapter, the conducting polymer polyaniline (PANI) was chosen as the matrix, which is functionalized by unsubstituted iron phthalocyanine (FePc) , cobalt phthalocyanine (CoPc) and tetra sulfonated iron phthalocyanine (TSFePc). The very purpose of choosing polyaniline is due to its simplified synthesis, environmentally stable nature and it shows various redox states depending on the extent and method of doping [5]. On the other hand, the extended π-electron system in metallophthalocyanines can interact with various gases like NO_x and NH_3 to form charge transfer complexes [6]; more specifically, iron and cobalt phthalocyanines are compounds known to undergo changes in the oxidation state of both ligand and the metal ion which make them suitable candidates for better sensitivity and selectivity to toxic gases like NO_2 and CO [7,8]. These are also chemically and thermally stable up to 400-500ºC [9]. Hence, in the present investigation, the conducting polyaniline was modified by incorporating redox dopants like sulphonic acid substituted as well as un-substituted iron phthalocyanines (TSFePc, FePc) and cobalt phthalocyanine (CoPc) in the form of dopant ion by both chemical and electrochemical route. These were studied for sensing behaviour towards toxic NO_2 gas pollutant at ppm levels. The use of functional dopants to modify conducting polymers is

advantageous in principle because complex syntheses of functional monomers are avoided. The effect of these dopants on structure, morphology and various properties including sensitivity to NO_2 have been described in this chapter.

Section – A : Studies on iron and cobalt phthalocyanine doped Polyaniline (PANI).

3.2. Chemical Synthesis of iron phthalocyanine (FePc) and cobalt phthalocyanine (CoPc) doped PANI (FePc-PANI and CoPc-PANI).

Due to the lack of solubility of unsubstituted iron and cobalt phthalocyanine in water, the reaction was carried out in 1:1 NMP-Water mixed solvent as reaction medium. The procedure for the synthesis of HCl doped PANI (PANI-HCl) was same as reported elsewhere [10,11]. In a typical reaction for the synthesis of FePc functionalized PANI (HCl doped), distilled aniline 4ml (44 mmol) was treated with 25 ml of 2M hydrochloric acid to give homogeneous solution. Iron phthalocyanine 0.249 g (0.44 mmol) dissolved in 150 ml of NMP solvent was added into the above solution with vigorous stirring. An equimolar quantity of ammonium per sulphate with respect to aniline was dissolved in 150 ml of water and slowly added into the reaction mixture with constant stirring. The reaction mixture was maintained at 5ºC for 4 hours. After 4 hours, the polymer was precipitated by pouring the solution into 1000 ml of water. The resulting green mass was washed with water to remove excess acid, filtered and vacuum dried for 24 hours. The concentration of FePc in PANI was varied by carrying out similar reaction by changing the mol percentage of FePc from 0.2 to 2 mol % w.r.t aniline concentration. The yields procured from the reactions are reported in Table 3.1. A similar procedure mentioned

above was followed for the synthesis of cobalt phthalocyanine doped PANI and the yields are reported in Table 3.2.

Table 3.1 Summary of the yield of reaction FePc and Aniline

No	FePc added (mol%)	Yield of FePc-PANI (g)	PANI Conversion (%)
1	0	3.447 (PANI alone)	84
2	0.2	3.519	86.1
3	0.5	3.680	88.3
4	1	4.01	92.4
5	2	4.395	96.6

Table 3.2 Summary of the yield of reaction CoPc and Aniline

No	CoPc added (mol%)	Yield of CoPc-PANI (g)	PANI Conversion (%)
1	0	3.447 (PANI alone)	84
2	0.2	3.468	85.1
3	0.5	3.617	86.6
4	1	3.849	88.7
5	2	4.104	90.2

The plots of the PANI conversion versus metal phthalocyanine concentration are shown in Fig. 3.1. It can be seen from the plot, that the yield of the reaction is following the equation $A + Bx - Cx^2$ where A is the yield of PANI as such without the addition of phthalocyanine and it corresponds to 84.The coefficients B corresponds to enhancement of the reaction due to phthalocyanine and C corresponds to retardation of reaction which is apparently diffusion controlled. The phthalocyanine is a bulky material, which doesn't

allow the aniline to reach the active site Fe or Co attached to the ligand. It can also be seen from the values of coefficient B, the catalytic activity of iron phthalocyanine is more than that of cobalt phthalocyanine and it is also reflected on the yields of the reactions.

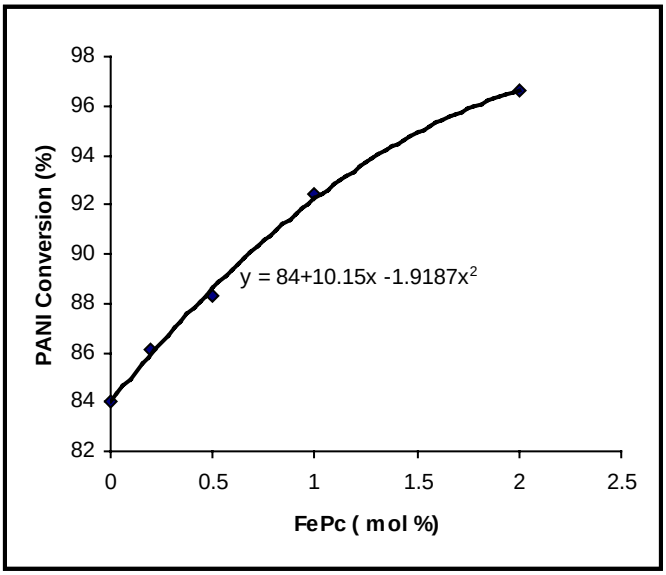

(a)

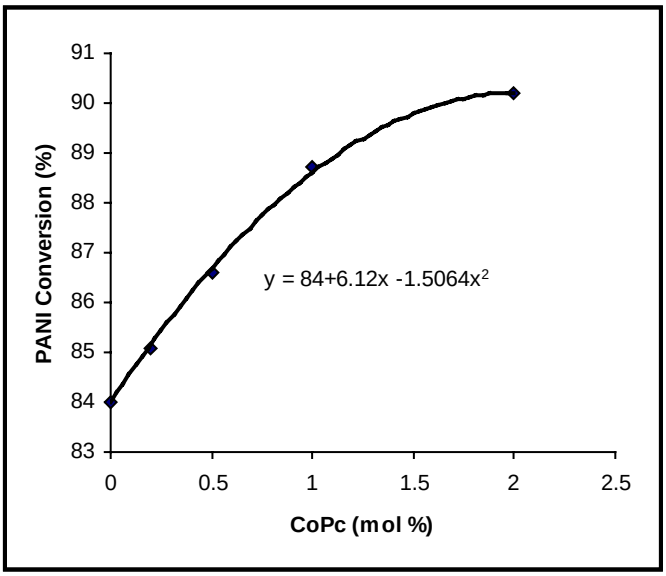

(b)

Fig .3.1. (a) The plot of PANI conversion versus FePc concentration. (b) The plot of PANI conversion versus CoPc concentration.

3.3. Results and Discussion

3.3.1. Characterisation of Structure

The efficacy of incorporation of various phthalocyanine groups in the polymer was characterized thoroughly by the following physico-chemical techniques.

3.3.1.1. FT-IR studies

The functionalization of conducting polyaniline with FePc and CoPc was characterized by recording FT-IR spectra of the newly synthesized polymers. Figs. 3.2 and 3.3 shows the FT-IR spectra of FePc, CoPc incorporated polyaniline respectively. In the FT-IR spectrum of HCl doped PANI, Fig. 3.2 (a), the absorption band at 1150 cm^{-1} represents protonation of imine nitrogen [12,13]. The absorption peaks at 1578 cm^{-1} and 1490 cm^{-1} are assigned to quinoid (Q) and benzenoid (B) structures of emeraldine form of PANI respectively [14,15]. Apart from this, the polymer shows C–N aromatic stretching vibrations at 1290 cm^{-1} [16]. After functionalization with metal phthalocyanines, there is no significant difference in the peak positions of their respective IR spectra apart from the change in the intensity of 1290 cm^{-1} absorption band. Hence, the spectra of FePc and CoPc functionalized PANI are more or less spectral sum of their individual compounds. This could be due to the formation of two phases namely metal phthalocyanine and PANI. The change of intensity of the 1290 cm^{-1} band, which corresponds to the C-N stretching vibration, can be due to molecular ordering in PANI. This is further confirmed by the X-ray diffraction and conductivity studies of these samples. The assignment of IR bands and their peak positions for FePc, CoPc, PANI, FePc-PANI and CoPc-PANI are given in Tables 3.3 and 3.4.

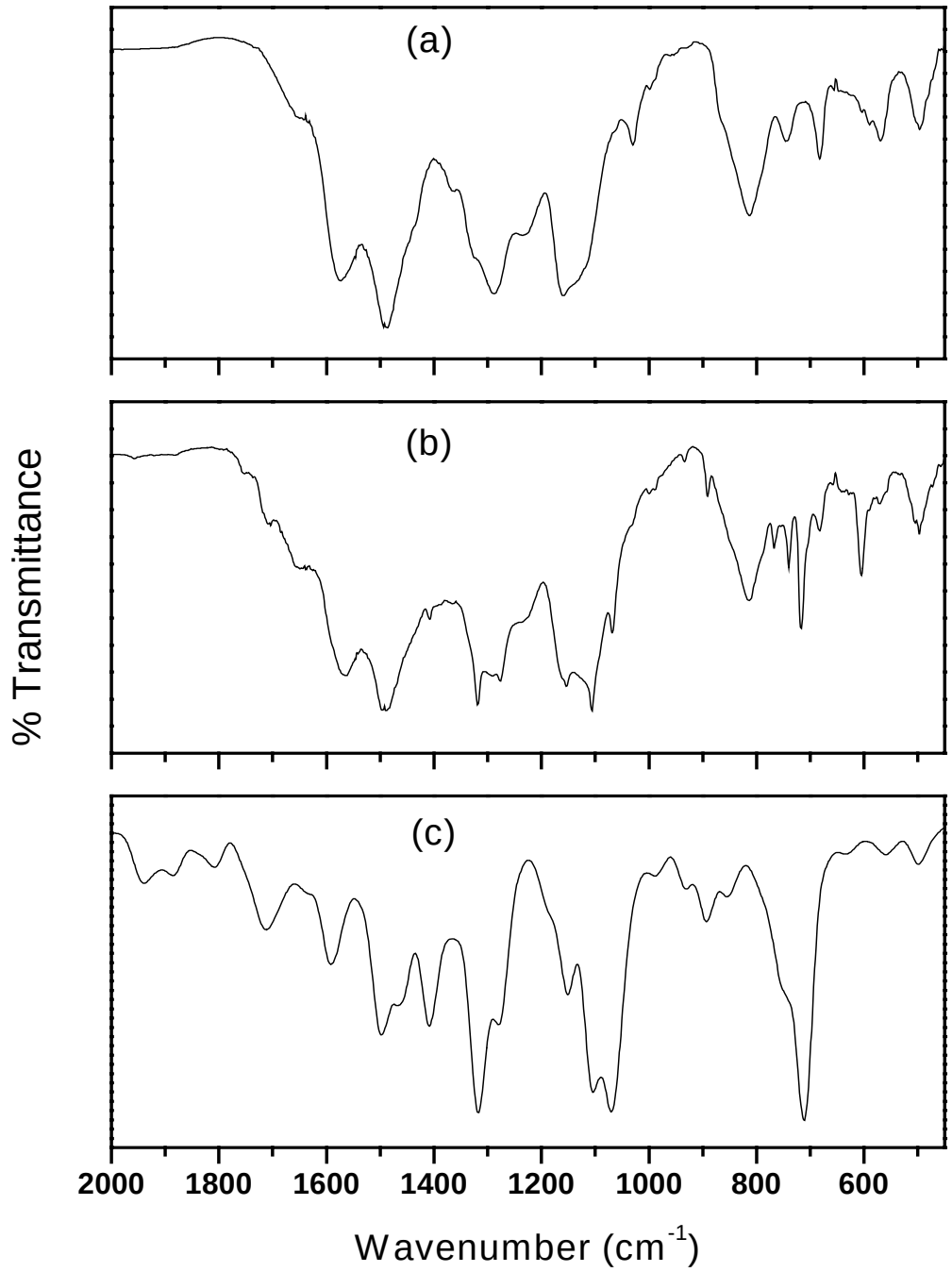

Fig. 3.2. FT IR Spectra of (a) HCl doped PANI; (b) FePc functionalized PANI; (c) FePc

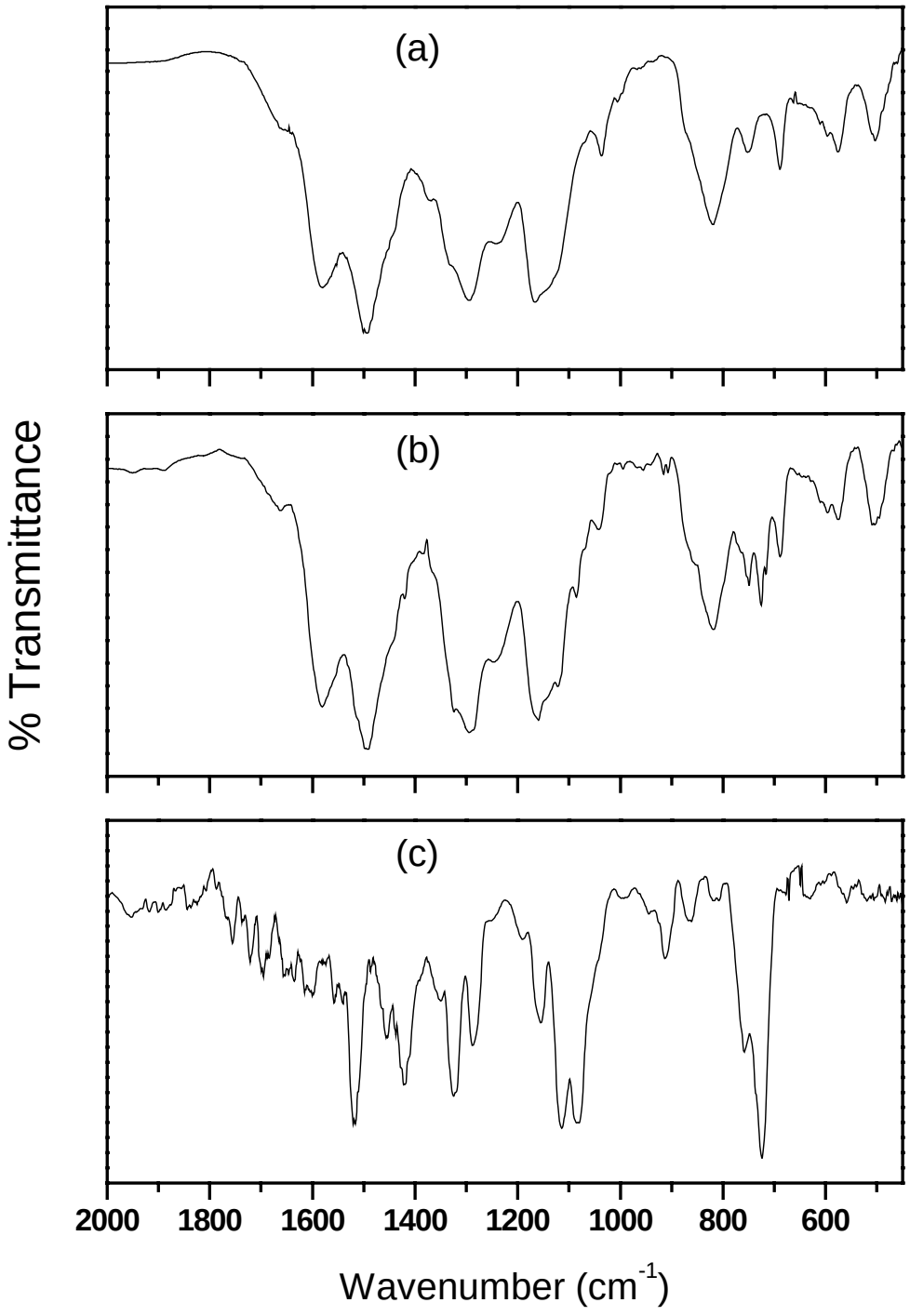

Fig. 3.3. FT IR Spectra of (a) HCl doped PANI; (b) CoPc functionalized PANI; (c) CoPc

Table 3.3 Frequency assignment of bands in the FTIR spectra of FePc and CoPc

Peak positions (cm^{-1})		IR band assignments
FePc	**CoPc**	
1715 w	1719 w	υ(C=C) stretching in phthalocyanine skeleton
1601 m	1608 w	υ(C-C) stretching Vibration
1509 s	1519 vs	β(C-H) bending Vibration
1411 s	1421 m	υ(C-H) stretching Vibration
1319 vs	1324 s	υ(C-C) stretching Vibration
1291 m	1297 m	υ(C-N) stretching Vibration
1105 s	1114 vs	β(C-H) bending in plane
1071 vs	1084 vs	β(C-H) in plane deformation
907 w	912 w	γ(C-H) out of plane deformation
712 vs	724 vs	υ(C-N) stretching Vibration

vs: very strong, s: strong, m: medium, w: weak

Table 3.4 Assignment of bands in the FTIR spectra of PANI, FePc-PANI and CoPc-PANI

Peak positions (cm^{-1})			IR band assignments
PANI	**FePc-PANI**	**CoPc-PANI**	
1577 s	1577 s	1578 s	Quinoid ring stretching
1490 vs	1489 vs	1491 vs	Benzenoid ring stretching
1290 s	1289 s	1290 s	υ(C-N) stretching vibration of aromatic ring
1160 s	1158 s	1160 s	$B\text{-}N^{+}H\text{-}B$ stretching Vibration
816 vs	815 vs	817 vs	para disubstituted benzene ring
745 m	743 m	747 m	γ(C-H) out of plane deformation
682 m	682 m	684 m	υ(C-C) ring stretching
570 m	603 m	570m	Out of plane (C-H) bending vibration
501 m	501 m	502 m	γ(C=C) out of plane ring bending

vs: very strong, s: strong, m: medium,

3.3.1.2. Wide Angle X-ray Diffraction (WAXD) Studies

The synthesized FePc-PANI and CoPc-PANI were characterized by WAXD. The X-ray diffraction pattern of FePc is shown in Fig. 3.4 and those for FePc-PANI in Fig.3.5. Similarly the diffraction pattern of CoPc and CoPc-PANI are shown in Figs. 3.6 and 3.7. The major reflections in the diffraction pattern of FePc, CoPc, PANI, FePc-PANI and CoPc-PANI and their *d*-spacing values are presented in Table 3.5. The diffraction pattern of FePc and CoPc are well documented in the literature [17]. The X-ray diffraction profile of HCl doped PANI synthesized in pure aqueous medium Fig. 3.5 (a') is in good agreement with the reported data [18], while that in NMP-water mixture has less crystallinity and appears to be that for PANI cast form NMP [26]. PANI exists in EB-I and ES-I/ ES-II crystalline forms.

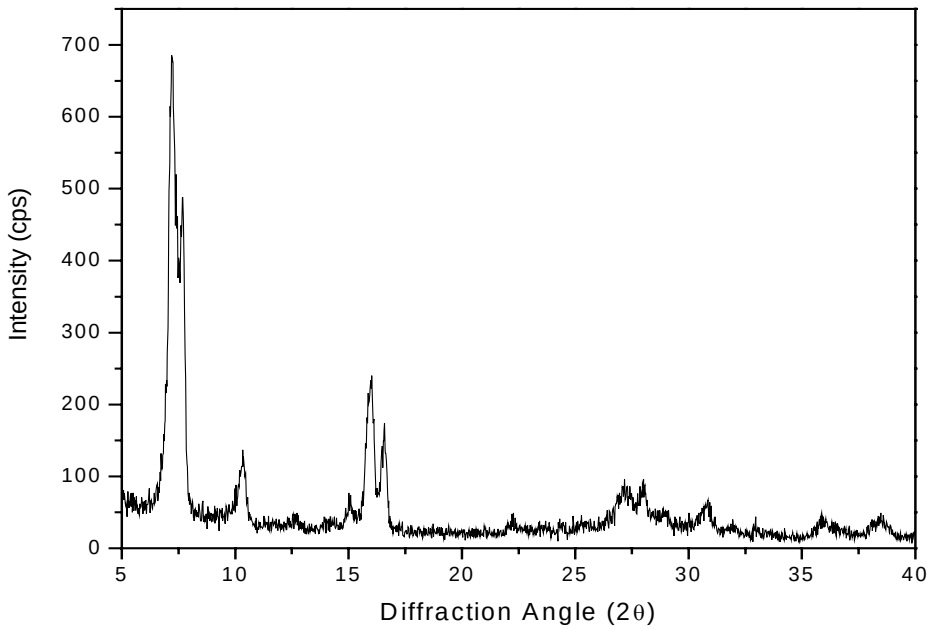

Fig. 3.4. X-ray diffractogram of FePc

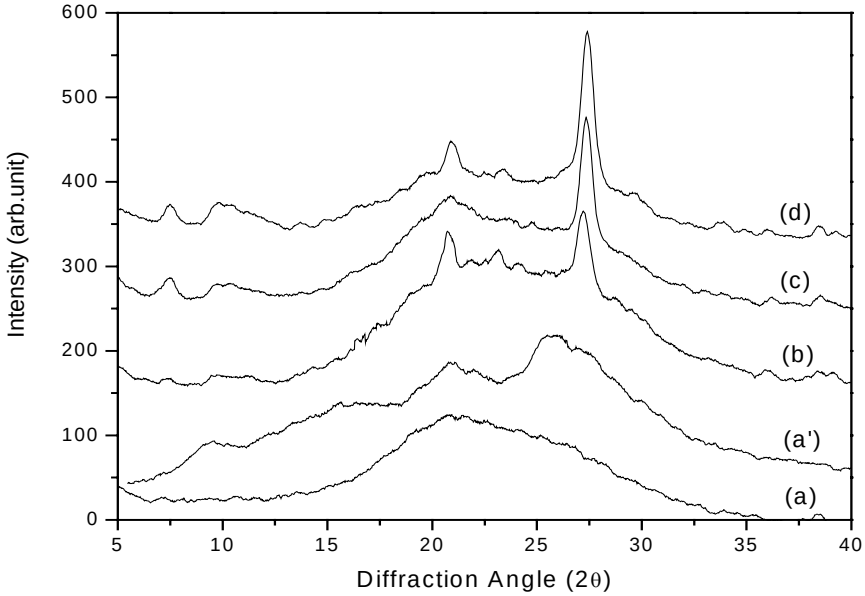

Fig. 3.5. X-ray diffraction pattern of various mol % of FePc incorporated PANI (a) PANI-NMP-Water medium, (a') PANI-Water medium (b) 0.2 mol % FePc, (c) 0.5 mol % FePc (d) 1 mol % FePc

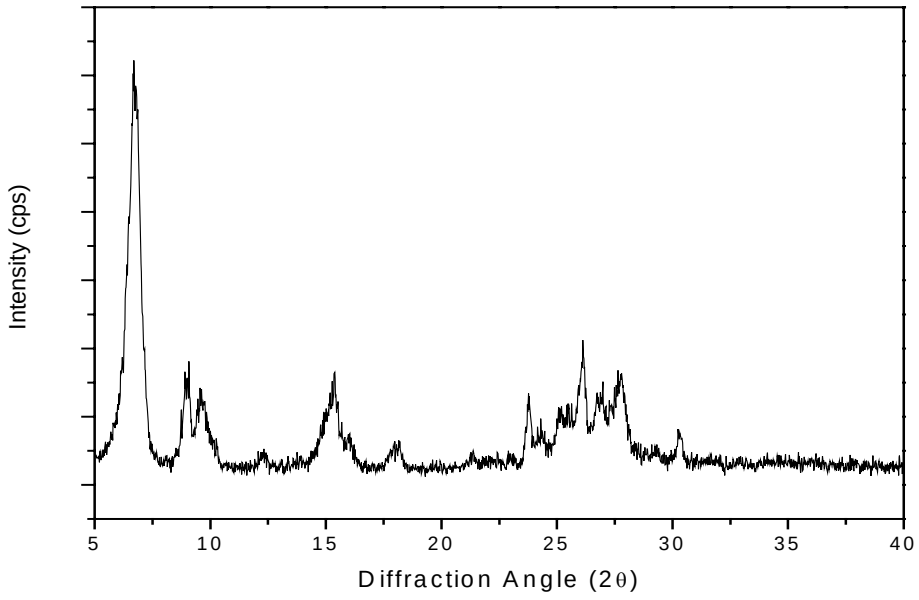

Fig. 3.6. X-ray diffractogram of CoPc

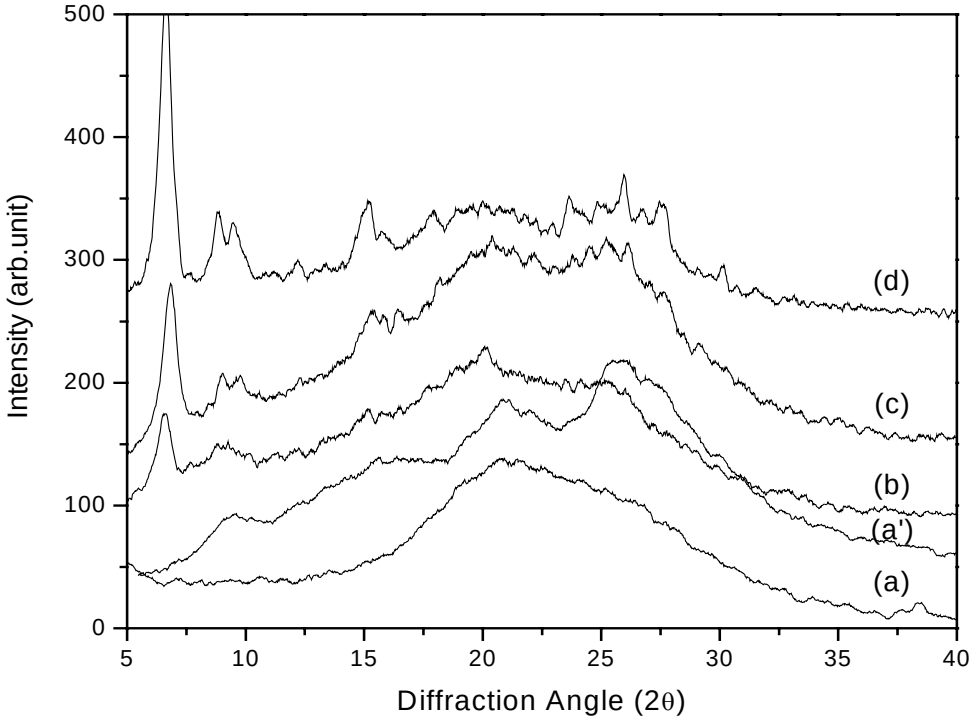

Fig. 3.7. X-ray diffraction pattern of various mol % of CoPc incorporated PANI (a) PANI-NMP-Water medium, (a') PANI-Water medium, (b) 0.2 mol % CoPc, (c) 0.5 mol % CoPc (d) 1 mol % CoPc

After incorporation with phthalocyanine the peak at 2θ = 27 in PANI continues to intensify with the increase in the concentration of FePc, which could be due to increase in molecular ordering along particular direction and/or stacking becomes better in the presence of phthalocyanine. According to Wang et al. [28] crystallinity decreased with increasing HCl concentration during synthesis over the range from 0.001 N to 7 N. The reason for this was that at high concentrations of HCl, addition of Cl atoms to the quinoid ring occurs. It was also reported that the crystallinity of the sample depends on the size of

Table 3.5. Major reflections in the X-ray diffraction patterns

Compound	2 Theta	I/Io	d-spacing
FePc	7.4 10.3 16.1 27.3	100 18.9 35.5 12.7	11.9 8.58 5.49 3.26
CoPc	6.7 8.9 9.6 15.3 23.8 26.1 27.6	100 26.8 23.2 22.8 20.1 29.8 29.1	13.18 9.87 9.20 5.78 3.73 3.41 3.22
PANI (synthesised under water medium)	8.9 15.0 20.3 25.4 27.0	37 54 74 100 78	9.92 5.9 4.37 3.5 3.3
FePc-PANI	7.4 9.8 20.3 27.0	64 65 78 100	11.9 9.01 4.37 3.3
CoPc-PANI	6.7 8.9 9.6 15.3 23.8 26.1 27.6	100 67 66 69 71 74 70	13.2 9.9 9.2 5.8 3.7 3.4 3.2

both oxidant and dopant. Dopant and oxidant with smaller size lead to higher crystallinity. In the present case, the planarity of the phthalocyanine can influence the morphology of the PANI and give better ordered structure. This is also confirmed from the intensity of C-N stretching mode at 1290 cm^{-1} which found to increase in phthalocyanine containing PANI. In both the cases of FePc and CoPc, it is seen that

above certain concentration, there is a peak at low 2θ region (<10 degrees), which is due to the phthalocyanine crystals. Hence, above this concentration there is a phase separation in which phthalocyanine crystals are obtained. In CoPc-PANI, the X-ray diffraction pattern as in Fig. 3.7(c) indicates the clear separation of two phases for concentration above 0.5 mol % of CoPc in PANI. This has been well reflected in the electrical conductivity data of both FePc and CoPc incorporated PANI that, it decreased with the increase of phthalocyanine concentration.

3.3.2. Measurement of properties

3.3.2.1. Electrical Conductivity

The electrical conductivity of the polymer samples were measured by two probe technique and the plot of conductivity versus mol % of FePc and CoPc in PANI are shown in Fig. 3.8. In all cases the primary dopant was the protonic acid HCl, when the phthalocyanine concentration was increased from 0.2 to 2 mol %, the electrical conductivity of PANI decreases. Here Pc is insulating, which are placed between PANI granules. As explained in IR and XRD characterisation techniques, these polymers contain phthalocyanine in phase separated form. Since FePc and CoPc by themselves have high resistivity with low charge carrier mobility, these may obstruct the charge flow along and in between the conducting polymeric chain leading to decrease in the conductivity of metal phthalocyanine loaded samples. The conductivity value of samples with different concentration of phthalocyanine are presented in Table 3.6.

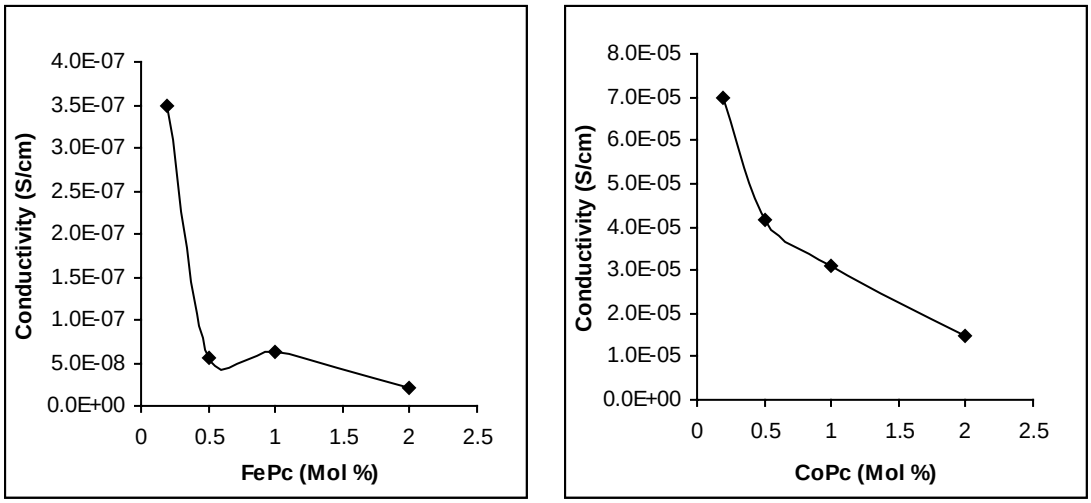

(a) **(b)**

Fig. 3.8. Plot of conductivity versus metal phthalocyanine concentration in PANI (a) FePc – PANI, (b) CoPc - PANI

Table 3.6. Room temperature conductivity data for FePc and CoPc incorporated PANI

Mol %	Conductivity -σ_{RT} (S/cm)	
	FePc-PANI	**CoPc-PANI**
0	1.19×10^{-4}	1.19×10^{-4}
0.2	3.48×10^{-7}	6.98×10^{-5}
0.5	5.50×10^{-8}	4.15×10^{-5}
1	6.20×10^{-8}	3.09×10^{-5}
2	1.99×10^{-8}	1.47×10^{-5}

3.3.2.2. FePc and CoPc incorporated PANI as Chemical sensor

The chemical sensors were made from the above synthesized samples according to the procedures explained in experimental chapter. The gas sensing ability of FePc and

CoPc functionalized PANI was checked with respect to 100 ppm NO_2 gas at room temperature. The fabricated sensor was taken in a specially designed chamber which in turn was connected to Keithley interfaced with computer. The change in resistance upon exposure to NO_2 gas was monitored online. The response characteristics of PANI with different concentration of metal phthalocyanines namely, FePc and CoPc is shown in Fig 3.9 and 3.10. As soon as the sample comes in contact with NO_2 gas, a decrease in resistance was observed in FePc and CoPc incorporated PANI samples. In conventional PANI doped with HA type acid (where A: Cl^-, Br^-, ClO_4^- , etc.) the sensing mechanism is governed by the protonation and deprotonation phenomena leading to a decrease in resistance on exposure to NO_2 gas [19] but, a very low sensitivity and speed of response was observed on the other hand FePc and CoPc modified polyaniline showed a better sensititvity and speed of response than pure PANI.

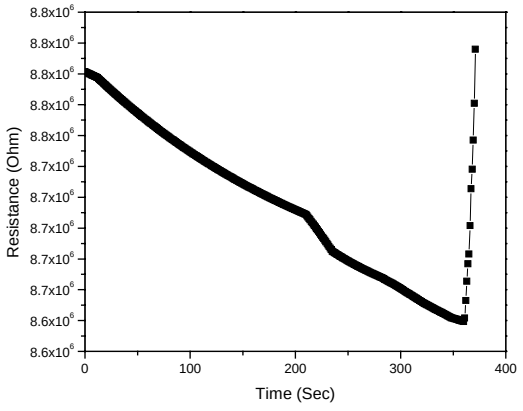

(a)

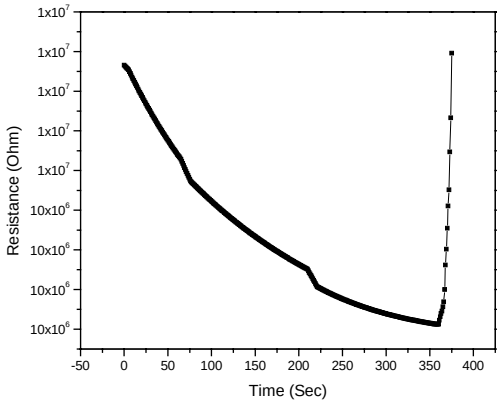

(b)

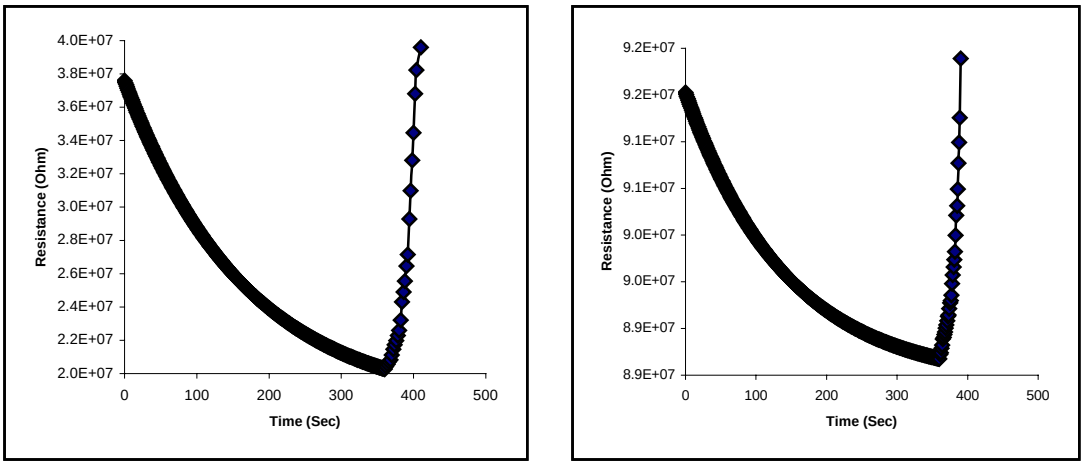

(c) (d)

Fig. 3.9. Response characteristics of FePc incorporated PANI towards NO_2 gas. (a) 0.2 mol % FePc-PANI, (b) 0.5 mol % FePc-PANI, (c) 1 mol % FePc-PANI and (d) 2 mol % FePc-PANI

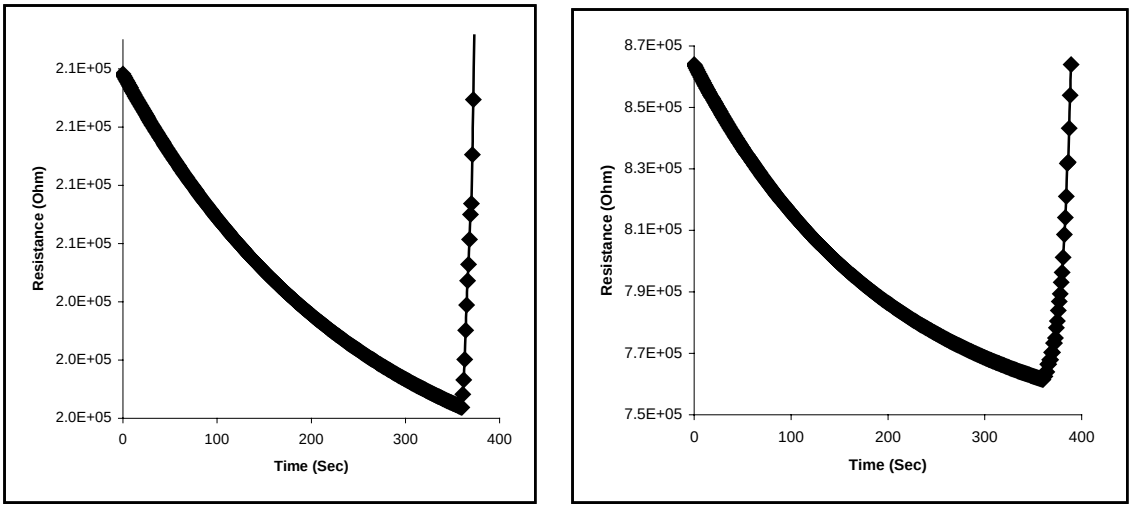

(a) (b)

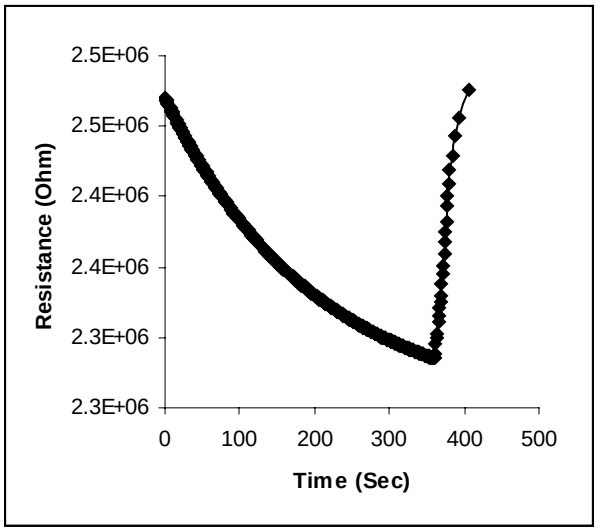

(c)

Fig. 3.10. Response characteristics of CoPc incorporated PANI towards NO_2 gas.
(a) 0.2 mol % CoPc-PANI, (b) 1 mol % CoPc-PANI and (c) 2 mol % CoPc-PANI

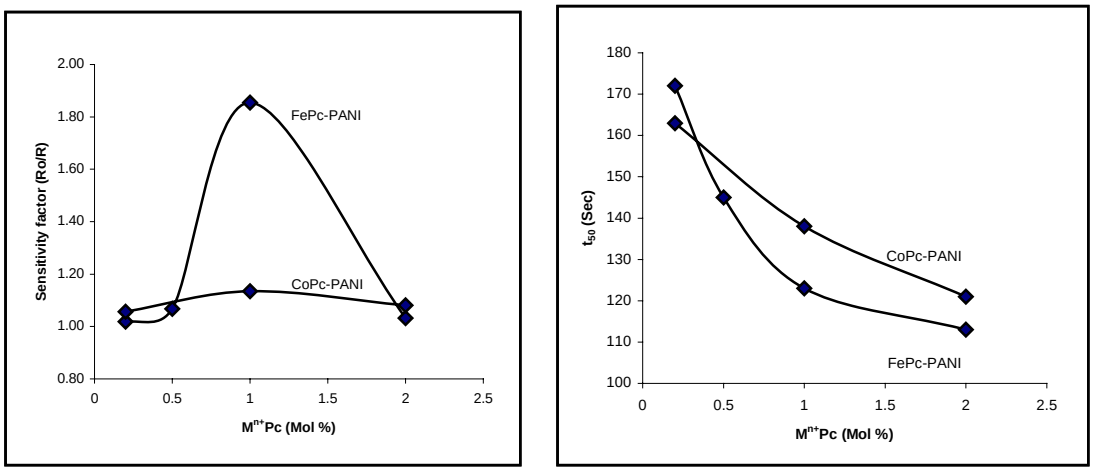

(a) (b)

Fig. 3.11. Sensor characteristics of FePc and CoPc incorporated PANI towards NO_2 gas
(a) Plot of sensitivity factor versus concentration of $M^{n+}Pc$
(b) Speed of response (t_{50}) versus concentration of $M^{n+}Pc$

It's well documented in the literature that the metal phthalocyanines behave like p-type semiconductor when treated with electron acceptor and n-type with electron donors[20], hence when they are exposed to oxidizing gas like NO_2, holes are created leading to an increase in conductivity (decrease in resistance) of the incoporated PANI samples. This observation is similar to the results obtained by Jones et al[21]. The sensitivity factor (S) for FePc and CoPc-PANI was calculated using the formula

$$\mathbf{S = Ro/R}$$

Where, Ro is the resistance before exposure to NO_2 gas and R is the resistance after exposure to gas.

The plot of sensitivity factor and speed of response versus different concentrations of FePc and CoPc in PANI are shown in Fig 3.11. The sensitivity factor and speed of response of phthalocyanine functionalized PANI samples are presented in the Table 3.7 for comparison. Both FePc and CoPc modified PANI showed maximum sensitivity at an optimum concentration of 1 mol % metal phthalocyanine in PANI and the response time was found to decrease with increase of phthalocyanine concentration. The increase of sensitivity after addition of phthalocyanine is due to the presence of functional molecule but above certain concentration these get aggregated and phase separated leading decrease in the sensitivity. Hence, there appears a critical concentration of the phthalocyanine at which maximum sensitivity is obtained.

Table 3.7 Sensor characteristics of FePc and CoPc functionalized PANI towards NO_2 gas

Compound	Mol % of $M^{n+}Pc$	Sensitivity factor (S)	Speed of response (t_{50}) (Sec)
FePc-PANI	0.2	1.02	172
	0.5	1.07	145
	1	1.85	123
	2	1.03	113
CoPc-PANI	0.2	1.06	163
	1	1.13	138
	2	1.08	121

The reversibility of the samples were checked by applying vacuum, where in it showed a fall in resistance to the original value. Almost 60 to 90 % recovery was achieved. Reproducible and stable responses were obtained for these sensor samples. Although the FePc and CoPc incorporated polymer samples showed some sensitivity to NO_2 gas, the work was started aiming at homogeneous incorporation of metal phthalocyanine onto polyaniline back bone. However, its electrical conductivity values were found to decrease with the loading of FePc and CoPc and this could happen due to the formation of two phase system namely phthalocyanine and PANI its heterogeneous nature formed during synthesis and it has also been reflected in the IR and XRD studies. Hence, for further studies, it was proposed to functionalize the polyaniline with water soluble sulfonated metal phthalocyanines, which can form homogeneous solution along with the monomer aniline leading to better and uniform distribution of metal phthalocyanine onto the polymer matrix without phase segregation. Further, tetra-sulfonated phthalocyanine can be readily used for the electrochemical synthesis of functionalized PANI.

Section – B : Studies on tetra sulfonated iron phthalocyanine (TSFePc) doped Polyaniline (PANI)

3.4. Chemical synthesis of tetra sulfonated iron phthalocyanine doped PANI (TSFePc-PANI).

Typically, synthesis of TSFePc doped PANI was carried out as follows: Freshly distilled aniline 4 ml (44 mmol) was treated with 25 ml of 2 M dil hydrochloric acid. The aqueous solution of TSFePc was prepared by dissolving 0.414 g of TSFePc (1 mol % w.r.t aniline) 100 ml of water and it was added in drop wise to the acidified aniline solution. An aqueous solution of ammonium per sulphate containing 9.98 g in 200 ml of water was added into the above reaction mixture with constant stirring. The reaction was carried out at 5ºC by keeping it in ice bath for 4 hours. At the end of 4 hours, the reaction mixture was poured in a 1000 ml of water to precipitate out the product. The green mass obtained was filtered, washed with water to remove the excess dopant (during washing the color of TSFePc was not observed) and finally vacuum dried for 24 hours. Yield: 4.334 g. A similar procedure was followed for carrying out a series of above reaction by changing the concentration of dopant TSFePc from 0.1 to 1 mol % w.r.t aniline. The yields obtained for the above reactions are reported in Table 3.8.

Table 3.8. Summary of the yield of reaction TSFePc and Aniline

No	TSFePc added (mol%)	Yield of TSFePc-PANI(g)	PANI Conversion (%)
1	0	3.628 (PANI alone)	88.3
2	0.1	3.723	90.6
3	0.2	3.835	93.1
4	0.5	4.067	95.7
5	1	4.334.	97.1

When the PANI conversion was ploted (Fig. 3.12) against the concentration of TSFePc used, the reaction follows the equation $A + Bx - Cx^2$ as discussed in the section 3.2. Here the catalytic activity of phthalocyanine is more as seen from the higher value of B when compared to the FePc-PANI and CoPc-PANI systems.

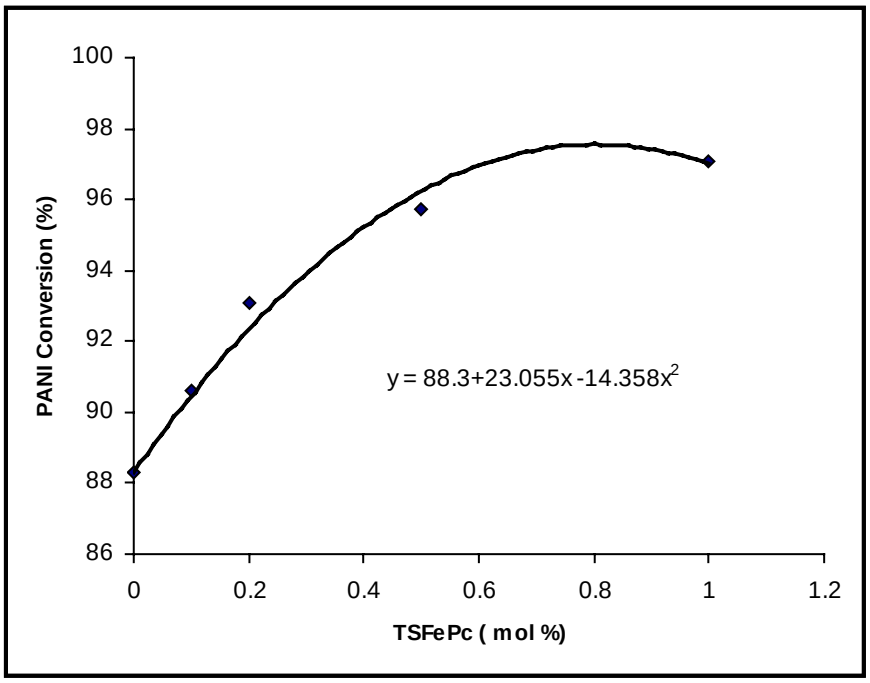

Fig .3.12. The plot of PANI conversion versus TSFePc concentration.

3.5. Results and Discussion

3.5.1. Characterisation of Structure

The structure of the newly synthesized phthalocyanine incorporated polymer was characterized thoroughly by the following physico-chemical techniques.

3.5.1.1. FT-IR studies

The functionalization of conducting polyaniline with TSFePc was confirmed by recording FT-IR spectra of the newly synthesized polymers. The FT-IR spectra of TSFePc functionalized polyaniline is shown in Fig. 3.13. One can see a significant difference in the peak positions of IR spectra of TSFePc functionalized PANI. The FT-IR spectra of TSFePc functionalized PANI showed a significant increase in the intensity of Q and B bands suggesting extra doping by sulfonic acid group. The band corresponding to the asymmetric and symmetric stretching of O=S=O group in TSFePc appeared at 1390 cm^{-1} and 1116 cm^{-1} in the functionalized PANI [22]. The band corresponding to benzenoid structure at 1494 cm^{-1} is found to shift towards lower energy (1489 cm^{-1}) with increased intensity [23,24] and the band corresponding to imine nitrogen at 1163 cm^{-1} in PANI also has been shifted to 1134 cm^{-1} [25]. Hence, it can be concluded that, there exits a strong interaction between the sulfonic acid group of TSFePc and the imine nitrogen carrying (+) ve charge which not only confirms the incorporation of TSFePc in PANI but also the additional doping by the same. The complete assignment of bands in the FTIR spectra of PANI and TSFePc-PANI are given in Table 3.9.

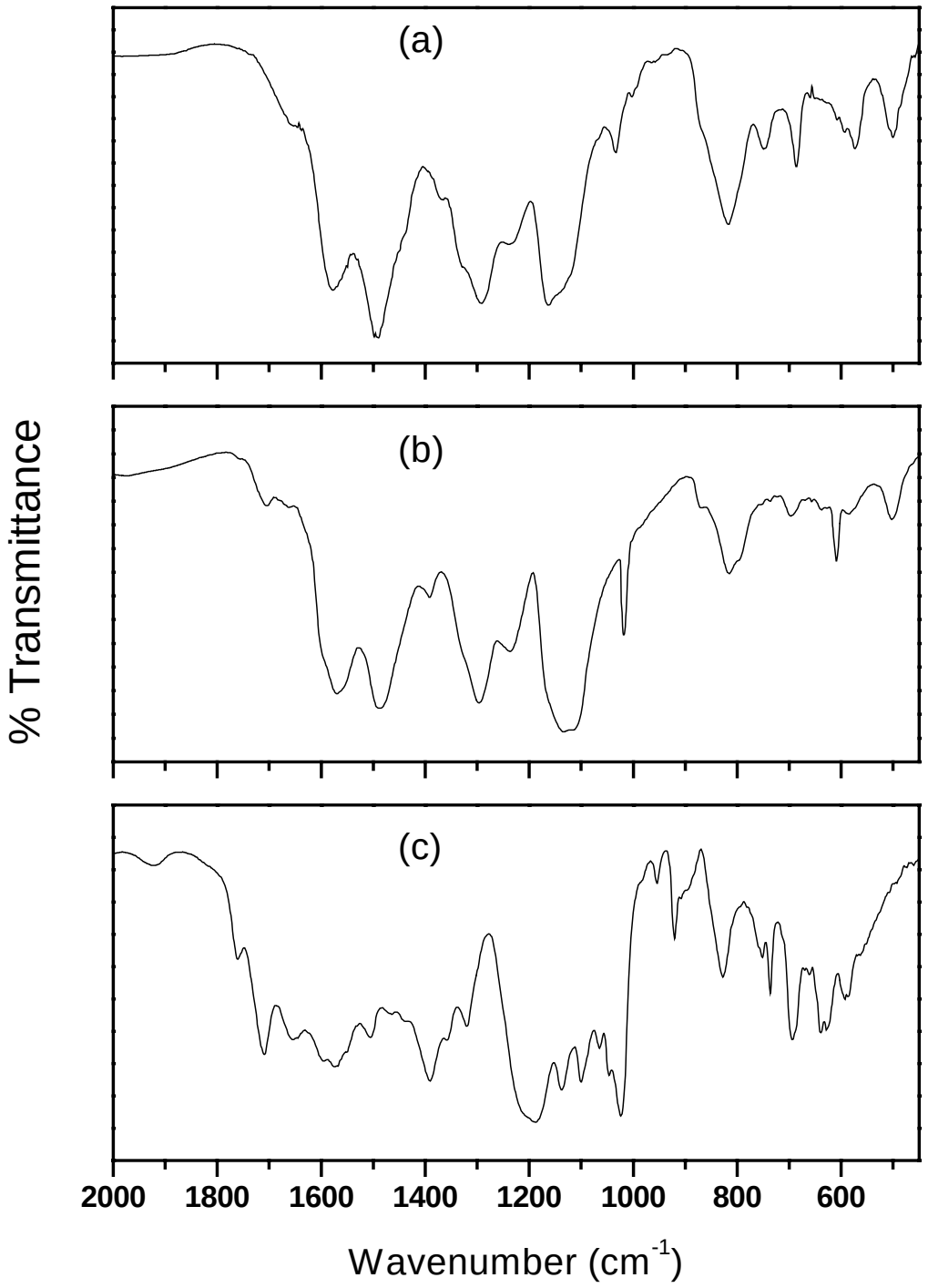

Fig. 3.13. FT IR Spectra of (a) HCl doped PANI; (b) TSFePc functionalized PANI; (c) TSFePc

Table 3.9 Assignments of bands in the FTIR spectra of PANI, TSFePc-PANI

Peak positions (cm^{-1})		IR band assignments
PANI	**TSFePc-PANI**	
-	1697 w	υ(C=C)stretching in Pc skeleton
1580 s	1567 s	Quinoid ring stretching
1494 s	1489 s	Benzenoid ring stretching
-	1390 w	Asymmetric stretching of O=S=O
1307 s	1294 vs	υ(C-N) stretching vibration of aromatic ring
1163 vs	1134 m	B-N^{+}H-B stretching Vibration
-	1016 m	symmetric stretching of O=S=O
817 s	813 s	para disubstituted benzene ring
748 m	702 m	γ(C-H) out of plane deformation
686 m	688 w	υ(C-C) ring stretching
571 m	589 m	Out of plane (C-H) bending vibration
501 m	499 m	γ(C=C) out of plane ring bending

vs: very strong, s: strong, m: medium, w: weak

3.5.1.2. Wide Angle X-ray Diffraction (WAXD) Studies

The synthesized TSFePc-PANI was characterized by WAXD and the patterns obtained are shown in Fig. 3.15. The X-ray profile of TSFePc alone is shown in Fig. 3.14. for comparison. The major reflections in the diffraction pattern of PANI, TSFePc-PANI and TSFePc is presented in Table 3.10. The crystal structure of HCl doped PANI are in well agreement with the reported data [18]. It can be seen that, it has a certain percentage of crystallinity before treating with TSFePc having 2θ values at 8.9, 15, 20.3, 25.4 and 27. The TSFePc was found to have well defined crystalline structure having reflections at 2θ values 9.1, 12.9, 19.4 and 26.

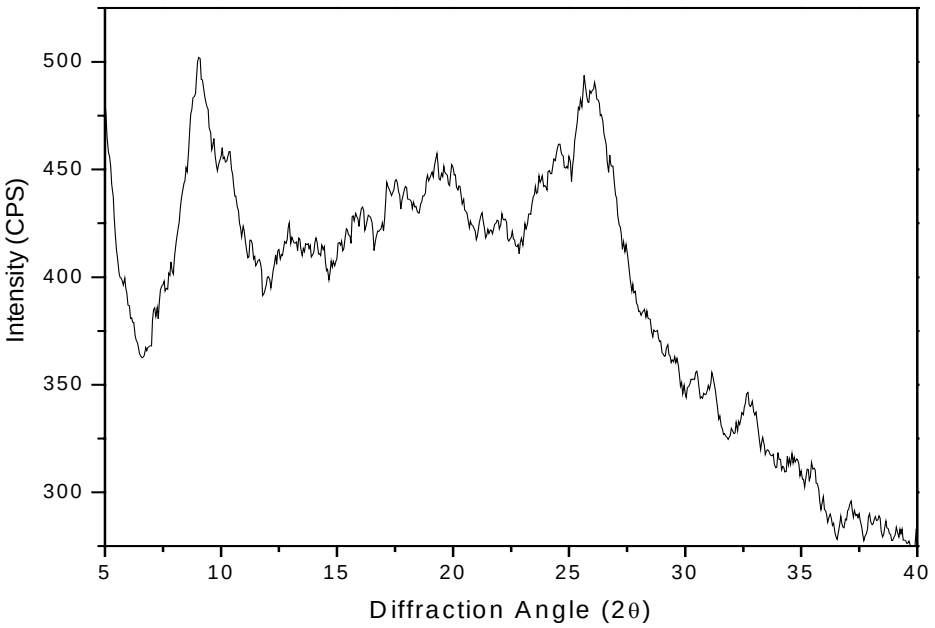

Fig. 3.14. X-ray diffractogram of TSFePc

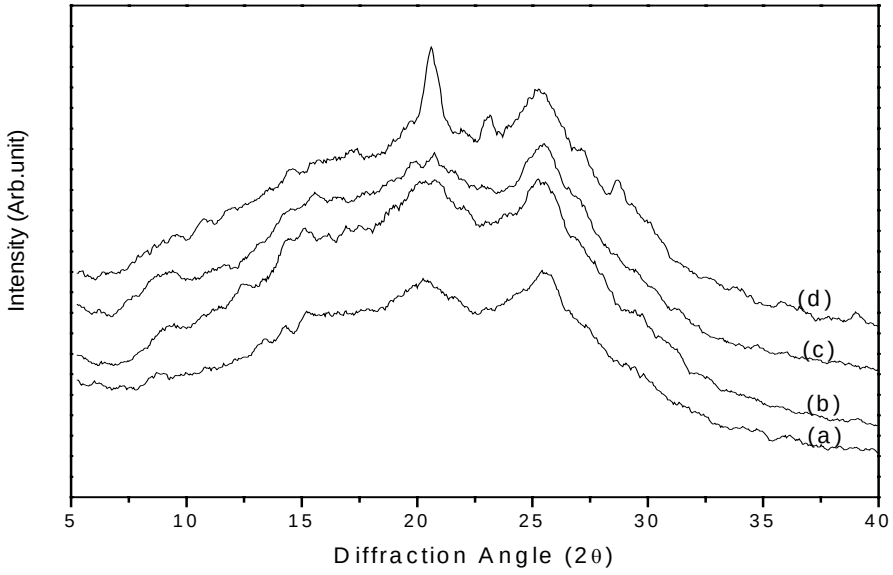

Fig. 3.15. X-ray diffraction pattern of various mol % of TSFePc incorporated PANI

(a) PANI, (b) 0.2 mol % FePc, (c) 0.5 mol % FePc (d) 1 mol % FePc

Table 3.10. Major reflections in the X-ray diffraction patterns

Compound	2 Theta	I/Io	d-spacing
PANI	8.9	37	9.92
	15.0	54	5.9
	20.3	74	4.37
	25.4	100	3.5
	27.0	78	3.3
TSFePc-PANI	20.3	100	4.37
	25.4	89	3.50
TSFePc	9.1	100	9.70
	12.9	84	6.85
	19.4	90	4.57
	26.0	96	3.42

However, its XRD peak intensities and breadth indicate much lower ordered structure, i.e. the crystallite size is much smaller than FePc. After functionalization of PANI with TSFePc, the very prominent peak at 9.1 is completely absent suggesting that there is no separate phthalocyanine phase left and that this phthalocyanine is homogeneously incorporated in the polymer matrix. The role of the counter-ion and solvent medium in determining the structure of doped PANI samples has been reported earlier. Pouget et al. [26] have observed two different crystalline forms of emeraldine base and its salt depending on the method of preparation, even though the chemical composition is the same in each case. Both crystalline arrangements belong to the orthorhombic system. The difference between them is found in the packing of chains and the counter ions within the

cell. Lux [27] has got totally different crystal structure upon precipitating the PANI powder in conc. sulfuric acid. In our system, the bulky counter ion TSFePc accommodates itself into the PANI structure to maintain the electroneutrality of the polymer which leads to a better stacking and increase in molecular ordering as noticed by the peak at 2θ value 20.3º. In present case also there is considerable increase of this peak intensity after incorporation of TSFePc in PANI (see curve d in Fig. 3.15).

3.5.1.3. UV- Visible studies

The typical UV-Vis absorption spectrum of TSFePc and TSFePc- PANI at 350-900 nm regions are shown in Figs. 3.16. and 3.17. For UV-Vis studies the solutions of TSFePc and TSFePc-PANI were prepared in water and formic acid. The UV-Vis spectrum of TSFePc is well reported in the literature [29]. It showed a strong absorption band at 770 nm termed the Q-band. In addition there is a strong absorption band in the UV region at 375 nm, denoted as B-band (or Soret band). It is well known that, polymers having conjugation by the overlap of P_z orbitals of SP^2 hybridized carbons exhibit one absorption band in the visible region ascribed to π-π^* electronic transition. In the UV-Visible spectra of TSFePc functionalized PANI, the π-π^* transition was seen at 375 nm and this showed red shift upon incorporating TSFePc into PANI. Apart from this, two additional bands were observed at 590 nm and 780 nm. The absorption band at 590 nm can be ascribed to the benzenoid to quinoid excitonic transition and the third band at 780 nm can be ascribed to the polaron to bipolaron transition [30] and this band shows a red shift upon functionalization with TSFePc. The change in wavelength of polaron to bipolaron transition is presented in Table 3.11. The intensity of Q-band in Pc is particularly

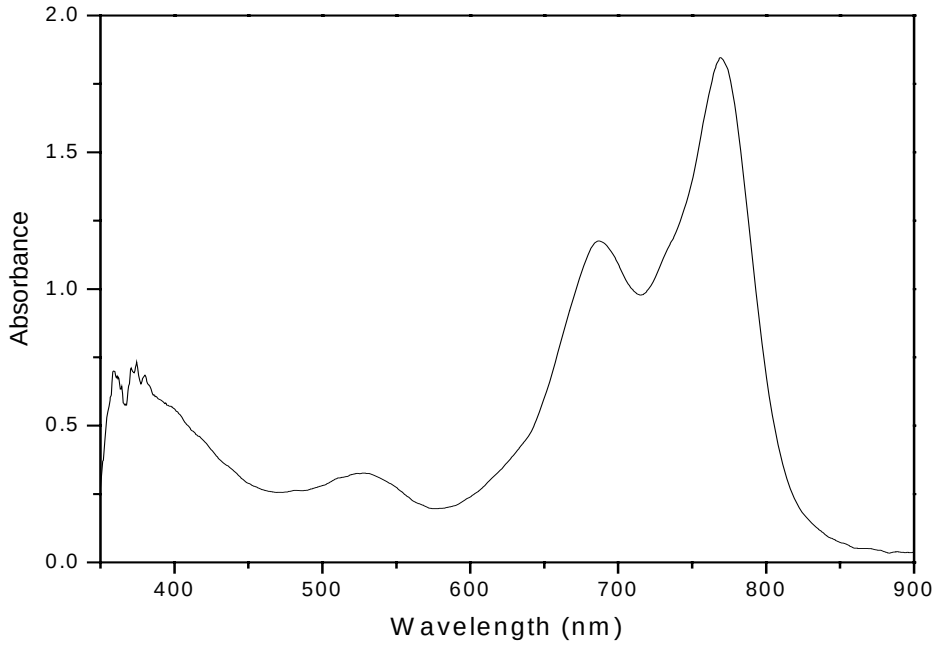

Fig. 3.16. UV-Vis absorption spectra of TSFePc

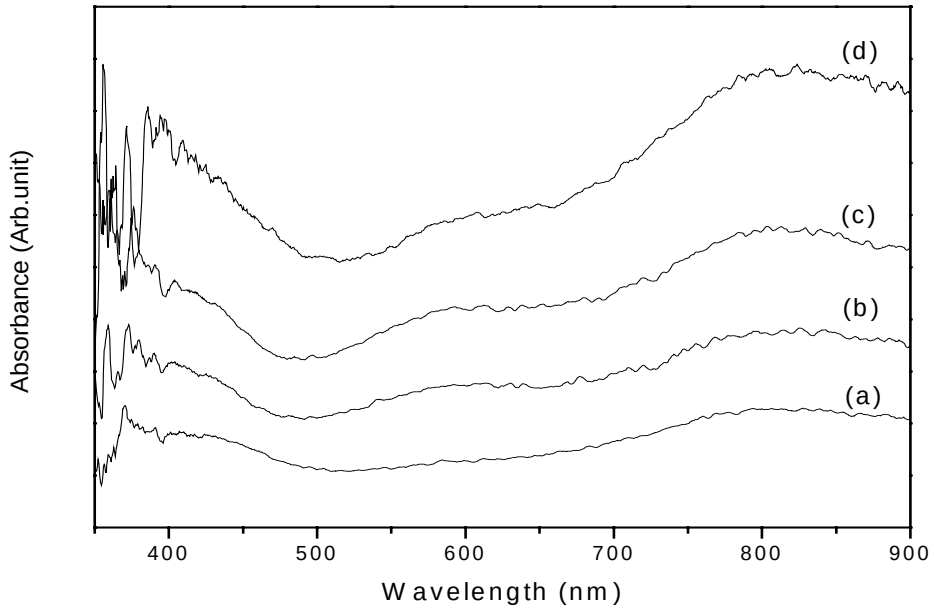

Fig. 3.17. UV-Vis absorption spectra of PANI incorporated with various mol % of TSFePc (a) PANI, (b) 0.2mol % TSFePc, (c) 0.5 mol % TSFePc (d) 1 mol % TSFePc

Sensitive to substitution and environment of the Pc macrocycle [31]. After functionalization, since TSFePc is well trapped inside the polymeric chains, the absorption due to Q-band is greatly suppressed. This also indicates that there are no free TSFePc aggregates formed and all the Pc matrics are fully dispersed at molecular level in PANI. It is also appropriate to mention that when PANI is functionalized with TSFePc, extended delocalisation of π electrons over the phthalocyanine macrocyclic frame work and the additional doping effect due to sulfonic group, makes it more conducting and this is indeed observed from the increase in the absorption at 830 nm as well as beyond it. The higher conductivity has been found to be true from the studies on electrical properties discussed later in the chapter.

Table 3.11 Polaron-bipolaron transition for TSFePc incorporated PANI

No	TSFePc (Mol %)	Polaron-bipolaron transition λ (nm)
1	0 (PANI)	804
2	0.2	809
3	0.5	812
4	1	826

3.5.1.4. Graphite Furnace Atomic Absorption spectroscopic (GFAAS) studies

The percentage of iron in the TSFePc functionalized PANI was estimated using this technique. From the percentage of iron, we calculated the amount of TSFePc get doped with PANI. The various mol % of TSFePc in PANI and the percentage of iron

present are presented in Table 3.12. It can be seen that the iron content in functionalized sample increases gradually upon increasing the mol % of TSFePc and the content is almost same as the content taken at the start of the reaction. This clearly indicates that the amount of sulphonated phthalocyanine added during synthesis has been fully functionalized and it has not been washed out during the work up of the product.

Table 3.12. The percentage of iron content in various mol % TSFePc functionalized PANI

Compound	Iron content (wt%)
PANI-0.2 mol% TSFePc	0.102
PANI-0.5 mol% TSFePc	0.239
PANI-1 mol% TSFePc	0.532

3.5.1.5. Energy Dispersive X-ray (EDX) studies

The percentage of two dopants namely chloride and sulfonated iron phthalocyanine were determined by analyzing the chlorine and iron content in the synthesized sample using EDX technique. The EDX spectra of the PANI with various mol percentage of TSFePc is shown in Fig. 3.18.

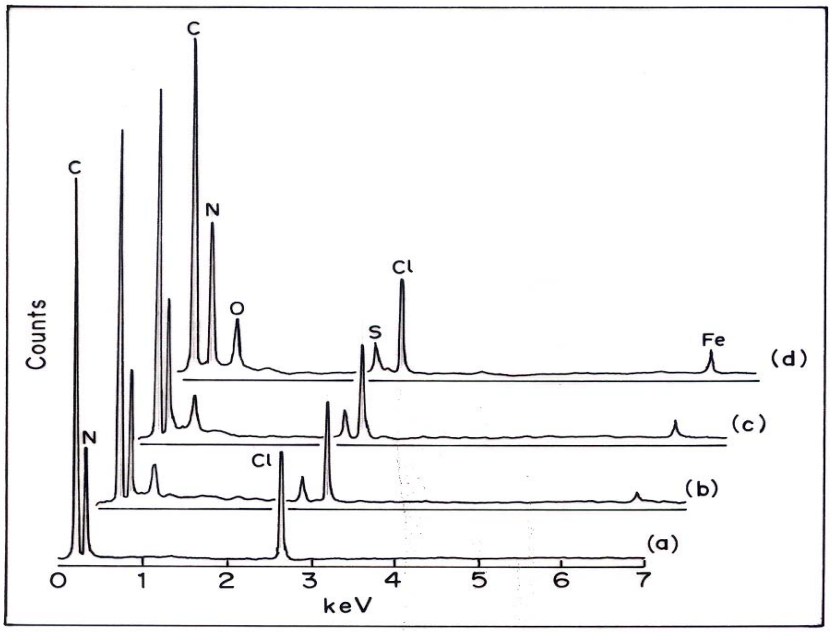

Fig. 3.18. The EDX spectra of the PANI with various mol percentage of TSFePc (a) PANI (b) 0.2 mol % TSFePc (c) 0.5 mol % TSFePc (d) 1 mol % TSFePc

3.5.2. Measurement of properties

The properties of the newly synthesized TSFePc–PANI like electrical conductivity, thermal stability, morphology of the sample and its application for NO_2 gas sensing are discussed in this section.

3.5.2.1. Electrical Conductivity

The electrical conductivity at room temperature for functionalized PANI shows that the sulfonated phthalocyanine functional molecule plays an important role in determining the PANI conductivity than the unsubstituted phthalocyanine. The plot of conductivity versus mol % of TSFePc in PANI are shown in Fig. 3.19. Apart from the primary dopant HCl, when the phthalocyanine concentration was increased from 0.1 to 1 mol %, the electrical conductivity of PANI was found to increase from 2.77 x 10^{-3} to 4.69

x 10^{-3} S/cm. This may be contrasted with the FePc (without sulfonic group) incorporated PANI where the conductivity decreased almost by an order of magnitude. In the case of TSFePc-PANI samples, it is expected that when the phthalocyanine with four sulfonic acid group at the periphery is incorporated into polyaniline chains, apart form conduction due to intrachain, the contribution from interchain conduction also increases due to the highly conjugated phthalocyanine moiety.

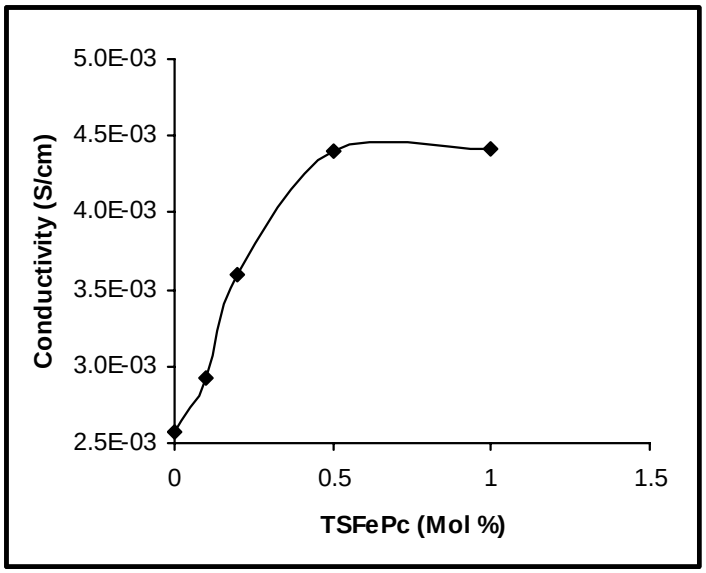

Fig. 3.19. Plot of conductivity versus TSFePc concentration in PANI

It links the two polymer chains through its sulfonic acid group withdrawing electron from the polymer backbone thereby creating more defects on it and hence the conductivity increases upto a certain concentration of phthalocyanine and after that the conductivity remains almost same. It is also reported in the literature [32] that when a bulky molecule is introduced into polyaniline, there is a change in the confirmation of polymer backbone from a coil like to a more expanded conformation. This change in conformation could

lead to extra doping effect called secondary doping which in turn increases the conductivity. The change in PANI chain conformation is clearly seen from the increase in the intensity of the peak at 20.3 in the X-ray diffractogram of functionalized PANI (see Fig. 3.15 (d)).

3.5.2.2. Thermal stability

Among the conducting polymers, PANI is claimed to have the highest environmental stability. From an industrial point of view it would be useful to be able to thermally process this material into useful product using conventional techniques such as extrusion, stretching, rolling, etc., which are generally carried out at elevated temperatures. Therefore, a study of the thermal properties was performed to examine the thermal stability of this material and to identify the maximum application temperature. The thermogram of TSFePc - PANI is shown in Fig. 3.20. along with the thermogram of PANI and TSFePc for comparison. The counter anion sulfonated phthalocyanine undergoes degradation in two steps, where in the first step sulfonic acid group is disassociated at 260ºC and in the second step phthalocyanine main molecule starts degrading at 514ºC [33]. In the TG thermogram, the HCl doped PANI and TSFePc functionalized PANI shows a similar pattern of thermogram but an increased thermal stability has been observed for TSFePc – PANI. All the functionalized polymers show two major weight losses. The first step weight loss corresponds to the removal of adsorbed water and the chloride dopant [34] and the second one is attributed to the structural decomposition of polymer backbone [35]. It can be seen that the thermal stability of the functionalized PANI increases as a function of sulfonated phthalocyanine.

This could be due to the stabilization of polymer backbone by the sulfonated phthalocyanine through its sulfonic acid group linking the polymer chains together to give better thermal stability. The weight retention of PANI-HCl at 600°C is 62 %.where as 0.5 mol % TSFePc and 1 mol % TSFePc functionalized PANI samples showed a weight retention of 66 and 69 % respectively. Hence we are confident enough to say that the phthalocyanine has a significant effect on the thermal stability of the doped polymer.

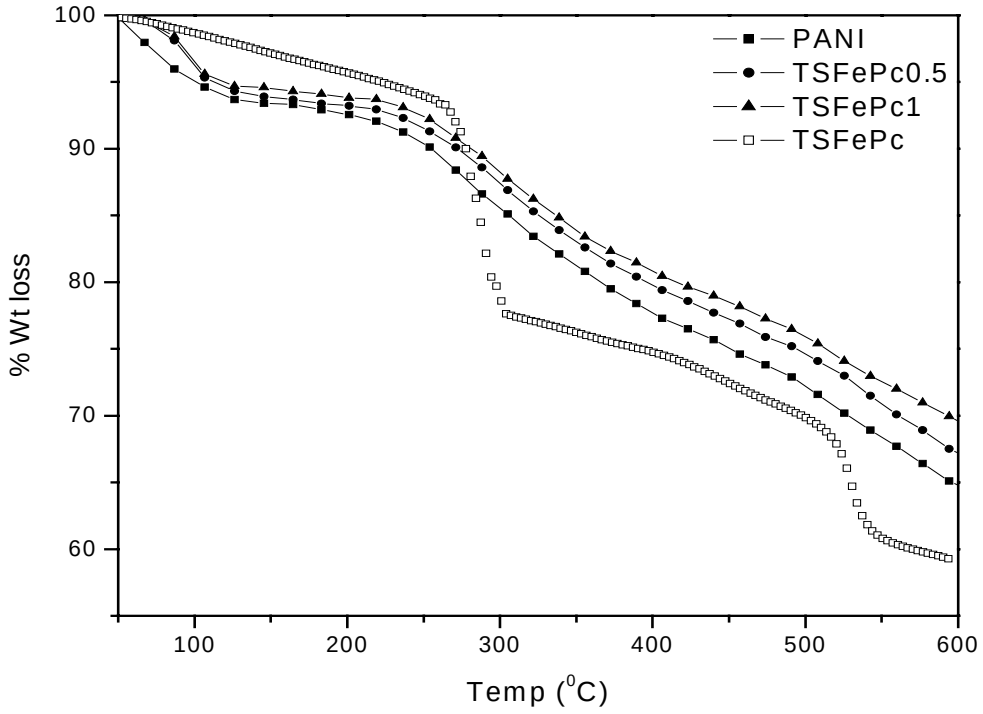

Fig.3.20. Thermogravimetric analysis of TSFePc functionalized PANI samples

3.5.2.3. Scanning Electron Microscopy (SEM) Analysis

The morphology of the synthesized polymer samples were analysed using scanning electron microscope, which clearly shows the samples were particulate in nature. The scanning electron microscopy of the samples are shown in Fig. 3.21.

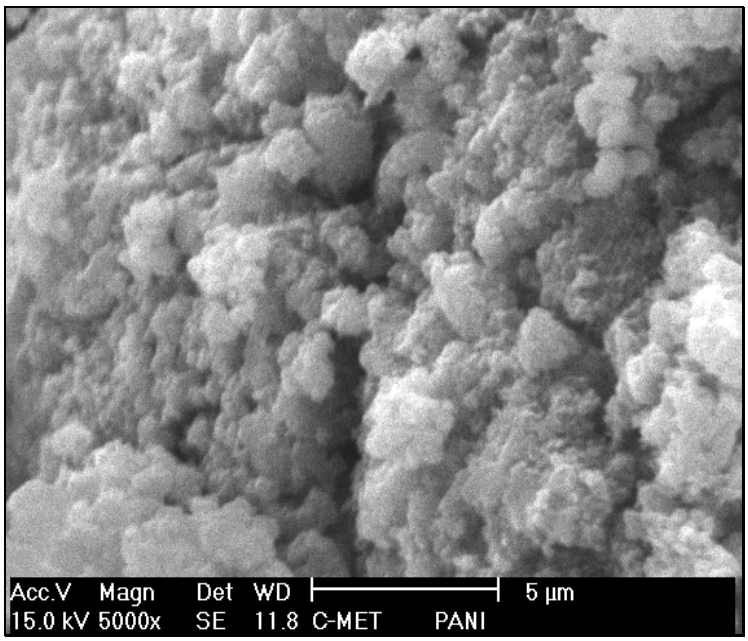

(a)

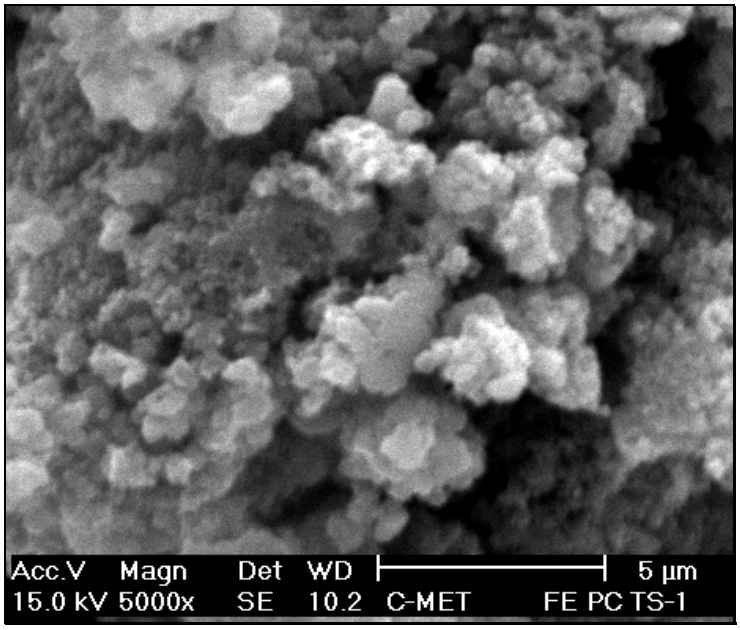

(b)

Fig. 3.21. Scanning Electron Micrograph (SEM) of (a) PANI-HCl
(b) TSFePc-PANI

3.5.2.4. Chemical sensor

The sensitivity of TSFePc functionalized PANI was tested with respect to 100 ppm NO_2 gas at room temperature. The fabricated sensor was taken in a specially designed chamber which in turn was connected to Keithley interfaced with a computer. The change in resistance upon exposure to NO_2 gas was monitored online. The response characteristics of PANI with different concentration of TSFePc, is shown in Fig. 3.22. when the sample was exposed to NO_2 gas, an increase in resistance was observed. The unsubstituted and substituted phthalocyanine incorporated PANI shows different mechanism of NO_2 gas sensing.

An unusual response in magnitude and sign observed in the case of TSFePc-PANI suggests a significant role of the incorporated sulfonated phthalocyanine in the polymeric chain. As the responses observed in the present case are in contrast with that of the conventional trend, the sensing behaviour is likely to involve a different process, especially interaction of NO_2 gas with sulfonated phthalocyanine. Although, the exact mechanism of sensing is not very clear at this stage, the probable phenomena for increase in resistance on exposure to NO_2 gas can be interpreted by considering the interaction of NO_2 gas with the dopant sulfonated phthalocyanine. In the NO_2 gas environment, NO_2 molecule takes up the proton from phthalocyanine sulfonic acid and decreases the doping level of PANI. As a result the conductivity of TSFePc-PANI drops. i.e. an increase in resistance was observed. Radhakrishnan et al. [36] have also observed similar characteristics with very high sensitivity factor and they have explained based on the diffusion of vapours through inter-domain spaces of the conducting polymer moieties. A pictorial representation of probable mechanism of interaction of NO_2 gas with

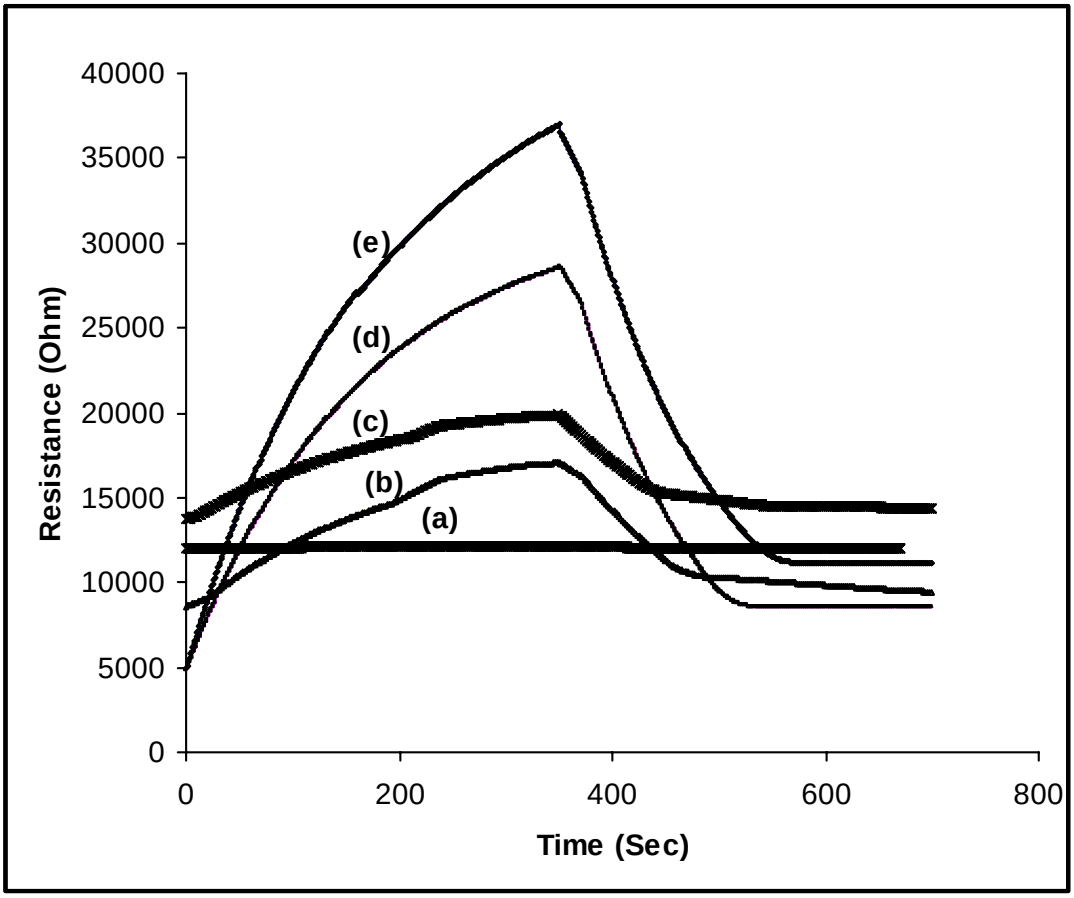

Fig. 3.22. Response characteristics of TSFePc incorporated PANI towards NO_2 gas. (a)PANI, (b) 0.1 mol % TSFePc-PANI , (c) 0.2 mol % TSFePc-PANI , (d) 0.5 mol % TSFePc-PANI and (e) 1 mol % TSFePc-PANI

phthalocyanine and the polymer is given at the end of this chapter. The sensitivity factor (S) was calculated using the formula

$$\mathbf{S = R/Ro}$$

Where, Ro is the resistance before exposure to NO_2 gas and R is the resistance after exposure to gas. The pure polyaniline was not found to be much sensitive to chemical vapours, whereas TSFePc-PANI polymers show enhanced sensitivity.

The plot of sensitivity factor and speed of response versus different concentrations of TSFePc in PANI are shown in Fig. 3.23. It's quite interesting to note the tremendous sensitivity of these samples to the vapours of nitrogen dioxide. The sensitivity factor and speed of response of these phthalocyanine functionalized PANI samples are presented in the Table 3.13. The response time t_{50} was found to decrease with increase in phthalocyanine concentration. The interesting aspect that emerges from these studies is that the sensitivity factor is higher and speed of response is much faster in TSFePc – PANI samples than FePc and CoPc incorporated PANI samples.

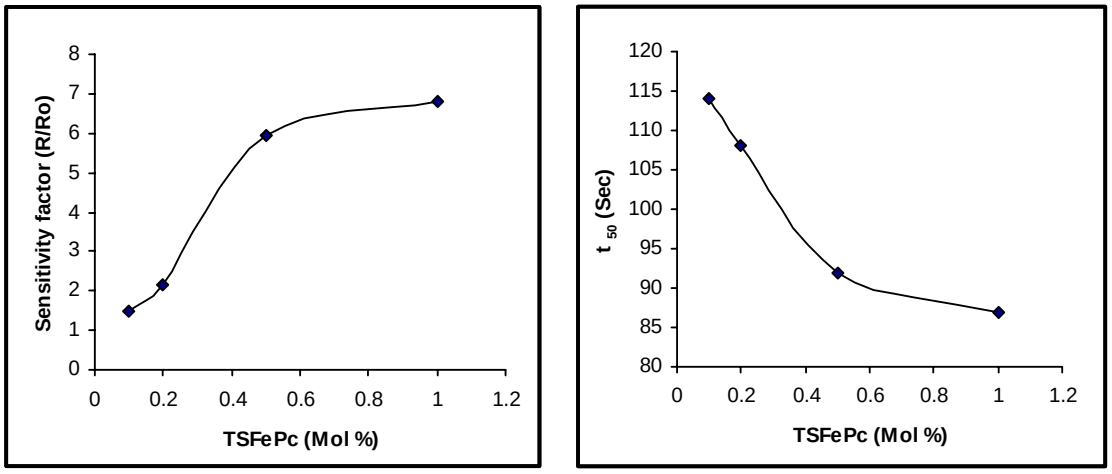

(a) (b)

Fig. 3.23. Sensor characteristics of TSFePc functionalized PANI towards NO_2 gas

(a) Plot of sensitivity factor versus concentration of TSFePc

(b) Speed of response (t_{50}) versus concentration of TSFePc

Table 3.13 Sensor characteristics of TSFePc functionalized PANI towards NO2 gas

Compound	Mol % of TSFePc	Sensitivity factor (S)	Speed of response (t_{50}) (Sec)
TSFePc-PANI	0.1	1.50	114
	0.2	2.14	108
	0.5	5.92	92
	1	6.81	87

The reversibility of the samples were checked by applying vacuum, it showed a fall in resistance to the original value and almost 60 to 90 % recovery was achieved. Reproducible and stable responses were obtained for these sensor sample.

3.6. Electrochemical Synthesis of tetra sulfonated iron phthalocyanine doped PANI (TSFePc-PANI).

The TSFePc was electrochemically doped into PANI by means of cyclic voltammetric (CV) and chronoamperometric techniques. The electrochemical cell was a classical three electrode cell consisted of platinum or ITO glass electrode with a geometric area of 1 cm^2 as working electrode for the deposition of functionalized PANI. The counter electrode was platinum and the standard calomel electrode (SCE) was used as reference.

The procedure for the synthesis of TSFePc incorporated PANI by cyclic voltammetric technique is as follows: 0.2 ml (2 mmol) of freshly distilled aniline was acidified with 10 ml of 2 M hydrochloric acid. 20 mg ($2x10^{-5}$ mol) of TSFePc dissolved

in 10 ml of water was added into the above solution and taken in a single compartment electrochemical cell. A very low concentration of monomer was used to prevent the polymer protrude out of the electrode surface. A thin film TSFePc incorporated PANI was deposited on platinum and ITO electrodes by cycling a potential of -0.2 volt to 1 volt for four cycles at 50 mV/s. The experiments were carried out at room temperature under nitrogen atmosphere. The thin film deposited on the electrode was taken out from the electrolytic bath, washed several times with water to remove excess acid and used it for further characterisation. A similar procedure was followed for the electrodeposition of PANI with different mol % (0.2, 0.5 and 1) of TSFePc. A typical cyclic voltammogram of TSFePc – PANI synthesis is shown in Fig.3.24.

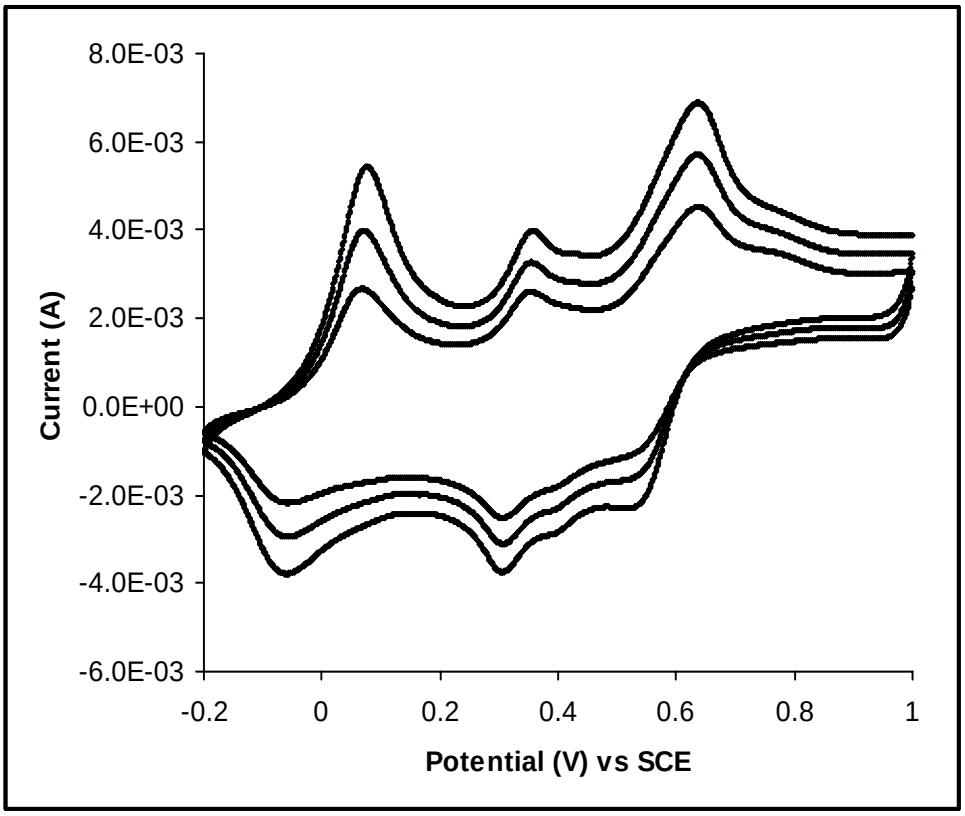

Fig. 3.24. Cyclic voltammogram obtained during electrodeposition of TSFePc-PANI

3.6.1. Fabrication of Chemical sensor

PET sheet was cleaned well and coated with thin film of gold by vacuum deposition technique. Interdigitated electrode was made by drawing a pattern on it and activated by keeping it at 1M $FeCl_3$ solution for 24 hours. Two leads were taken from the interdigitated electrode for electrical contact. Using interdigitated gold electrode as working electrode, the TSFePc–PANI was deposited onto it by means of chronoamperometric technique. The procedure for the deposition of TSFePc–PANI by chronoamperometric technique is same as mentioned above, here instead cycling the potential, a constant potential of 800mV was applied for 300 Sec. A typical chronoamperometric curve is shown in Fig.3.25. Care was taken to have uniform film of surface area of 1 cm^2. The modified PANI thin film deposited on the interdigitated electrode was removed from the electrolytic bath, rinsed with water to remove extraneous materials and finally dried in vacuum for 24 hours. The fabricated sensor was then tested with 100 ppm NO_2 gas in a specially designed testing chamber.

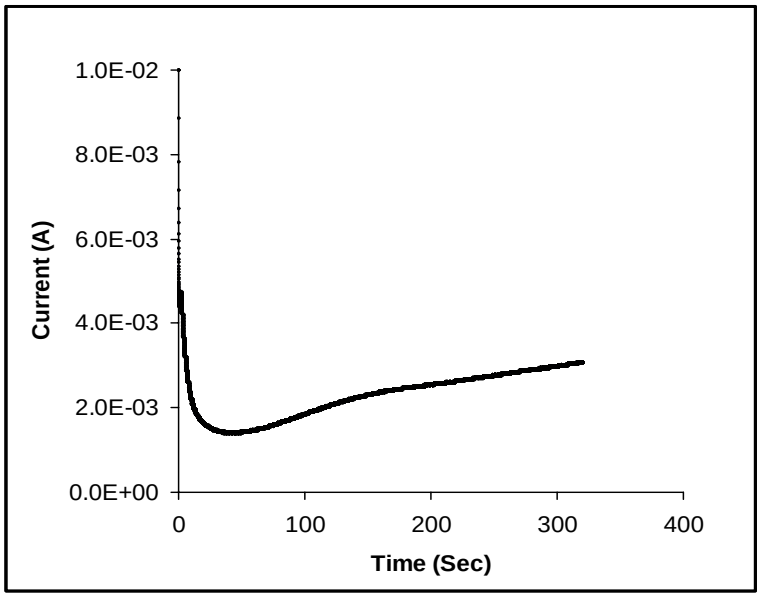

Fig.3.25. Chronoamperometric curve for the electrodepostion of TSFePc -PANI

3.7. Results and Discussion

3.7.1. Characterisation of Structure

The structure of the electrochemically synthesised TSFePc –PANI was characterized thoroughly by the following spectroscopic techniques.

3.7.1.1. FT-IR studies

The incorporation of TSFePc onto conducting polyaniline by electrochemical route was confirmed by FT-IR spectra of the polymers. IR spectra of the samples were recorded by scraping the deposited material from the platinum electrode and a thin wafer was formed by grinding it with IR grade KBr. Fig.3.26 shows the FT-IR spectra of emeraldine salt form of electrochemically synthesized PANI and TSFePc functionalized polyaniline. In the FT-IR spectra of PANI, the absorption band at 1155 cm^{-1} represents protonation of imine nitrogen. The absorption peaks at ca. 1575 cm^{-1} and 1494 cm^{-1} are assigned to quinoid (Q) and benzenoid (B) C=C stretches of emeraldine form of PANI respectively. Apart from this, the polymer shows C–N aromatic stretching vibrations and C-H out of plane bending vibration at 1310 cm^{-1} and 510 cm^{-1}. On the other hand, the FT-IR spectra of TSFePc functionalized PANI showed a significant difference in the wavenumber with respect to their corresponding bands in PANI. The bands corresponding to quinoid and benzenoid structure at ca. 1575 cm^{-1} and 1494 cm^{-1} is found to shift towards lower energy (ca. 1566 and 1490 cm^{-1}). with increased intensity. The band corresponding to the asymmetric stretching of O=S=O group in TSFePc and phthalocyanine (Pc) skeleton in the functionalized PANI seems to overlap with the bands corresponding to PANI and it appears as broad band at 1155 cm^{-1}.

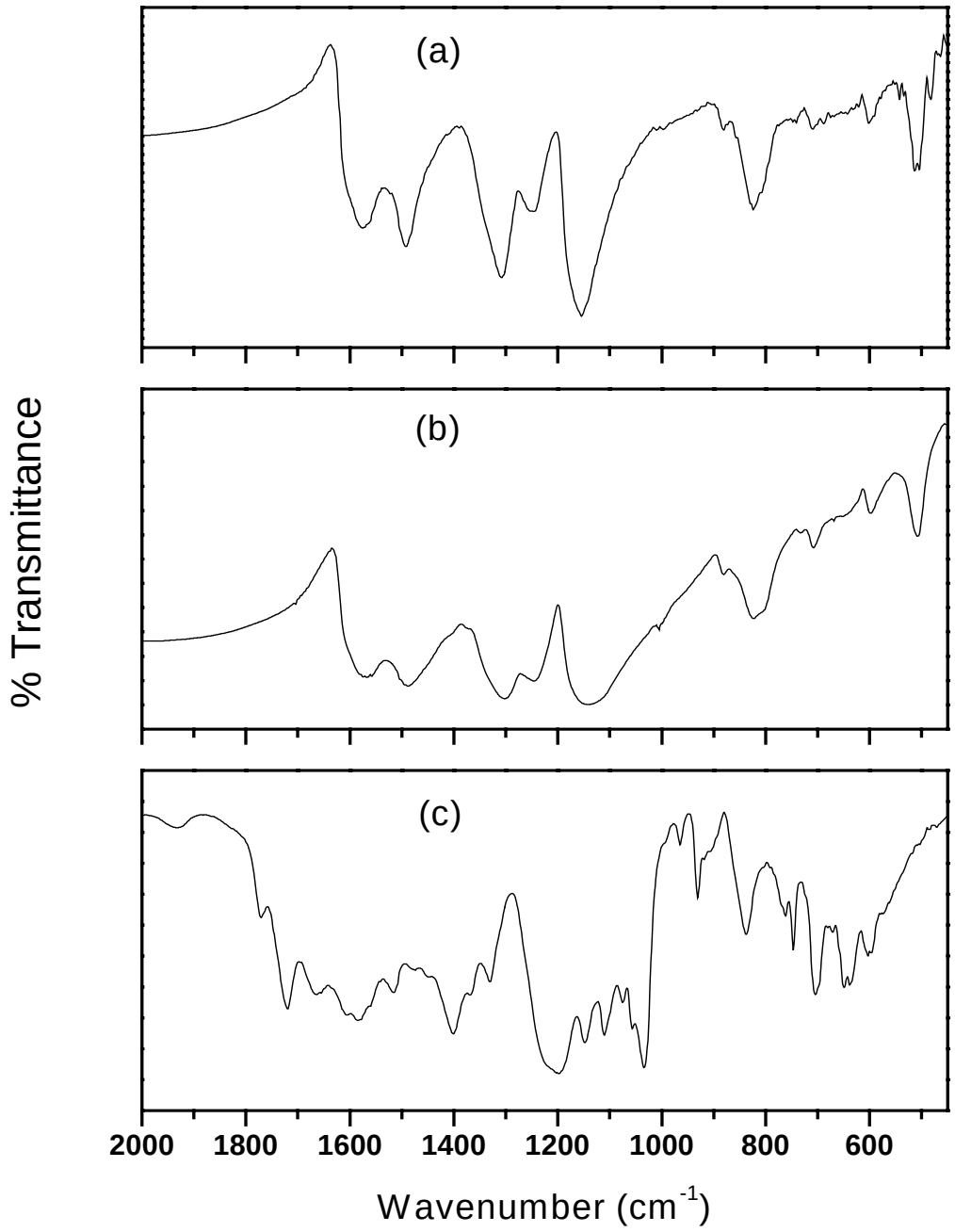

Fig.3.26. FTIR spectra of electrochemically functionalized polyanilines.

(a) HCl doped PANI, (b) TSFePc functionalized PANI, (c) TSFePc

Additionally the band at 708 cm^{-1} in the functionalized PANI corresponds to the Pc skeleton showing the signature of the TSFePc incorporation in polymer matrix. The major absorption bands and their assignments are presented in Table 3.14.

Table 3.14. FTIR band assignments for electrochemically functionalized PANI

Peak positions (cm^{-1})		**IR band assignments**
PANI	**TSFePc-PANI**	
1575 s	1566 s	Quinoid ring stretching
1494 s	1490 s	Benzenoid ring stretching
1310 s	1299 s	υ(C-N) stretching vibration of aromatic ring
1155 vs	1136 vs	$B\text{-}N^{+}H\text{-}B$ stretching Vibration and
-	1002 w	Symmetric stretching of O=S=O
824 s	822 s	para disubstituted benzene ring
-	708 m	γ(C-H) out of plane deformation of TSPc
600 w	600 w	υ(C-C) ring stretching
510 m	510 m	Out of plane (C-H) bending vibration

vs: very strong, s: strong, m: medium, w: weak

3.7.1.2. UV- Visible studies

The electronic absorption of conducting polymers are useful in investigating the oxidation and doping state of the polymer backbone [37].The UV-Vis spectrum of PANI and TSFePc loaded PANI films on the ITO plate were taken in the reflectance mode at 350-900 nm regions are shown in Fig. 3.27. The broad band at 393 nm and 768 nm in PANI can be ascribed to π - π^{*} electronic transition and polaron to bipolaron transition which are responsible for the conductivity of the polymer [38].

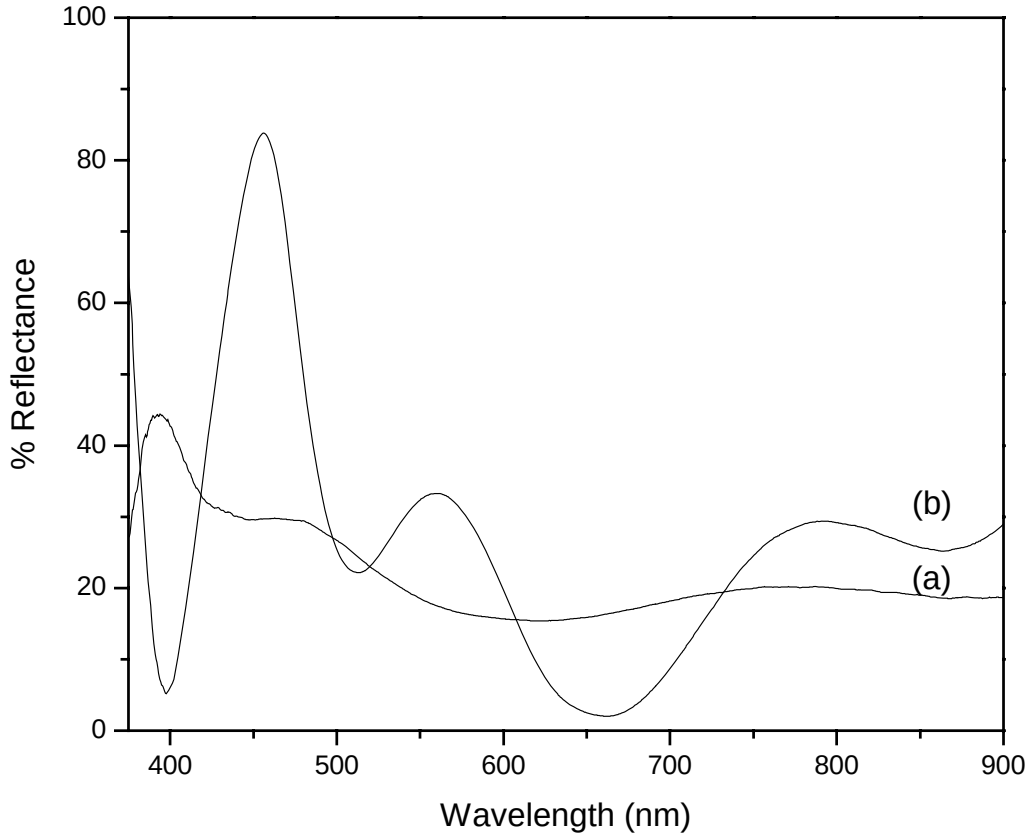

Fig. 3.27. The UV-Vis absorption spectrum of electrochemically deposited (a) PANI-HCl and (b) TSFePc functionalized PANI films.

Whereas the UV-Visible spectra of TSFePc functionalized PANI showed the π - π^* transition at 455 nm and two additional bands at 562 nm and 795 nm corresponding to benzenoid to quinoid excitonic transition and polaron to bipolaron transition. In Fig.3.27(b) the red shift in π - π^* transition and polaron to bipolaron transition are clearly visible and this is possible only when the extension of conjugation occurs after functionalization.

3.7.1.3. Wide Angle X-ray Diffraction (WAXD) Studies

The Electrochemically synthesized TSFePc-PANI was characterized by WAXD to identify its nature of crystallinity. The X-ray diffraction profiles of PANI and TSFePc-PANI are shown in Fig. 3.28. The X-ray diffraction studies were carried out by keeping the gold coated glass containing electrodeposited material over the sample holder slot

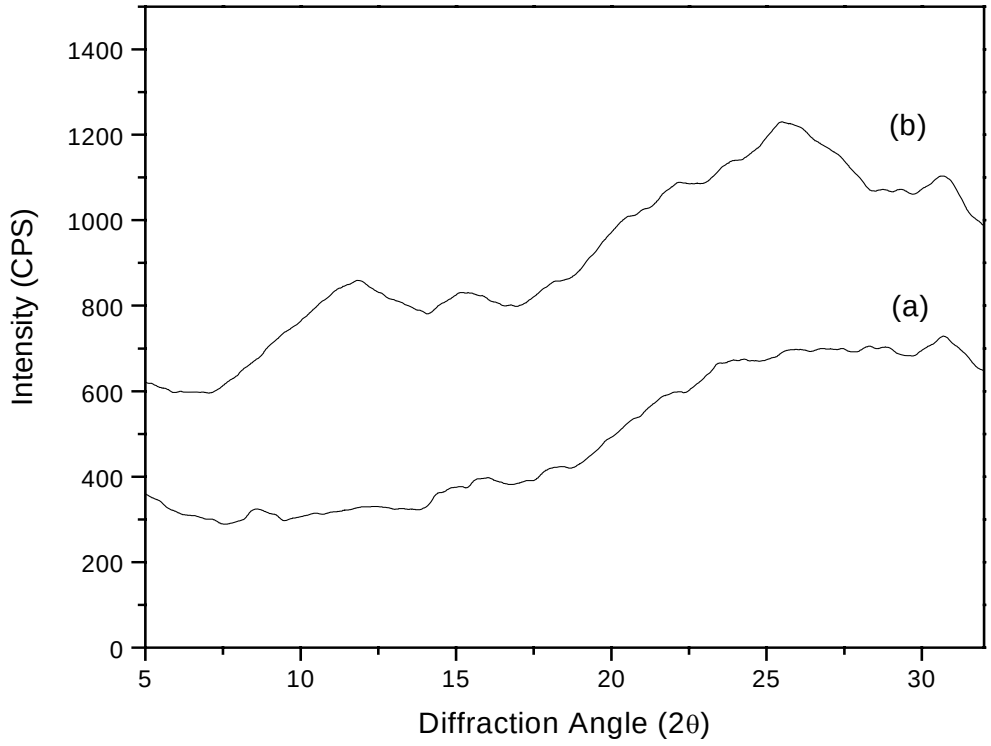

Fig. 3.28. Wide Angle X-ray diffraction patterns of electrodeposited (a) PANI and (b) 1 mol % TSFePc-PANI

The crystal structure of electrochemically synthesized PANI is amorphous in nature. After functionalization, its crystal structure has been modified giving rise to broad peaks centered at 2θ values 25.9 and 11.6. Here, solvent, pH of the medium and the dopant plays a role in determining the structure of TSFePc doped PANI. The broad peak

centered at 27.6 in PANI is found to shift towards lower 2θ value 25.9 thereby indicating the successful incorporation of bulky phthalocyanine molecule into the polyaniline chains

3.7.2. Measurement of properties

The properties like thermal stability, morphology of the synthesized TSFePc–PANI by electrochemical route and its application towards NO_2 gas sensing are discussed in this section.

3.7.2.1. Thermal stability

The electrodeposited sample was scrapped from platinum electrode and its thermogram was recorded. The thermogram of TSFePc-PANI is shown in Fig. 3.29. along with the thermogram of PANI prepared under the same condition for comparison.

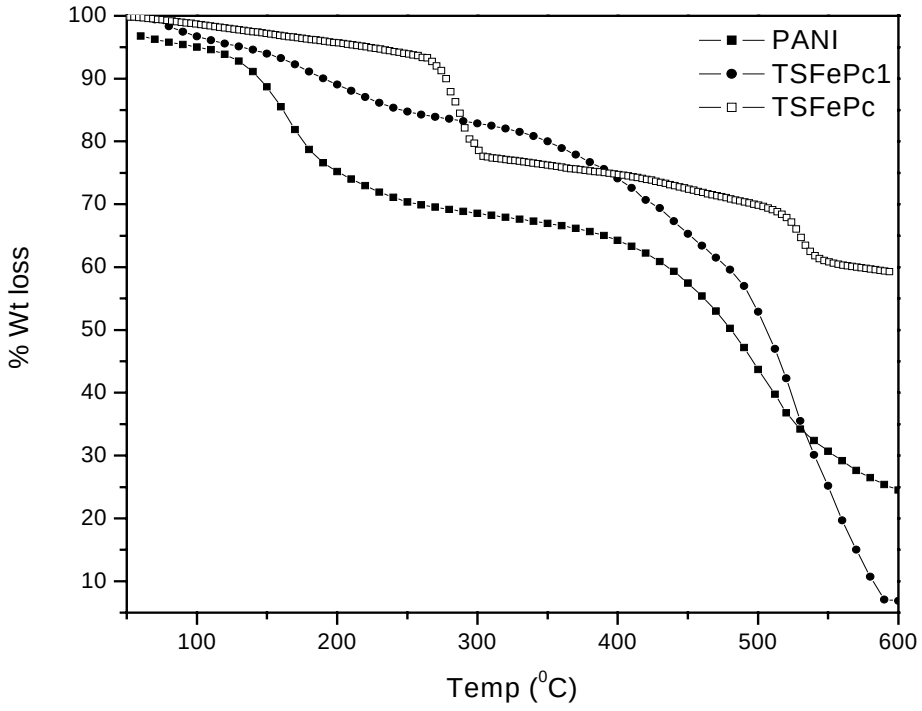

Fig. 3.29. TG thermogram of electrochemically synthesized PANI and TSFePc-PANI

The TG thermogram, although functionalization does increase the thermal stability of PANI, the overall thermal stability is less than that of chemically functionalized PANI. At 250ºC the functionalized PANI shows a weight loss of 15 % and it almost degrades completely at 580ºC where as chemically functionalized polymer shows only 6 % weight loss at 250ºC with a weight retention of 66 to 69 % at 600ºC. The functionalized polymers show major weight loss starting at 480ºC and it can be attributed to the structural decomposition of polymer backbone.

3.7.2.2. Scanning Electron Microscopy (SEM) Analysis

The morphology of the electrochemically synthesized TSFePc – PANI polymer films grown on gold coated PET film at a constant potential of ca. 0.8 V vs SCE for 300 sec were analysed using scanning electron microscope. Scanning electron microscopy of the samples are shown in Fig 3.30. It is interesting to observe a clearly defined nano fibrils in the average size of 50 nm where as the polyaniline synthesized by electrochemical route using HCl as dopant under the same condition show porous structure and doesn't show the fibrillar morphology. Hence it can be concluded that the morphology of the electrochemically grown film depends on the type of dopant employed during synthesis. A number of studies have investigated the effect of counter ion on PANI film morphology. Yang et al [39] has pointed out that use of polyelectrolytes such as poly(vinylsulfonate) and poly(styrenesulfonate) produce more globular surface structures.

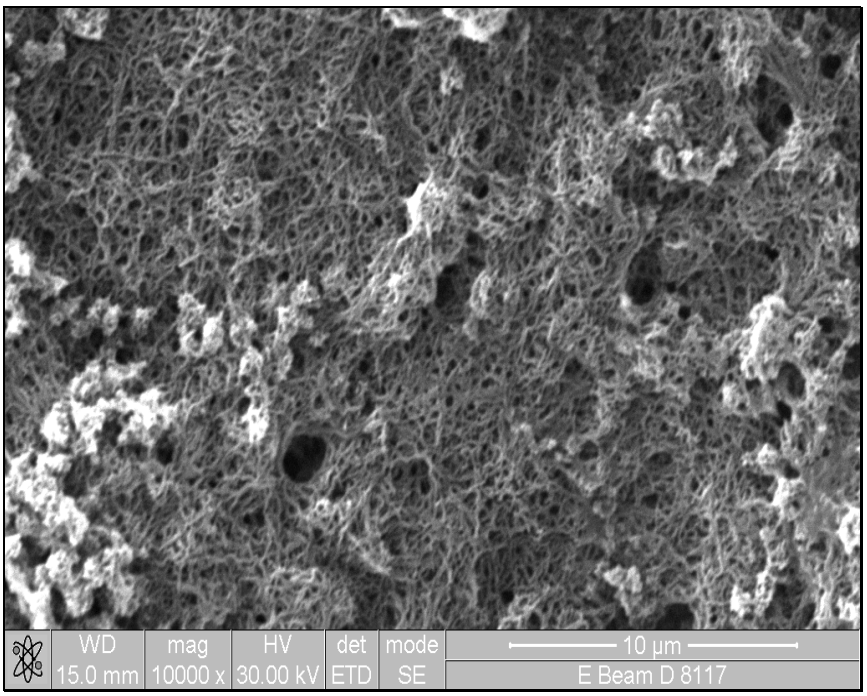
WD
15.0 mm
mag
10000 x
HV
30.00 kV
det
ETD
mode
SE
10 µm
E Beam D 8117

(a)

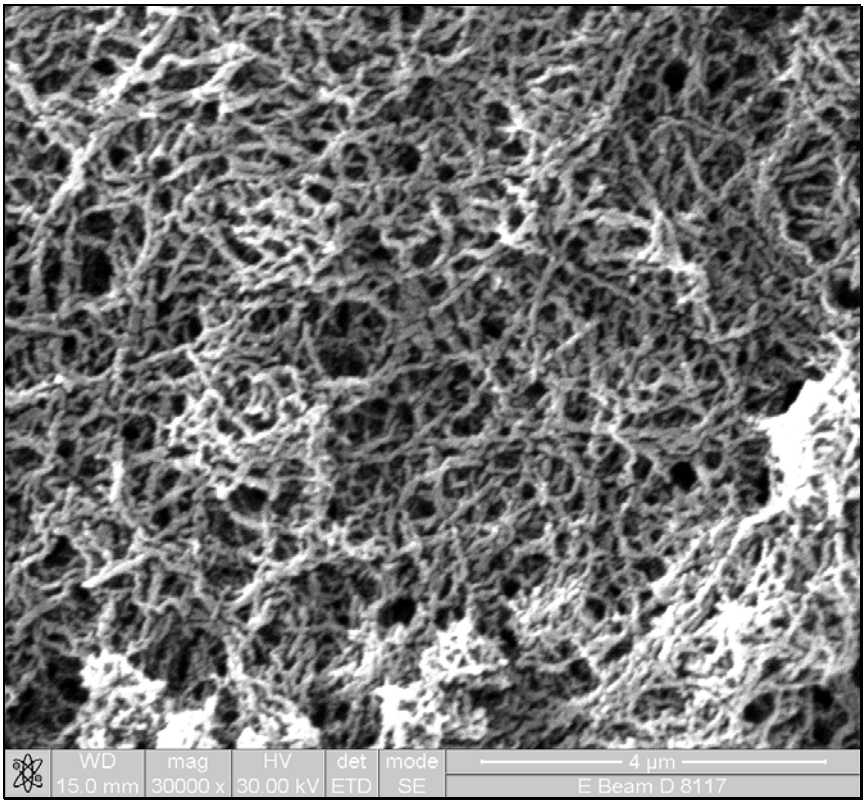
WD
15.0 mm
mag
30000 x
HV
30.00 kV
det
ETD
mode
SE
4 µm
E Beam D 8117

(b)

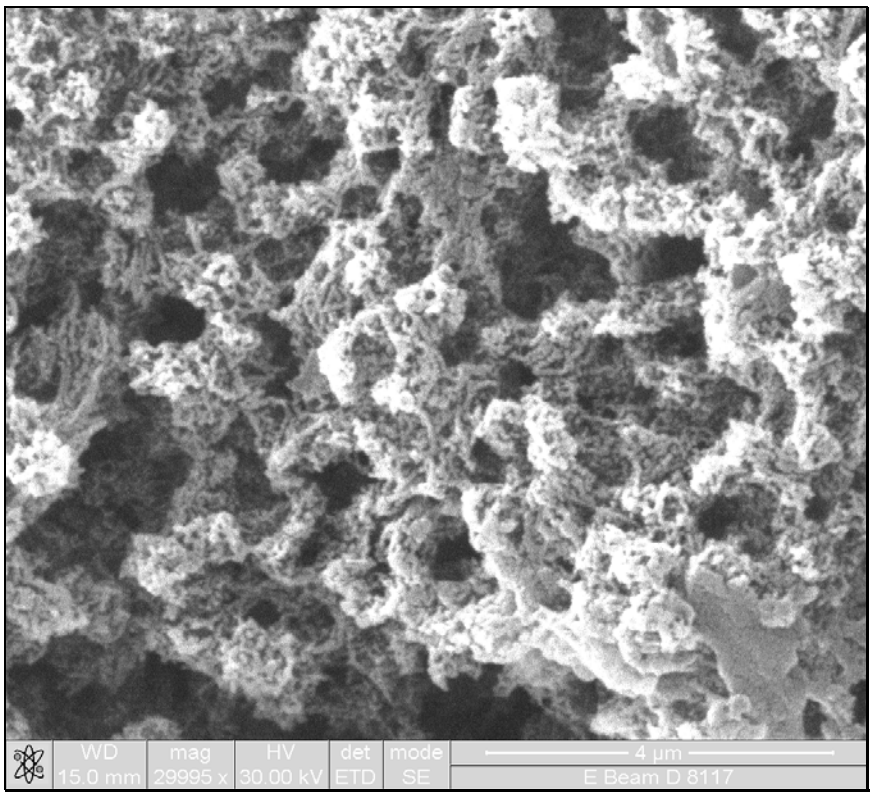

(c)

Fig. 3.30. Scanning electron microgram of electrochemically functionalized PANI with magnification (a) 10000 (b) 30000 and (c) HCl doped PANI

3.7.2.3. Electrochemical studies

The electrochemically grown film was characterized by cyclic voltammetric (CV) technique. The CV of PANI was carried out in aqueous medium containing 2 M HCl solution. The voltammograms were recorded with a potential sweep rate of 50 mV/s between -0.2 and 1V at room temperature. Where as the CV of TSFePc-PANI was carried out in DMF solvent containing 1x 10^{-4} M tetra butyl ammonium perchlorate (TBAP) which acts as supporting electrolyte. Here the potentials were cycled between 0 to -2V versus SCE at a sweep rate of 50 mV/s. Before each experiment the cell was bubbled with nitrogen.

The cyclic voltammogram of pure PANI film obtained is exactly similar to that reported in literature [40] and shown in Fig. 3.31. On the positive redox side, two redox couples were identified at 0.249V and 0.824V versus SCE. These redox processes have been assigned to the interconversion between the different oxidation states of polyaniline and accompanied by an electrochromic effect. The first one, at low potential values, has been associated with the interconversion between leucoemeraldine and emeraldine (accompanied by a color change from yellow to green) and the second one, to the interconversion between emeraldine to pernigraniline (green to violet). However, an

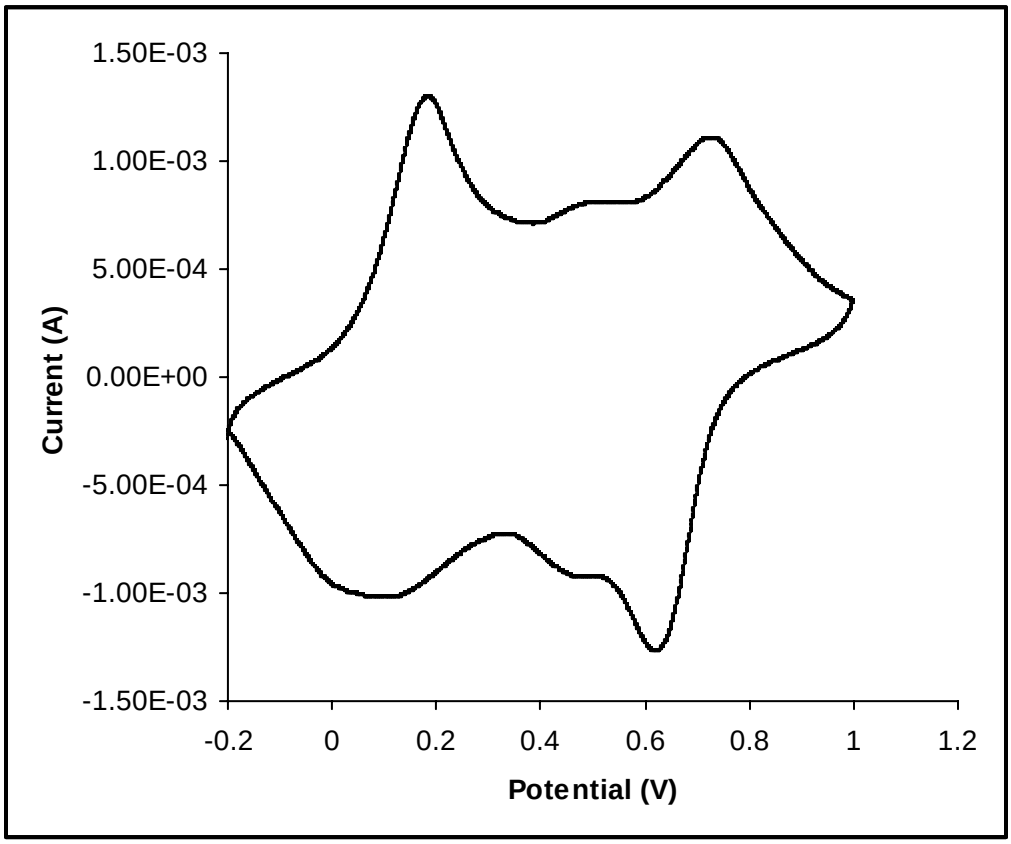

Fig. 3.31. Cyclic voltammogram of Pure PANI in H_2O/ 2M HCl, scan rate 0.05 V/s

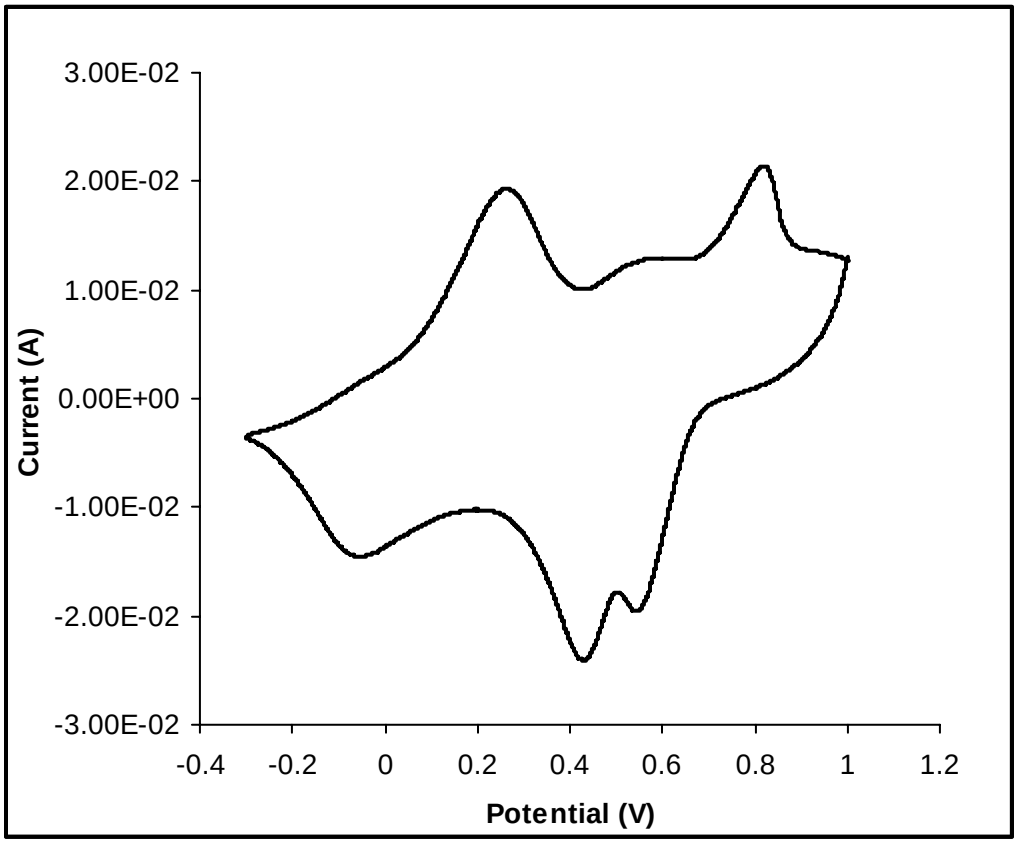

Fig. 3.32. Cyclic voltammogram of PANI in TSFePc-PANI in H_2O/ 2M HCl, scan rate 0.05 V/s

intermediate redox process appears at around 0.557V versus SCE , which is dependent on the electrolytic nature. Such peaks have been associated with degradation [41] on the polymer structure caused by undesirable reaction such as hydrolysis, chain scission and/or cross-linking. At some instances, large intensity of the intermediate peak was observed which could be due to high ionic strength of the medium [42]. The cyclic voltammogram of TSFePc functionalized PANI (TSFePc–PANI) are shown in Fig. 3.32. and 3.33. characteristics of PANI and TSFePc in TSFePc-PANI respectively. Sulfonated iron phthalocyanine displays three redox couples in the range 0 to -2V.

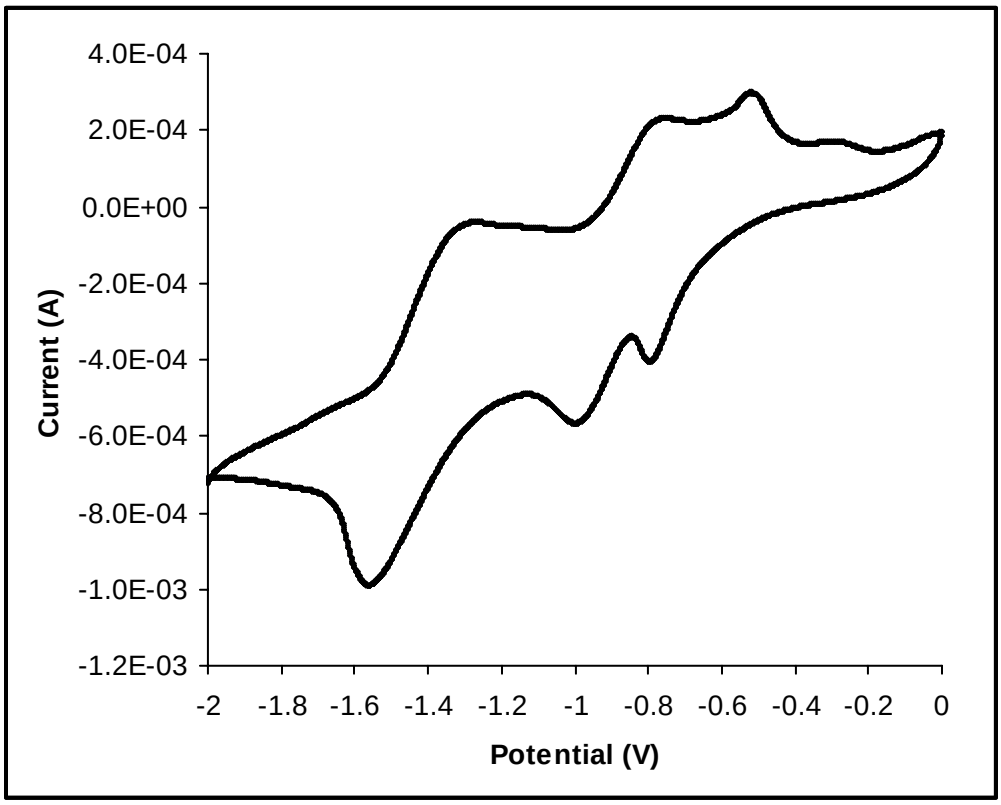

Fig. 3.33. Cyclic voltammogram of TSFePc-PANI in DMF/0.1 M TBAP. scan rate 0.05 V/s

Metallophthalocyanine electrochemistry in the solution phase is typified by multiple and often reversible redox processes localized on the metal center or the phthalocyanine ring. In a typical cyclic voltammogram of TSFePc–PANI, one can observe the multiple reduction of TSFePc at potentials -0.814, -1.016 and -1.58 V characteristics of ring reduction in TSFePc. But for the pure TSFePc compound, the reduction potentials appear at ca. -0.74, -1.08 and -1.15 V [43]. The shift in the reduction potentials of TSFePc-PANI towards more negative potential indicates the influence of PANI on the ring reductions of TSFePc. Apart from this, the oxidation of metal center to $[TSFe(III)Pc(-2)]^{+}$ occurs in the range -0.15 to +0.69 V and its highly dependent upon the solvent and counter ion [44].

3.7.2.4. Chemical sensor

The sensor was fabricated by electrochemically depositing the functionalized PANI onto the gold coated PET substrate and used it for testing with 100 ppm NO_2 gas at room temperature. A similar procedure as explained in the section 3.5.2.4. was followed for testing with gas. The response characteristics of TSFePc–PANI to NO_2 gas is shown in Fig. 3.34. Here the response is very rapid at the same time recovery is also fast when compared to the sensor fabricated by chemical method. This could be due to uniform and controlled alignment of phthalocyanine rings onto the polymer back bone and less amount of impurities formed during synthesis, which is being reflected on gas sensing.

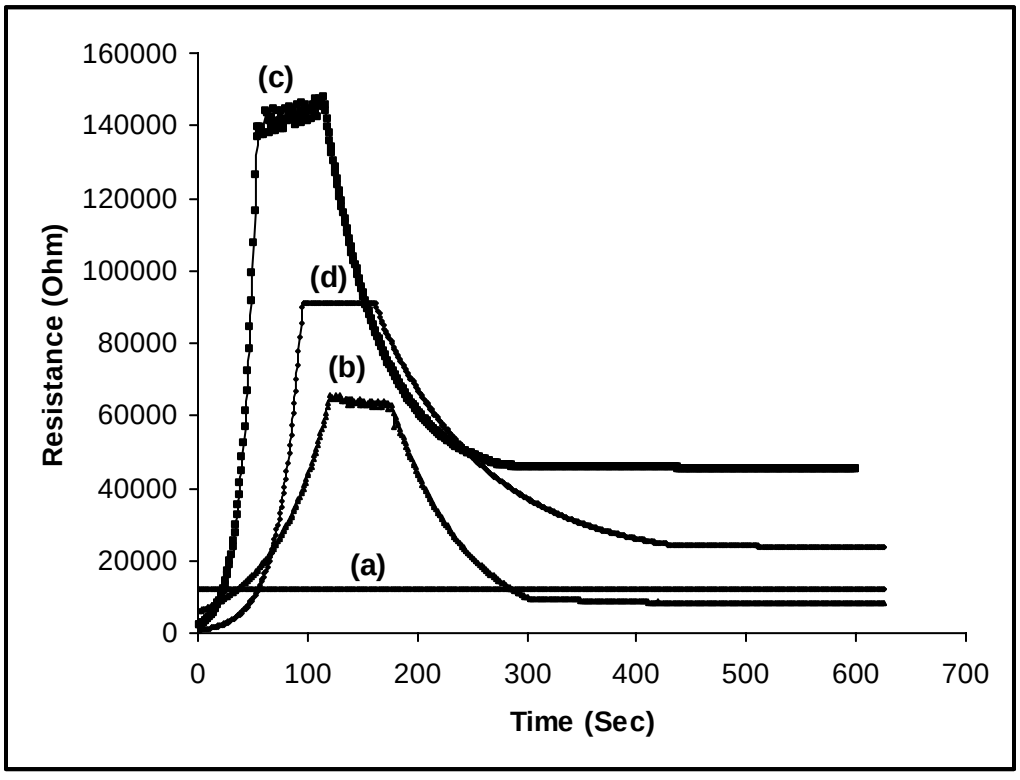

Fig. 3.34. Response characteristics of electrochemically functionalized TSFePc-PANI towards NO_2 gas. (a) PANI, (b) 0.2 mol % TSFePc-PANI , (c) 0.5 mol % TSFePc-PANI and (d) 1 mol % TSFePc-PANI

The sensitivity factor and response time are calculated as described earlier and is shown in Fig. 3.35. These calculated parameters are listed in Table 3.15. Here one can see the sensitivity factor increases with increase of Pc content in PANI and it reaches maximum at an optimum concentration of Pc i.e.; 0.5 mol % TSFePc in PANI at the same time it displayed a fast response t_{50} of 46 sec, when compared to sensor fabricated by chemical method which shows 70 times increase in sensitivity factor. The probable mechanism of sensing is same as to that explained in the section 3.5.2.4. and is pictorially represented in Fig. 3.36.

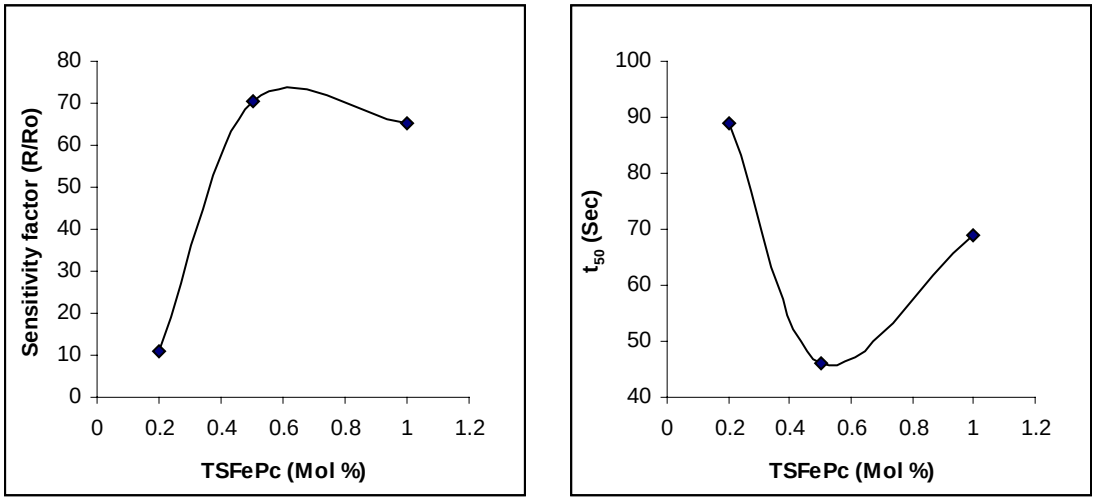

(a) **(b)**

Fig. 3.35. Sensor characteristics of Electrochemically functionalized TSFePc-PANI towards NO_2 gas

(a) Plot of sensitivity factor versus concentration of TSFePc

(b) Speed of response (t_{50}) versus concentration of TSFePc

Table 3.15. Sensor characteristics of TSFePc functionalized PANI towards NO_2 gas

Compound	Mol %	Sensitivity factor (S)	Speed of response (t_{50}) (Sec)
TSFePc-PANI	0.2	10.86	89
	0.5	70.35	46
	1	65.22	69

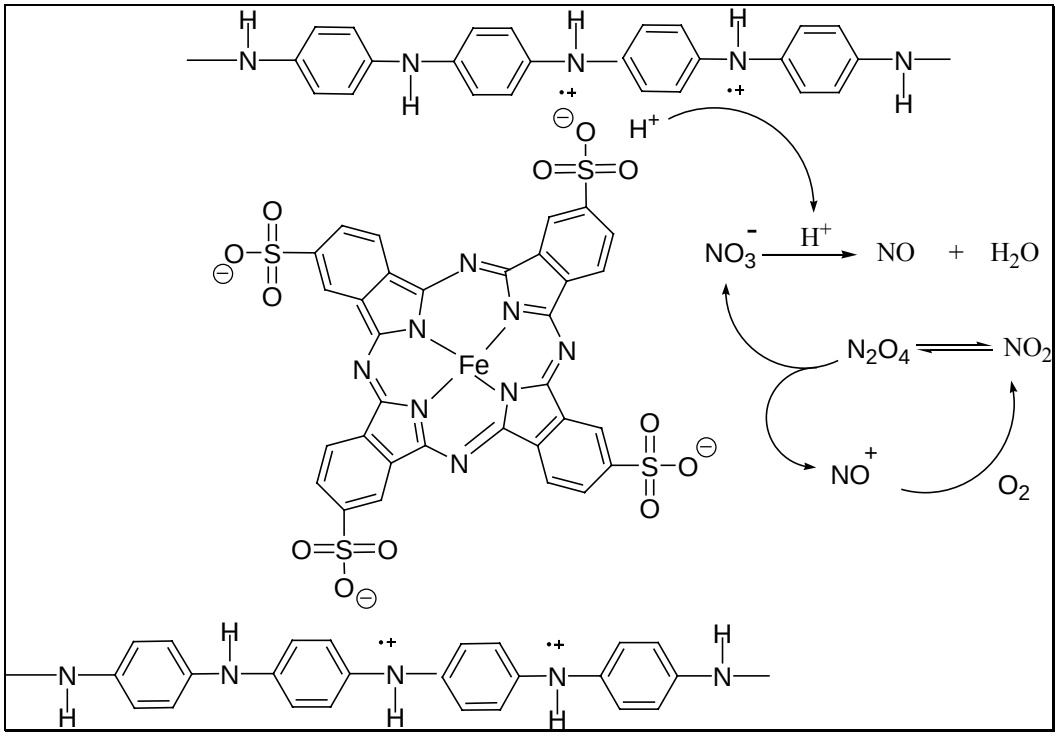

Fig. 3.36. Pictorial representation of gas sensing of TSFePc functionalized PANI towards NO_2 gas

3.8. Conclusion

Conducting polyaniline containing FePc, CoPc and TSFePc functional molecule were synthesized both chemically and electrochemically. The synthesized materials were characterised by spectroscopic techniques and their properties like (i) electronic conductivity (ii) thermal stability (iii) morphology and (iv) NO_2 gas sensing were studied in detail. TSFePc showed better interaction with the polymer backbone than its un-substituted analogs, which is revealed by IR technique. The extension of conjugation due to the incorporated TSFePc was revealed by a red shift in polaron-bipolaron transition that occurs in the UV-Vis region. A semi crystalline X ray pattern was observed along with a pronounced phase separation for FePc and CoPc incorporated PANI, whereas the same has not taken place with TSFePc-PANI which is further supported by conductivity data measured at room temperature. The electrical conductivity at room temperature was found to have inverse relation with FePc and CoPc concentration in PANI where as TSFePc functionalized PANI showed increase in conductivity. Here, the increase in conductivity may be due to electron withdrawing sulfonic acid group in TSFePc and a change in confirmation of polymer backbone from a coil like to a more expanded conformation, which develops extra doping, called secondary doping. After noting down the fall in the properties of FePc and CoPc incorporated PANI, further studies towards its properties on thermal stability and morphology are irrelevant and therefore those measurements were not carried out.

The chemically functionalized PANI was found to have better thermal stability than the same prepared under electrochemical route and in all these case the incorporated

phthalocyanine has improved the thermal stability of PANI. While sensing towards NO_2 gas, the electrochemically fabricated sensor displayed better response characteristics than the sensor which was fabricated by other route. The maximum speed of response (t_{50}) of 46 sec was achieved by TSFePc-0.5-PANI synthesized under electrochemical method where as the sensor of chemically prepared samples showed t_{50} of 87 sec. The sensitivity factor is found to be very high, S = 70.3 in the electrochemically prepared samples and its almost ten times higher than that of sensor material prepared by chemical route where as the FePc and CoPc modified PANI exhibited very poor performances both in sensitivity and speed of response. Hence it can be concluded that, in all respects the tetra substituted phthalocyanine functionalized PANI showed better performances than its un-substituted phthalocyanine.

3.9. References

[1] J. J. Miasik, A. Hooper and B. C. Tofield, J. Chem. Soc., Faraday. Trans. 1., 82 (1986) 1117.

[2] J. Janata, Anal. Chem., 62 (1990) 33R.

[3] C. Nylander, M. Armgarth and I. Lundstrom, Anal. Chem. Symp. Ser., 17 (1983) 203.

[4] T. Hanawa, S. Kuwabata and H. Yoneyama, J. Chem. Soc., Faraday Trans. 1., 84 (1988) 1587.

[5] E. M. Genies, A. Boyle, M. Lapkowski and C. Tsintavis, Synth.Met., 36 (1990) 139.

[6] C. C. Leznoff and A. B. P. Lever, Phthalocyanine , properties and applications, Vol.1, VCH, New york (1989).

[7] A. Belghachi and R. A. Collins, J. Phys. D: Appl. Phys. 21 (1988) 1647.

[8] R. Zhou, F. Josse, W. Gopel, Z. Z. Ozturk and O. Bekaroglus, Appl. Organomet. Chem., 10 (1996) 557.

[9] N. R. Armstrong, J. Porphyrins Phthalocyanines, 4 (2000) 414.

[10] J. D. Stenger-Smith, Prog. Polym. Sci., 23 (1998) 57.

[11] N. Gospodinova and L. Terlemezyan, Prog. Polym. Sci., 23 (1998) 1443.

[12] J. Tan, X. Jing, B. Wang and F. Wang, synth. Met., 24 (1988) 231.

[13] S. A. Chen and H. T. Lee, Macromolecules., 28 (1995) 2858.

[14] C.-T. Kue, C.-H.Chen, Synth. Met., 99 (1999) 165.

[15] Y. Wang, M. F. Rubner, Synth. Met., 47 (1992) 255.

[16] M. Lapkowski, K. Berrada, S. Quillard, G. Louarn and A. Pron, Macromolecules., 28 (1995) 1233.

[17] C. Ercolani, C. Neri, P. Porta, Inorg. Chem. Acta., 1:3, (1967) 415.

[18] F. Lux, Polymer., 35 (1994) 2915.

[19] J. J. Miasik, A. Hooper and B. C. Toefield, J. Chem, Soc, Faraday Trans-1., 82 (1986) 1117.

[20] M. Hanack and M. Lang, Adv. Materials., 6 (1994) 819.

[21] T. A. Jones, B. Bott and S. C. Thorpe, Sens. Actuator., 17 (1989) 467.

[22] R. M. silverstein, G. C. Bassler and T. C. Morrill, Spectrometric identification of organic compounds, 4th edi, John Wiley and sons, (1981).

[23] Y. Cao, S. Li, Z. Xue and D. Guo, Synth. Met., 16 (1986) 305.

[24] V. V. Chabukswar, S. Pethkar and A. A Athawale, Sens. Actuators B., 77 (2001) 657.

[25] W. J. Bae, K. H. Kim and W. H. Jo, Chem Comm., (2003) 2768.

[26] J. P. Pouget, M. E. Jozefowicz and A. J. Epstein, Macromolecules., 24 (1991) 779.

[27] F. Lux, E. J. Samuelson and E. T. Kang, Synth. Met., 69 (1995) 167.

[28] F. S. Wang, J. S. Tang, L. Wang, H. F. Zhang and Z. Mo, Mol. Cryst. L iq. Cryst., 160 (1988) 175.

[29] J. F. Myers, G. W. R. Canham and A. B. P. Lever, Inorg. Chem., 14 (1975) 461.

[30] A. R. Hopkins, P. G. Rasmussen and R. A. Basheer, Polym. Prepr., 36 (1995) 396.

[31] C. C. Leznoff and A. B. P. Lever, Phthalocyanine , Vol.1, properties and applications, VCH, New york (1989).

[32] A. G. MacDiarmid, A. J. Epstein, Synth. Met., 65 (1994) 103.

[33] R. Seoudi, G. S. El-Bahy and Z. A. El Sabed, J. Mol. Struct., 753 (2005) 119.

[34] V. G. Kulkarni, L. D. Campbell and W. R. Mathew, Synth. Met., 30 (1989) 321.

[35] J. Yue, A. J. Epstein, Z. Zhong and P. K. Gallagher, Synth. Met., 41 (1991) 765.

[36] S. Radhakrishnan and S. D. Deshponde, Sensor, 2 (2002) 185.

[37] J. G. Masters, Y. Sun and A. G. Mac Diarmid, Synth. Met., 41 (1991) 715.

[38] J. A. Malmonge, C. S. Campoli, L. F. Malmonge and G. O. Chierice, Synth. Met., 119 (2001) 87.

[39] J. H. Hwang and S. C. Yang, Synth. Met., 29 (1989) E271.

[40] D. E. Stilwell and S. M. Park, J. Electrochem Soc., 135 (1988) 2497.

[41] W. S. Huang, B. D. Humphrey and A. G. MacDiarmid, J. Chem. Soc., Faraday Trans-1., 82 (1986) 2385.

[42] A. J. Motheo, J. R. Santos, E. C. Venancio and L. H. C. Mattoso, Polymer., 39 (1998) 6977.

[43] L. D. Rollmann and R. T. Iwamoto, J. Am. Chem, Soc., 90 (1968) 1455.

[44] A. B. P. Lever and J. P. Wilshire, Inorg. Chem., 17 (1978) 1145.

CHAPTER-4

Synthesis and properties of tetra sulfonated nickel phthalocyanine doped PANI

4.1. Introduction

Chemical modification of conducting polymer surfaces with metal phthalocyanines and porphyrins has expanded the scope of these materials in various fields like, nonlinear optics, electrochromic devices, electronic devices, and sensors for gas and chemical detection [1-3]. Compared to unsubstituted parent metal phthalocyanines, peripherly substituted phthalocyanines are better candidates for applications in the above described fields due to their ease of solubility in aqueous medium, better and uniform incorporation into the matrix. As described in chapter 3 of this thesis, tetrasulfonated phthalocyanine was giving better homogeneity both in chemical and electrochemical synthesis. With the possibility of immobilizing the water soluble NiPc onto the polyaniline matrix, it can become an interesting material for gas sensing application, as phthalocyanines are known for their change in physico-chemical properties upon coming in contact with foreign species [4].

Many properties of the phthalocyanine can be varied by changing the metal and substituting at the periphery of the phthalocyanine macrocycle. For example , (i) its redox properties of phthalocyanine can be varied [5], (ii) the solubility can be increased by reducing the stacking property [6], the interaction between analyte and the functional molecule can be varied etc. Hence, in the present study, the emeraldine salt form of conducting polyaniline was modified both chemically and electrochemically using tetra sulfonated nickel phthalocyanine (TSNiPc) as co-dopant. The aim of choosing sulfonated nickel phthalocyanine as functional molecule is due to the following reason. The transition metal complex or metal ions anchored to conducting polyaniline matrixes represent useful material for sensing atmospheric pollutant toxic gases. In addition to this

it indentifies the effect of nickel towards NO_2 gas sensing under indentical macrocyclic frame work and compare its physico-chemical properties with the other phthalocyanine functionalized polyaniline systems. The various physico-chemical properties emerged from these functionalized conducting polymer prepared under chemical and electrochemical routes were compared at the end of this chapter.

Section–A : Studies on chemically synthesized tetra sulfonated nickel phthalocyanine (TSNiPc) doped Polyaniline (PANI)

4.2. Synthesis of tetra sulfonated nickel phthalocyanine doped PANI (TSNiPc-PANI).

In a first set of experiment, the sodium salt of sulfonated nickel phthalocyanine (TSNiPc) 0.430 g (1 mol % w.r.t aniline concentration) is converted into its corresponding sulfonic acid by passing the sulfonated phthalocyanine salt solution through a column containing cation exchange resin (Amberlite-120) to replace the sodium ions with H^+ ions. Polymerisation of aniline along with the functional dopant phthalocyanine was conducted in aqueous medium for 4 hours at room temperature using ammonium persulfate as oxidizing agent. A typical procedure for the synthesis of phthalocyanine functionalized PANI is as follows: 4 ml of fresh distilled aniline was acidified with stoichiometric equivalent of 25 ml 2 M HCl solution. The above prepared nickel phthalocyanine sulfonic acid was added drop by drop into the acidified aniline to give homogeneous solution. Finally, an aqueous solution of ammonium persulphate containing 9.98 g was slowly added into the above solution to initiate the polymerization. During the course of reaction, the colour of the solution changed from blue to dark green.

At the end of 4 hour, the green mass was precipitated by pouring into 1000 ml of distilled water. The functionalized PANI product was filtered and the excess oxidizing agent and acid were removed by washing it repeatedly with water and finally vacuum dried for 24 hours. Yield: 4.233 g. A similar procedure was followed to prepare PANI with various mol % of functional dopant TSNiPc (0.1 to 1 mol % w.r.t aniline). The yields obtained for the above reactions are reported in Table 4.1.

Table 4.1. Summary of the yield of reaction TSNiPc and Aniline

No	TSNiPc added (mol%)	Yield of TSNiPc-PANI (g)	PANI conversion (%)
1	0	3.628 (PANI alone)	88.3
2	0.1	3.674	89.4
3	0.2	3.780	91.1
4	0.5	3.963	92.6
5	1	4.233	94.1

The plot of PANI conversion versus metal phthalocyanine concentration is shown in Fig. 4.1. It's clear that, the yield of the reaction is following the equation:

$$y = A + Bx - Cx^2$$

where *A* is the yield of PANI and it corresponds to 88.3. The coefficient B corresponds to the concentration of phthalocyanine enhancing the reaction and C corresponds to retardation of polymerization reaction and its diffusion controlled. After certain

concentration of phthalocyanine, the bulky phthalocyanine molecule doesn't allow the aniline to reach the active site Ni attached to the ligand and hence there is a retardation in polyaniline formation.

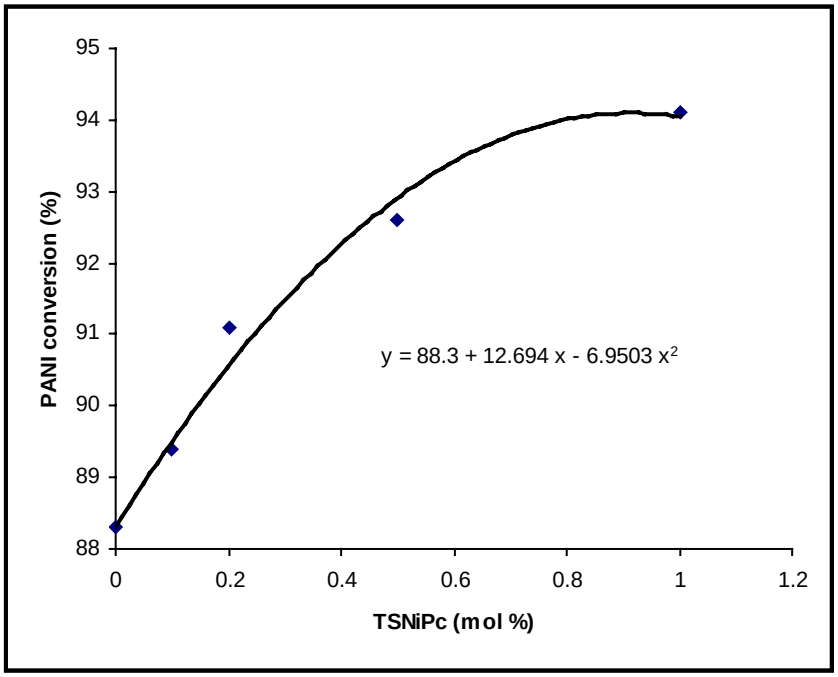

Fig. 4.1. The plot of PANI conversion versus TSNiPc concentration.

4.3. Results and Discussion

4.3.1. Characterization of Structure

The following physico-chemical techniques were done in order to elucidate the structure of newly synthesized nickel phthalocyanine incorporated PANI.

4.3.1.1. FT-IR Studies

Infrared spectroscopy is a powerful tool to determine the structural changes that occur during functionalization of polyaniline chain. The efficacy of incorporation of sulfonated nickel phthalocyanine into the PANI matrix was confirmed by analyzing the stretching and bending vibrations of their respective characteristics groups in PANI. The IR spectra of TSNiPc functionalized PANI (TSNiPc-PANI) along with TSNiPc and PANI are shown in Fig. 4.2. The FT-IR spectrum of functionalized PANI was broadened and shifted from original stretching frequencies of PANI. The signature of phthalocyanine skeleton was seen at 1707, 1389 and 1026 cm^{-1} corresponding to -(C=C)- stretching, asymmetric and symmetric stretching of O=S=O group in Pc respectively. It has been reported [7] that quinoid and benzenoid stretching frequencies undergo shift in peaks in the range 10-15 cm^{-1} when it's subjected to strong intermolecular interactions. In our system, the interaction between the sulphonated phthalocyanine and the polymer backbone is revealed by shift in the stretching frequencies of quinoid and benzeniod groups towards lower wavenumber 1572 and 1487 cm^{-1}. Hence, it can be concluded from certain degree of shift in the IR frequencies, that functionalization has taken place. All the characteristic group frequencies and their assignments are listed in Table 4.2.

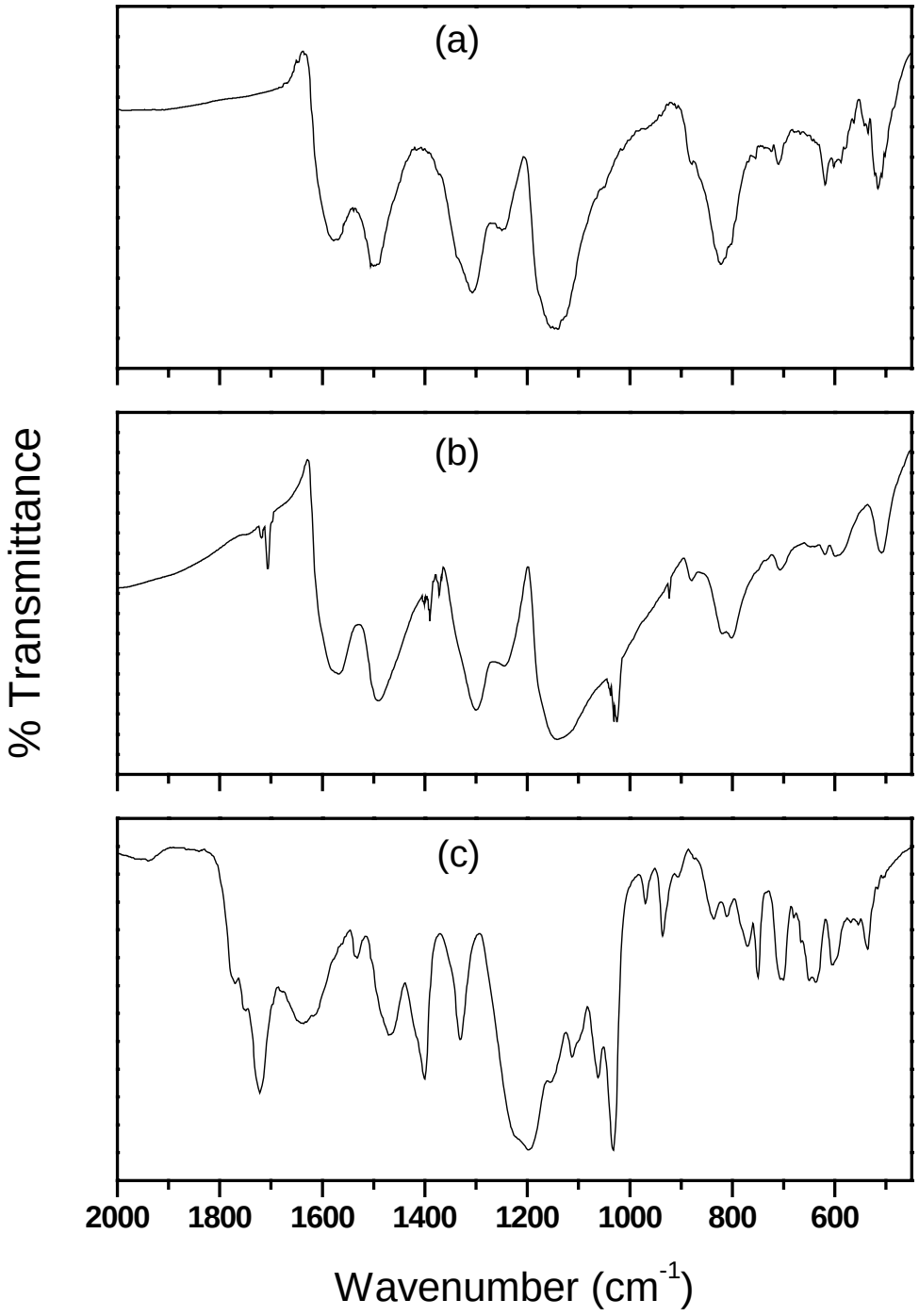

Fig. 4.2. FT-IR Spectra of (a) HCl doped PANI; (b) TSNiPc functionalized PANI; (c) TSNiPc

Table 4.2 Assignment of bands in the FTIR spectra of TSNiPc-PANI

Peak positions (cm^{-1})		IR band assignments
PANI	**TSNiPc-PANI**	
-	1707 w	υ(C=C)stretching in Pc skeleton
1580 s	1572 s	Quinoid ring stretching
1494 s	1487 s	Benzenoid ring stretching
-	1389 w	Asymmetric stretching of O=S=O
1307s	1293 vs	υ(C-N) stretching vibration of aromatic ring
1163 vs	1142 m	$B\text{-}N^{+}H\text{-}B$ stretching Vibration
-	1026 m	symmetric stretching of O=S=O
817 s	805 s	para disubstituted benzene ring
748 m	711 m	υ(C-C) ring stretching
606 m	604 m	Out of plane (C-H) bending vibration
510 m	506 m	γ(C=C) out of plane ring bending

vs: very strong, s: strong, m: medium, w: weak

4.3.1.2. UV- Visible studies

The optical spectra of polyaniline has been the subject of intensive study to identify various types of transition occurring in PANI. Fig. 4.3. shows the electronic spectra of TSNiPc and the TSNiPc incorporated PANI samples. The spectra were recorded by preparing the TSNiPc and TSNiPc-PANI solutions in water and formic acid. The UV-Vis spectrum of TSNiPc showed its characteristics electronic transitions at 754 nm and 407 nm termed Q and B bands. As discussed in the last chapter that, the Q band is more intense than the B band and it is highly sensitive to the substitution or environment

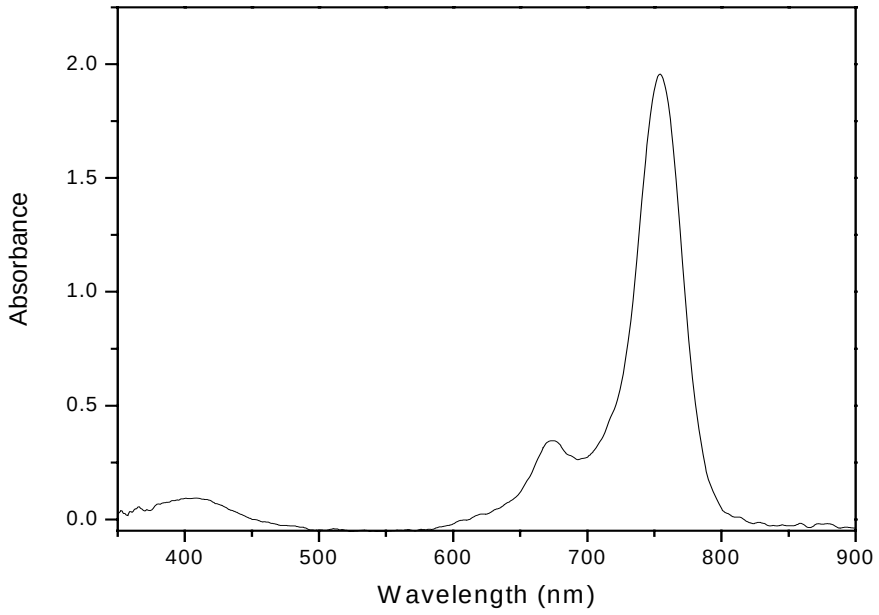

Fig. 4.3. UV-Vis absorption spectra of TSNiPc

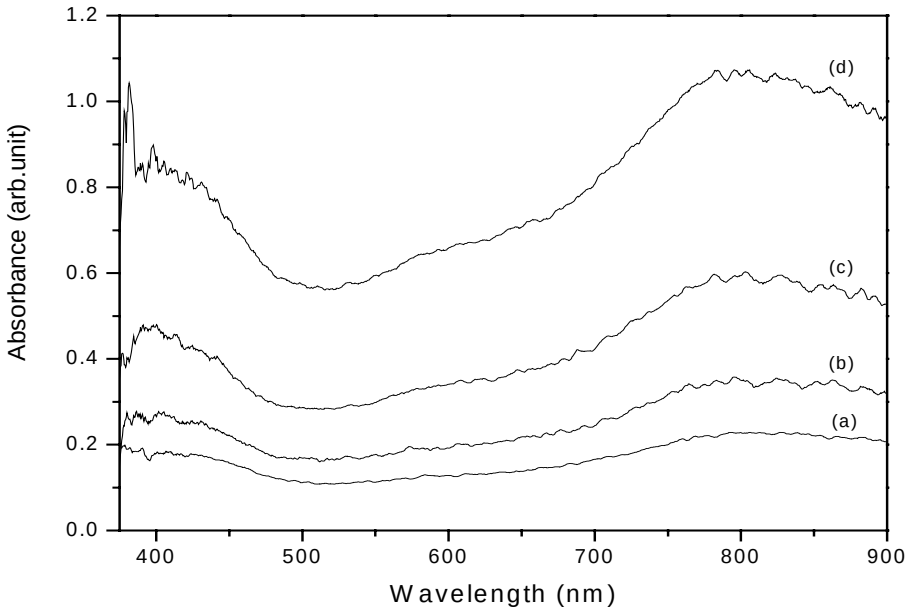

Fig. 4.4. UV-Vis absorption spectra of PANI incorporated with various mol % of TSNiPc (a) PANI, (b) 0.2mol % TSNiPc, (c) 0.5 mol % TSNiPc (d) 1 mol % TSNiPc

of the macrocycle. The electronic spectra of phthalocyanine modified PANI samples are broadened and its intensity increases with phthalocyanine concentration. The broad electronic transition observed at 820 nm is due to the formation of charge carrying polarons. Electronic conductivity measurement confirms the changes in electronic structure and the formation of charge carriers in the phthalocyanine functionalized polymer system. In addition to the broad band at 820 nm, the absorption band in the UV region at 420 nm is due to the π - π^* transition and it is related to the extent of conjugation between the adjacent rings in the polymer chain [8]. This band shows a bathochromic shift from 420 nm for PANI to 430 nm for TSNiPc-PANI.

4.3.1.3. Wide Angle X-ray Diffraction (WAXD) studies

Although various authors have reported the synthesis and structure of PANI, its structure is still in debate. A systematic structural study has been undertaken by Wang et al [9]. These authors point out strong variation in crystallinity (between 12 and 32%) of doped PANI, depending on preparation method, oxidant and dopant. Detailed investigation of the structure by Pouget et al [10] claimed their emeraldine materials as class-I and class-II based on the method of preparation. The class-I material can be converted into class-II by dissolution in NMP and casting it. Class-I emeraldine base (EB-I) and class-I emeraldine salt (ES-I) are inter-convertable by HCl doping and NH_4OH dedoping and the same holds for class-II material. Emeraldine base EB-I is amorphous in nature where as the salt ES-I is 50% crystalline. Emeraldine base EB-II is reported to have 50% crystallinity but its crystalline component is different from the crystal structure of doped form ES-II which also possess approximately 50% crystallinity with orthorhombic unit cell.

In the present investigation, PANI doped with HCl alone has certain percentage of crystallinity having peaks centered at 2θ values 8.9, 20.3 and 25.4. After functionalization with TSNiPc in acidic medium, notable changes in crystallinity has been observed due to the addition of macrocyclic phthalocyanine moiety into polymer matrix. The X-ray diffraction profile for TSNiPc and Pc functionalized polymers are shown in Figs. 4.5. and 4.6. From the XRD patterns, it can be seen that more ordering is taking place upon introduction of planar phthalocyanine moiety which leads to increase in the intensity of peaks at 8.4, 14.9, 20 and 25.4. There are no peaks corresponding to original TSNiPc which indicates that there is no phase separation or free phthalocynaine present in the samples. The observed XRD patterns for the functionalized samples are similar to the pattern for ES-I obtained by Pouget et al. [10].

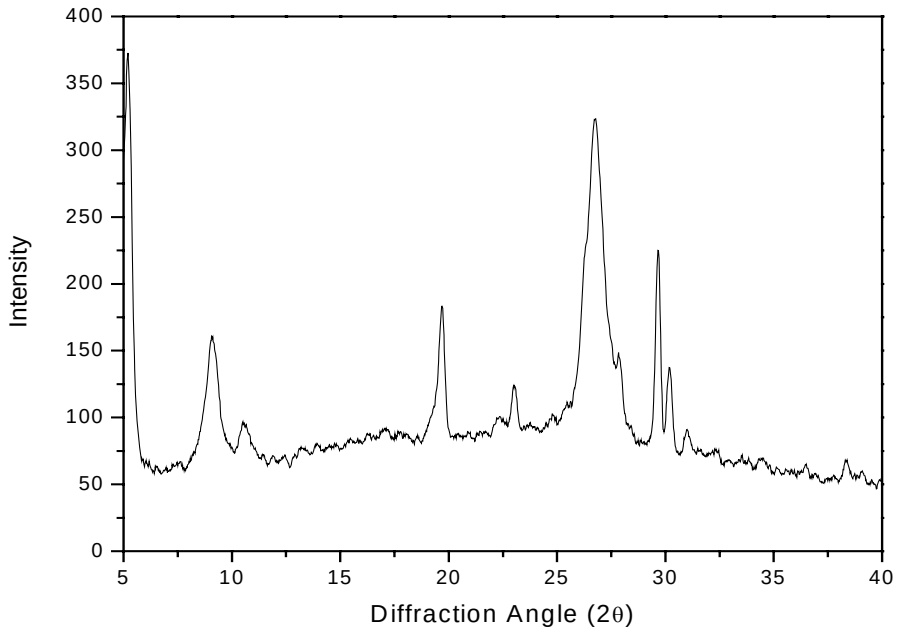

Fig. 4.5. X-ray diffractogram of TSNiPc

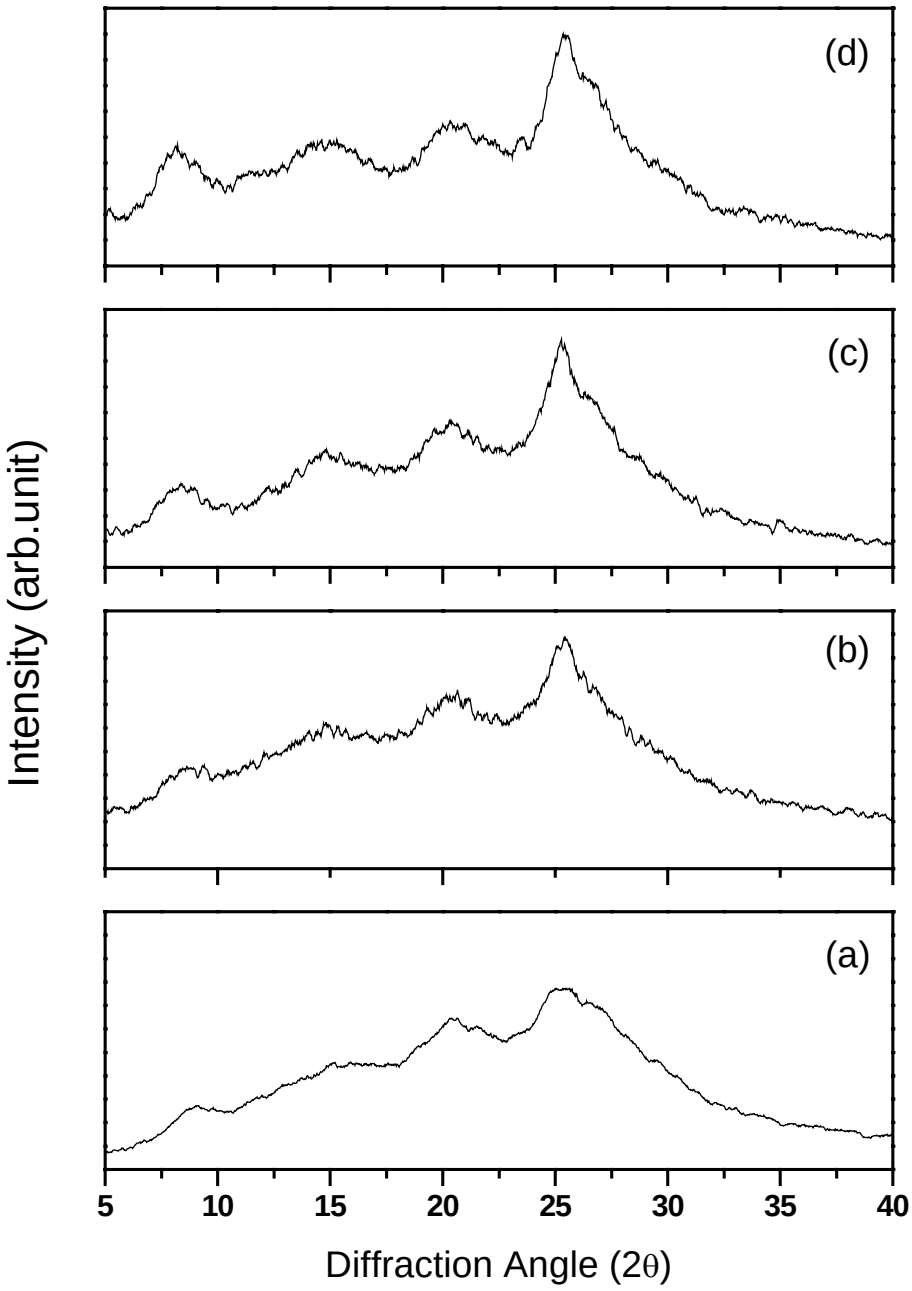

Fig. 4. 6. X-ray diffraction pattern of various mol % of TSNiPc incorporated PANI
(a) PANI, (b) 0.2 mol % TSNiPc, (c) 0.5 mol % TSNiPc (d) 1 mol % TSNiPc

It is also note worthy to point out the increase in crystallinity with respect to secondary doping by sulfonated phthalocyanine which is similar to the effects observed by Macdiarmid et al [11]. During secondary doping i.e., introduction of bulky sulphonated dopant uncoils the polymer leading to orientation along a particular direction. The major reflections in the diffraction pattern of TSNiPc, PANI and TSNiPc-PANI and their d-spacing values are presented in table 4.3.

Table 4.3. Major reflections in the X-ray diffraction patterns

Compound	2 Theta	I/Io	d-values
PANI	8.9	37	9.92
	15.0	54	5.9
	20.3	74	4.37
	25.4	100	3.5
	27.0	78	3.3
TSNiPc-PANI	8.4	55	10.5
	14.9	57	5.94
	20.0	65	4.44
	25.4	100	3.5
TSNiPc	9.1	49	9.7
	10.6	29	8.33
	19.6	54	4.52
	23.0	37	3.86
	26.8	100	3.32
	29.7	69	3.0
	30.2	41	2.95

4.3.1.4. Graphite Furnace Atomic Absorption spectroscopic (GFAAS) studies

The amount of phthalocyanine incorporated in PANI was estimated by analyzing the percentage of nickel content in the sample. It can be seen that the nickel content in functionalized sample increases gradually upon increasing the mol % of TSNiPc and the content is almost same as the content taken at the start of the reaction. This clearly indicates that the amount of sulphonated phthalocyanine added during synthesis has been fully functionalized and it has not been washed out during the work up of the product. The various mol % of TSNiPc in PANI and the percentage of nickel present are presented in Table 4.4.

Table 4.4. The percentage of nickel content in various mol % TSNiPc functionalized PANI

Compound	Nickel content (wt%)
PANI-0.2 mol% TSNiPc	0.106
PANI-0.5 mol% TSNiPc	0.246
PANI-1 mol% TSNiPc	0.541

4.3.1.5. Energy Dispersive X-ray (EDX) studies

The percentage of two dopants namely chloride and sulfonated nickel phthalocyanine were determined by analyzing the chlorine and nickel content in the synthesized sample using EDX technique. The EDX spectra of the PANI with various mol percentage of TSNiPc is shown in Fig. 4.7.

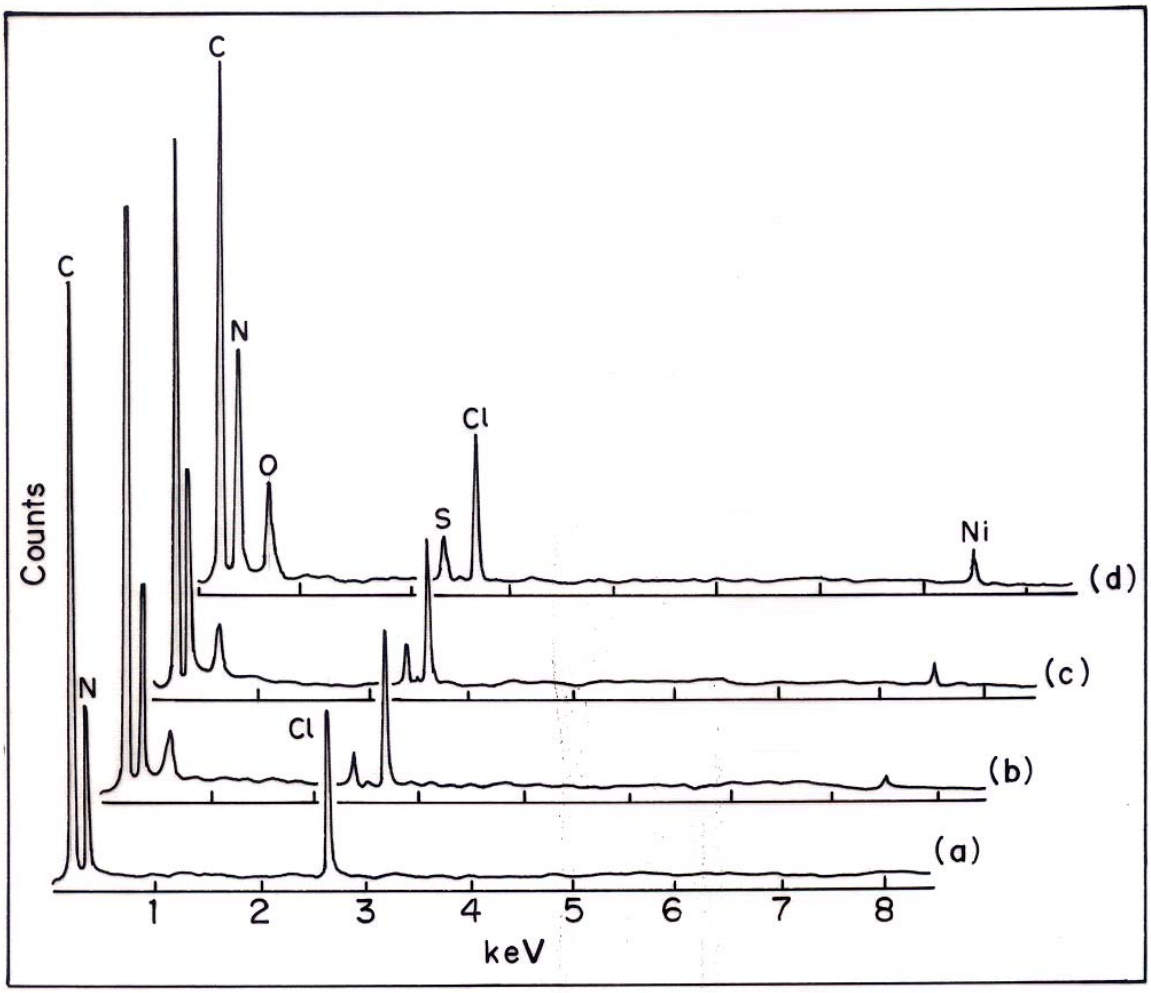

Fig. 4.7. The EDX spectra of the PANI with various mol percentage of TSNiPc (a) PANI (b) 0.2 mol % TSNiPc (c) 0.5 mol % TSNiPc (d) 1 mol % TSNiPc

4.3.2. Measurement of properties

4.3.2.1. Electrical Conductivity

The electrical conductivity of the functionalized PANI samples were studied at room temperature using two probe technique. The results for the conductivity as a function of TSNiPc concentration are depicted in Fig. 4.8. Interesting part in the

conductivity measurements is to observe the effect of phthalocyanine on the overall conductivity behaviour in these samples. It can be seen that the addition of phthalocyanine increases the conductivity as observed in the previous chapter. HCl doped PANI displayed a conductivity of 2.58 x 10^{-2} S/cm, after incorporation with sulfonated phthalocyanine, its conductivity has increased from 3.3 x 10^{-2} S/cm for 0.1 mol % to 3.8 x 10^{-2} S/cm for 1 mol % TSNiPc. The increase in conductivity may be due to chain alignment as influenced by the counter ion and this effect can be seen from the increase in crystallinity of TSNiPc-PANI polymer from XRD studies.

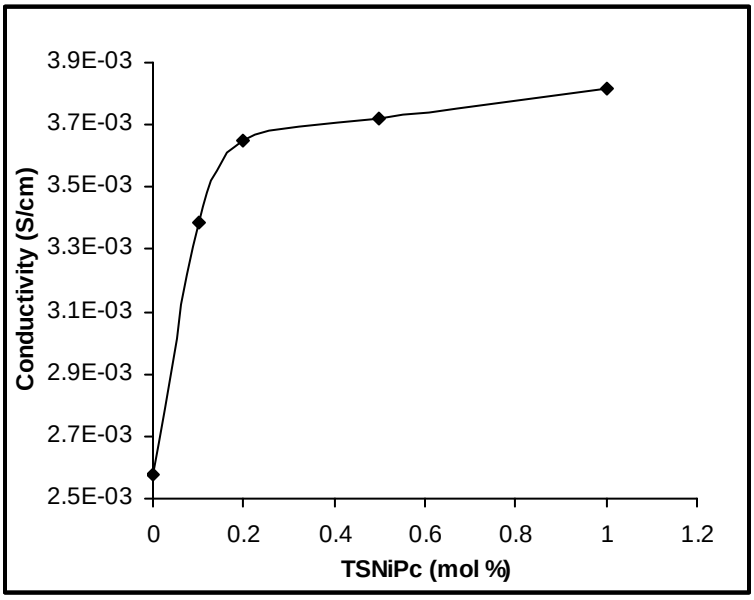

Fig. 4.8. Plot of conductivity versus TSNiPc concentration in PANI

In these polymers, the phthalocyanine acting as counter ion, force the backbone of main chains to take a conformation such that the polyaniline rings in the different main chains parallel to the planar molecule and to one another; the same effect was called as secondary doping by Cao et al. [12]. Several authors have reported the conductivity of PANI prepared under different acidic media like DBSA, naphthalenesulfonic acid, CSA,

acetic and tartaric acid. PANI-CSA films cast from m-cresol has become a subject of interest due to high conductivity. The increase in conductivity has been explained based on secondary doping effect. In the case of TSNiPc-PANI samples, apart from increase in crystallinity, phthalocyanine with four sulfonic acid groups at the periphery is incorporated into polyaniline, hence the possibility of interchain conduction also increases through the highly conjugated phthalocyanine moiety placed in between the polymer chain.

4.3.2.2. Thermal stability

Often serious disadvantages such as insolubility, infusibility and hence non processability mask the great potential of conducting polymers. The studies on the thermal stability of the conducting polymers are of great importance because conducting polymer has to be stable under processing conditions of the host thermoplastic polymers. In the present study, TSNiPc-PANI polymers were subjected to thermal analysis and the results obtained are shown in Fig. 4.9. The thermal degradation was actually carried from room temperature to 700°C. From the thermogram, it is evident that the thermal stability of polyaniline has increased with the addition of phthalocyanine. As mentioned in the previous chapter, phthalocyanine undergoes degradation in two stages: in the first stage sulpfonic acid group is leaving at 260ºC and in the second stage phthalocyanine skeleton starts degrading at 514ºC [13]. All functionalized polymers showed degradation in two stages. The first stage weight loss was from 50°C to 200ºC which involves removal of moisture and chloride dopant ion. The second stage weight loss is the polymer degradation, which starts from 250ºC onwards. The enhancement in the thermal stability

of the TSNiPc functionalized samples can be seen from the thermogram, as it could be due to the incorporated phthalocyanine macrocyclic moiety rendering more stability to the polymeric chain.

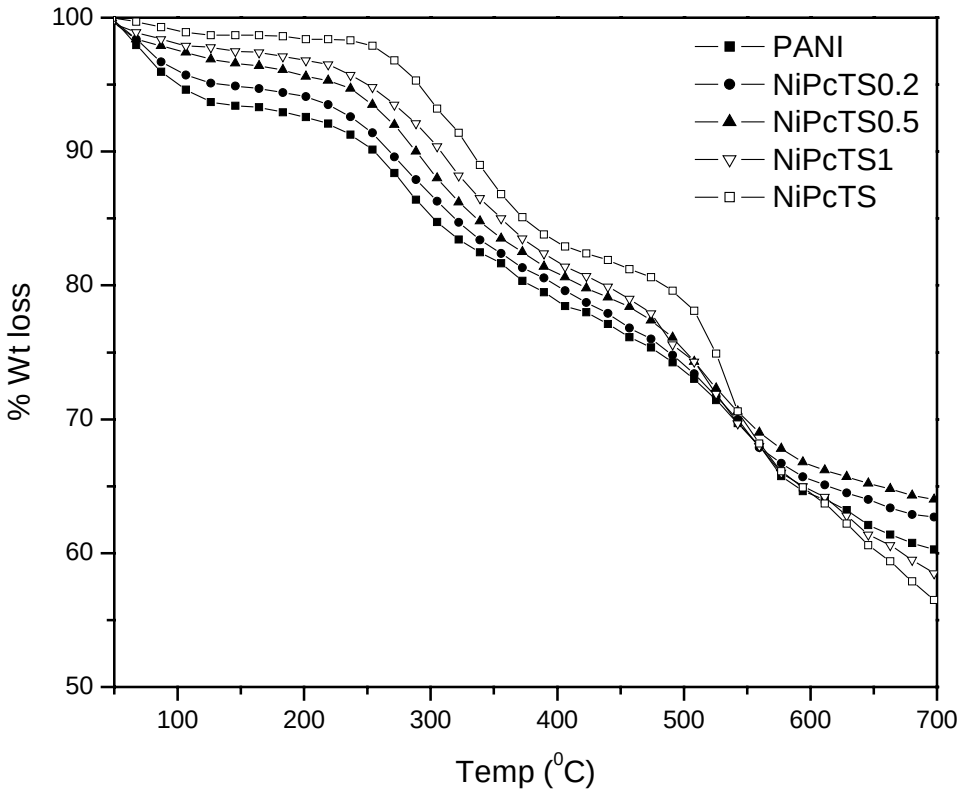

Fig. 4.9. Thermogravimetric analysis of TSNiPc-PANI samples

4.3.2.3. Scanning Electron Microscopy (SEM) Analysis

The morphology of the chemically synthesized polymer samples were analyzed using scanning electron microscope, which clearly shows the samples were of particulate in nature. The scanning electron microscopic images of the samples are shown in Fig. 4.10. The morphology changes from globular to flaky after incorporation of TSNiPc.

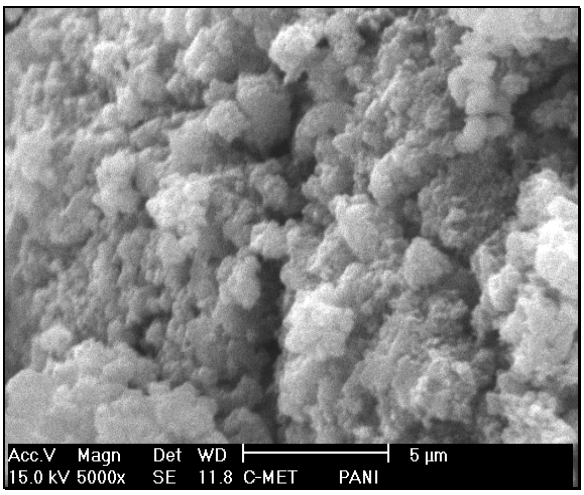

(a)

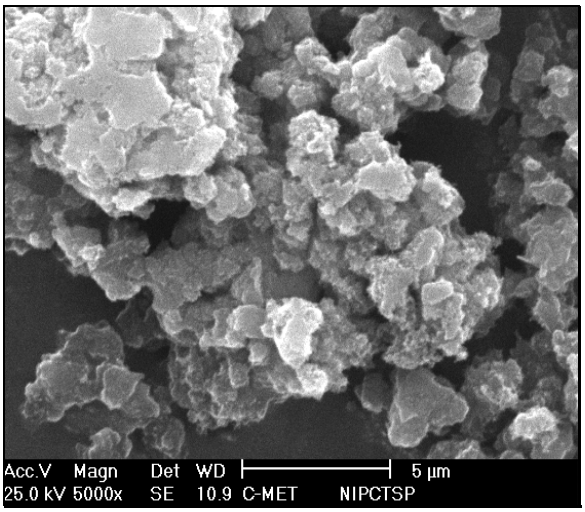

(b)

Fig. 4.10. Scanning Electron Micrograph (SEM) of (a) PANI-HCl
(b) TSNiPc-PANI

4.3.2.4. Chemical sensor

Thin layer of molecular and polymeric compounds gain increasing interest as sensitive, selective and stable coatings for chemical sensors for small inorganic compounds like CO, NO_2, NH_3 and volatile organic compounds (VOCs). In this section, the gas sensing ability of pure PANI as well as TSNiPc-PANI was checked. For this

study, the samples were prepared as described in detail in chapter-II. The pure PANI was not found to be much sensitive to chemical vapours and it doesn't dissolve in solvents from which it can be cast as film. Hence, it was mixed with PEO-$CuCl_2$ complex for making surface cells by applying a thin paste of TSNiPc-PANI dispersed in PEO-$CuCl_2$ complex on interdigitated PCB [14]. Such surface cell type sensors were prepared for different compositions of PANI-TSNiPc.

These samples were then exposed to 100 ppm NO_2 gas in a specially designed pre-evacuated glass chamber. Both PANI and TSNiPc-PANI showed increase in resistance with 100 ppm NO_2 gas, but the magnitude of change in resistance was high with TSNiPc functionalized PANI. The response of TSNiPc-PANI film towards 100 ppm NO_2 gas is shown in Fig. 4.11. The influence of NO_2 on the resistance of PANI film is relatively complicated. Agbor et al [15] has reported, a decrease in resistance when PANI film in the form of emeraldine base was exposed to NO_2 gas. It seems contradictory to our results. The difference was attributed to the different protonation states of PANI used. Agbor et al. has used emeraldine base form and ours was emeraldine salt form protonated by HCl and TSNiPc. It is well known that emeraldine salt has the greatest conductivity in the PANI family and its conductivity will decrease if its oxidation state becomes higher [16]. Our results can be explained by the higher oxidation state of PANI due to the oxidation by NO_2 gas. Li et al [17] have also got similar results on exposing molybdic acid doped PANI film with NO_2 gas. The interaction of NO_2 with TSNiPc-PANI material and the subsequent changes in electronic states contributed to high response is represented in the pictorial form at the end of this chapter. The sensitivity factor (S) was calculated from the sensor characteristics of TSNiPc-PANI using the expression

$$S = R/Ro$$

where R is the resistance after exposure and Ro is the resistance before exposure.

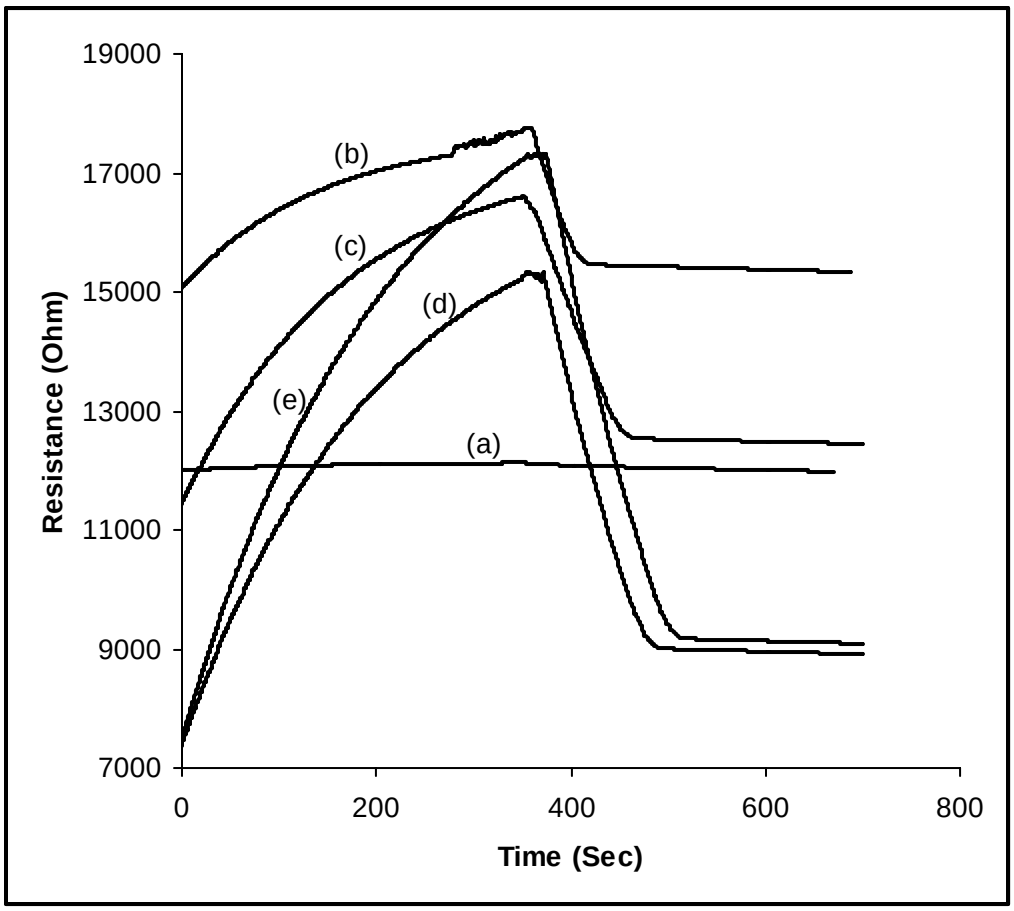

Fig. 4.11. Response characteristics of TSNiPc incorporated PANI towards NO_2 gas. (a) PANI, (b) 0.1 mol % TSNiPc-PANI , (c) 0.2 mol % TSNiPc-PANI , (d) 0.5 mol % TSNiPc-PANI and (e) 1 mol % TSNiPc-PANI

These chemical sensors operating at room temperature displayed moderate half time response t_{50} of 131 s and 103 s for 0.1 and 1mol% NiPcTS doped PANI. A slight increase in sensitivity factor from 1.1 to 2.3 was observed for the NiPcTS doped PANI. These were found to be less sensitive than the iron phthalocyanine doped PANI described in

earlier chapter. The sensitivity factor (S) and response time (t_{50}) calculated for different phthalocyanine concentration are shown in Fig. 4.12.

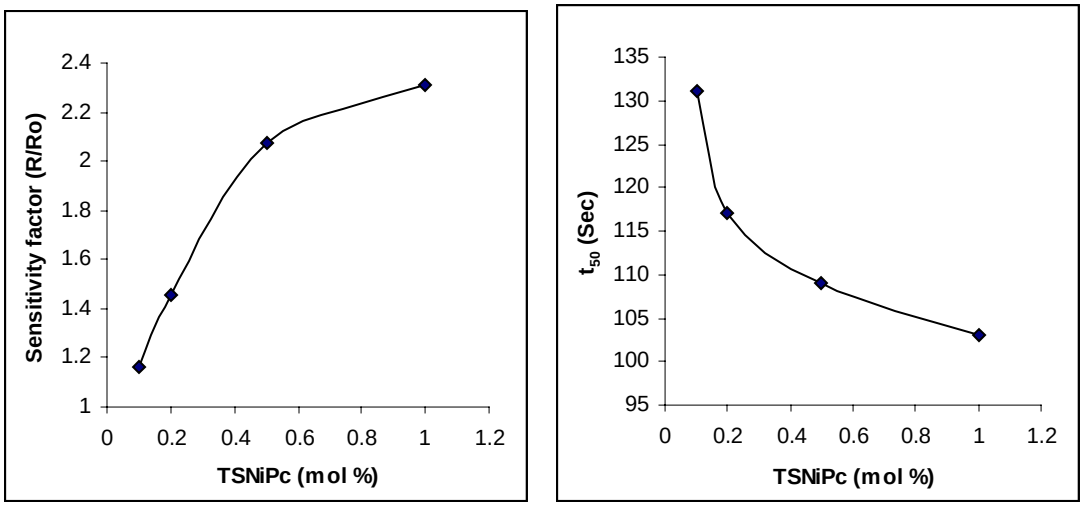

(a) **(b)**

Fig. 4.12. Sensor characteristics of TSNiPc functionalized PANI towards NO_2 gas

(a) Plot of sensitivity factor versus concentration of TSNiPc

(b) Time of response (t_{50}) versus concentration of TSNiPc

The sensitivity factor and speed of response of TSNiPc functionalized PANI samples are presented in the Table 4.5.

Table 4.5. Sensor characteristics of TSNiPc functionalized PANI towards NO_2 gas

Compound	**Mol % of TSNiPc**	**Sensitivity factor (S)**	**Speed of response (t_{50}) (Sec)**
TSNiPc-PANI	0.1	1.16	131
	0.2	1.45	117
	0.5	2.07	109
	1	2.30	103

Section – B : Studies on electrochemical synthesis and properties of tetra sulfonated nickel phthalocyanine doped PANI.

4.4. Synthesis of TSNiPc-PANI by electrochemical route

Electrochemical polymerization of TSNiPc-PANI was carried out in an electrolytic bath containing 0.2 ml (2 mmol) of freshly distilled aniline, 10 ml of 2M hydrochloric acid and 10 ml of $2x10^{-5}$ molar nickel phthalocyanine tetra sulfonic acid solution. The electrochemical cell consisted of platinum or ITO glass as working electrode with a geometric area of 1 cm^2. The reference electrode was standard calomel electrode (SCE) and the platinum foil was used as counter electrode. The electrochemical cell was purged with dry nitrogen gas to remove dissolved oxygen in the electrolyte. Fig. 4.13. shows the growth of TSNiPc-PANI by the potentiodynamic method at a sweep rate of 50 mV/s by cycling the potential between -0.2 volt and 1 volt. The deposited film was rinsed successively with distilled water to remove the acid and excess functional material. A similar procedure was followed for the electrodeposition PANI with different mol % (0.2, 0.5 and 1) of TSNiPc. The films obtained were then characterized by FT-IR, UV-Vis and WXRD techniques to elucidate its structure. The electrochemical studies were also done by cyclic voltammetric techniques in the DMF and aqueous solvents.

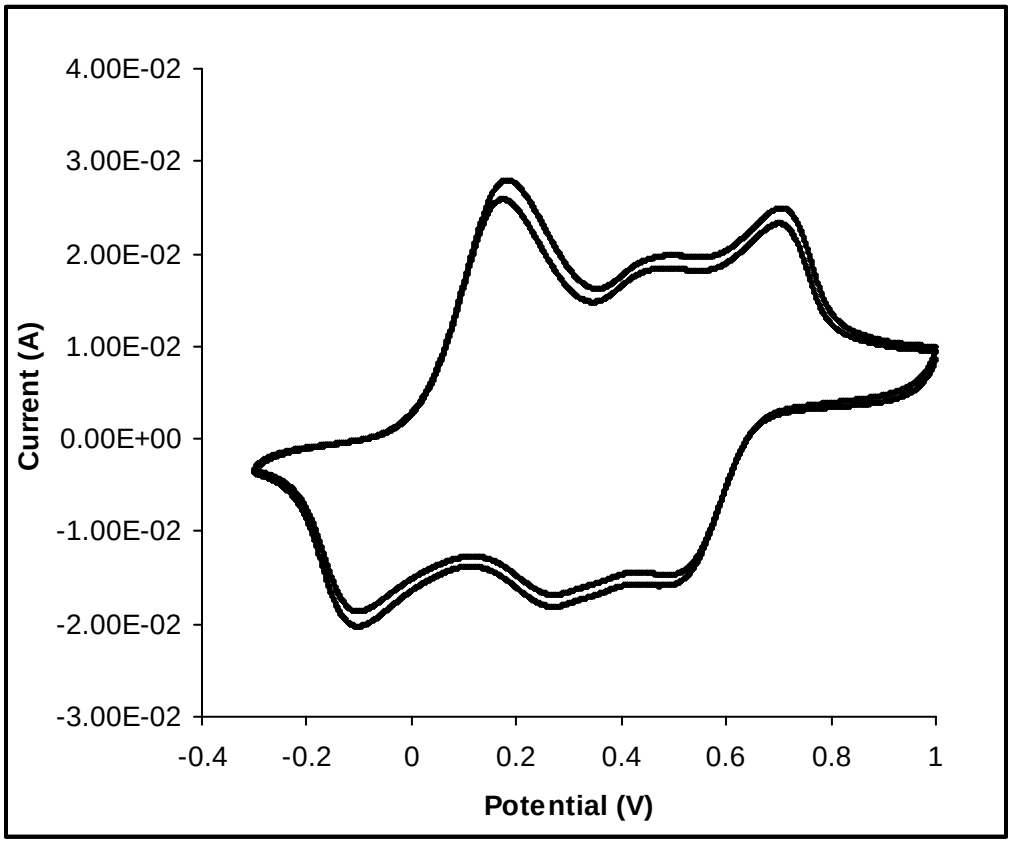

Fig. 4.13. Cyclic voltammogram obtained during electrodeposition of TSNiPc-PANI

4.4.1. Fabrication of Chemical sensor

The sensor was fabricated by electrodepositing the TSNiPc–PANI over the interdigitated gold electrode by means of potentiostatic method. In this experiment, a constant potential of 800 mV was applied to the interdigitated gold electrode for 300 s. PANI with various mol % (0.2, 0.5, 1) of TSNiPc are deposited by taking different concentration of TSNiPc along with aniline monomer and the electrolyte. In all these experiments an initial decrease in current was observed due to the adsorption of organic molecules at the electrode surface. The subsequent behaviour of the current is dependent on the applied potential. The shape of the transient is also the function of experimental

conditions such as (i) nature of anion present (ii) concentration of monomer and (iii) preparation of electrode surface. A typical chronoamperometric curve is shown in Fig. 4.14. Care has been taken to form uniform film of surface area 1 cm^2.

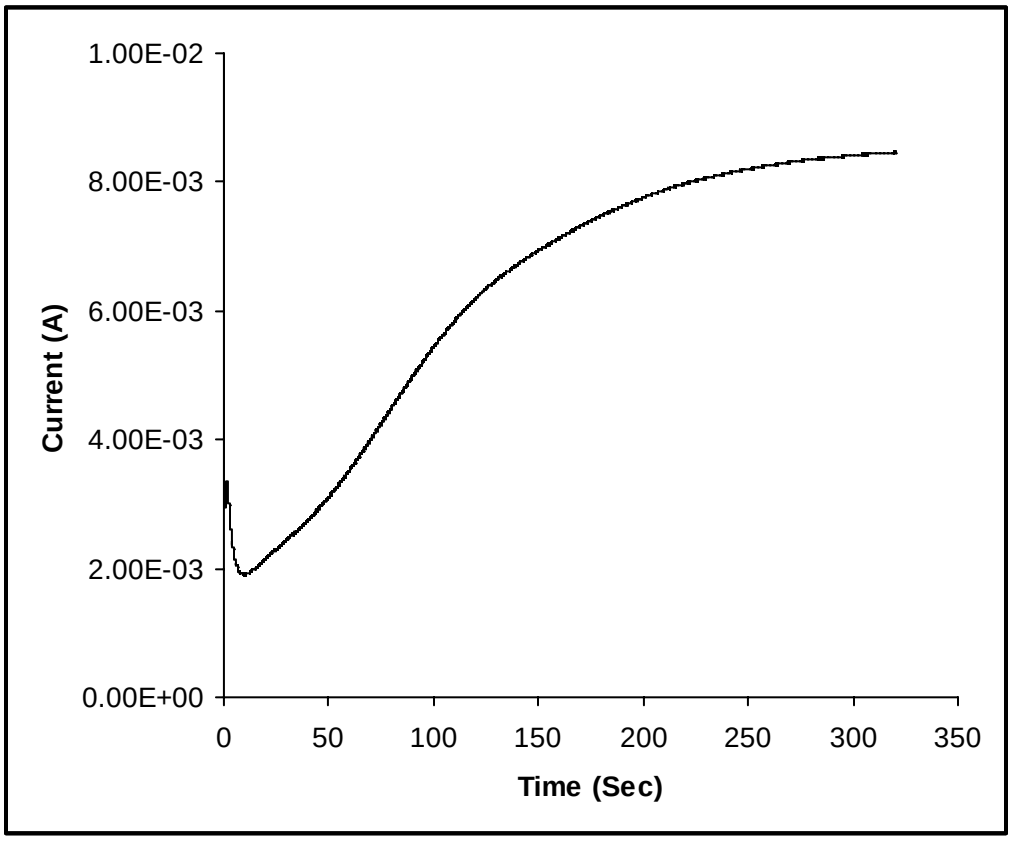

Fig. 4.14. Chronoamperometric curve for the electrodepostion of TSNiPc -PANI

4.5 Results and Discussion

4.5.1. Characterisation of Structure

The structure of the nickel phthalocyanine incorporated PANI was characterized thoroughly by the following physico-chemical techniques.

4.5.1.1. FT-IR Studies

Fig. 4.15. shows the IR spectra of electrochemically functionalized TSNiPc-PANI samples. Although major difference is not seen between pure PANI and the functionalized PANI, the bands associated with quinoid-benzenoid groups and –C=N- stretching frequencies have been broadened and shifted towards lower wavenumber. It has been reported that the intensity of the band at 1566 cm^{-1} relative to 1485 cm^{-1} is a measure of the degree of oxidation of the polymer [18] and it increases after extra doping by sulfonated phthalocyanine. This is a clear indication that sulfonated phthalocyanine interacts with PANI matrix thereby weakening the –(C=C)- stretching of the quinoid-benzenoid ring structures. Since the amount of phthalocyanine present is small, we couldn't observe the characteristics peaks for phthalocyanine except the band at 1007 cm^{-1} corresponding to symmetric stretching of sulphonic acid group and 1707 cm^{-1} for the skeletal stretching of Pc ring. All the usual stretching frequencies corresponding to γ(C-H) out of plane deformation, υ(C-C) ring stretching and υ(C-N) stretching vibration of aromatic ring are assigned and presented in Table 4.6.

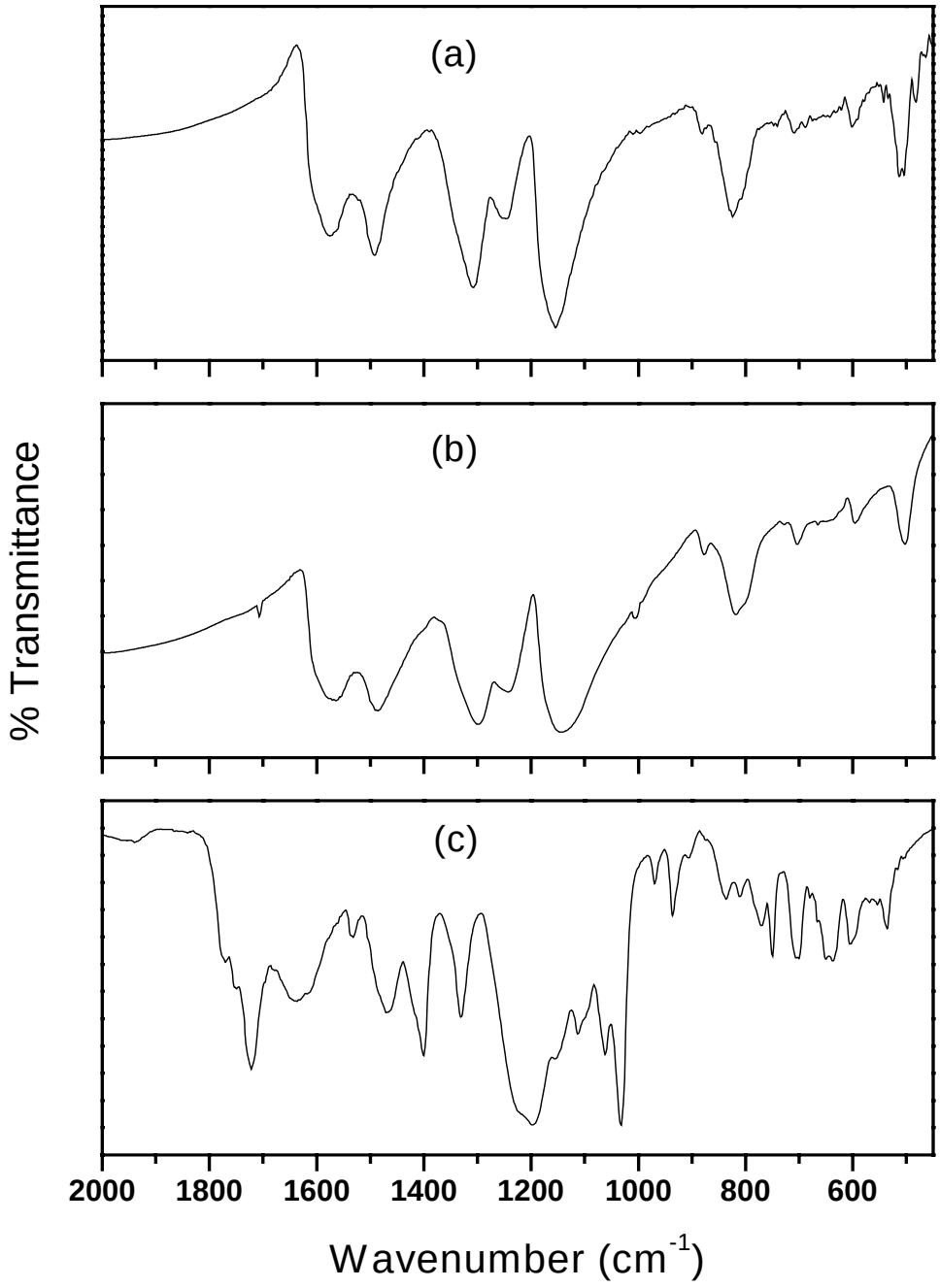

Fig. 4. 15. FTIR spectra of electrochemically functionalized polyanilines. (a) HCl doped PANI, (b) TSNiPc functionalized PANI, (c) TSNiPc

Table 4.6. FTIR band assignments for electrochemically functionalized TSNiPc-PANI

Peak positions (cm^{-1})		IR band assignments
PANI	**TSNiPc-PANI**	
-	1707 w	υ(C=C)stretching in Pc skeleton
1575 s	1566 s	Quinoid ring stretching
1494 s	1485 s	Benzenoid ring stretching
1310 s	1297 s	υ(C-N) stretching vibration of aromatic ring
1155 vs	1140 vs	$B\text{-}N^{+}H\text{-}B$ stretching Vibration and
-	1007 w	Symmetric stretching of O=S=O
824 s	820 s	para disubstituted benzene ring
-	702 m	γ(C-H) out of plane deformation of TSPc
600 w	594 w	υ(C-C) ring stretching
510 m	505 m	Out of plane (C-H) bending vibration

4.5.1.2. UV- Visible Studies

The diffuse reflectance spectra of the electrochemically prepared 1 μm thick PANI and TSNiPc-PANI film prepared under 2M HCl medium on an ITO substrate has absorption bands at 393 and 768 nm representing the well known characteristics transitions, π - π^* and polaron to bipolaron transitions. These bands are likely to shift towards higher λ_{max}, when the polymer backbone is subjected to interact with highly conjugated phthalocyanine moiety [19]. In general, electronic and vibrational energy levels of molecules are affected by their environment. The polymer – functional dopant interaction is determined by the electronic charge distributions in the ground and excited

electronic states of the absorbing entity. All these effects are reflected in the shapes and intensities of the absorption bands. Hence the absorption bands of TSNiPc-PANI sample has been red shifted, appearing at 465 and 817 nm. The difference in the absorption spectra of PANI and TSNiPc-PANI is clearly distinct due to increase in delocalization of charge and /or higher free carrier concentration. A long tail for the absorption extends to 1000nm which is quite prominent for the TSNiPc incorporated PANI. A shoulder appearing at 500 – 600 nm can be ascribed to benzenoid to quinoid electronic transition. Fig. 4.16 depicts the UV-Vis spectra of pure PANI and TSNiPc functionalized PANI.

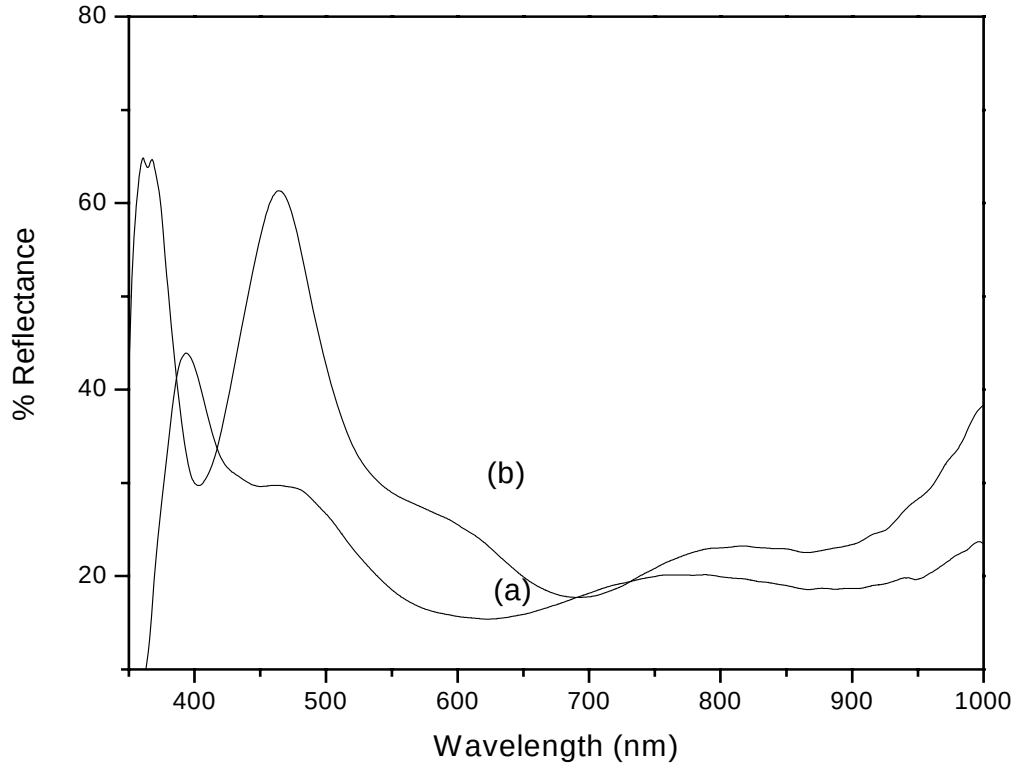

Fig. 4.16. The UV-Vis absorption spectrum of electrochemically deposited (a) PANI-HCl and (b) TSNiPc functionalized PANI films.

4.5.1.3. Wide Angle X-ray Diffraction (WAXD) Studies

As the SEM picture reveals the formation of nano fibers, the X-ray diffraction studies were carried out on the electrodeposited PANI and TSNiPc-PANI samples to identify its nature of crystallinity. X-ray diffraction reveals significant differences in structure development of PANI and TSNiPc-PANI during electrodeposition. The HCl doped PANI was found to have amorphous halo. Upon doping with TSNiPc, a partial crystallinity develops due to isotropic packing resulting from the stacked π - π interaction of bulky phthalocyanine dopant. The appearance of an appreciably sharp crystalline peak at 2θ = 11.5 and a broad and weak diffraction appeared at 2θ value 25.4 for TSNiPc doped PANI may be due to the change in the crystalline form of the sample.

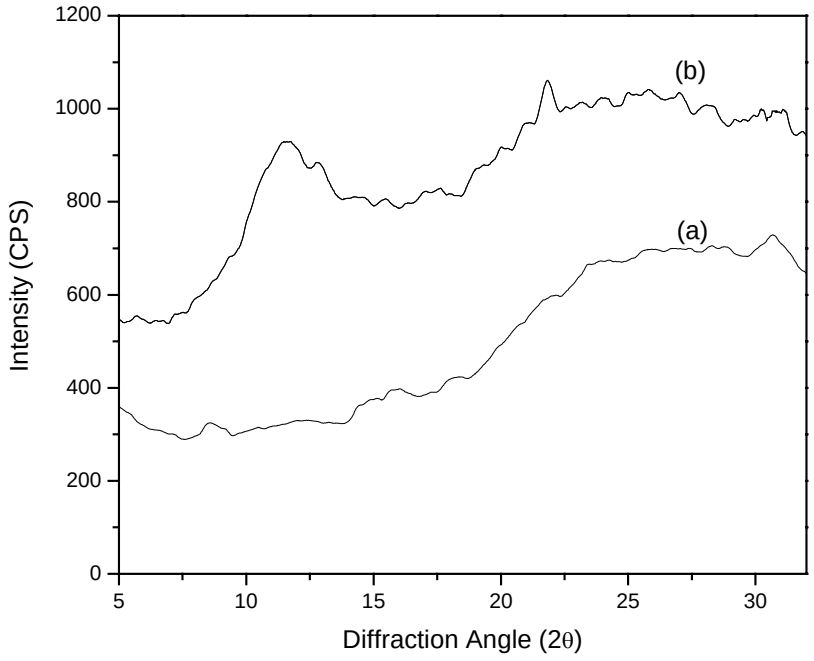

Fig. 4.17. Wide Angle X-ray diffraction patterns of electrodeposited (a) PANI and (b) 1 mol % TSNiPc-PANI

4.5.2. Measurement of properties

The properties like thermal stability, morphology of the synthesized TSNiPc – PANI by electrochemical route and its application towards NO_2 gas sensing are discussed in this section.

4.5.2.1. Thermal stability

The thermogram of electrochemically synthesized TSNiPc-PANI was recorded to study its thermal stability. The thermogram of TSNiPc-PANI is shown in Fig. 4.18. along with the thermogram of PANI prepared under the same condition for comparison. The electrochemically synthesized PANI shows two degradation steps but its overall thermal stability is less compare to chemically synthesized PANI. Here, the major weight loss corresponding to degradation of polymer back bone starts at 419ºC in PANI whereas in TSNiPc-PANI major degradation starts at 438ºC. This shows that thermally stable phthalocyanine moiety imparts good thermal stability to polymeric backbone. At 600ºC, PANI showed a weight retention of 24% where as the electrochemically functionalized PANI degrades almost completely.

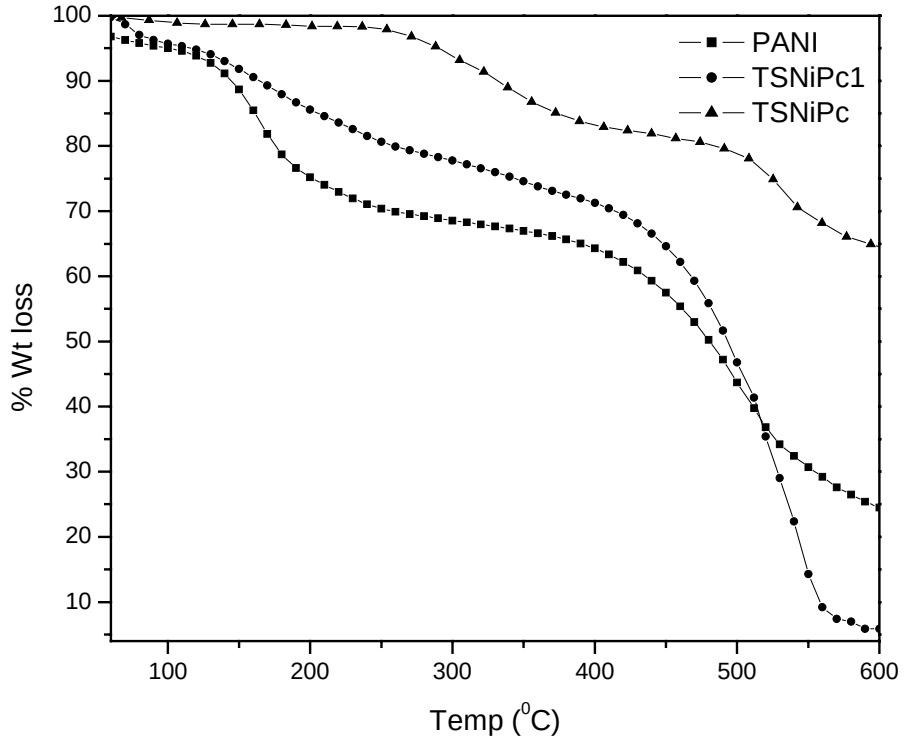

Fig. 4.18. TG thermogram of electrochemically synthesized PANI and TSNiPc-PANI

4.5.2.2. Scanning Electron Microscopy (SEM) Analysis

The morphology of the electrochemically synthesized TSNiPc – PANI polymer film grown on gold coated PET film at a constant potential of ca. 0.8 V vs SCE for 300 sec was analyzed using scanning electron microscope. Scanning electron microscopy of the growth surfaces of PANI-HCl and TSNiPc-PANI are shown in Fig. 4.19. SEM images of PANI functionalized with TSNiPc reveal a striking contrast between PANI synthesized under similar electrochemical condition. It is interesting to observe a clearly defined nano fibrils of average size 50 nm with TSNiPc-PANI, whereas the polyaniline synthesized using HCl as dopant under similar condition show porous structure and

doesn't show the fibrillar morphology. It is clear from the above discussion that the morphology of the electrochemically grown film depends on the type of functional dopant TSNiPc employed during synthesis.

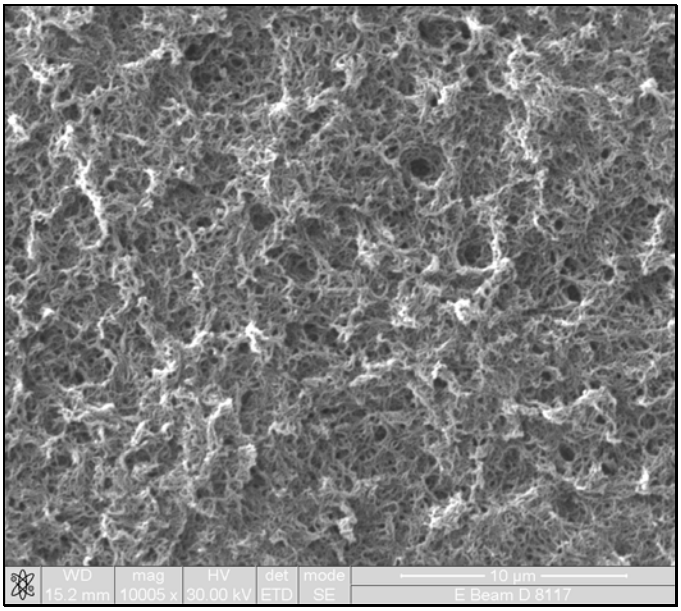

(a)

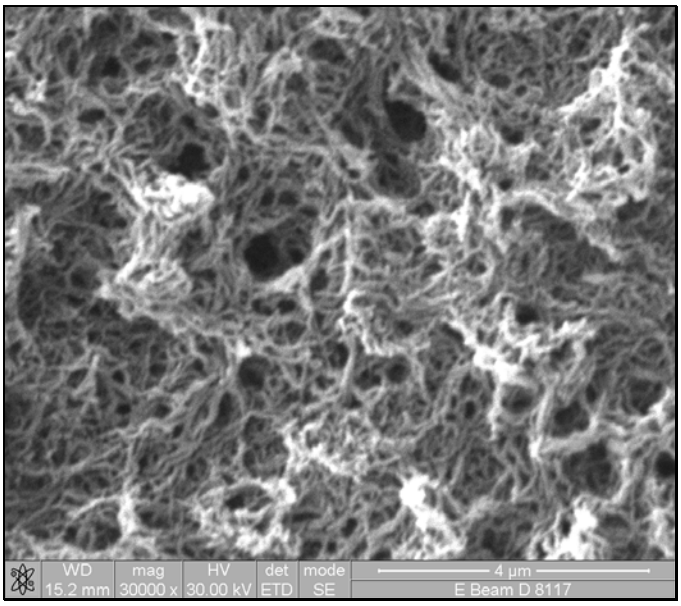

(b)

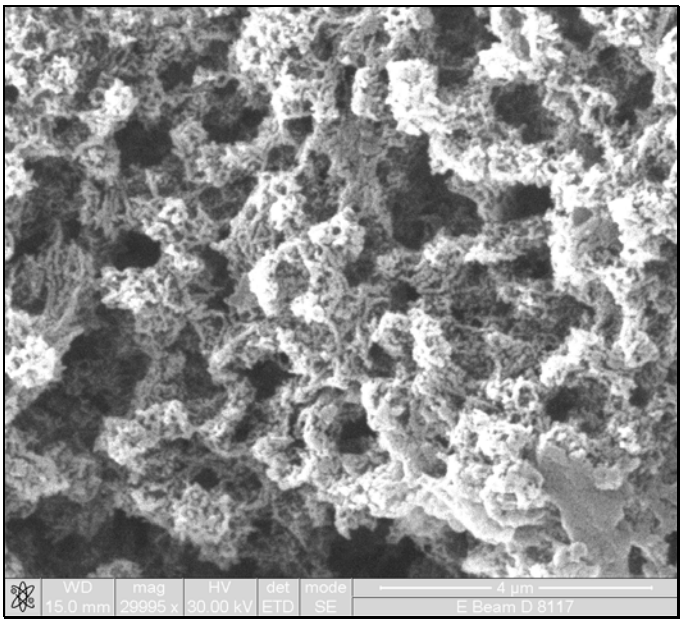

(c)

Fig. 4.19. Scanning electron micrograph of electrochemically functionalized TSNiPc-PANI with magnification (a) 10000, (b) 30000 and (c) HCl doped PANI

4.5.2.3. Electrochemical studies

The motivation behind the electrochemical study of TSNiPc-PANI is to find the applications in the field of electrocatalysis, photoelectrochemistry, energy storage and corrosion protection of metals. For example, the redox property of polyaniline has been used to study the oxidation of methanol [20] and formic acid [21]. Similarly many authors have exploited the redox property of metal phthalocyanine [22-24]. The conducting polymer would act as either an electron source during oxidation or an electron sink during reduction. As a result, polymers would be electroactive and participate in the electrochemical reaction. For this reason electrochemistry has been playing a central role in characterizing the conducting polymers.

The cyclic voltammetry (CV) of PANI was carried out in aqueous medium containing 2 M HCl solution. The voltammograms were recorded with a potential sweep rate of 50 mV/s between -0.2V and 1V versus SCE at room temperature. Whereas the CV of TSNiPc-PANI was carried out in DMF solvent containing 1x 10^{-4} M tetra butyl ammonium per chlorate (TBAP), which acts as supporting electrolyte. Here, the potentials were cycled between 0V to -2V versus SCE at a sweep rate of 50 mV/s. The electrochemical cell was bubbled with nitrogen before starting each experiment. The cyclic voltammogram of pure PANI and PANI in TSNiPc-PANI are shown in Figs. 4.20 and 4.21.

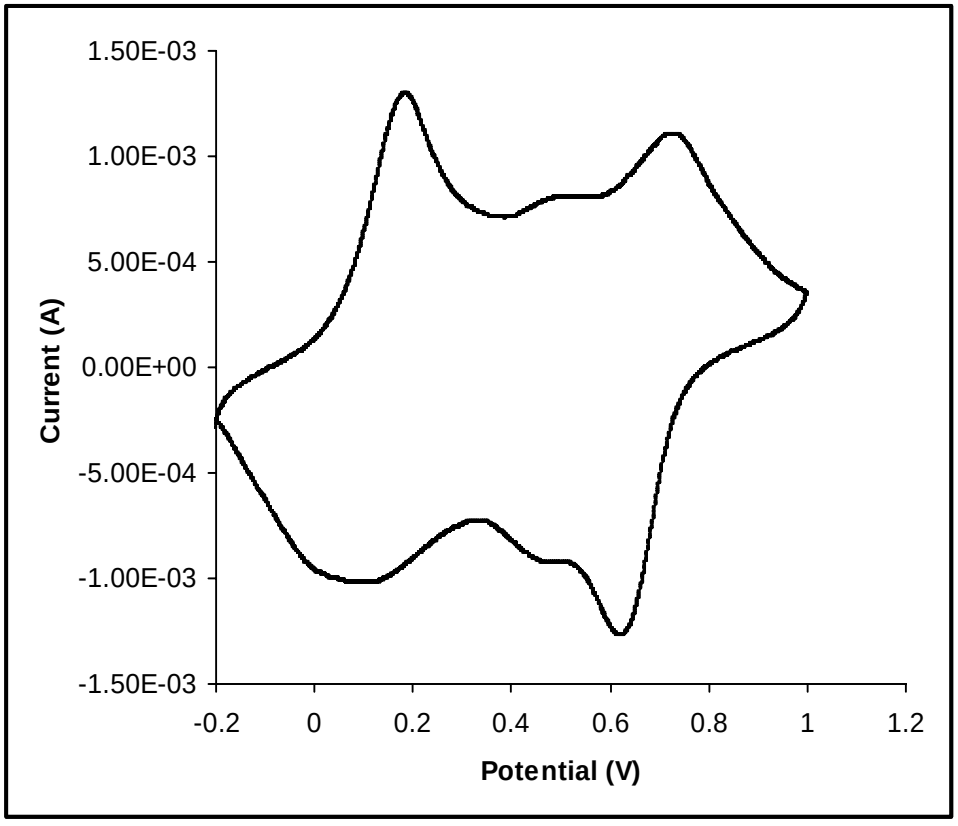

Fig. 4.20. Cyclic voltammogram of Pure PANI in H_2O/ 2 M HCl .scan rate 0.05 V/s

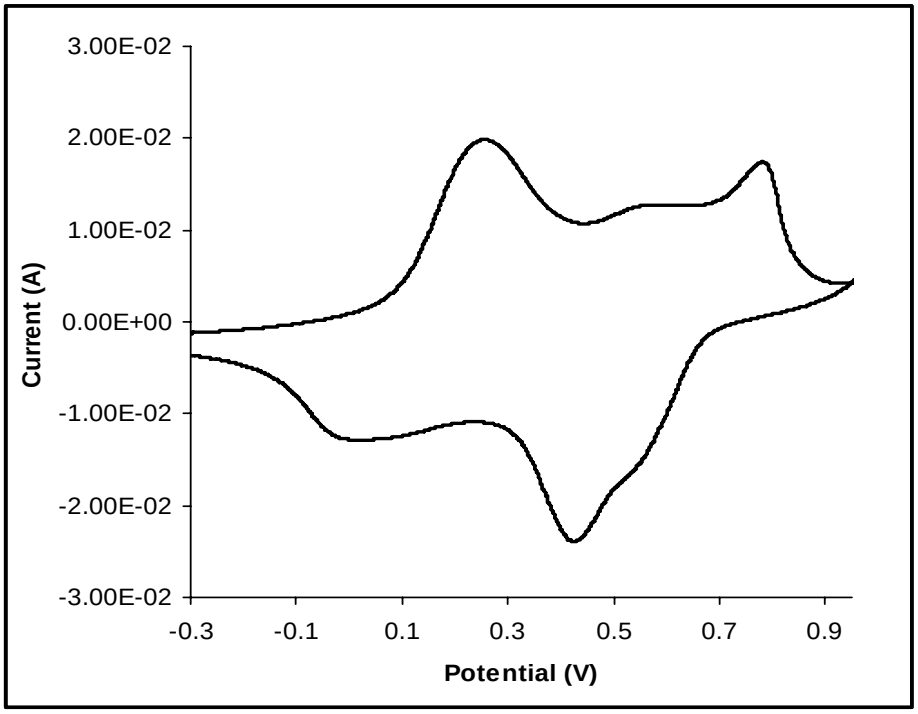

Fig. 4.21. Cyclic voltammogram of PANI in TSNiPc-PANI in H2O/ 2 M HCl .scan rate 0.05 V/s

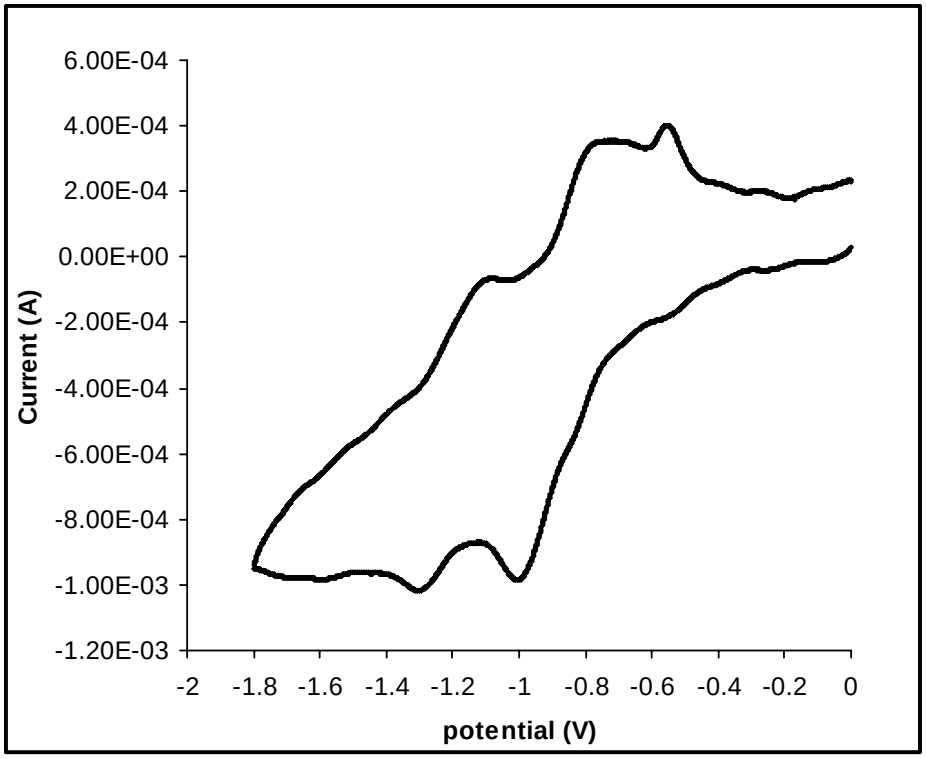

Fig. 4.22. Cyclic voltammogram of TSNiPc-PANI in DMF/0.1 M TBAP. scan rate 0.05 V/s

When compared with pure PANI, The cyclic voltammogram of PANI in TSNiPc-PANI is almost similar in its pattern but the oxidation peaks have been slightly shifted towards more (+) ve potential side. It shows two redox couples, the first couple appeared at 0.265V versus SCE is associated with redox interconversion between polyleucoemeraldine and polyemeraldine and the second couple at 0.794V versus SCE corresponds to polyemeraldine and polypernigraniline interconversions. At the potentials of the second oxidation peak, polyaniline is unstable in aqueous solution and undergoes degradation of a hydrolytic nature. The middle peak in the voltammogram has caused many controversies. According to Genies et al. [25] the middle peak is due to formation of the phenazine ring by involving an aniline nitrenium cation. The PANI film was found to be reasonably stable when the potential was cycled between -0.2 and 1V for more than 10 cycles.

The redox characteristics of TSNiPc was identified by carrying the cyclic voltammogram of TSNiPc functionalized PANI (TSNiPC – PANI) and is shown in Fig. 4.22. Most of the applications rely critically upon the redox properties of MPc species localized on the metal center or the phthalocyanine ring. The central metal ion may be incapable of a redox process in the usual electrochemical regime especially transition metal species such as Ni(II) and Cu(II). However in the case of transition metal species like iron, it may undergo oxidation or reduction at potentials comparable to the Pc ring processes [26]. Sulfonated nickel phthalocyanine displays only two redox couples as compared to iron phthalocyanine system in the range 0 to -2V.

In a typical cyclic voltammogram of TSNiPc – PANI, one can observe reduction of TSNiPc at potentials -1.012 and -1.31V characteristics of ring reduction such as

TSNiPc(-2) to $[TSNiPc(-3)]^-$ and $[TSNiPc(-3)]^-$ to $[TSNiPc(-4)]^{2-}$. But for the pure TSNiPc compound, the reduction potentials appear at ca. -0.71 and -1.14 V [27]. The shift in the reduction potentials of TSNiPc-PANI towards more negative potential indicates the effect of PANI as well as the polarization of the phthalocyanine by the metal center on the ring reductions of TSNiPc. Reduction at the metal center is not seen in the system and it is true in the case of nickel as it doesn't undergo reduction to Ni^+ as reported in the literature [28].

4.5.2.4. Chemical sensor

The sensors fabricated by electrochemical method possess several advantages over sensor material prepared by chemical route, such as purity of the product and easy control of sensor film thickness. In addition, the doping level can be controlled by varying the current and potential with time. The procedure explaining the fabrication of sensor and its testing with 100 ppm NO_2 gas is already described in chapter II. As long as the absorption ability of the sensitive film is improved from the view point of material design, the interaction between the adsorbed gas molecules and the sensitive film would be enhanced to improve the gas sensitivity. Accordingly, the TSNiPc-PANI film with regular nano fibre structure obtained in our experiments anticipated to have excellent gas sensitivity owing to its morphology. When the TSNiPc-PANI film was exposed to NO_2 gas, the resistance of the film increases sharply but the magnitude of increase is less as compared to TSFePc-PANI film. The reversibility of the process was also checked with the removal of guest gas from the test chamber by applying vacuum and it showed almost 80% of recovery as seen from the sensor response characteristics. The response

characteristics of TSNiPc – PANI to NO_2 gas is shown in Fig. 4.23. The interaction of NO_2 gas with TSNiPc-PANI is similar as explained in the pervious chapter. The possible interaction mechanism of NO_2 gas with, TSNiPc-PANI material is represented in Fig. 4.25.

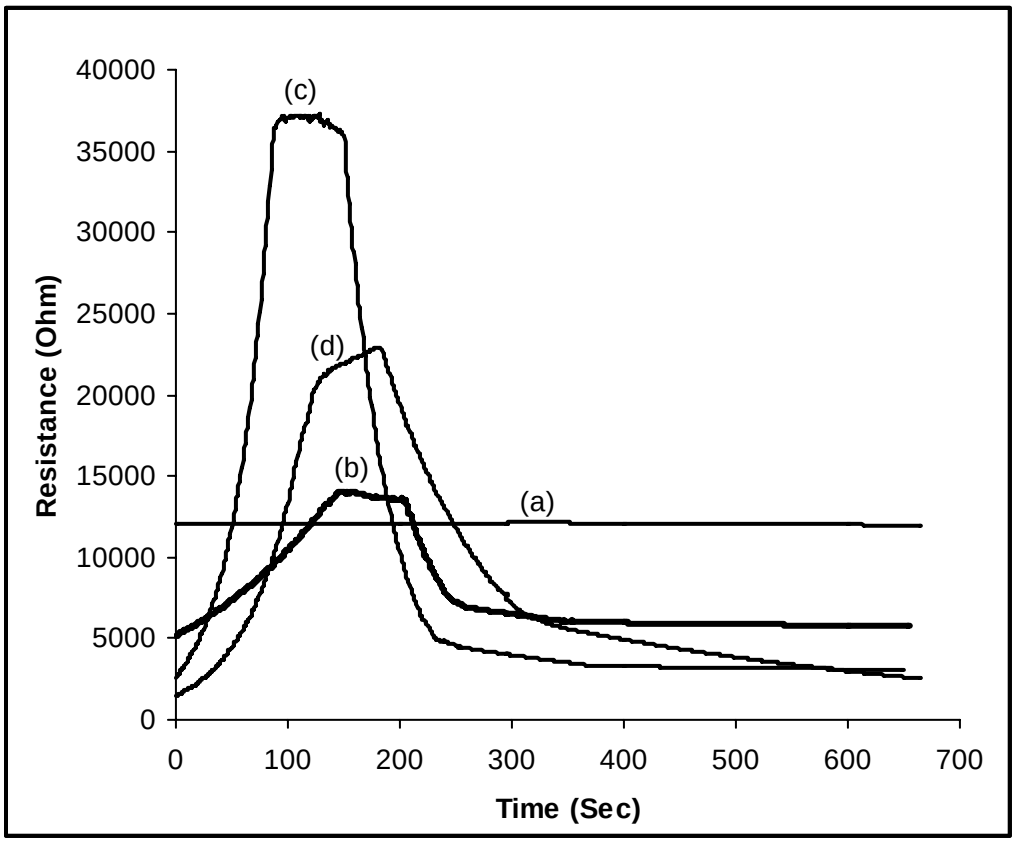

Fig. 4.23. Response characteristics of electrochemically functionalized TSNiPc-PANI towards NO_2 gas. (a) PANI, (b) 0.2 mol % TSNiPc-PANI, (c) 0.5 mol % TSNiPc-PANI and (d) 1 mol % TSNiPc-PANI

The sensitivity factor and response time was calculated as mentioned previously and is shown in Fig. 4.24. and the values are presented in Table 4.7. It can be seen that a maximum sensitivity is reached with 0.5 mol% NiPcTS itself with further addition of

phthalocyanine doesn't have much influence on the sensitivity. Sample with 0.5 mol% NiPcTS showed a maximum sensitivity factor (R/R_o) of 14 with a half time response t_{50} of 67 s. The sensitivity results obtained for electrochemically modified PANI is well superior to chemically modified PANI but much inferior to FePcTS doped PANI.

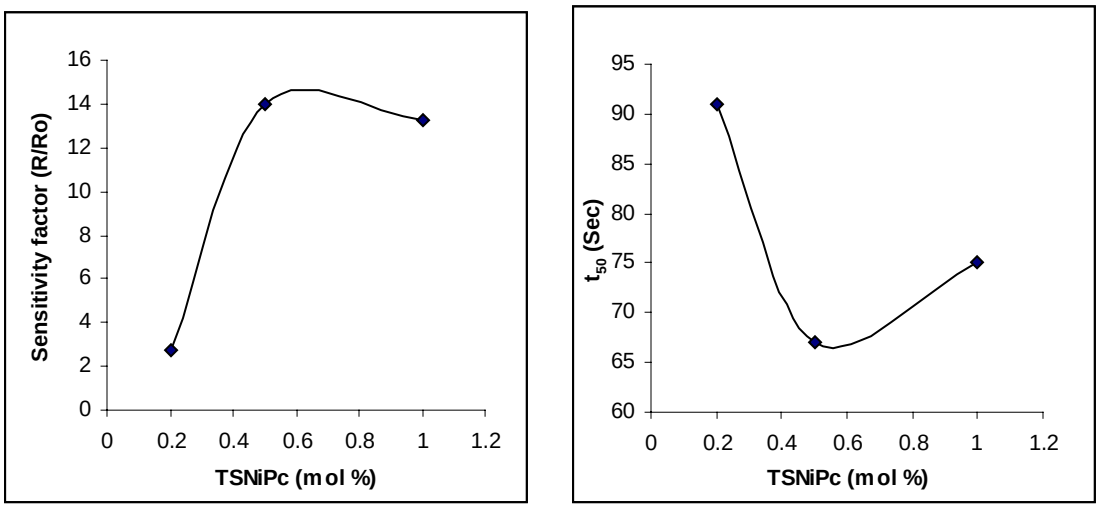

(a) **(b)**

Fig. 4.24. Sensor characteristics of Electrochemically functionalized TSNiPc-PANI towards NO_2 gas

(a) Plot of sensitivity factor versus concentration of TSNiPc

(b) Time of response (t_{50}) versus concentration of TSNiPc

Table 4.7. Sensor characteristics of TSNiPc functionalized PANI towards NO_2 gas

Compound	**Mol %**	**Sensitivity factor (S)**	**Speed of response (t_{50}) (Sec)**
TSNiPc-PANI	0.2	2.69	91
	0.5	14.00	67
	1	13.28	75

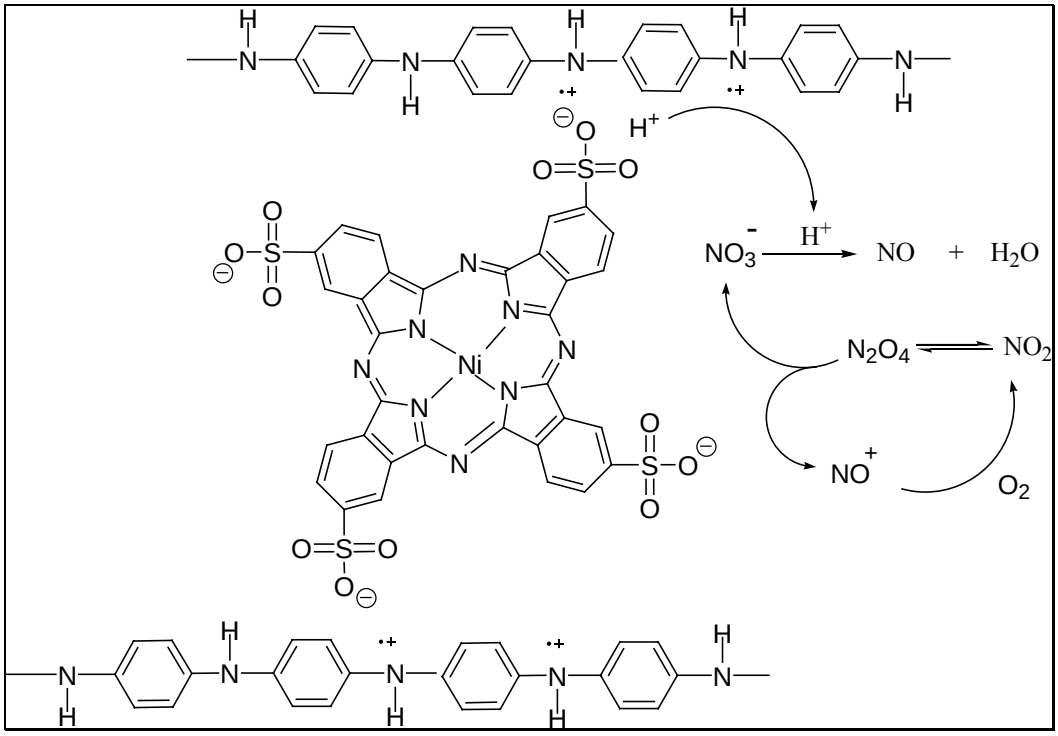

Fig. 4.25. Pictorial representation of gas sensing of TSNiPc functionalized PANI towards NO_2 gas

4.6. Conclusion

This chapter describes the incorporation of functional molecule TSNiPc into conducting polyaniline by chemical and electrochemical methods. The synthesized polymer samples were thoroughly characterized by various spectroscopic techniques like IR, UV, WXRD, AAS and their properties like electronic conductivity, thermal stability, morphology and its application towards NO_2 gas sensing were studied in detail. In IR, the signature of phthalocyanine and the shift in the characteristic bands of PANI confirm its functionalization. As seen from the optical spectra, the incorporated phthalocyanine increases the intensity of polaron to bipolaron transition in PANI indicating the effect of

phthalocyanine on polyaniline backbone. Notable changes in the crystallinity has been observed in the WXRD studies of TSNiPc-PANI. The increase in crystallinity of TSNiPc-PANI could be due to more ordering of polymer chain with the addition of macrocyclic phthalocyanine unit and this has been confirmed by the increase of charge transport revealed by the conductivity studies carried at room temperature. The amount of phthalocyanine incorporated in PANI was examined by metal ion analysis through GFAAS and EDAX techniques. As observed from the thermogravimetric studies, the thermal stability of chemically synthesized polymer samples were found to be better than the electrochemically deposited TSNiPc-PANI.

Cyclic voltammetric studies of the electrochemically deposited polymer samples showed two redox peaks in the (-)ve potential side characteristics of phthalocyanine ring reduction. From the CV studies, it can be understood that these materials can also be used as electrocatalytic study of thiol oxidation. The possibility of use of these functionalized polymers as gas sensors has been exploited by detecting its sensitivity towards 100 ppm NO_2 gas. It can be justified that, formation of nano fibers in the electrochemical deposition of TSNiPc-PANI could be the reason for higher sensitivity and faster response to NO_2 gas. The electrochemically synthesized TSNiPc-PANI samples showed almost seven times higher sensitivity than the chemically functionalized samples. A fast response time (t_{50} of 67 sec) was observed with electrochemically prepared PANI containing 0.5 mol % TSNiPc. The TSNiPc incorporated PANI is a very interesting polymeric material in terms of its electrical conductivity, thermal stability and most importantly it can be promising material for the sensor application for detecting low concentrations of NO_2 gas.

4.7. References

[1] D. C. Dyer and J. W. Gardner, Sens. Actuators. A., 62 (1997) 724.

[2] M. Cole, J. W. Gardener, A.W.Y. Lim and J. E. Brignell, Sens. and Actuator B., 58 (1999) 518.

[3] H. S. Nalwa, Handbook of Organic Conductive Molecules and Polymers, Vol.4 John Wiley and Sons Ltd, London, 1997.

[4] B. Bott and T. A. Jones, Sens. Actuator B., 5 (1984) 4.

[5] C. C. Leznoff and A. B. P. Lever, Phthalocyanine , Vol.3, properties and applications, VCH, New york (1989).

[6] G. Schmid, E. Witke, U. Schlick, S. Knecht and M. Hanack, J. Mater. Chem., 5 (1995) 855.

[7] J. Tan, X. Jing, B. Wang and F. Wang, synth. Met., 24 (1988) 231.

[8] Y. Wei, W. W. Focke, G. E. Wnek, A. Ray and A. G. MacDiarmid, J. Phys. Chem., 93 (1993) 495.

[9] F. S. Wang, J. S. Tang, L. Wang, H. F. Zhang and Z. Mo, Mol. Cryst. Liq. Cryst., 160 (1988) 175.

[10] J. P. Pouget, M. E. Jozefowicz and A. J. Epstein, Macromolecules., 24 (1991) 779.

[11] A. G. MacDiarmid, A. J. Epstein, Synth. Met., 69 (1995) 85.

[12] Y. Cao, P. Smith and A. J. Heeger, Synth. Met., 48 (1992) 91.

[13] R. Seoudi, G. S. El-Bahy and Z. A. El Sabed, J. Mol. Struct., 753 (2005) 119.

[14] S. Radhakrishnan and A. B. Mandale, Synth. Met., 62 (1994) 217.

[15] N. E.Agbor, M. C.Pretty and A. P.Monkman, Sens. Actuator B., 28(1995)173.

[16] E. T. Kang, K. G. Neoh, K. L. Tan, Prog. Polym. Sci., 23 (1998) 277.

[17] D. Li, Y. Jiang, Z. Wu, X. Chen and Y. Li, Sens. Actuator B., 66 (2000) 125.

[18] N. S. Sariciftci, H. Kuzmay, H. Neugebauer and A. Neckel, J. Chem. Phys., 92 (1990) 4530.

[19] R. M. silverstein, G. C. Bassler and T. C. Morrill, Spectrometric identification of organic compounds, John Wiley and sons, 4th edi, 1981.

[20] M. Gholamain, J. Sundram and A. Q. Contractor, Langmuir., 3 (1987) 741.

[21] M. Ulmann, R. Kostecki, J. Augustynski, D. J. Strike and M. Koudelka-Hep, Chimica., 46 (1992) 138.

[22] C. Coutanceau, A. Rakotondrainibe, P. Crouigneau, J. M. Leger and C. Lamy, J. Electroanal. Chem., 386 (1995) 173.

[23] N. Kobayashi and W. A. Nevin, App. Organometallic. Chem., 10 (1996) 579

[24] N. Phougat and P. Vasudevan, J. Power. Source., 69 (1997) 161.

[25] E. M. Genies, A. Boyle, M. Lapkowski and C. Tsintavis, Synth. Met., 36 (1990) 139.

[26] C. C. Leznoff and A. B. P. Lever, Phthalocyanine , properties and applications, Vol.3, VCH, New york (1989).

[27] A. B. P. Lever, S. Licoccia, K. Magnell, P. C. Minor and B. S. Ramaswamy, Adv. Chem. Ser., 201 (1982) 237.

[28] J. T. S. Irvine, B. R. Eggins and J. Grimshaw, J. Electroanal. Chem., 271 (1989) 161.

CHAPTER-5

Synthesis and properties of tetra sulfonated Copper phthalocyanine doped PANI

5.1. Introduction

Copper phthalocyanine and its substituted derivatives have enjoyed considerable industrial importance for use in dyestuffs, paints, colours for metal surfaces, fabrics and plastics. However, they are being intensively developed for a host of other high technology applications such as photodynamic cancer therapy, display devices, electrocatalysis, photocatalysis, photovoltaic devices and chemical sensors [1]. Recent researches show that various metals substituted phthalocyanine (Pc) or their peripherally substituted derivatives exihibit different responses to the sensing gas. Among the metal substituted Pc, CuPc has been found to have superior properties than the others in terms of sensitivity, reproducibility in the detection of gases [2].

Since phthalocyanine has rigid and highly extended and fused conjugated structures it is difficult to make thin films or coatings from them. Even the films cast from solutions are found to be brittle. In order to make use of these materials for particular application they are dissolved or dispersed on an insulating polymer matrix. Such dispersions are cast as films and studied for various applications. Copper phthalocyanine and its derivatives have been incorporated into various insulating polymer matrices such as PTFE, Poly imide, Poly-N-vinyl carbazole, etc to study its viability in optoelectronic and molecular electronic applications [3-4]. Copper phthalocyanine possessing carboxyl terminals are incorporated into polyaniline and the resulting material was blended with PMMA to improve its conductivity [5]. Similarly, co-facially stacked polymeric phthalocyanines have been incorporated into high strength polyaramide fibers and doped after extrusion to yield stable conductive fibers [6].

When phthalocyanines are incorporated into conducting polymers, extended conjugated structures become available both on the dopant and on the matrix polymer to provide useful and intriguing properties such as increased catalytic activity, improved durability and high electronic conductivity. Thus, the usual functions of the phthalocyanine such as electrochromism, electrocatalysis, change in physico chemical properties upon coming in contact with foreign species, etc. can be readily exploited by incorporating them into suitable conducting polymers such as polyaniline, polypyrrole, etc. by chemical or electrochemical means. Although, the science and technology of phthalocyanine has advanced well, its potentiality with conducting polymer has not been well explored especially towards its utility in gas sensing and till date, no report is found on the NO_2 gas sensing behavior of polyaniline functionalized with sulfonated copper phthalocyanine. The present chapter discusses the functionalisation of emeraldine salt form of polyaniline with tetra sulfonated copper phthalocyanine by chemical and electrochemical method. The various physico-chemical properties like crystallinity, electrical conductivity, thermal stability, morphology, redox behavior and sensing towards NO_2 gas were evaluated and compared at the end of this chapter.

Section–A : Studies on chemically synthesized tetra sulfonated copper phthalocyanine (TSCuPc) doped Polyaniline (PANI)

5.2. Synthesis of tetra sulfonated copper phthalocyanine doped PANI (TSCuPc-PANI).

In the first step, the sodium salt of sulfonated copper phthalocyanine (TSCuPc) 0.433 g (1 mol % w.r.t aniline concentration) was dissolved in 25 ml of distilled water

and converted into its corresponding sulfonic acid as described in the previous chapter. Polymerisation of aniline along with the functional dopant phthalocyanine was carried out in aqueous medium. A typical procedure for the functionalisation of PANI involves, acidifying 4 ml of distilled aniline with stoichiometric equivalent of 25 ml 2 M HCl and 25 ml of TSCuPc solution. An aqueous solution of ammonium per sulphate containing 9.98 g in 200 ml of water was added into the above reaction mixture with constant stirring. The reaction was carried out at 5ºC by keeping it in ice bath for 4 hours. At the end, green mass of TSCuPc functionalized PANI product was collected by pouring the reaction mixture in 1000 ml of water. The green mass obtained was filtered, washed repeatedly with distilled water to remove excess oxidizing agent and acid and finally vacuum dried for 24 hours. Yield: 4.307 g. The same procedure was followed for carrying out series of above reaction by changing the concentration of dopant TSCuPc from 0.1 to 1 mol % w.r.t aniline. The yields obtained for the above reactions are reported in Table 5.1

Table 5.1. Summary of the yield of reaction TSCuPc and Aniline

No	TSCuPc added (mol%)	Yield of TSCuPc-PANI(g)	PANI conversion (%)
1	0	3.628 (PANI alone)	88.3
2	0.1	3.709	90.1
3	0.2	3.837	92.3
4	0.5	4.048	94.4
5	1	4.307	95.7

When the PANI conversion was ploted against the concentration of TSCuPc used, the yield of the reaction follows the equation given below as discussed in the section 3.2.

$$y = A + Bx - Cx^2$$

where A is the yield of PANI obtained i.e., 88.3. The coefficient B corresponds to the concentration of phthalocyanine enhancing the reaction and C corresponds to retardation of polymerization. Its clear from the above equation that, there is enhancement in the polymer formation upto certain concentration of phthalocyanine which indicates the catalytic effect due to the added phthalocyanine. However, above 0.6 mole % the large molecules do not allow the aniline to reach the active site Cu attached to the ligand and hence there is a retardation in the additional polyaniline formation at these concentrations.

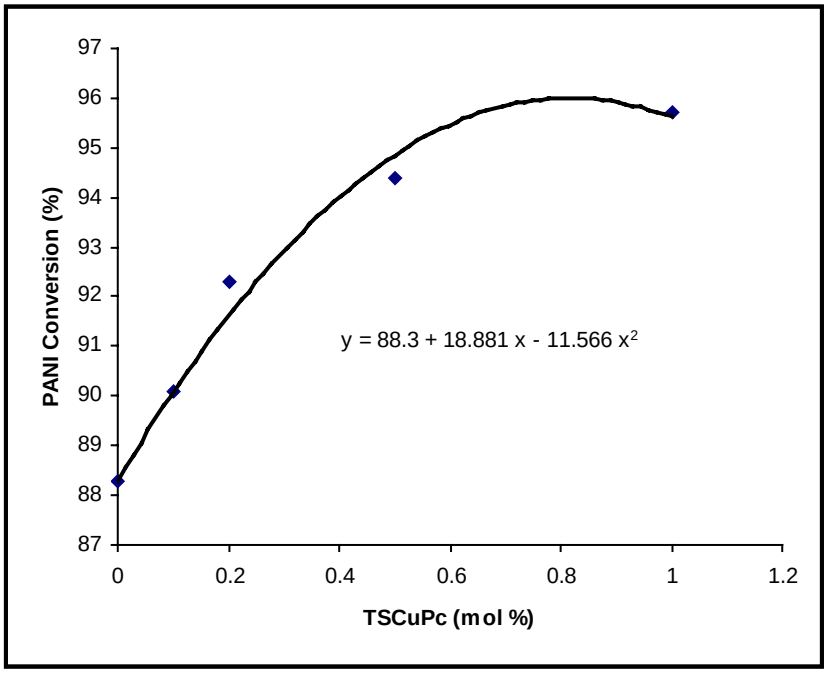

Fig. 5.1. The plot of PANI conversion versus TSCuPc concentration

5.3. Results and Discussion

5.3.1. Characterisation of Structure

The structure of the copper phthalocyanine incorporated PANI was characterized thoroughly by the following physico-chemical techniques.

5.3.1.1. FT-IR studies

The IR spectra of TSCuPc functionalized PANI (TSCuPc-PANI) along with TSCuPc and PANI are shown in Fig. 5.2. In the IR spectra of PANI, Fig. 5.2(a), the intense bands at 1580 and 1494 cm^{-1} have been assigned, respectively, to the ring stretching modes of the quinoid and benzenoid rings. The band at 1307 cm^{-1} is assignable to C-N stretching adjacent to the quinoid structure. The band at 1163 cm^{-1} has been attributed to the B-N^{+}H-B stretching Vibration while the band at 817 cm^{-1} is due to the C-H out of plane bending of 1,4-disubstituted benzene. After incorporation, the spectral changes observed as shown in Fig. 5.2(b) are almost similar to those observed in the IR spectral studies of earlier chapters. For example, the band due to the benzenoid structure at 1494 cm^{-1} shows a red shift. The band due to the quinoid structure at 1580 cm^{-1} also weakens and shows a small red shift. The characteristic asymmetric and symmetric stretchings of sulfonic acid in TSCuPc appeared as a small band at 1389 and 1027 cm^{-1} [7]. Similarly other characteristic bands at 748, 606 and 510 cm^{-1} corresponding to –(C-C)- stretching and ring out of plane bending showed greatly decreased intensity. The infrared spectral results suggest that there is a substantial interaction between PANI and the co-dopant TSCuPc. All the characteristic group frequencies and their assignments are presented in Table.5.2.

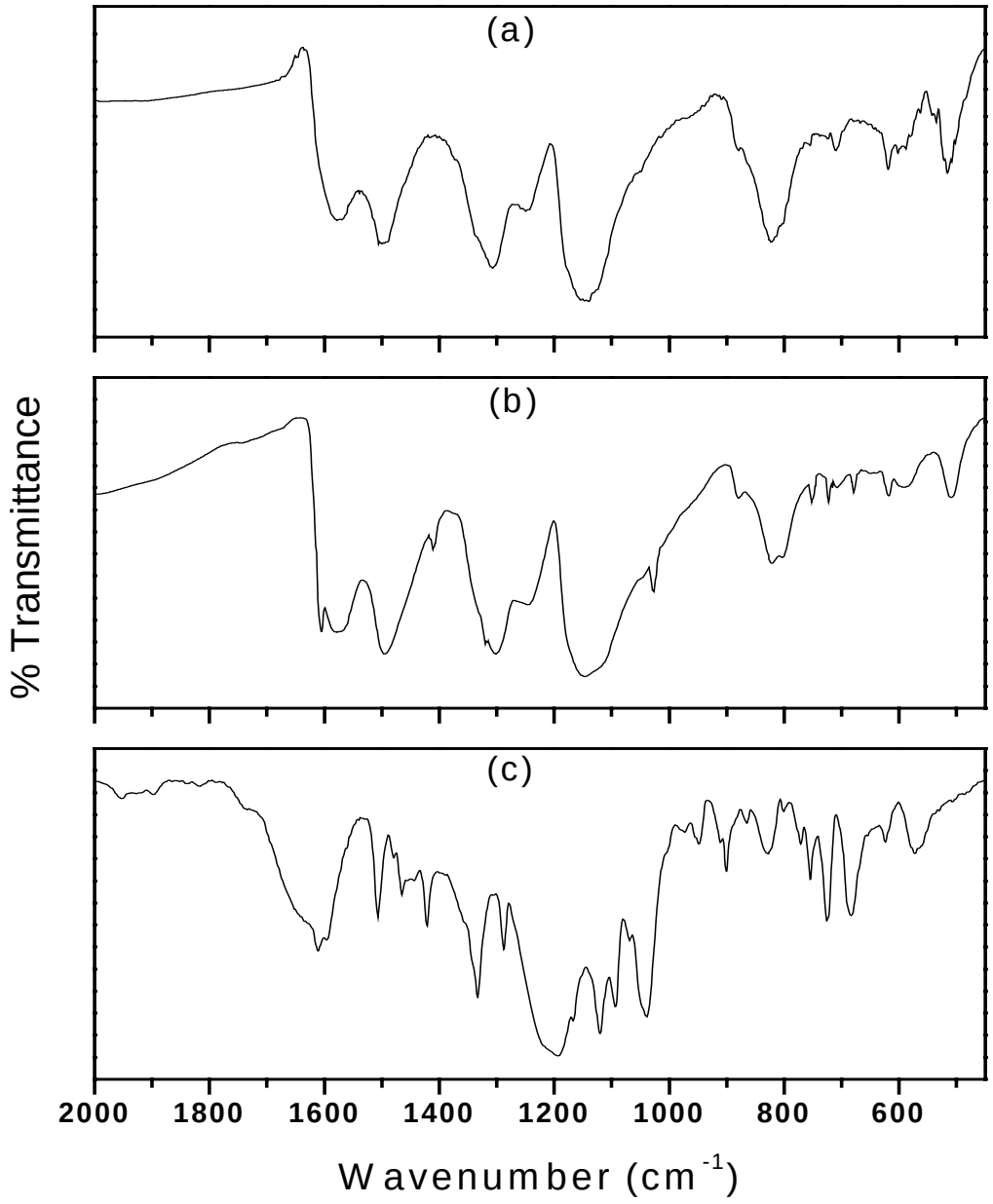

Fig. 5.2. FT IR Spectra of (a) HCl doped PANI; (b) TSCuPc functionalized PANI; (c) TSCuPc

Table:5.2 Assignment of bands in the FTIR spectra of TSCuPc-PANI

Peak positions (cm^{-1})		IR band assignments
PANI	**TSCuPc-PANI**	
-	1599 w	υ(C=C)stretching in Pc skeleton
1580 s	1567 s	Quinoid ring stretching
1494 s	1485 s	Benzenoid ring stretching
-	1389 w	Asymmetric stretching of O=S=O
1307s	1294 vs	υ(C-N) stretching vibration of aromatic ring
1163 vs	1137 m	$B\text{-}N^{+}H\text{-}B$ stretching Vibration
-	1027 m	symmetric stretching of O=S=O
817 s	801 s	para disubstituted benzene ring
748 m	703 m	υ(C-C) ring stretching
606 m	601 m	Out of plane (C-H) bending vibration
510 m	494 m	γ(C=C) out of plane ring bending

vs: very strong, s: strong, m: medium, w: weak

5.3.1.2. UV- Visible studies

The electronic spectra of TSCuPc and TSCuPc-PANI were recorded in water and formic acid medium. The electronic absorption spectrum of TSCuPc shown in Fig 5.3. displays two major absorption bands designated as Q and B bands appeared at 762 and 407 nm. It can also be noticed that the Q band shows characteristic splitting present in all phthalocyanine derivatives [8,9] and it appears due to extensive coupling between the

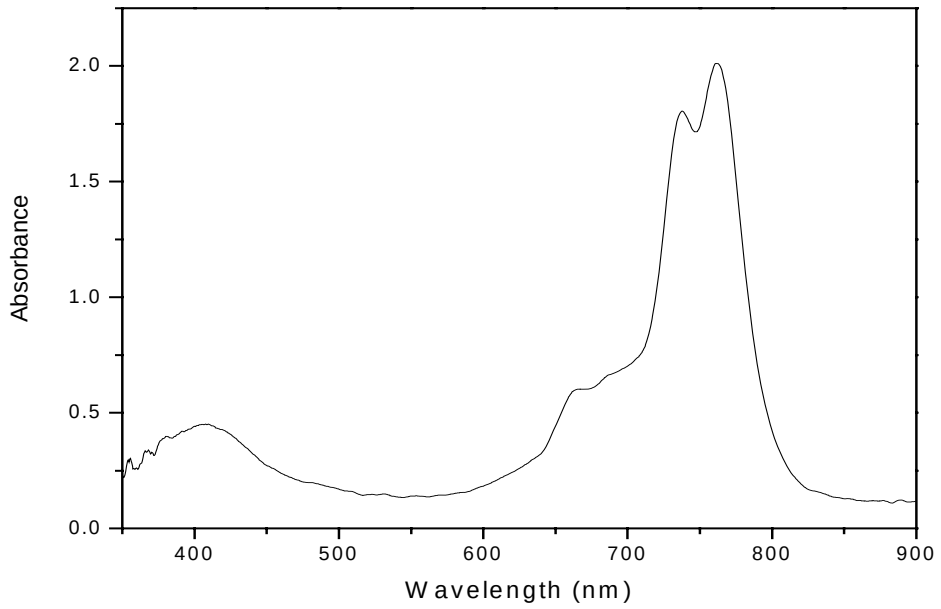

Fig. 5.3. UV-Vis absorption Spectra of TSCuPc

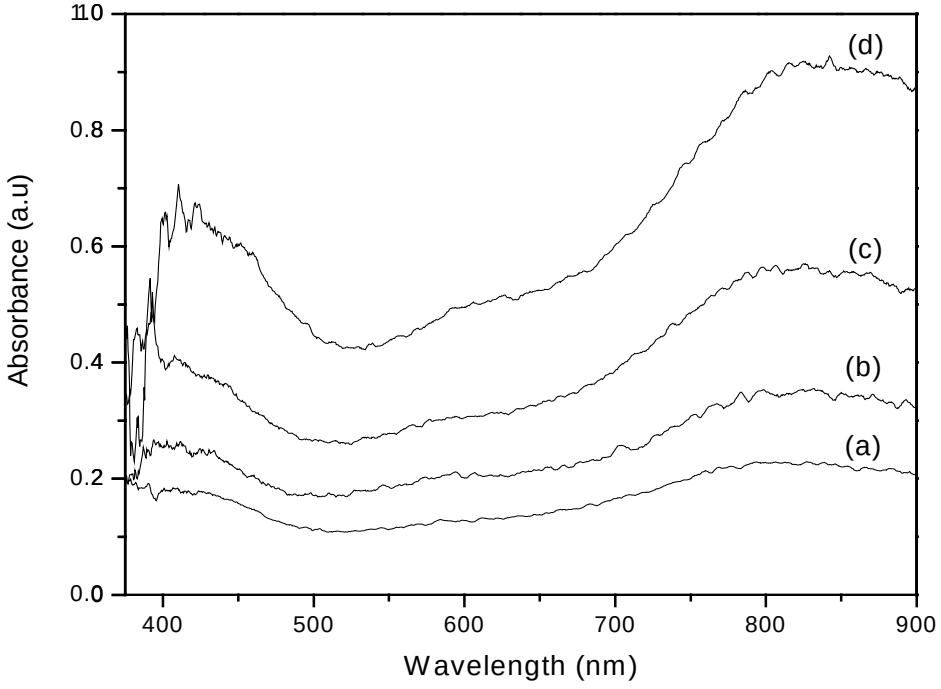

Fig. 5.4. UV-Vis absorption spectra of various mol % of TSCuPc in PANI

(a) PANI, (b) 0.2mol % TSCuPc, (c) 0.5 mol % TSCuPc (d) 1 mol % TSCuPc

π -systems of adjacent ring. The Q band represents the π - π* transition taking place from the highest occupied molecular orbital (HOMO) to the lowest unoccupied molecular orbital (LUMO) of the macrocyclic ligand and the high energy region of the B band explains the π-d transition taking place in the complex [10]. Since the Q band is sensitive to nearby chemical environment, its peak has vanished after getting incorporated into PANI matrix. The absorption spectra of PANI as a function of TSCuPc concentration are shown in Fig. 5.4. In the spectra of TSCuPc-PANI (Fig 5.4(d)), the band at higher energy region 427 nm corresponds to the π - π^* transition and the wide band at lower energy region 839 nm represents the polaron to bipolaron transition which are responsible for the charge carriers in the polymer. An increase in intensity was noted for this band with the increase of phthalocyanine concentration in PANI, which clearly indicates the contribution made by the phthalocyanine moiety to the free charge carrier density in the polymer matrix. Apart from the increase in intensity, both the bands showed slight red shift with the function of Pc concentration in PANI and this is expected due to the extended delocalization of π electrons. A shoulder at 595 nm has been observed characteristic of quiniod to benzeniod transition.

5.3.1.3. Wide Angle X-ray Diffraction (WAXD) Studies

The crystal structures of the various forms of PANI with different counter-ions continue to be under active investigation. The X-ray profile of PANI doped with HCl is well known and discussed in detailed [11]. It's reported that the structure of PANI is determined by the method of preparation, oxidant and type of dopant used. The PANI prepared by us was found to have certain percentage of crystallinity having peaks

centered at 2θ values 8.9, 20.3 and 25.4. When it was functionalized with TSCuPc, ordering of polymeric chain takes place and hence we could observe certain increase in the intensity of the peaks centered at 2θ values 6.8, 15, 20.1 and 25.4. The X-ray diffraction pattern of TSCuPc and TSCuPc-PANI are shown in Figs. 5.5. and 5.6. It's worth noticing that, after incorporation, the characteristics peaks for TSCuPc have not been observed in the diffraction patterns of TSCuPc-PANI, which suggests that the long range ordering of phthalocyanine is lost and the molecules are well dispersed throughout the polymer matrix. The introduction of phthalocyanine unit has the tendency to induce some molecular rearrangements of PANI due to strong π-π interaction between the adjacent ring regularly spaced along the polymer chain backbone. Hence, it is observed that a sharp peak at 2θ = 6.8 which does not belong to TSCuPc appears and the peak at 25.4 degrees increases in intensity.

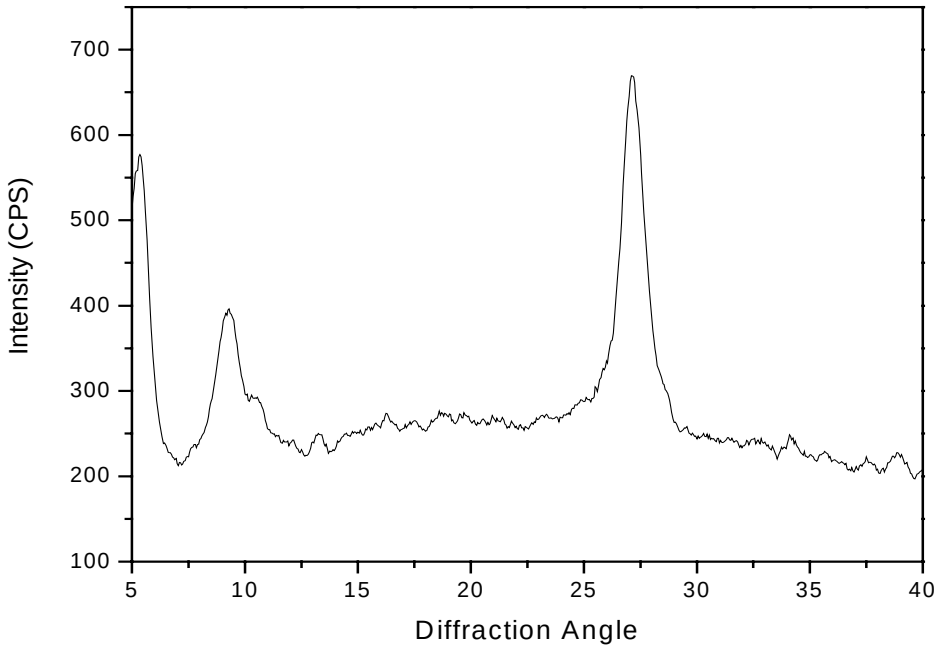

Fig. 5.5. X-ray diffractogram of TSCuPc

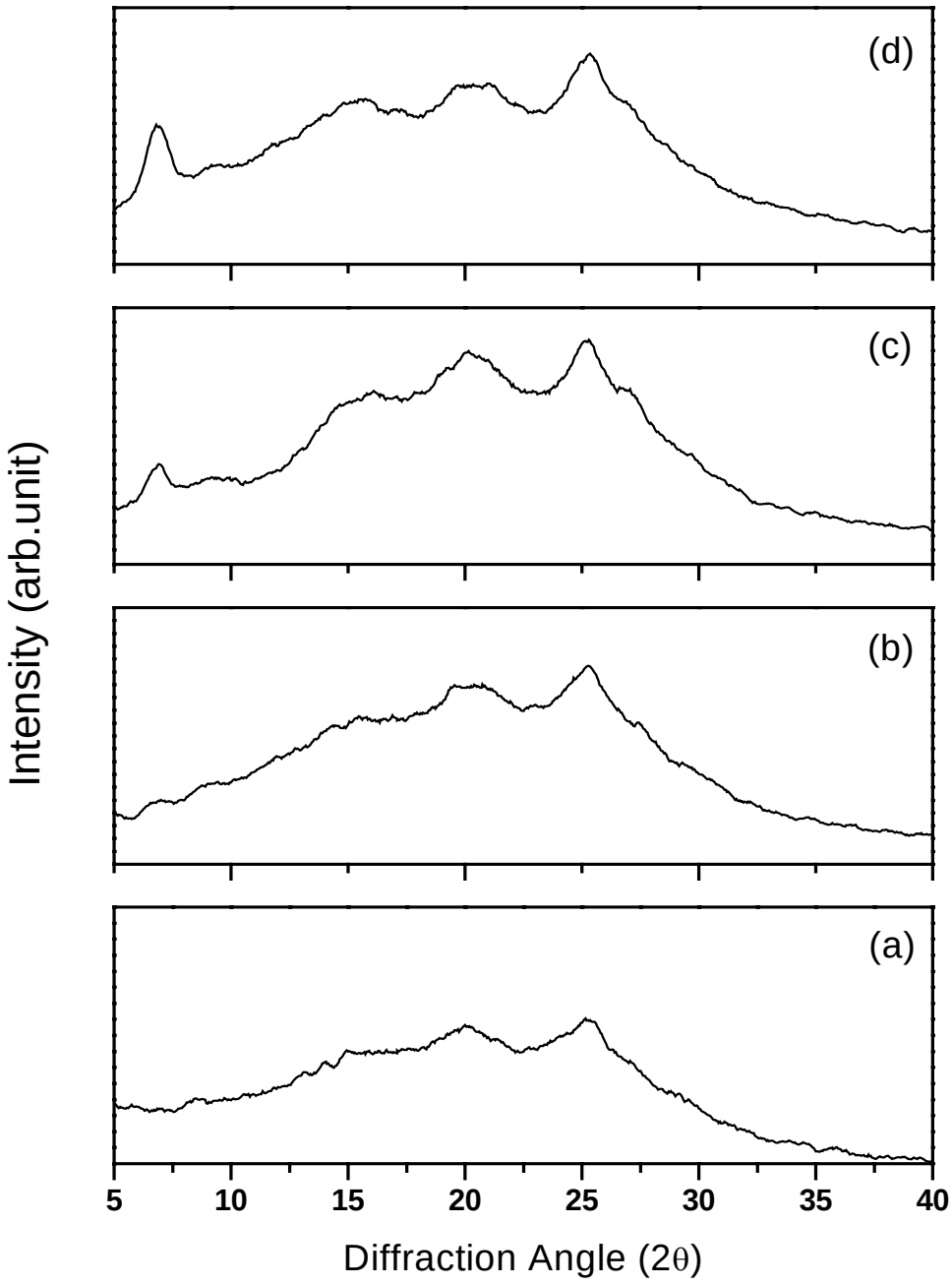

Fig. 5. 6. X-ray diffraction pattern of various mol % of TSCuPc incorporated PANI (a) PANI, (b) 0.2 mol % TSCuPc, (c) 0.5 mol % TSCuPc (d) 1 mol % TSCuPc

The major reflections in the diffraction pattern of TSCuPc, PANI and TSCuPc-PANI and their d-spacing values are presented in table 5.3.

Table 5.3 Major reflections in the X-ray diffraction patterns

Compound	2 Theta	I/Io	d-values
PANI	8.9	37	9.92
	15	54	5.9
	20.3	74	4.37
	25.4	100	3.5
	27	78	3.3
TSCuPc-PANI	6.8	72	12.98
	15.0	83	5.9
	20.1	88	4.41
	25.4	100	3.50
TSCuPc	5.3	85	16.65
	9.3	59	9.5
	27.2	100	3.27

5.3.1.4. Graphite Furnace Atomic Absorption spectroscopic (GFAAS) studies

The amount of phthalocyanine incorporated in PANI was estimated by analyzing the percentage of copper content in the sample. It can be seen that the copper content in functionalized sample increases gradually upon increasing the mol % of TSCuPc and the content is almost same as the content taken at the start of the reaction. This clearly indicates that the amount of sulphonated phthalocyanine added during synthesis has been fully functionalized and it has not been washed out during the work up of the product.

The various mol % of TSCuPc in PANI and the percentage of copper present are presented in Table 5.4.

Table 5.4. The percentage of copper content in various mol %

TSCuPc functionalized PANI

Compound	**copper content (wt%)**
PANI-0.2 mol% TSCuPc	0.111
PANI-0.5 mol% TSCuPc	0.254
PANI-1mol% TSCuPc	0.557

5.3.1.5. Energy Dispersive X-ray (EDX) studies

The percentage of two dopants namely chloride and sulfonated copper phthalocyanine were determined by analyzing the chlorine and Copper content in the synthesized sample using EDX technique. The EDX spectra of the PANI with various mol percentage of TSCuPc is shown in Fig. 5.7.

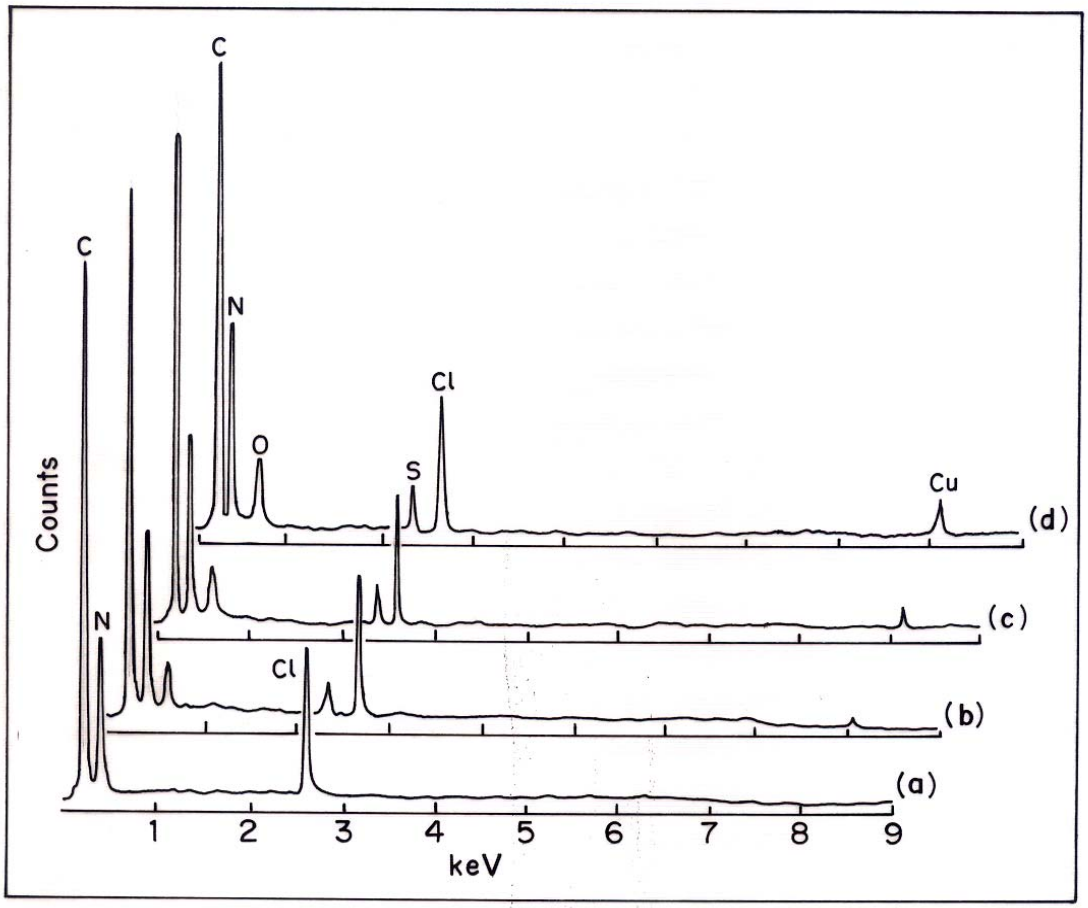

Fig. 5.7. The EDX spectra of the PANI with various mol percentage of TSCuPc (a) PANI (b) 0.2 mol % TSCuPc (c) 0.5 mol % TSCuPc (d) 1 mol % TSCuPc

5.3.2. Measurement of properties

The properties like electrical conductivity, thermal stability, morphology of the synthesized TSCuPc–PANI by electrochemical route and its application towards NO_2 gas sensing are discussed in this section.

5.3.2.1. Electrical Conductivity

A two-probe electrical contact arrangement coupled with Keithley electrometer and a home made cell was employed for evaluating the DC conductivity of these samples. In this study, the conductivities were measured at room temperature as a function of co-dopant concentration TSCuPc. Fig. 5.8. shows the variation of conductivity with respect to phthalocyanine concentration in PANI. The conductivity PANI-HCl was noticed as 2.58 x 10^{-2} S/cm and this found to increase with the addition of sulfonated phthalocyanine. PANI containing 1 mol % of phthalocyanine displayed a conductivity of 5.07 x 10^{-2} S/cm. In general, phthalocyanine is an organic semiconductor, conduct electron or hole in one direction through conjugated chains. When the phthalocyanine molecules organize itself to form stacks, there will be a strong π-π interaction between the adjacent ring and hence it will have tendency to conduct the electron in a cofacial manner when excess electrons or holes are introduced into the conduction or valence band [12]. When phthalocyanines are incorporated into polyaniline matrix, extended conjugated structures are available both on the dopant and on the polyaniline matrix and hence it provides better pathway for the transport of charges along and in between the polyaniline matrix. However, the effect of structural disorder also plays a vital role in the transport phenomena of polymers.

Several authors have reported the conductivities of polyaniline doped with sulfonic acids like DBSA, CSA, MSA and PTSA. We have the studied the effect of phthalocyanine sulfonic acid on the conductivity of PANI and it is quite interesting to note that conductivity of PANI increases as a function of phthalocyanine concentration. The self–secondary doping effect was shown to induce significant enhancement in

electrical properties [13]. The enhancement of the conductivity in these materials is either by the generation of extended states in doped molecules or by charged defects with electronic structures. Incorporation of phthalocyanine dopant modifes the structural properties of polyaniline. This modification plays an important role in enhancing the conductivity of the polymer. Also sulfonic acid of the phthalocyanine units may interact with amine/imine hydrogens, which enhances the electrical properties of the polymers

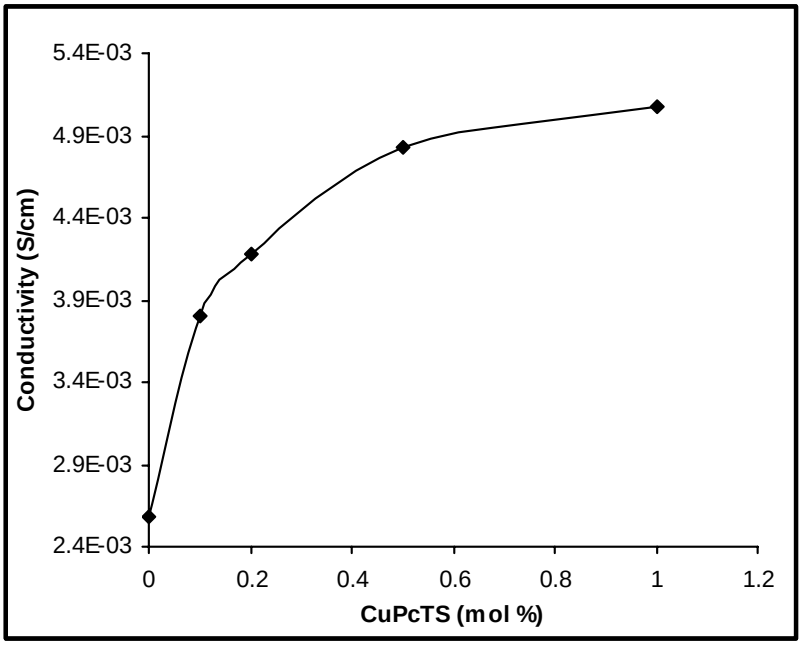

Fig. 5.8. Plot of conductivity versus TSCuPc concentration in PANI

5.3.2.2. Thermal stability

The TG thermogram of TSCuPc-PANI is shown in Fig. 5.9. along with PANI-HCl and TSCuPc for comparision. Its very clear from the thermogram that the thermal stability of polyaniline has increased with the addition of TSCuPc. In general, sulfonated phthalocyanine displays two stage degradative pattern corresponding to the removal of sulfonic acid group and degradation of phthalocyanine moiety where as in TSCuPc, we

could observe only one degradation starting at 445°C, which implies that among the sulfonated phthalocyanine, the copper phthalocyanine is said to have better thermal stability, correspondingly the thermally stability of functionalized polymer also has increased by 5 – 8°C at 445°C.

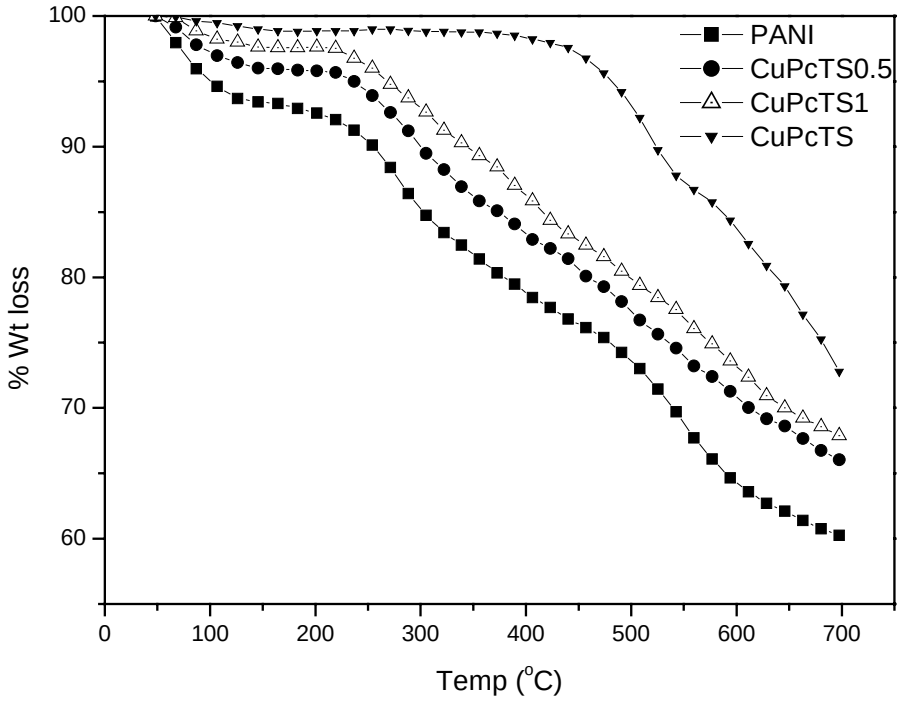

Fig. 5.9. Thermogravimetric analysis of TSCuPc-PANI samples

Here again, TSCuPc functionalized polymers showed two stage weight losses. The first one corresponds to the removal of adsorbed water and the chloride dopant [14], and the second one attributed to the structural decomposition of polymer backbone [15]. At 700°C, the weight retention of PANI-HCl is 60 %.where as 0.5 mol % TSCuPc and 1 mol % TSCuPc functionalized PANI samples showed a weight retention of 66 and 68 % respectively. Hence we can say that the phthalocyanine has a significant effect on the

thermal stability of the doped polymer. Here the thermal stabilization of polymer backbone primarily comes from the sulfonated phthalocyanine where it links the polymer chains together through its sulfonic acid group to give better thermal stability.

5.3.2.3. Scanning Electron Microscopy (SEM) Analysis

The scanning electron microscopy images of the samples are shown in Fig. 5.10. The morphology of the chemically synthesized polymer samples clearly shows the samples were particulate in nature but these become more flaky / platelet like with the incorporation of TSCuPc.

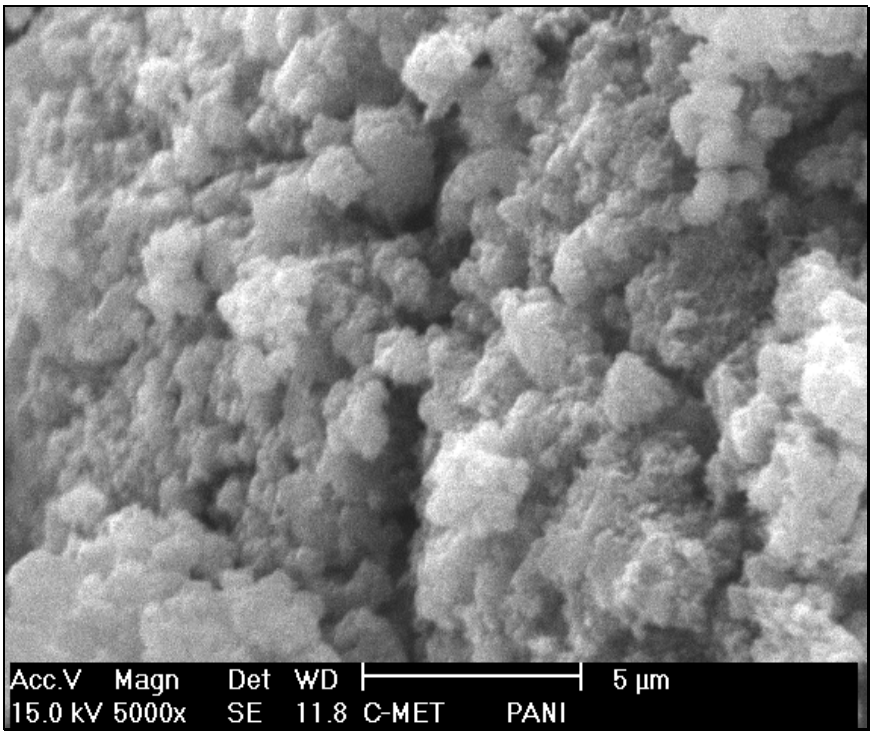

(a)

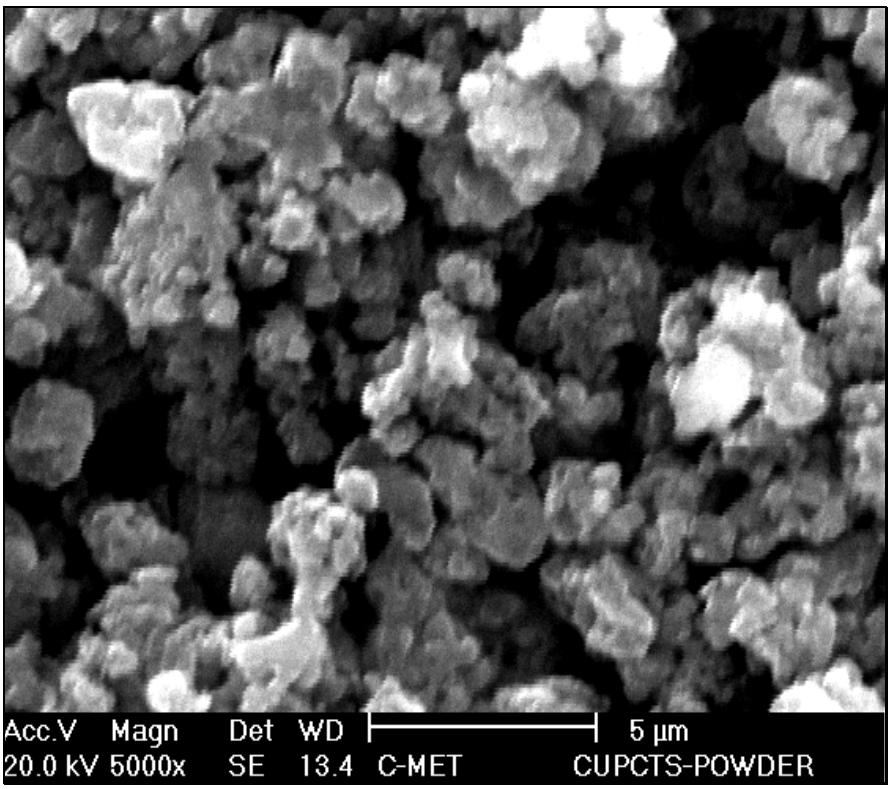

(b)

Fig.5.10. Scanning Electron Micrograph (SEM) images for (a) PANI-HCl (b) TSCuPc-PANI

5.3.2.4. Chemical sensor

Among the chemical sensor based on measurements of conductivity or dielectric constant of the sensitive layers when exposed to chemical vapours, the most commonly used materials like oxides of tin, titanium and zirconium show high sensitivity only at temperature exceeding 100°C [16], which can be harmful in many circumstances especially when explosives are involved. Hence efforts have been made in recent years to look for alternative sensing materials which show high sensitivity under room temperature ambient condition. Among these, conducting polymers have shown very

promising results, Since they exhibit large changes in conductivity over small concentration ranges of certain chemicals.

We have investigated the sensing characteristics of polyaniline containing various concentrations of functional molecule TSCuPc and report here some of the interesting features observed. The TSCuPc-PANI was mixed with PEO-$CuCl_2$ and made into paste. This paste was applied on an interdigitated electrode pattern so as to obtain a sensor element in a surface cell configuration. The sensor elements were tested by connecting it to Keithley electrometer which in turn interfaced with computer. The change in electrical resistance of the sensor element was monitored online through Test point software. Fig. 5.11. shows the response characteristics of sensor element containing various mol % of TSCuPc in PANI towards 100 ppm NO_2 gas. When the gas was introduced into the testing chamber, we observed only a smaller change in resistance for PANI-HCl whereas TSCuPc functionalized PANI showed change in resistance of almost 30 times for PANI with 1 mol % TSCuPc. It was seen that there is an increase in resistance after exposure to gas showing a response time t_{50} of 60 -100 seconds depending on the composition of PANI. It is interesting to note that the recovery is also fast and we could achieve a recovery of 85 %. From the response characteristics, the sensitivity (S) and response time (t_{50}) were calculated and shown in Fig. 5.12. In order to understand the above results, one has to analyse and study the interaction between the chemical vapour and the polymeric material as well as the process involved in the sensing action.

In the literature, Phthalocyanine and PANI individually interact with NO_2 gas showing decrease in resistance and the explanation is based on the increase in the number of holes when exposed to NO_2 gas [17,18]. In the present case, we could observe an

increase in resistance and this change in resistance could be due to the interaction of NO_2 gas with the dopant sulfonated phthalocyanine. (as discussed in the previous chapters) which in turn transfers the charge to the polymer backbone. The possible mechanism of interaction of NO_2 gas with the functionalized polymer is shown in Fig 5.25. The sensitivity factor (S) was calculated from the sensor characteristics of

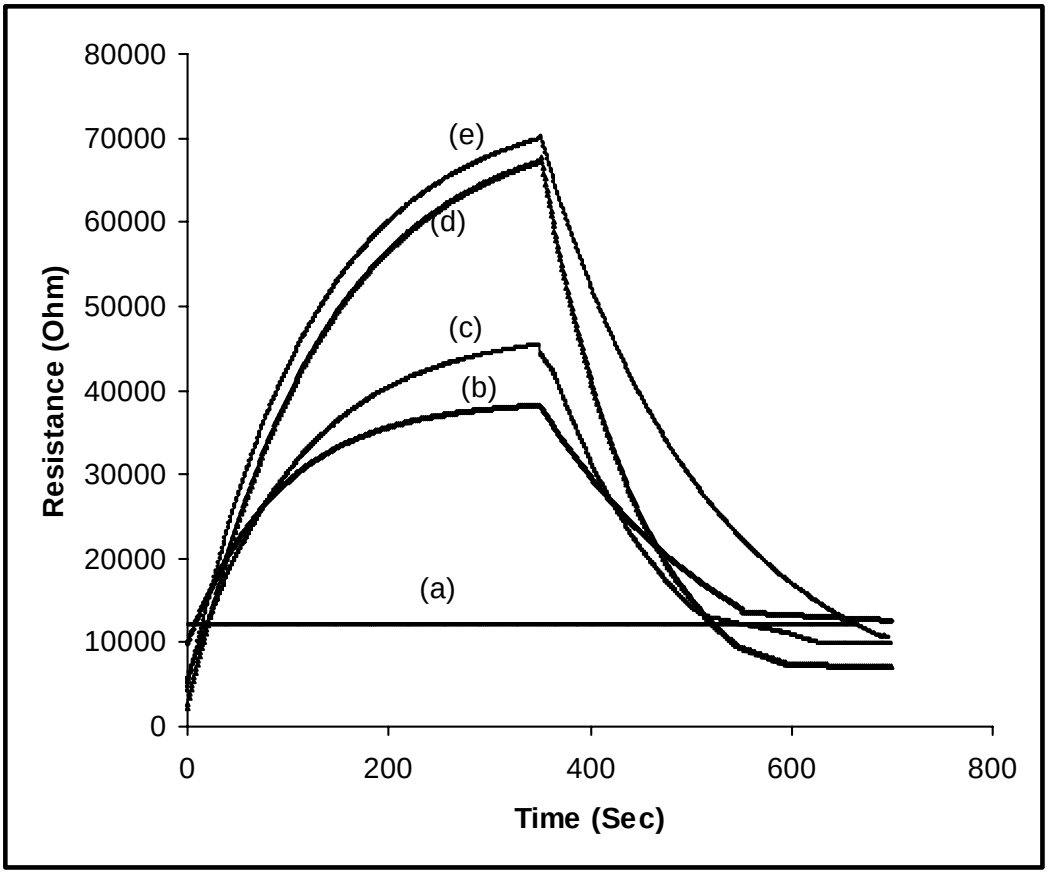

Fig. 5.11. Response characteristics of TSCuPc incorporated PANI towards NO_2 gas. (a) PANI, (b) 0.1 mol % TSCuPc-PANI , (c) 0.2 mol % TSCuPc-PANI , (d) 0.5 mol % TSCuPc-PANI and (e) 1 mol % TSCuPc-PANI

TSCuPc-PANI as mentioned in the last chapter. The chemical sensor made from 0.1 and 1 mol % CuPcTS doped PANI samples displayed a half time response t_{50} of 89 sec and 62 sec respectively. A high sensitivity factor (R_f/R_o) of about 30 was achieved with even

0.6 mol % CuPcTS. Above this concentration, there does appear to be more improvement in the sensor characteristics. Table 5.5 presents the sensitivity factor and speed of response obtained from the sensor characteristics of TSCuPc-PANI.

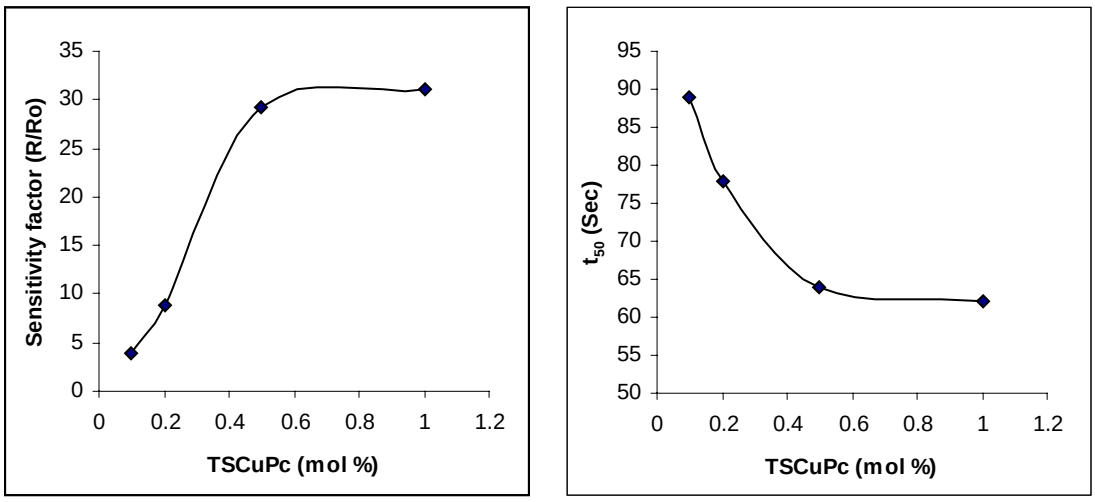

(a) **(b)**

Fig. 5.12. Sensor characteristics of TSCuPc functionalized PANI towards NO_2 gas

(a) Plot of sensitivity factor versus concentration of TSCuPc

(b) Time of response (t_{50}) versus concentration of TSCuPc

Table: 5.5. Sensor characteristics of TSCuPc functionalized PANI towards NO_2 gas

Compound	Mol % of TSCuPc	Sensitivity factor (S)	Speed of response (t_{50}) (Sec)
TSCuPc-PANI	0.1	3.8	89
	0.2	8.7	78
	0.5	29.3	64
	1	30.9	62

Section – B : Studies on electrochemical synthesis and properties of tetra sulfonated copper phthalocyanine (TSCuPc) doped PANI.

5.4. Synthesis of TSCuPc-PANI by electrochemical route

Electrochemical synthesis of polyaniline has some advantage including greater control over the oxidation potential and the fact that the products don't need to be exhaustively purified from excess monomer, oxidant and acid due to the deposition of polymer on the working electrode. Electrochemical polymerization of TSCuPc-PANI was carried out by the potentiodynamic method at a sweep rate of 50 mV/s by cycling the potential between -0.2 volt and 1 volt. The electrochemical cell was a classical three electrode cell consisted of platinum or ITO glass electrode with a geometric area of 1 cm^2 as working electrode for the deposition of functionalised PANI. The platinum and the standard calomel electrode (SCE) was used as the counter and reference electrodes. The experiments were carried out at room temperature under nitrogen atmosphere. The procedure for the synthesis of TSCuPc incorporated PANI by cyclic voltammetric technique is as follows. 0.2 ml (2 mmol) of freshly distilled aniline was acidified with 10 ml of 2 M hydrochloric acid. Then 10 ml of $2x10^{-5}$ molar copper phthalocyanine tetra sulfonic acid solution was added to the acidified aniline and taken in a single compartment electrochemical cell. During polymerization, the conjugate base ($CuPc(SO_3^-)_4$ of the dopant was incorporated into the polymer matrix. A thin film of TSCuPc-PANI deposited on the electrode was taken out from the electrolytic bath, washed repeatedly with water to remove acid and other impurities. A typical cyclic voltammogram obtained during the synthesis of TSCuPC-PANI is shown in Fig. 5.13.

A similar procedure was followed for the electrodeposition PANI with different mol % (0.2, 0.5 and 1) of TSCuPc. The various physico-chemical properties of the film were then studied by FT-IR, UV-Vis and WXRD techniques to elucidate its structure. The electrochemical studies were also done by cyclic voltammetric techniques in the DMF and aqueous solvents.

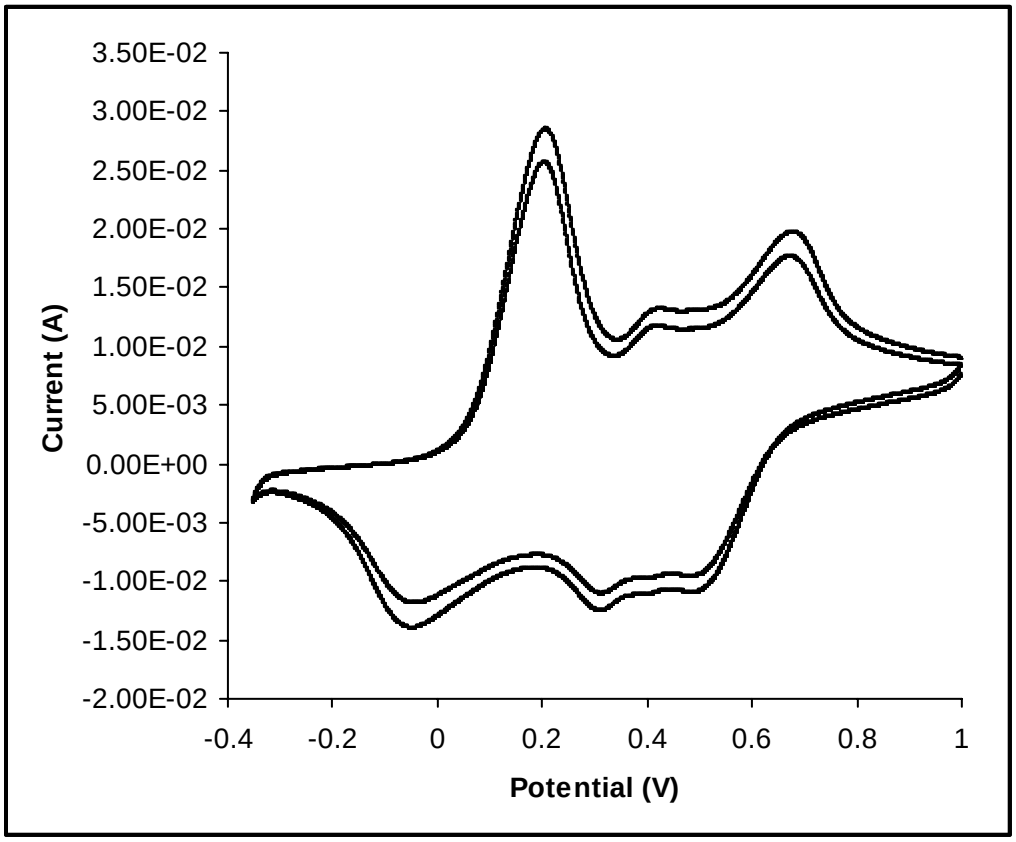

Fig. 5.13. Cyclic voltammogram obtained during electrodeposition of TSCuPc-PANI

5.4.1. Fabrication of Chemical sensor

The sensor was fabricated by electrodepositing the TSCuPc–PANI over the interdigitated gold electrode by means of potentiostatic method. In these experiment, a constant potential of 800mV was applied to the interdigitated gold electrode for 300 Sec.

PANI with various mol of TSCuPc (0.1, 0.5 and 1 mol %) were deposited by taking different concentrations of TSCuPc along with monomer and the electrolyte. A typical chronoamperometric curve is shown in Fig. 5.14. Since the sensitivity of the film depends on the thickness of the film, care was taken to have uniform film of surface area 1 cm^2.

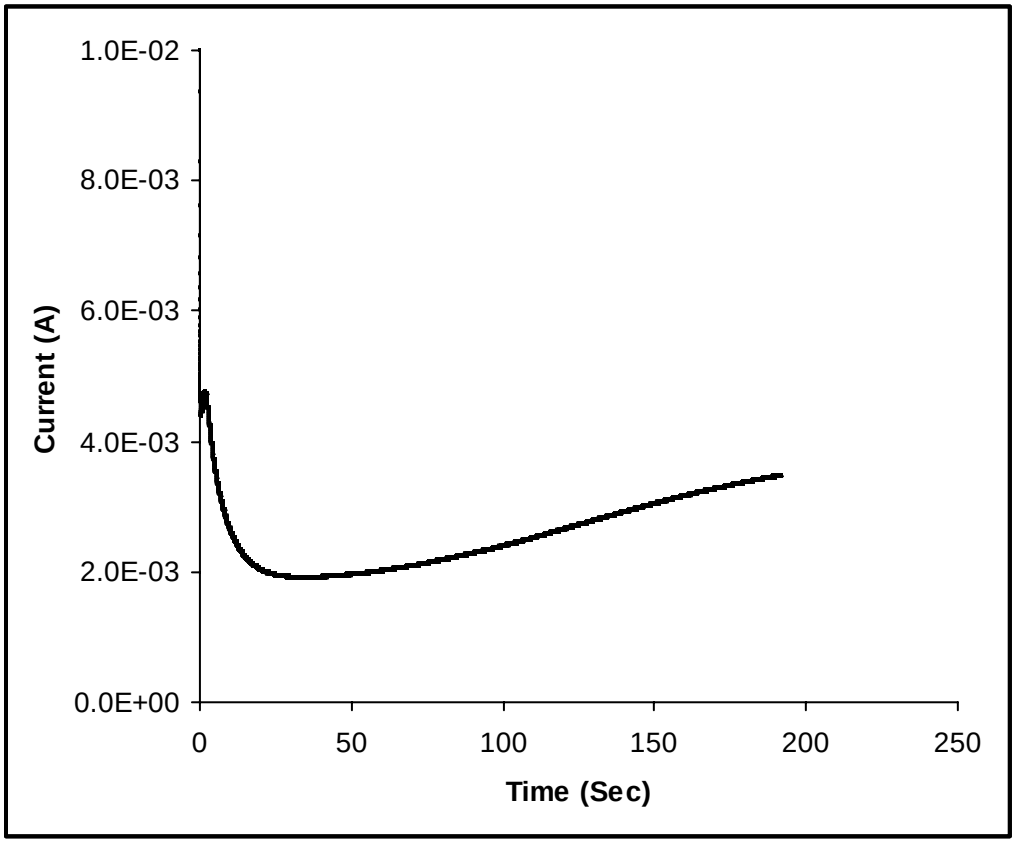

Fig.5.14. Chronoamperometric curve for the electrodepostion of TSCuPc -PANI

5.5. Results and Discussion

5.5.1. Characterisation of Structure

The structure of the copper phthalocyanine incorporated PANI film was characterized thoroughly by the following physico-chemical techniques.

5.5.1.1. FT-IR studies

Detailed examinations of the IR spectra of TSCuPc and electrochemically functionalized PANI (TSCuPc-PANI) have been made and their assignments of bands are presented in Table 5.6. By looking at the IR spectra shown in Fig 5.15. its clear that, the incorporation of TSCuPc has taken place in PANI matrix. The characteristic peaks of PANI has been broadened and slightly shifted towards lower wavenumber. For example, the –(c=c)- stretching of quiniod and benezeniod peaks appeared at 1575 and 1494 cm^{-1} are sharp in PANI where as the same in TSCuPc-PANI has been broadened and are not well resolved due to the overlapping bands of sulphonated phthalocyanine with PANI. The stretching vibrations of C-N bond of quinone and benzene ring of PANI appeared at 1310 cm^{-1} while the same has been shifted to 1301 cm^{-1} in TSCuPc-PANI. Apart from the usual bands, the asymmetric and symmetric stretching modes of O=S=O in the sulfonic acid appeared as weak bands at 1390 and 1027 cm^{-1}. Therefore, the FTIR spectra of TSCuPc-PANI polymer presented in Fig. 5.15 (b) provide clear evidence for the effective incorporation of sulfonated phthalocyanine.

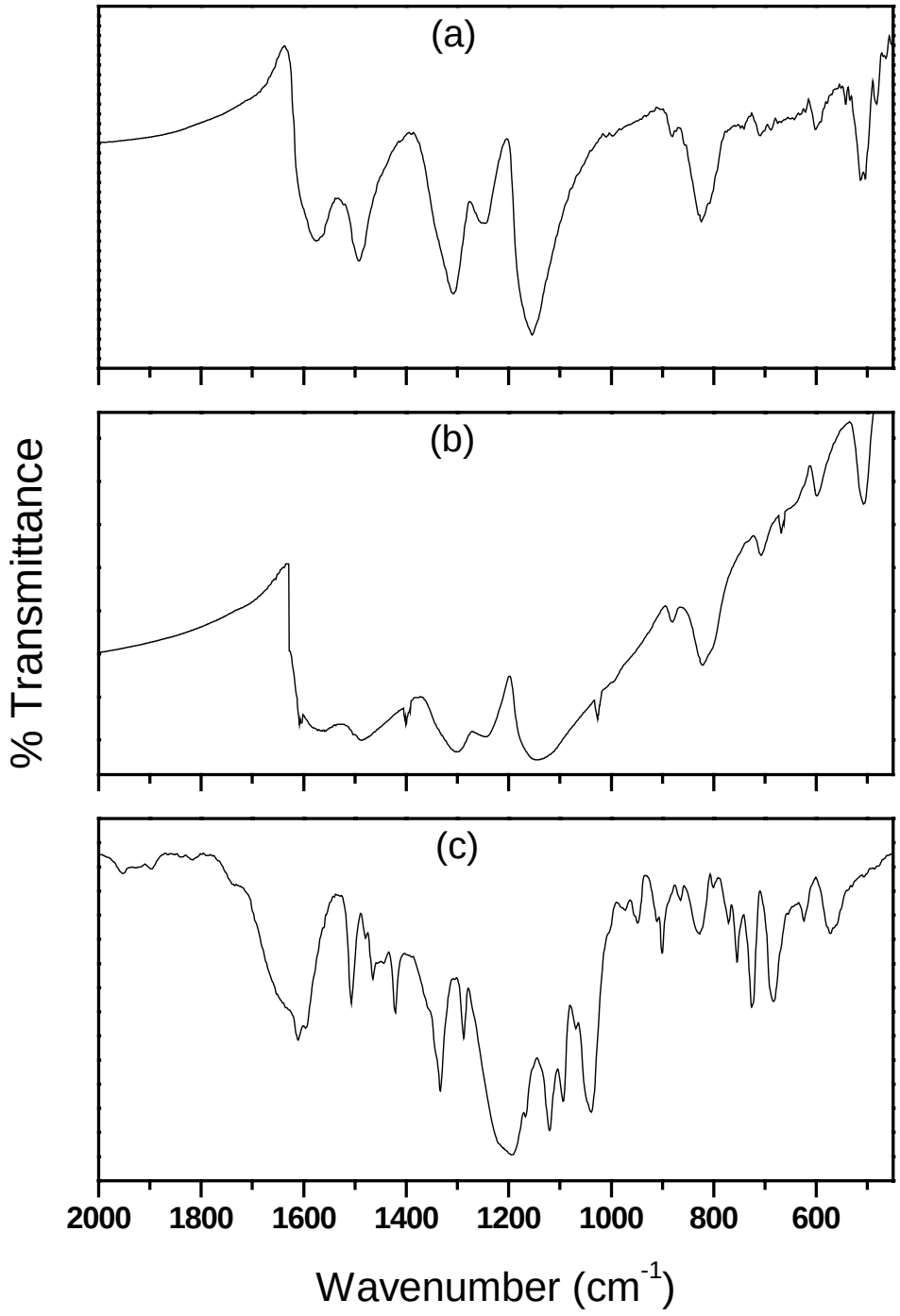

Fig. 5. 15. FTIR spectra of electrochemically functionalized polyanilines. (a) HCl doped PANI, (b) TSCuPc functionalized PANI, (c) TSCuPc

Table 5.6. FTIR band assignments for electrochemically functionalized PANI

Peak positions (cm^{-1})		IR band assignments
PANI	**TSNiPc-PANI**	
-	1607 w	υ(C=C)stretching in Pc skeleton
1575 s	1562 s	Quinoid ring stretching
1494 s	1486 s	Benzenoid ring stretching
-	1390 w	Asymmetric stretching of O=S=O
1310 s	1301 s	υ(C-N) stretching vibration of aromatic ring
1157 vs	1139 vs	$B\text{-}N^{+}H\text{-}B$ stretching Vibration and
-	1027 w	Symmetric stretching of O=S=O
824 s	821 s	para disubstituted benzene ring
-	668 m	γ(C-H) out of plane deformation of TSPc
599 w	596 w	υ(C-C) ring stretching
510 m	511 m	Out of plane (C-H) bending vibration

vs: very strong, s: strong, m: medium, w: weak

5.5.1.2. UV- Visible studies

Fig. 5.16. depicts the diffuse reflectance spectra of electrochemically prepared 1 μm thick PANI and TSCuPc-PANI film prepared under 2M HCl medium on an ITO substrate. These bands can shift as a result of change in the morphological or oxidative properties of the polymer [19]. The interpretations for PANI are same as discussed in the previous chapters. The TSCuPc-PANI film exhibits an absorption peak at 472 nm

(benzenoid π - π^* transition absorbance) and at 821 nm with a steadily increasing free carrier tail starting from around 850 nm to the near IR region. This behavior is consistent with a delocalized polaron band structure and an expanded coil like conformation for the polymer chain [20] indicating the PANI films are in conducting state. The intensity of the bipolaron peak at 821 nm increased with increase in TSCuPc concentration indicating higher doping levels. The absorption bands appearing at this lower energy region suggest the creation of polaronic and bipolaronic band structures during doping. The band at 559 nm is attributed either to the electronic transition from low valence levels to polaron or bipolaron levels [21].

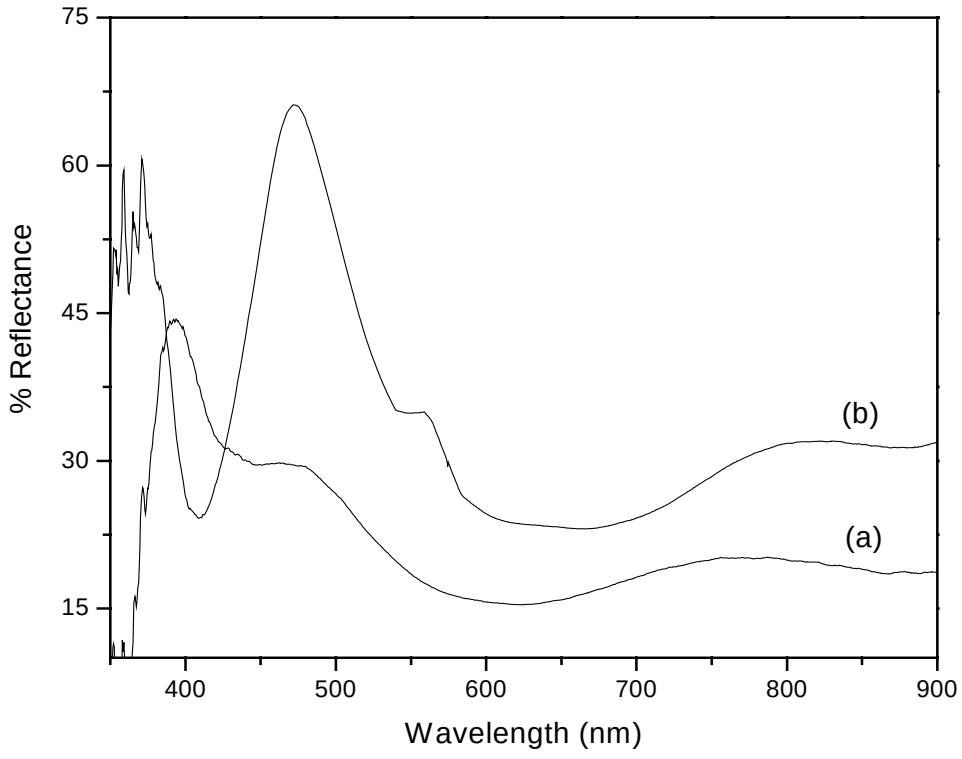

Fig. 5.16. The UV-Vis absorption spectrum of electrochemically deposited (a) PANI-HCl and (b) TSNiPc functionalised PANI films.

5.5.1.3. Wide Angle X-ray Diffraction (WAXD) Studies

X-ray diffraction was used to further probe the structure of TSCuPc-PANI nano fibers. The X-ray diffraction profiles of electrochemically synthesised PANI and TSCuPc functionalized PANI are shown in Fig. 5.17. The diffraction pattern for TSCuPc-PANI doesn't contain any characteristic peaks for phthalocyanine which clearly indicates that, the phalocyanine has been uniformly distributed in the polymer matrix. Apart from broad peak centered at 2θ =27, we could observe a new peak at 15.6 ° which belongs neither to PANI nor phthalocyanine. This unusual sharp peak may be due to the scattering from highly oriented PANI chain obtained by electro functionalisation of PANI in presence of TSCuPc as co-dopant. This sharp peak is absent in PANI synthesized under similar condition. This indicates that the TSCuPc is acting as a template in directing the PANI chain to form nano fibers.

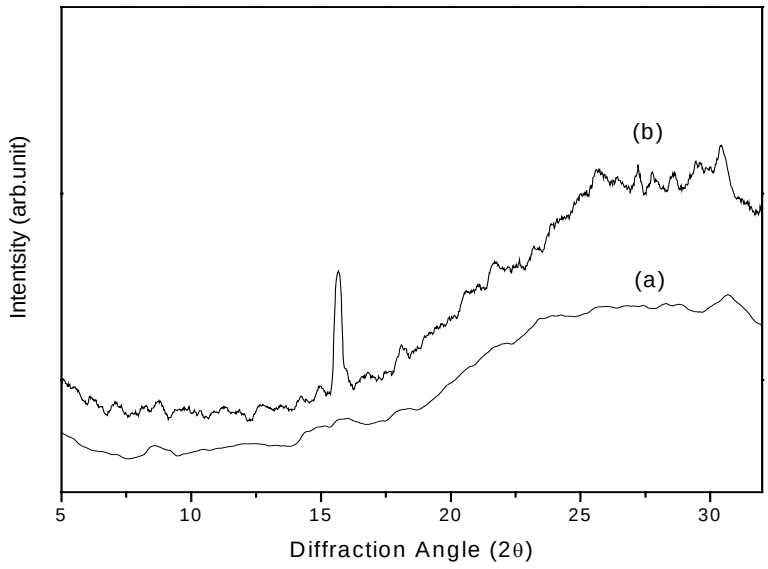

Fig.5.17. Wide Angle X-ray diffraction patterns of electrodeposited (a) PANI and (b) 1 mol % TSCuPc-PANI

5.5.2. Measurement of properties

The properties like thermal stability, morphology of the synthesized TSCuPc – PANI by electrochemical route and its application towards NO_2 gas sensing are discussed in this section.

5.5.2.1. Thermal stability

The thermal stability of electrochemically functionalized TSCuPc-PANI was found to have similar degradative pattern as compared with earlier systems. The thermogram of TSCuPc-PANI is shown in Fig. 5.18. Here, the thermal stability of TSCuPc-PANI was found to be almost 10 % higher than of pure PANI at 300ºC. The major weight loss corresponding to degradation of polymer back bone starts at 419ºC in PANI where as in TSCuPc-PANI the major degradation starts

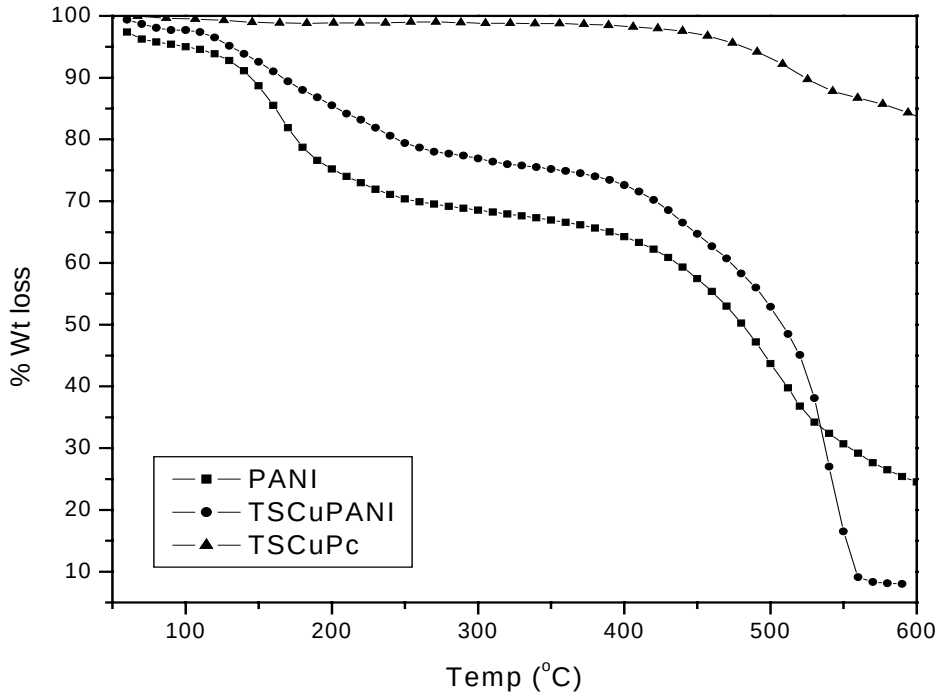

Fig. 5.18. TG thermogram of electrochemically synthesized PANI and TSCuPc-PANI

at 464ºC. This shows that phthalocyanine imparts good thermal stability to polymeric backbone. It is surprise to see, at 600ºC, the electrochemically functionalized PANI degrades almost completely where as PANI showed weight retention of 24%.

5.5.2.2. Scanning Electron Microscopy (SEM) Analysis

The morphology of the electrochemically synthesized TSCuPc – PANI polymer film grown on gold coated PET film was analysed using scanning electron microscope. SEM images of the growth surfaces for PANI-HCl and TSCuPc-PANI are shown in Fig. 5.19. PANI functionalized with TSCuPc reveals a striking contrast between PANI synthesized under similar electrochemical condition. It is interesting to observe a clearly defined nano fibrils of average size 50 nm with TSCuPc-PANI, where as the polyaniline synthesized using HCl as dopant under same condition show porous structure and doesn't show the fibrillar morphology. It's clear from the above discussion that the morphology of the electrochemically grown film depends on the type of functional dopant TSCuPc employed during synthesis and it acts as a template in forming nano fibrils. During the growth of PANI, the chain coils in such a way that , the sulfonated phthalocyanine acting as a dopant forms a stack with the neighboring Pc unit due to π - π^* interaction, which direct the polyaniline chain to grow in a spiral fashion leading to nano fibrous pattern

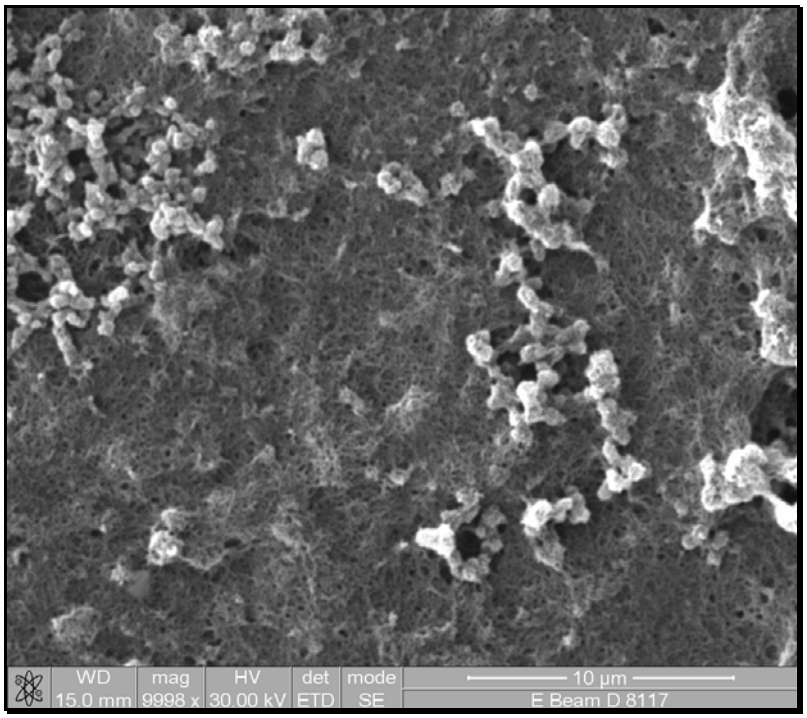
WD
15.0 mm
mag
9998 x
HV
30.00 kV
det
ETD
mode
SE
10 µm
E Beam D 8117

(a)

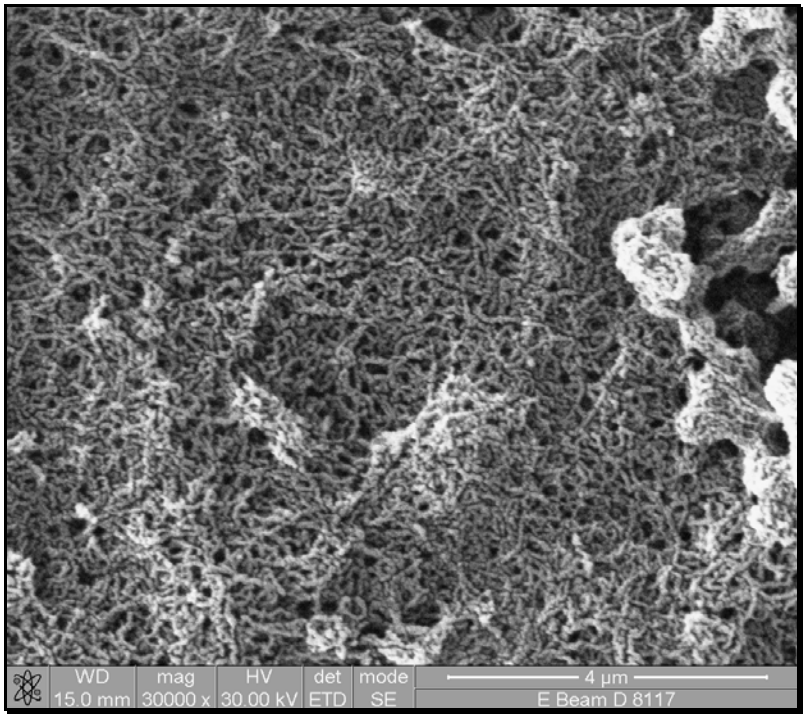
WD
15.0 mm
mag
30000 x
HV
30.00 kV
det
ETD
mode
SE
4 µm
E Beam D 8117

(b)

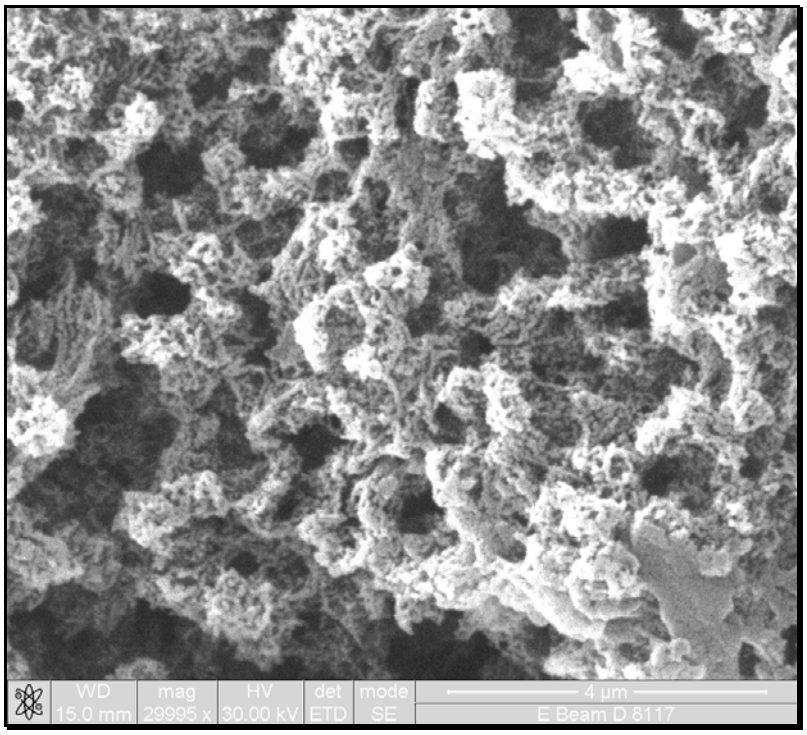

(c)

Fig. 5.19. Scanning electron micrograph of electrochemically functionalized TSCuPc-PANI with magnification (a) 10000, (b) 30000 and (c) HCl doped PANI

5.5.2.3. Electrochemical studies

The electrochemical experiments were carried out with certain objectives in mind including the investigation of this new material for energy storage or semiconducting applications and electrocatalysis. The redox properties of the TSCuPc-PANI polymer has been, in general investigated by cyclic voltammetric technique containing a traditional three-electrode cell with two platinum foil electrodes and a saturated calomel reference electrode (SCE) at room temperature. The electrochemical properties of the TSCuPc-PANI film was studied separately for PANI and TSCuPc in aqueous and non aqueous medium in order to get well defined redox peaks. An electrolytic bath containing 2M HCl

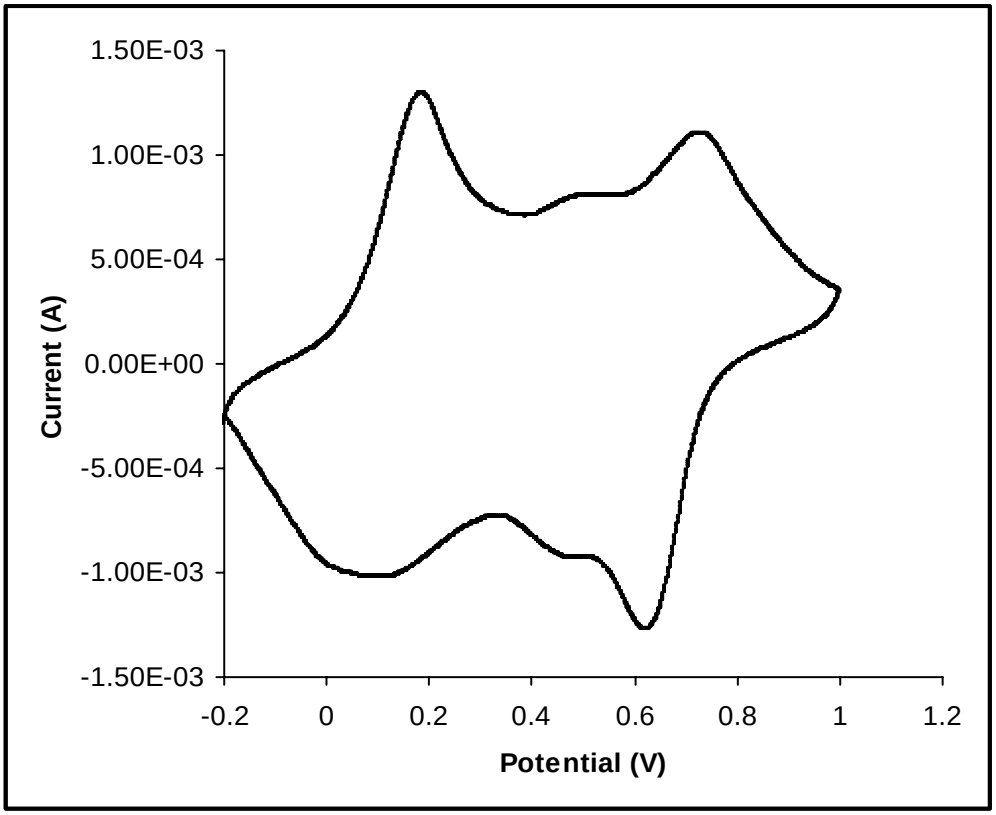

Fig. 5.20. Cyclic voltammogram of Pure PANI in H2O/ 2 M HCl .scan rate 0.05 V/s

in water was used to study the redox properties of PANI and the voltammograms were recorded by cycling the potential between -0.2 and 1V versus SCE at a sweep rate of 50 mV/s. The cyclic voltammogram of pure PANI and PANI in TSCuPc-PANI are shown in Fig. 5.20 and Fig. 5.21. The cyclic voltammogram of PANI in TSCuPc-PANI showed two redox couples appearing at 0.253V and 0.825V versus SCE, first one characteristics of redox interconversion between polyleucoemeraldine and polyemeraldine and the second couple between polyemeraldine and polypernigraniline. The peak potential of the

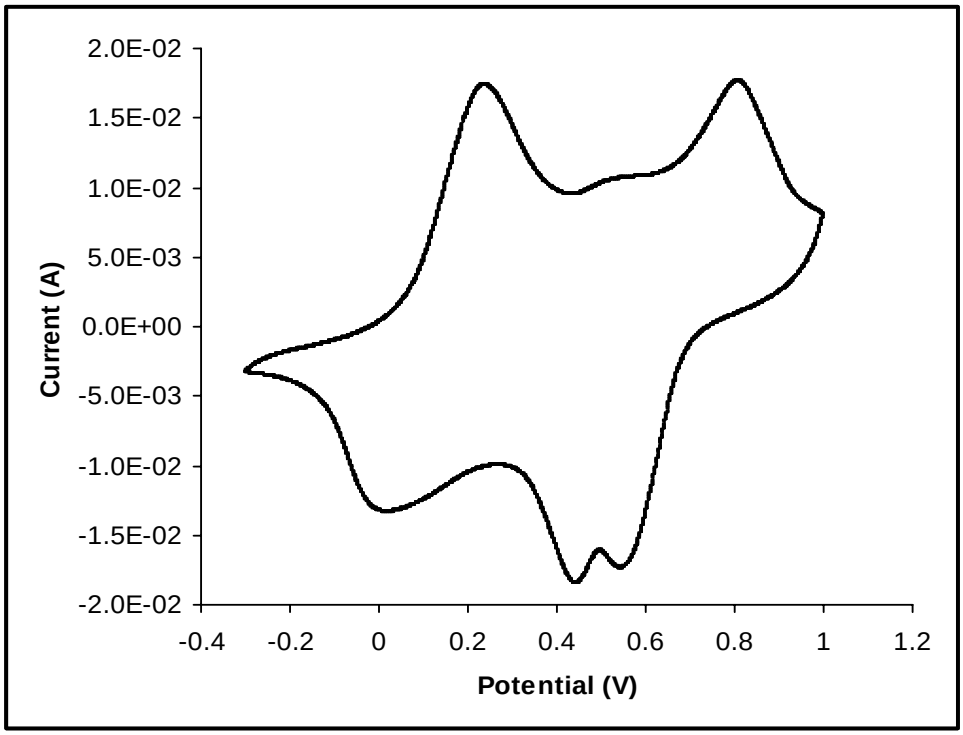

Fig. 5.21. Cyclic voltammogram of PANI in TSCuPc-PANI in H2O/ 2 M HCl .scan rate 0.05 V/s

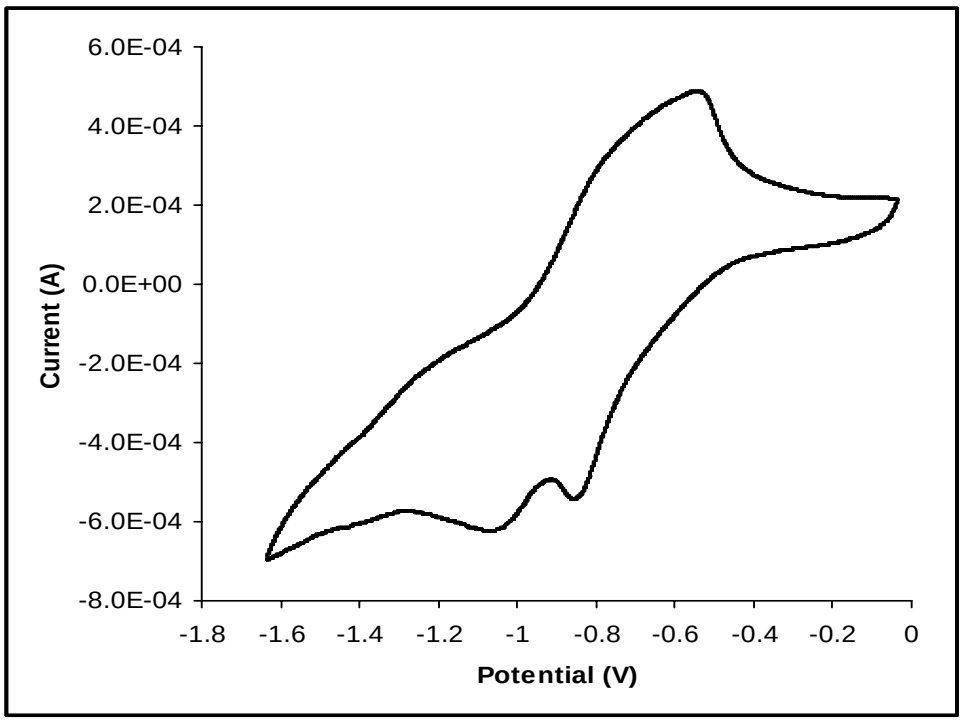

Fig. 5.22. Cyclic voltammogram of TSCuPc-PANI in DMF/0.1 M TBAP. scan rate 0.05 V/s

second redox reaction depends on the type of acid used as electrolyte and the solution pH [22]. The CV of TSCuPc in TSCuPc-PANI was carried out in DMF solvent containing $1x10^{-4}$ M tetra butyl ammonium perchlorate (TBAP). Here the potentials were cycled between 0 to -2V versus SCE at a sweep rate of 50 mV/s. In a typical cyclic voltammogram of TSCuPc – PANI, the process observed in the potential range from –0.7 to -1.4V can be explained as ring reduction processes of TSCuPC-PANI which is similar to the electrochemistry of TSCuPc, Copper phthalocyanines show well behaved two redox processes [23] centered on the ligand, from $[TSCu(II)Pc(-1)]^{+}$ to $[TSCu(II)Pc(-3)]^{-}$ at potentials very similar to those of TSNiPc. The similarities in the reduction potentials between these phthalocyanines indicate that reduction involves the phthalocyanine ligand rather than being metal centered. The reduction potentials of TSCuPc were observed at -0.86 and -1.12 V characteristics of ring reduction such as TSCuPc(-2) to $[TSCuPc(-3)]^{-}$ and $[TSCuPc(-3)]^{-}$ to $[TSCuPc(-4)]^{2-}$. The pure TSCuPc compound, displayed its redox waves at -0.745 and -1.14 V. It's reasonable to envisage that the alteration in the redox properties of the phthalocyanine molecule could be due to the surrounding polymer matrix. PANI as well as the polarization of the phthalocyanine by the metal center on the ring reductions of TSCuPc induces a small cathodic shift in the reduction potentials. The cyclic voltammogram of TSCuPc functionalized PANI (TSCuPc-PANI) displaying the redox characteristics of TSCuPc is shown in Fig. 5.22.

5.5.2.4. Chemical sensor

A great deal of polyaniline sensor research has been focused on changing the polymer structure to facilitate interaction between vapor molecules and polymer either by modifying the polymer backbone or the interchain connections [24]. Nanofibers of

polyaniline are found to have superior performance relative to conventional materials due to their much greater exposed surface area. Since nano structured polyaniline have much greater surface area, the use of nanowires, nanotubes, nanofibers could greatly improve diffusion, as well as much greater penetration depth for gas molecules relative to their bulk counterparts. The small diameter of the nanofibers coupled with the possibility of gas approaching from all sides should give sensors with improved performances. However, very few reports are available on nano structured conducing polymer sensors, probably due to the lack of facile and reliable methods for making conducting polymer nanostructures.

We have successfully prepared a film of TSCuPc-PANI by electrochemical method and used it for our sensor studies. During electrodeposition of TSCuPc-PANI, TSCuPc acts a template in forming the nano fibre and it has an added advantage of sensing the NO_2 gas. Here, solvents are not used for casting into film form and hence the interference due to the solvents are avoided. The real time resistance changes of the TSCuPc-PANI films are monitored with Keithley electrometer, upon exposure to 100 ppm NO_2 gas. The response given by the sensor elements made from PANI-HCl and TSCuPc-PANI (prepared under the same condition) were compared in Fig. 5.23. Since the film were in the nano fibrous form, its sensing action with NO_2 gas was very fast. We could notice a fast response with high sensitivity factor for PANI containing 0.5 mol % of TSCuPc, but the recovery was found to be slow for this compared to other composition. PANI containing 0.5 mol % TSCuPc showed a minimum response time t_{50} of 29 sec with a high sensitivity factor of 335.4. The response time and sensitivity factor for various composition of TSCuPc-PANI were calculated and shown in Fig. 5.24. The use of redox

active TSCuPc might change the oxidation state of polyaniline, thereby changing the degree of conjugation of the polyaniline backbone and the conductivity. Thus the possibility of adding functional guest into polyaniline matrix, could greatly broaden the

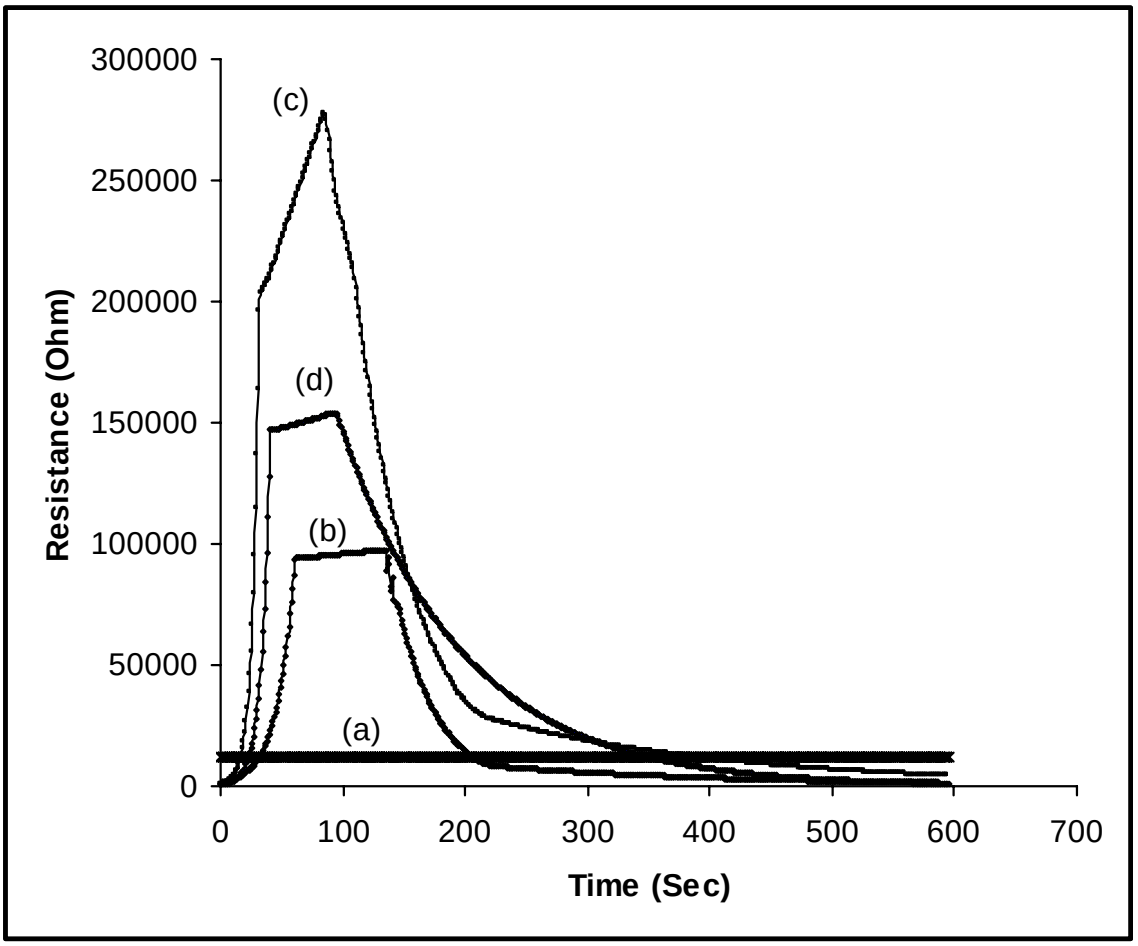

Fig. 5.23. Response characteristics of electrochemically functionalized TSCuPc-PANI towards NO_2 gas. (a) PANI, (b) 0.2 mol % TSCuPc-PANI, (c) 0.5 mol % TSCuPc-PANI and (d) 1 mol % TSCuPc-PANI

scope of polyaniline towards gas sensor. The guest-matrix interaction provides new mechanism of sensing action towards the NO_2 gas and it is represented in Fig. 5.25.

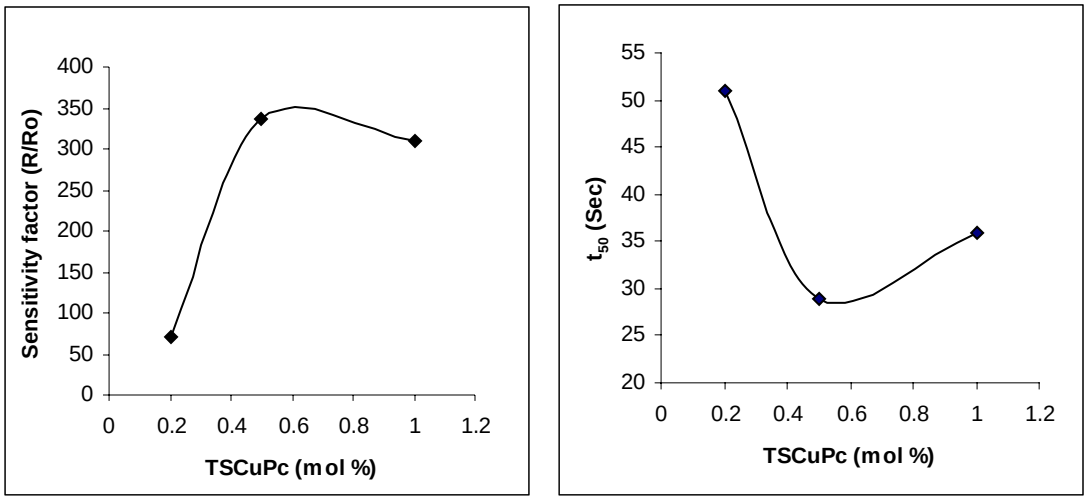

(a) **(b)**

Fig. 5.24. Sensor characteristics of Electrochemically functionalized TSCuPc-PANI towards NO_2 gas

(a) Plot of sensitivity factor versus concentration of TSCuPc

(b) Speed of response (t_{50}) versus concentration of TSCuPc

Table 5.7. Sensor characteristics of TSCuPc functionalized PANI towards NO_2 gas

Compound	**Mol %**	**Sensitivity factor (S)**	**Speed of response (t_{50}) (Sec)**
TSCuPc-PANI	0.2	71.7	51
	0.5	335.4	29
	1	310.7	36

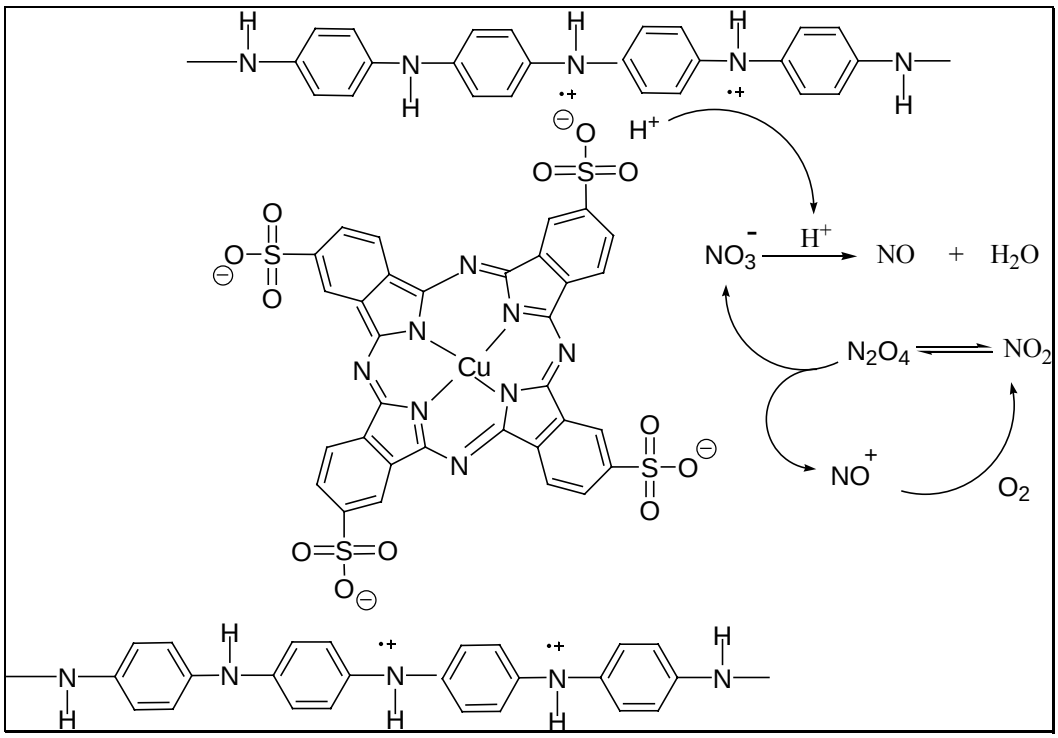

Fig. 5.25. Possible mechanism for gas sensing of TSCuPc functionalized PANI towards NO_2 gas

5.6. Conclusion

The chemical and electrochemical incorporation of TSCuPc into polyaniline has been successfully carried out during polymerization of aniline. The catalytic nature of TSCuPc was seen from the yield of TSCuPc-PANI polymer obtained. The structure of TSCuPc-PANI was elucidated from the FT-IR spectra, UV-Vis spectra and Wide Angle X-ray Diffraction studies. All the above techniques confirmed the efficacy of TSCuPc incorporation in polyaniline matrix. The ordering of polyaniline chain with the introduction of phthalocyanine was seen from increase in the intensity of XRD patterns.

The effect of phthalocyanine sulfonic acid on the charge transport of the polymer was analysed by measuring the D.C conductivity of TSCuPc-PANI samples which

displayed an increase in conductivity as a function of phthalocyanine concentration. The newly synthesized TSCuPc-PANI polymer exhibits better thermal stability than emeraldine salt form of PANI as seen from the thermogravimetric analysis. The morphology of the chemically and electrochemically synthesized polymer samples were analysed through SEM. The chemically prepared samples were particulate in nature where as the TSCuPc-PANI film prepared through electrochemical method showed nano fibrous morphology.

The redox behaviour of electrochemically prepared TSCuPc-PANI film was investigated by cyclic voltammetric technique and it showed two redox processes centered on the ligand. The TSCuPc-PANI nano fibers synthesized by electrochemical method gave significantly better performance towards NO_2 gas sensing in terms of both sensitivity and time response due to the high surface area and small nano fiber diameter. Therefore, these TSCuPc-PANI nano fibers appear to be superior as a chemical sensor materials operating at room temperature. To further examine these materials, different concentrations of various analytes will be used to determine the range of response and the limits of detection.

5.7. References

[1] N. R. Armstrong, J. Porphyrins Phthalocyanines., 4 (2000) 414.

[2] R. Zhou, F. Jose, W. Gopel, T. Z. Z. Ozturks and O. Bekaroglus, App. Organometallic. Chem., 10, (1996) 557.

[3] M. Kaneko and D. Wohrle, Adv. Polym. Sci., 84 (1988) 141.

[4] D. Wohrle, H. Kaune and B. Schumann, Makromol. Chem., 187 (1986) 2947.

[5] S. Venkatachalam, and P. V. Prabhakaran, Eur. Polym. J., 29 (1993) 711.

[6] T. Inabe, J. W. Lyding, M. K. Moguel and T. J.Marks, J. Phys., C3 (1983) 625

[7] Pretsch, Structure determination of organic compounds. Tables of spectral data, 3 rd Edn., Springer, USA, (2000).

[8] A. Davidson, J. Chem. Phys., 77 (1982) 162.

[9] Q. Chen, D. Gu, J. Shu, X. Tang and F. Gan, Mater. Sci. Eng., B25 (1994) 171.

[10] M. M. El-Nahass, K. F. Abd El-Rahman, A. A. M. Farag and A. A. A. Darwish, Int. J. Mod. Phy B., 18 (2004) 421.

[11] F. Lux, Polymer., 35 (1994) 2915.

[12] T. J. Marks, Angew. Chem. Int. Ed. Engl. 29, (1990) 857.

[13] A. G. MacDiarmid, A. J. Epstein, Synth. Met., 65 (1994) 103.

[14] V. G. Kulkarni, L. D. Campbell and W. R. Mathew, Synth. Met., 30 (1989) 321.

[15] J. Yue, A. J. Epstein, Z. Zhong and P. K. Gallagher, Synth. Met., 41 (1991) 765.

[16] J. Janata, Principles of Chemical Sensors, Plenum, New york, (1989).

[17] L. Valli, Adv. Colloid and Interface. Sci., 116 (2005) 13

[18] N. E. Agbor, M. C. Pretty and A. P. Monkman, Sensor and Actuator., B 28 (1995) 173.

[19] C.C. Han and S. P. Hang, Macromolecules 34 (2001) 4937.

[20] Y. Xia, A. G. MacDiarmid and A. J. Epstein, Macromolecules., 27 (1994) 7212.

[21] M. Higuchi, D. Imoda and T. Hiroa, Macromolecules., 29 (1996) 8277.

[22] W. S. Huang, B. D. Humphrey and A. G. MacDiarmid, J. Chem. Soc., Faraday Trans-1., 82 (1986) 2385.

[23] A. B. P. Lever, S. Licoccia, K. Magnell, P. C. Minor and B. S. Ramaswamy, Adv.Chem. Ser., 201 (1982) 237.

[24] T. Kikas, H. Ishida, J. Janata, Anal. Chem., 74 (2002) 3605.

CHAPTER-6

Summary and Conclusion

Summary and Conclusion

Conducting polymers functionalized with groups which enhance specific physical and/or chemical properties, without causing disruption to electronic properties of the conjugated backbone, have become increasingly prominent in recent years. These materials are promising candidates for sensor, electrochromic, redox catalytic and energy conversion applications. In this respect, polyaniline substituted with redox or molecular recognizing groups represent very attractive combination for developing new materials.

Polyaniline (PANI) and their derivatives, have been investigated as the active layer of gas sensors since early 1990s. The sensors made from polyaniline have many improved characteristics like room temperature operation, shorter response time, ease of synthesis etc. when compared to metal oxide based sensors that operate at high temperature.

Much effort has been devoted in the past, to improve the sensitivity, selectivity, response time and stability of gas sensors by modifying the sensing materials. Incorporating a second component into polyaniline in the form of dopant is one of the most important methods to develop new materials for devices. Hence in the present investigation, the emeraldine salt form of polyaniline was incorporated with tetra sulfonated metal phthalocyanines in the form of dopant ion. The functional molecules namely iron, nickel and copper tetra sulfonated phthalocyanines were used to incorporate into polyaniline matrix by chemical and electrochemical methods. The efficacy of incorporation and the structure of functionalized polyaniline was elucidated by various physico-chemical techniques. Initially, the polyaniline was modified with un-substituted iron and cobalt phthalocyanines. Due to lack of solubility in the reaction medium, the

product of the reaction ended up with polyaniline-phthalocyanine composite with decrease in electrical conductivity measured at room temperature. Hence, it was decided to use water soluble tetra sulfonated metal phthalocyanines as dopant during the synthesis of polyaniline. It is interesting to mention here, that the yield of polyaniline has increased in the presence of phthalocyanine, which could be due to the catalytic effect of phthalocyanine and it is more pronounced in the case of sulfonated iron phthalocyanine incorporated PANI. Based on the yield obtained, the catalytic effect of Phthalocyanine for polymerization can be arranged in the order TSFePc > TSCuPc > TSNiPc.

The formation of two phases namely, phthalocyanine and PANI could be seen from the IR spectra of FePc-PANI and CoPc-PANI compounds where as the sulfonated phthalocyanine incorporated PANI doesn't show any phase separation. This is further evidenced from the wide angle x-ray diffraction studies. Apart from this, the effect of phthalocyanine incorporation in PANI was seen as a shift in the frequency of benzeniod structure towards lower wave number region. A significant increase in the intensity of Q and B band in the IR spectra of functionalized PANI suggests the extra doping by sulfonated phthalocyanine. The peaks corresponding to asymmetrical and symmetrical stretching of sulfonic acid in phthalocyanine has been shifted and appeared at 1350 cm^{-1} and 1120 cm^{-1} further confirms functionalisation of PANI by sulfonated phthalocyanine. In electrochemically functionalized PANI due to the small amount of phthalocyanine present, major difference is not seen between pure PANI and the functionalized PANI. The bands associated with quinoid-benzenoid groups and –C=N- stretching frequencies have been broadened and are not well resolved due to the overlapping of characteristic bands of sulphonated phthalocyanine with PANI.

The structure of sulfonated phthalocyanine functionalized PANI was studied by WAXD, PANI doped with HCl alone has certain percentage of crystallinity having peaks centered at 2θ values 8.9, 20.3 and 25.4 characteristic of orthorhombic crystal system. After functionalisation with sulfonated phthalocyanine, notable changes in the crystallinity of PANI has been observed due to the addition of macrocyclic phthalocyanine moiety into polymer matrix. In TSFePc-PANI, the very prominent peak at 2θ = 9.1 characteristic of TSFePc is completely absent suggesting that there is no separate phthalocyanine phase left. At the same time there is an increase in the intensity of peak at 2θ value 20.3º suggesting a better stacking and increase in molecular ordering of PANI chain. In the case of TSNiPc-PANI and TSCuPc-PANI samples, there is an increase in the intensity of the peaks centered at 2θ values 15, 20 and 25 has been observed with the increase of phthalocyanine concentration in PANI which has been explained based on increase in the molecular ordering of polymer chains induced by phthalocyanine.

Since the SEM picture revealed the nano fiberous morphology for the electrodeposited PANI and Pc functionalized PANI films, the X-ray diffraction studies were carried out to identify its structure. A partial crystalline nature was seen at 2θ value 11.5 and 15.6 for TSNiPc and TSCuPc loaded PANI. This unusual sharp peak may be due to the scattering from highly oriented PANI chain obtained by electro functionalisation of PANI in the presence of sulfonated Pc as co-dopant. This sharp peak is absent in PANI synthesized under similar condition.

The UV-Vis spectral studies were carried out in water and formic acid medium. The electronic spectra of phthalocyanines showed two characteristic bands Q and B

bands. The intensity of Q-band in Pc is sensitive to the environment of the Pc macrocycle. Hence, it has vanished after functionalisation with PANI. The UV-Vis spectra of all functionalized PANI displayed three characteristic bands at 350, 540 and 770 nm corresponding to the π - π^* transition, benzenoid to quinoid excitonic transition and polaron to bipolaron transitions. The π - π^* and polaron to bipolaron transitions in PANI showed red shift, which is expected due to the extension of conjugation with the highly conjugated phthalocyanine moiety. The diffuse reflectance spectra of electrochemically prepared PANI and Pc functionalized PANI films on ITO plates displayed clearly defined bands at 450, 550 and 800 nm region corresponding to the interpretations given for absorption spectra of chemically synthesized samples.

The amount of phthalocyanine incorporated was quantitatively analyzed by means of GFASS and EDX techniques. The metal ion analyzed by GFASS technique revealed the proportionate increase in metal ion concentration as consistent with the concentration of sulfonated phthalocyanine used. In EDX, there is an increase in the intensity of N, O, S and metal ion peaks with slight decrease in the intensity of Cl. This indicates that few Cl dopants are replaced by the sulfonated phthalocyanine molecules.

The electrical conductivity of all the samples were carried out by two probe technique. It is interesting to note that, in all the three sulfonated metal phthalocyanines, the conductivity was found to increase with increase in phthalocyanine concentration. This is due to the fact that, when the phthalocyanine with four sulfonic acid group at the periphery is incorporated into polyaniline chains, extended conjugated structures are available both on the dopant and on the polyaniline matrix and hence it provides better pathway for the transport of charges along and in between the polyaniline matrix. The

self-secondary doping effect can also induce significant improvement in electrical properties. Sulfonic acid of the phthalocyanine units may interact with amine/imine hydrogens, and modifies the electrical properties of the polymers. Although the increase in conductivity is not so much pronounced, the maximum difference in conductivity between the PANI and 1mol % incorporated sulfonated metal phthalocyanine-PANI was found with TSCuPc-PANI and it can be arranged in the order

TSCuPc-PANI > TSFePc-PANI > TSNiPc-PANI

The electrical conductivity of Polyaniline modified with un-substituted phthalocyanine doesn't show any increase in conductivity instead a steady fall in conductivity was noted and this could happen (i) when there is no proper interaction between the phthalocyanine and PANI and (ii) the charge transport is restricted due to the formation of two phases namely, insulating phthalocyanine and conducting PANI. In the case of tetra sulfonated phthalocyanine incorporated PANI, there exists a strong interaction between the Pc and PANI and the dopant plays an important role in the conductivity of the polymer. This is further confirmed from the IR and WAXD studies.

The thermo gravimetric analysis of the functionalized PANI under N_2 atmosphere displayed two major weight losses. The initial weight loss is due to the removal of water and chloride dopant and the second one due to the structural decomposition of polymer backbone. The added phthalocyanine has significant effect on the thermal stability of PANI. Here, stabilization of polymer chiefly comes through the sulfonated phthalocyanine linking the PANI chains together to give better thermal stability. At 600°C, the weight retention of PANI-HCl is 62 % where as PANI containing 1 mol % TSCuPc showed a maximum weight retention of 73 %. Hence, based on the weight

retention at 600°C, the thermal stability of sulfonated phthalocyanine functionalized PANI can be arranged in the order TSCuPc-PANI > TSFePc-PANI > TSNiPc-PANI.

The morphology of all the phthalocyanine loaded PANI samples synthesized through chemical method clearly shows the samples were globular particulate in nature where as in the case of electrochemically synthesized TSPc-PANI samples, to our surprise a clearly defined nano-fibrils of average size 50 nm has been observed. The polyaniline synthesized by electrochemical route using HCl as dopant under the same condition doesn't show the fibrillar morphology instead a porous structure was observed. Hence, it can be concluded that the functional dopant may act as a template in forming nano-fibrils. During the growth of PANI, the chain coils in such a way that, the sulfonated phthalocyanine forms a stack with the neighboring Pc unit due to π - π^* interaction, which direct the polyaniline chain to grow in a spiral fashion leading to nano fibrous pattern.

The redox behaviour of electrochemically synthesized Pc containing PANI films were studied by cyclic voltametric technique separately for PANI and TSCuPc in aqueous and non aqueous medium to get well defined redox peaks. In all Pc functionalized PANI films, PANI showed two redox couples appearing at 0.253V and 0.825V versus SCE, characteristics of redox interconversion between polyleucoemeraldine and polyemeraldine and the second couple between polyemeraldine and polypernigraniline. The electrochemical properties of sulfonated Pc, in PANI was studied in DMF solvent containing $1x\ 10^{-4}$ M tetra butyl ammonium perchlorate (TBAP) between 0 to -2V versus SCE at a sweep rate of 50 mV/s. Sulfonated iron phthalocyanine displayed three redox couples at potentials -0.814, -1.016 and -1.58 V where as nickel

and copper possess only two redox potentials at -1.012, -1.31 and -0.86, -1.12 V characteristics of ring reductions.

Apart from this, the oxidation of metal center to $[TSFe(III)Pc(-2)]^{+}$ occurs in the range -0.15 to +0.69 V. The transition metal species such as Ni(II) and Cu(II) may be incapable of a redox process in the usual electrochemical regime. It's reasonable to envisage that the alteration in the redox properties of the phthalocyanine molecule could be due to the surrounding polymer matrix. PANI as well as the polarization of the phthalocyanine by the metal center on the ring reductions of TSCuPc induces a small cathodic shift in the reduction potentials.

The potentiality of the Pc functionalized PANI samples was tested to explore its final utility towards sensing of 100 ppm NO_2 gas. When the samples were exposed to NO_2 gas a decrease in resistance was observed with FePc and CoPc loaded PANI which appear to be a common process. On the other hand, an increase in resistance was observed with sulfonated Pc incorporated PANI samples. Hence, a different mechanism of NO_2 gas sensing has been suggested for the substituted phthalocyanine incorporated as dopants in PANI.

In unsubstituted FePc and CoPc incorporated PANI, phthalocyanines behave like p-type semiconductor and when exposed to oxidizing gas like NO_2, holes are created leading to an increase in conductivity (decrease in resistance) of the overall polymer samples. FePc and CoPc modified PANI showed maximum sensitivity (R_o/R) at an optimum concentration of 1 mol % metal phthalocyanine in PANI. These materials were phase separated at high concentration of the additives. Also, their conductivity was not high which suggests that these were not effective dopants.

The interesting aspect that emerges from these sensor studies is that the sulfonated Pc-PANI samples showed higher sensitivity factor and speed of response than FePc and CoPc incorporated PANI samples.

Among the sensors made from chemically synthesized sulfonated phthalocyanine-PANI samples, 1 mol % TSCuPc incorporated PANI showed maximum sensitivity factor (R/R_o) of 30.9 with a response speed of 62 sec where as TSFePc and TSNiPc-PANI displayed only 6.8 and 2.3 with a response speed of 87 and 103. From the sensitivity values, it can be concluded that the sensitivity increases with increases in Pc concentration and it almost gets saturated for PANI containing 1 mol % Pc. It is interesting to note that the recovery is also fast and almost 70 – 85 % recovery was achieved in these samples.

In the case of sensors fabricated by electrochemical method, the response is very rapid and at the same time recovery is also fast when compared to the sensor made from chemical method. The high sensitivity of electrochemically synthesized samples can be due to uniform, controlled alignment of phthalocyanine rings onto the polymer back bone and nano structured polyaniline obtained during synthesis. In all electrochemically functionalized PANI samples, the maximum sensitivity was reached at an optimum concentration of 0.5 mol % of TSPc in PANI where as in chemically synthesized samples, it is reached only at 1 mol % Pc. A high sensitivity factor of 335 was achieved by TSCuPc-PANI with rapid response time of 29 sec. The TSFePc and TSNiPc functionalized PANI showed a moderate sensitivity factor of 70 and 14 with a response time of 46 and 67 sec. Hence it can be concluded that the TSCuPc-PANI nano fibers synthesized by electrochemical method gave significantly better performance towards

NO_2 gas sensing in terms of both sensitivity and time response due to the high surface area and small nano fiber diameter. Apart from this, the TSCuPc-PANI is found to have high conductivity which suggests better charge transfer efficiency which can also be a reason for high sensitivity with rapid response to NO_2 gas. A relation can be drawn by comparing the conductivity, sensitivity and catalytic behaviour of metal phthalocyanines is given in Table 6.1.

Table 6.1 Comparison on conductivity, sensitivity and catalytic behaviour of metal phthalocyanines

$TSM^{2+}Pc$-PANI	**Conductivity** ($ohm^{-1}cm^{-1}$)	**Sensitivity factor to NO_2**	**Catalytic efficiency** (Yield %) [a]
M^{2+} = Fe	0.0044	70.3	40
M^{2+} = Ni	0.0038	14.0	20
M^{2+} = Cu	0.0051	335.4	90
PANI	0.0025	1.01	---

[a] S. L. Jain et al, J. Mol. Catalysis A., 195, (2003) 283.

It is seen from the above data, that the sensitivity factor is essentially related to the catalytic efficiency and charge transfer process of the phthalocyanine group introduced as dopant in the PANI. Therefore, among the sulfonated metal phthalocyanine incorporated PANI, the TSCuPc-PANI appear to be superior as a chemical sensor materials operating at room temperature. Additionally, the morphology also plays an

important role since nano fibrous morphology is seen in the electrochemically deposited films, which give better response than the chemically synthesized polymers.

These studies have clearly brought out the importance of functionalization of conducting polymers for specific application such as a chemical sensor. It is not only the type of functional group that is important but also the method of its incorporation, its interaction with the polymer as well as the effect on supermolecular structure, which lead to final performance of the polymer as the active material in the device. Considering the fact that only a small concentration (5 molecules for 1000 monomer unit) of the functional groups gives tremendous changes in the sensitivity factor, these modified conducting polymers are quite similar to olefactory nerves occurring in nature which have sensing moieties attached to the long chain. Thus, these sensors can lead to the development of artificial electronic nose, which can sniff out toxic gases and send alarms.

Fellowships, Award and Publications

Research Fellowships:

Junior and Senior Research Fellowships from Council of Scientific and Industrial Research for a period of five years on the basis of National Entrance Test.

Awards:

Best Paper Award for a research paper " Iron phthalocyanine modified polyaniline for Toxic gas sensor application" presented during MACRO-2006, an International Conference on "Polymers for Advanced Technology" organized by National Chemical Laboratory, Pune-8.

Publications:

1. S. Francis Amalraj and S. Radhakrishnan. "Iron phthalocyanine modified polyaniline for Toxic NO_2 gas sensor application", Communicated to Sensor and Actuator.
2. S. Francis Amalraj and S. Radhakrishnan "A highly sensitive NO_2 gas sensor based on electrical conductivity changes in copper phthalocyanine functionalised polyaniline". (manuscript under preparation).
3. S. Francis Amalraj and S. Radhakrishnan "Electrochemically functionalised Polyaniline-Phthalocyanine nano fibers for NO_2 gas sensing" (manuscript under preparation).

Papers presented in National and International conference:

1. S. Francis Amalraj and S. Radhakrishnan. "Copper Phthalocyanine Functionalised Polyaniline - A potential toxic gas sensor" presented in ICAM 2008, an International conference on " Advanced Materials" organized by Mahatma Gandhi university, Kottayam, India.
2. S. Francis Amalraj and S. Radhakrishnan. "Iron phthalocyanine modified polyaniline

for Toxic gas sensor application" presented during MACRO 2006, an International Conference on "Polymers for Advanced Technology" organized by National Chemical Laboratory, Pune-8.

3. S. Francis Amalraj and S. Radhakrishnan. Presentation on the topic "conducting polyaniline modified with copper phthalocyanine for electrocatalytic application". Regional symposium on polymer science and technology, Society of polymer science, India.